REFERENCE ONLY

UNIVERSITY OF LONDON THESIS

Degree PhD Year 2006 Name of Author McNEIL, E.

Neutrophil Function in S100A9 Null Mice

Eileen M^{c}Neill

Cancer Research UK London Research Institute

and

University College London

September 2005

Supervisors

Dr. Nancy Hogg	Prof. Peter Beverley
Cancer Research UK	University College London

This thesis is submitted in part fulfilment of the requirements for the degree of Doctor of Philosophy at the University of London

ProQuest LLC
789 East Eisenhower Parkway
P.O. Box 1346
Ann Arbor, MI 48106-1346

Abstract

S100A9 and its heterodimeric binding protein, S100A8, are low molecular weight calcium-binding proteins of the S100 protein family that are abundantly expressed in myeloid cells. They constitute 40% of neutrophil cytosolic protein and 1% of monocyte cytosolic protein. To elucidate the function of this protein complex, a study of the S100A9 null mice, which also lack S100A8, was undertaken.

Myelopoiesis in the S100A9 null mice was shown to be normal, with the resulting neutrophils and monocytes showing no differences in differentiation or activation state. No compensatory upregulation of other S100 proteins was found in S100A9 null neutrophils, which exhibit a significantly lower buoyant density than wildtype neutrophils.

The basic calcium homeostasis of the S100A9 null neutrophils was normal. However a reduced calcium flux in response to suboptimal levels of MIP-2, KC, MIP-1α, PAF and C5a but not FMLP was observed. This lesion in calcium response was shown to be in the IP_3-mediated calcium release pathway.

Adhesion of the S100A9 null neutrophils along with migration and *in vitro* chemotaxis was normal. In addition no differences in the cytoskeletal morphology of the S100A9 null cells was seen. No defect in *in vivo* migration of neutrophils or monocytes could be seen in a peritonitis model initiated by thioglycollate, TNFα or IL-1β.

Activation of the NADPH oxidase, measured in kinetic and phagocytosis-activated studies, was unaltered by the loss of S100A9. There was no effect of S100A9 deletion in an *in vitro* bacterial killing assay or in an *in vivo* model of *Streptococcus pneumoniae* lung infection.

Expression of S100A8/9 has been associated with wound healing and cancer. No defect in wound healing or injected tumour growth was found in S100A9 null mice. However a model of chemical-induced carcinogenesis in the S100A9 null mice demonstrated both an increased rate of papilloma formation and increased papilloma multiplicity.

Acknowledgements

Firstly I'd like to thank my supervisor Nancy Hogg and the rest of the Leukocyte Adhesion Lab past and present for their help and encouragement. In particular: Ali, Paula, Andrew, Robbie, Melanie, Kath and Mat. A special mention goes to Josie Hobbs for her help and perfect understanding of all frustrations S100-related!

None of the work presented in this thesis would have been possible without the Biological Resources Unit. In particular I'd like to thank Barbara, Anna and George for looking after, and helping manage, my mouse colony. Also Gill, Clare and Rob for their vital help with the *in vivo* work presented here.

Thanks should also go to George Elia for performing the skin histochemistry included in this thesis. I would also like to thank my collaborator Aras Kadioglu for performing the infection studies.

A final thankyou goes to all my friends and family for their support and understanding through what has not always been a particularly straightforward project!! A big thanks also goes to everyone who helped proof-read my thesis, which was a massive help in the final stages.

Table of contents

Table of figures

Table of tables

Abbreviations

2-APB	2-aminoethyldiphenylborinate
AA	Arachidonic acid
AM	Acetoxymethyl ester
APC	Antigen processing cell
ARP2/3	Actin related protein 2/3
B	Body cavity
BCECF	2',7' -bis(2-carboxyethyl)-5(6)-carboxyfluorescein
BIM	bisindolylmaleimide I
BrdU	Bromodeoxyuridine
BSA	Bovine serum albumin
C	Complement
cADPR	Cyclic adenosine diphosphate ribose
CaM	Calmodulin
cDNA	Complementary DNA
CFA	Cystic fibrosis antigen
CFU	Colony forming unit
CGD	Chronic granulomatous disease
CMP	Common myeloid progenitor
DAG	Diacylglycerol
DAPI	4',6'-diamidino-2-phenylindole
DCDHF	Dichlorodihydrofluorescein
DMBA	7,12-dimethylbenz(a)antharacene
DNA	Deoxyribonucleic acid
ECL	Enhanced chemiluminescence
EDTA	Ethylene diamine tetraacetic acid
EGF	Epidermal growth factor
ER	Endoplasmic reticulum
ES	Embryonic stem cell
ETYA	5,8,11,14-eicosatetraynoic acid
FACS	Fluorescence activated cell-sorting
FCS	Foetal calf serum
FITC	Fluorescein isothiocyanate
FMLP	N-formyl-methionyl-leucyl-phenylalanine
GAG	Glycosaminoglycan
G-CSF	Granulocyte colony stimulating factor
GDP	Guanosine diphosphate
GM-CSF	Granulocyte/macrophage colony stimulating factor

GMP	Granulocyte-monocyte progenitor
GPCR	G-protein-coupled receptor
GT	Granulation tissue
GTP	Guanosine tris-phosphate
HBSS	Hanks balanced salt solution
HE	Hyperproliferative epithelium
HF	Hair follicle
HRP	Horseradish peroxidase
ICAM-1	Intracellular adhesion molecule 1
Ig	Immunoglobulin
IGF	Insulin-like growth factor
IL	Interleukin
IP_3	Inositol 1,4,5-triphosphate
JAM	Junctional adhesion molecule
KGF	Keratinocyte growth factor
LAD1	Leukocyte Adhesion deficiency 1
LFA-1	Leukocyte function-associated antigen 1
LPS	Lipopolysaccharide
mAb	Monoclonal antibody
M-CSF	Macrophage colony stimulating factor
MIP	Macrophage inflammatory protein
ML	Migrating lip
MMP	Matrix metalloproteinase
MPO	Myelo-peroxidase
mRNA	Messenger RNA
MRP	Migration inhibitory factor-related protein
NAADP	Nicotinic acid adenine dinucleotide phosphate
NAD	Nicotinamide adenine dinucleotide
NADPH	Nicotinamide adenosine dinucleotide phosphate
OAG	1-oleolyl-2-acyl-sn-glycerol
pAb	Polyclonal antibody
PAF	Platelet activating factor
PAGE	Polyacrylamide gel electrophoresis
PAMP	Pathogen associated molecular pattern
PBS	Phosphate buffered saline
PCR	Polymerase chain reaction
PdBu	Phorbol-12,13-dibutyrate
PE	Phycoerytherin
PECAM	Platelet/endothelial cell adhesion molecule
PH	Pleckstrin homology

PIP_2	Phosphatidylinositol (4,5)-bisphosphate
PKC	Protein kinase C
PLC	Phospholipase C
PMA/TPA	Phorbol-12Myristate-13-acetate
PMSF	Phenylmethylsulfonyl fluoride
PRR	Pattern recognition receptor
PSGL-1	P selectin glycoprotein ligand 1
PTX	Pertussis toxin
RAGE	Receptor for advanced glycation end-products
RNA	Ribonucleic acid
RPMI	Roswell park memorial institute medium
RT-PCR	Reverse transcription PCR
S1P	Sphingosine-1-phosphate
SD	Standard deviation
SDS	Sodium dodecyl sulphate
SEM	Standard error of the mean
SERCA	Sarcoplasmic/Endoplasmic reticulum calcium ATPase
SOCE	Store operated calcium entry
T	Tumour
TAE	Tris-acetate buffer
TGF	Transforming growth factor
TLR	Toll-like receptor
TNFα	Tumour necrosis factor α
TRP	Transient receptor potential
V	Vessel
VCAM	Vascular cell adhesion molecule
W	Wound

CHAPTER 1

1 Introduction

1.1 Calcium signalling

Calcium is a simple ubiquitous cellular signal. From the moment of fertilisation, when activation of the egg occurs by introduction of a sperm-transported phospholipase C to initiate calcium oscillations, calcium regulates an array of diverse cellular processes. As calcium participates in the transduction of a variety of signals, a complex network of calcium handling mechanisms exist. Calcium levels within the unstimulated cell are held at ~100nM rising to a level of ~1μM upon stimulation (reviewed in (Berridge et al., 2000)). The calcium that is needed to make up a cellular signal can broadly be either of extracellular origin, entering the cell by one of many cell surface ion channels, or released from the internal calcium stores through different calcium channels. The activation of these processes occurs either by the activating signal directly opening a calcium channel, for example the voltage operated calcium channels found in excitable cells, or by the production of a calcium mobilising second messenger.

1.1.1 Extracellular calcium entry

Study of calcium entry pathways in non-excitable cells has been a focus of intensive research in recent years. Pathways of this type are either directly activated by extracellular ligand-gated ion channels, by second messengers, such as lipid mediators including DAG and arachidonic acid, or by the depletion of the

intracellular stores. This store operated calcium entry process allows the cell to refill depleted intracellular stores. The activation of a family of store operated calcium channels on the cell surface by either physical interaction with the calcium stores or following production of a diffusible factor is hypothesised to be the means by which this process occurs. (Reviewed in (Berridge et al., 2003; Hardie, 2003; Spassova et al., 2004)).

1.1.2 Intracellular calcium release

The primary origin of intracellular calcium signals is the endoplasmic reticulum (ER). As well as the role of this cellular organelle in protein synthesis, the membrane bound sacks or tubes of the ER provide a reservoir of calcium within the cell. Calcium levels within the ER are ~100-500μM where calcium is held by high capacity buffering proteins such as calsequestin and calretinin (reviewed in (Berridge, 2002)). The most well defined intracellular calcium release pathways in non-excitable cells are those elicited by the IP_3 receptor and the ryanodine receptor. Both these receptors are located in the membrane of the endoplasmic reticulum in non-excitable cells and act as ligand gated ion channels allowing the release of calcium into the cytosol. Calcium release via the IP_3 receptor occurs following ligation by the lipid mediator IP_3. This mediator is produced by enzymes of the phospholipase C family that hydrolyse the membrane lipid PIP_2 to form DAG and IP_3. The ryanodine receptor gains its name from the plant alkaloid ryanodine that was used to define this receptor. Ryanodine has a stimulatory activity at low concentrations and an inhibitory function at higher concentrations. Along with these better defined second messengers, putative roles for NAADP and sphingosine-1-phosphate (S1P) in releasing calcium are under

study. (Basic program of calcium signalling reviewed in (Berridge et al., 2003; Berridge et al., 2000)).

1.1.3 The OFF process

Following elevation of the cytosolic calcium concentration, the signal must then be transduced into a specific effect. This can occur by direct activation of calcium-sensitive enzymes and ion channels, or be further transduced by calcium-binding effector proteins. Along with the activation of the calcium driven cellular processes, the calcium signal itself must be terminated and the calcium in the cytosol be removed. The clearance of the calcium signal happens by activation of calcium pumps that return calcium to the internal stores (Sarcoplasmic/endoplasmic reticulum calcium ATPase (SERCA) pump), pump calcium out of the cell (Na^+/Ca^{2+} exchanger), or facilitate uptake into the mitochondria (mitochondrial uniporter). This process is aided by calcium buffering proteins that have a high on-rate for calcium binding. They rapidly take up free calcium and gradually release it back into the cytosol to be removed in keeping with their slow off-rate (reviewed in (Berridge et al., 2003)).

1.1.4 Calcium signal transduction

It is the job of calcium binding proteins to take the basic elemental signal of increased calcium and translate this into a diverse array of cellular functions. The most common calcium-binding protein motif is the EF-hand that is shared by many proteins having calcium buffering or calcium sensor activities. The classical helix-loop-helix EF-hand motif contains a 12 amino acid ion-binding pattern: **X*Y*Z*Y*X**Z** where XYZ are the ligands participating in metal ion coordination (EF-Hand structural reviews: (Ikura, 1996; Lewit-Bentley and Rety,

2000)). The underlying mechanism by which EF-hand sensor proteins transduce their signal is by a large change in conformation following calcium binding, altering their interaction with downstream effector proteins.

1.2 S100 proteins

S100 proteins are a major EF-hand family subgroup with approximately 19 members. S100 proteins are so named after their biochemical property of being soluble in 100% ammonium sulphate (S100 fraction). The first member of this group, S100B, was identified in the S100 fraction of bovine brain homogenate (review (Donato, 2001)). Proteins of this family show a relatively tissue-specific distribution pattern. For example S100A1 is highly expressed in cardiac tissue and S100B is highly expressed in neuronal tissue. A summary of the tissue distribution and putative functions of the S100 family is shown in Table 1.1. The majority of S100 family members are clustered on chromosome 1 in humans and chromosome 3 in mice. Following the discovery of the chromosomal organisation of the S100 family members, a nomenclature based on the order in which they are found in the human chromosome was suggested and generally adopted in the late 1990s (Ridinger et al., 1998; Schafer et al., 1995). Genomic analysis of the S100 family has indicated they are absent in *Arabidopsis thaliana, Drosophila melanogaster, Caenorhabditis elegans* and *Saccharomyces cerevisiae*. The most evolutionary primitive organism to express any S100 protein is *Squalus acanthius* (Spiny dogfish) from the *Chondricthyes* class (Sharks, Skate and Rays). The protein expressed by this organism is most closely related to S100A1, indicating this may be the ancestral member of the S100 family (Ravasi et al., 2004). The S100 family demonstrate 50% similarity between members at the

Human S100 Family Member	Ortholog in Mouse?	Tissue Distibution According to Swiss-Prot Database (Human)	Putative Functions (Human and/or Mouse)	References for putative functions
S100A1	Yes	Highly prevalent in heart, also found in skeletal muscle and brain	Modulates cardiac calcium signalling and stimulates Ca^{2+} induced Ca^{2+} release.	Most et al., 2004; Most et al., 2003; Treves et al., 1997
S100A2	Yes	Subset of epithelial cells including human mammary epithelial cells and keratinocytes	Chemoattracts eosinophils. Regulates F-actin-tropomyosin interaction. Inhibits tumour progression	Gimona et al., 1997; Komada et al., 1996; Wicki et al., 1997
S100A3	Yes	Skin specific	None	
S100A4	Yes	Ubiquitously expressed	Promotes metastatic activity of tumour cells. Modulates cell migratory machinery	C'Naaman et al., 2004; Kim and Helfman, 2003; Taylor et al., 2002; Wang et al., 2005
S100A5	Yes	Kidney	None	
S100A6	Yes	Ubiquitous	Regulates cell-cycle progression	
S100A7	Yes	Fetal ear, skin, tongues, highly up-regulated in psoriatic epidermis	Chemoattracts lymphocytes. Anti-microbicidal.	Glaser et al., 2005; Jinquan et al., 1996
S100A8	Yes	Myeloid cells	Chemoattractant. Anti-microbicidal and apoptosis inducing function in complex with S100A9. Regulates neutrophil oxidase activity and arachidonic acid transport in complex with S100A9.	Cornish et al., 1996; Kerkhoff et al., 2005; Kerkhoff et al., 2001; Steinbakk et al., 1990; Yui et al., 1997

Human S100 Family Member	Ortholog in Mouse?	Tissue Distibution According to Swiss-Prot Database (Human)	Putative Functions (Human and/or Mouse)	References for putative functions
S100A8	Yes	Myeloid cells	Chemoattractant. Anti-microbicidal and apoptosis inducing function in complex with S100A9. Regulates neutrophil oxidase activity and arachidonic acid transport in complex with S100A9.	Cornish et al., 1996; Kerkhoff et al., 2005; Kerkhoff et al., 2001; Steinbakk et al., 1990; Yui et al., 1997
S100A9	Yes	Myeloid cells	Chemoattractant. Anti-microbicidal and apoptosis inducing function in complex with S100A9. Regulates neutrophil oxidase activity and arachidonic acid transport in complex with S100A9.	Kerkhoff et al., 2005; Kerkhoff et al., 2001; Ryckman et al., 2003b; Steinbakk et al., 1990; Yui et al., 1997
S100A10	Yes	Connective and epithelial tissues	Interacts with Annexin II. Forms part of cornified epithelium.	Broome et al., 2003; Eckert et al., 2004; Waisman, 1995
S100A11	Yes	Haematopoetic and reproductive tissues (highly prevalent in sertoli cells)	Interacts with Annexin I. Forms part of cornified epithelium.	Broome et al., 2003; Eckert et al., 2004; Seemann et al., 1996

Human S100 Family Member	Ortholog in Mouse?	Tissue Distibution According to Swiss-Prot Database (Human)	Putative Functions (Human and/or Mouse)	References for putative functions
S100A12	No	Monocytes and lymphocytes	RAGE ligand	Hofmann et al., 1999
S100A13	Yes	Heart and skeletal tissue	Participation in fibroblast growth factor-1 release	Mouta Carreira et al., 1998
S100A14	Yes	Highly prevalent in colon, moderate levels in thymus, kidney, liver and lung.	None	
S100A15	No	Unknown	None	
S100B	Yes	Highly prevalent in brain	Modulation of neuronal calcium signalling. Mediates neurite outgrowth	Dyck et al., 2002; Huttunen et al., 2000; Nishiyama et al., 2002; Xiong et al., 2000
S100P	Yes	Placenta	None	
S100Z	Putative sequence	Spleen and leukocytes	None	

Table 1.1 Summary of S100 family members showing site of expression and putative functions if known.

Sites of expression according to Swiss-Prot database accessed via www.genecards.org. Table adapted from (Donato, 1999; Marenholz et al., 2004).

amino-acid-level, although their DNA sequence similarity is less. The regions of greatest divergence between family members are in the non-coding regions indicating a potential role for these regions in tissue specific control of expression (Zimmer et al., 1996).

The gene structure of S100 proteins are highly conserved in humans and rodents, consisting of 3 exons, with the coding sequence beginning in exon 2 and ending in exon 3 (figure 1.1) (Zimmer et al., 1996). The basic structural unit of the S100 protein is a symmetrical unit comprising of two EF-hand domains joined by a flexible linker (figure 1.1). Most S100 proteins generally exist as dimers, with the formation of homodimers being the most common stoichometry. S100 proteins are defined by the presence of an atypical N-terminal EF-hand domain consisting of 14 rather than 12 residues. Typically the conformational change in the EF-hand induced by calcium binding is small in the N-terminal EF-hand and more dramatic in the C-terminal motif. The hydrophobic patch revealed by calcium binding to the S100 protein is relatively shallow and an S100 dimer typically presents two symmetrically opposed hydrophobic zones. It is these hydrophobic pockets that appear to allow interaction of the S100 protein with its target (Bhattacharya et al., 2004).

In addition to their ability to bind calcium, S100 proteins are also reported to bind other divalent cations including zinc and copper. The site of binding has been shown to be near the dimer interface surface in the crystal structure of S100A7, S100B and S100A12. (Recent structural data for S100 reviewed in (Bhattacharya et al., 2004)). The specificity of their effector function is thought to be provided primarily by their distinct tissue specific expression and sub-cellular localization.

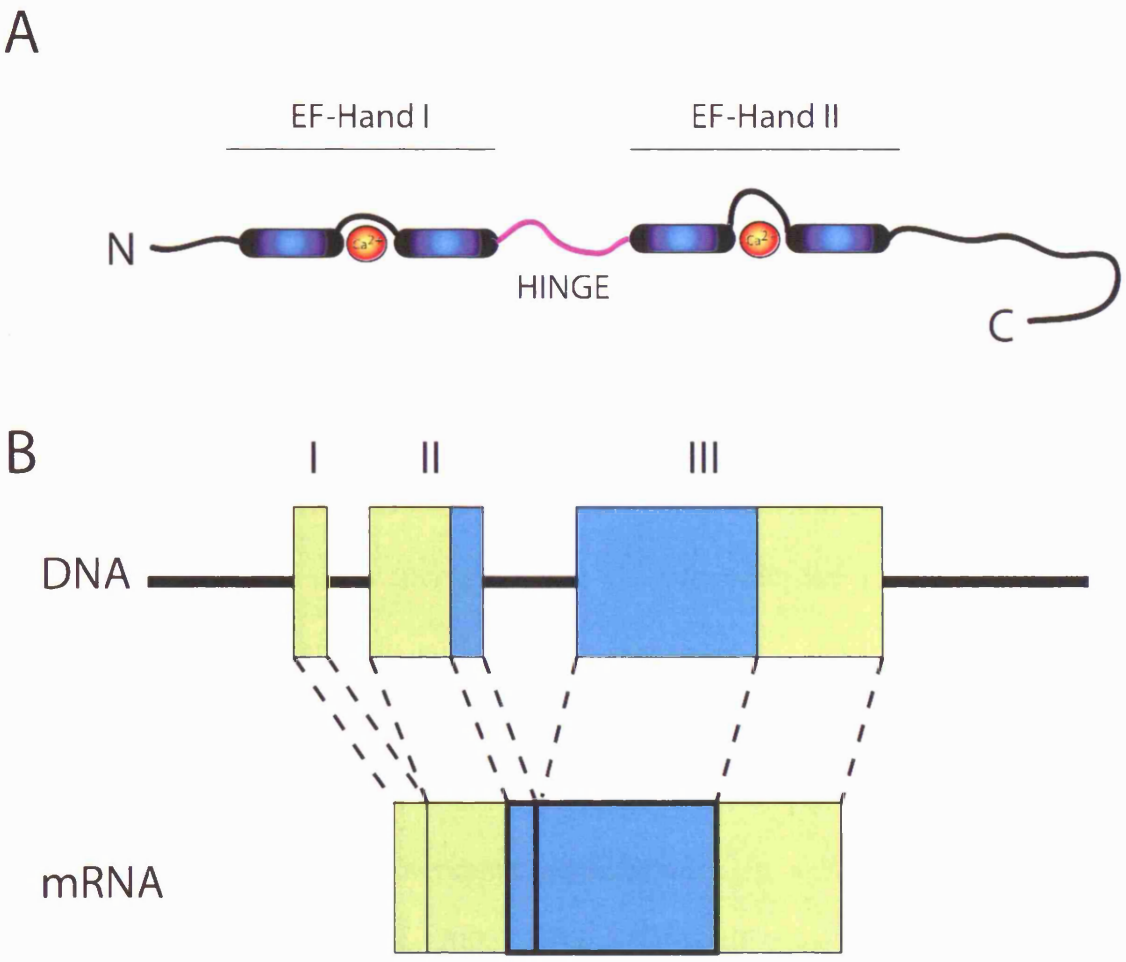

Figure 1.1 S100 protein and gene structure

A: General structure of S100 proteins showing the two EF-hand motifs, with EF-hand II having an extended calcium binding loop.

B: Typical S100 protein gene structure, with the boxes showing the three exon regions and the blue regions indicating the coding sequences. The corresponding mRNA structure is also shown.

1.2.1 S100 null animals

Numerous functions have been associated with S100 proteins. Much of this evidence comes from *in vitro* studies and provides a broad spectrum of possible functions many of which seem to have no defined mechanism of action. To date several S100 null animals have been produced in order to address the function of these proteins in an *in vivo* biological system. The majority of these transgenic animals have been viable and fertile, showing no gross abnormalities (a summary of the S100 null animals published to date can be found in Table 1.2). Only S100A8 has been shown to have a non-redundant function in development to date. The S100A8 null mice are lethal at embryonic day 11.5, possibly implying a role in maternal-foetal interaction (Passey et al., 1999). S100A1 is expressed at high levels in cardiomyocytes. S100A1 null mice have a lesion in the calcium response to β-adrenergic stimulation in cardiomyocytes and show lack of compensation for increased cardiac work in a model of acute hemodynamic stress (Du et al., 2002). The S100B null mice show enhanced calcium transients in response to caffeine in astrocyte cell cultures (Xiong et al., 2000). In addition these mice show an enhanced reactivity in a model of experimental epileptogenesis where seizures are induced by electrical stimulation of the amygdala, a process known as kindling (Dyck et al., 2002). The S100A4 null mice have shown an increased susceptibility to spontaneous tumour formation (Grum-Schwensen et al., 2005). S100A11 null animals are normal, viable and fertile showing no abnormalities to date in the cells that demonstrate the highest basal expression of this protein, sertoli cells (Mannan et al., 2003).

S100 Family Member	Phenotype	Reference
S100A1	Decreased cardiac contractility and increased susceptibility to haemodynamic stress *in vivo*	Du et al., 2002
S100A4	Spontaneous tumour formation	C'Naaman et al., 2004
S100A4	Decreased engraftment of syngeneic tumour cell-line	Grum-Schwensen et al., 2005
S100A8	Embryonic lethal	Passey et al., 1999
S100A9	Decreased chemoattractant-induced calcium signalling *in vitro*	Hobbs et al., 2003
S100A9	Altered neutrophil migration *in vitro*	Manitz et al., 2003
S100A11	No obvious phenotype	Mannan et al., 2003
S100B	Enhanced memory function in *in vivo* behavioural tests	Nishiyama et al., 2002
S100B	Enhanced epileptogenesis in an *in vivo* kindling model	Dyck et al., 2002

Table 1.2 Summary of S100 family knockout mice

Adapted from (Marenholz et al., 2004).

1.2.2 S100A9

S100A9 is of considerable interest to leukocyte biologists by nature of its extraordinarily high expression in neutrophils, constituting 40% of neutrophil cytosolic protein in its dimeric form with S100A8 (Edgeworth et al., 1991). Originally identified in a number of studies and given a variety of names including "the cystic fibrosis antigen" (CFA), "migration inhibitory factor-related protein 14 (MRP-14), p14, calgranulin A and L1 light chain amongst others (reviewed (Hessian et al., 1993)). Cloning of the S100A9 cDNA revealed these proteins to be the same entity and latterly it has been given the name S100A9 according to the new nomenclature of these proteins. Uncharacteristically for S100 proteins, S100A9 exists as a hetero-, rather than homo-, dimer bound to another family member, S100A8. The stochiometry of this complex was evaluated by immuno-affinity chromatography and complexes of 1:1 S100A8:S100A9 were found in human granulocytes and monocytes along with higher order complexes (Edgeworth et al., 1991). Further evaluation of the dimer formation revealed that the most favourable conformational arrangement of S100A8/9 was as a 1:1 heterodimer, with other S100A9/A9 or S100A8/A8 homodimeric complexes not demonstrating the unique interface complementarities of the heterodimer (Hunter and Chazin, 1998). There are several reports of higher order S100A8/9 complexes with the formation of calcium-induced tetramers being the most recently reported (Teigelkamp et al., 1991; Vogl et al., 1999). Yeast two-hybrid analysis also revealed the heterodimer to be the preferred conformation for the human proteins with only the murine

homologs showing homodimerization (Propper et al., 1999). The C-terminus was shown to have an important role in dimer formation in that study (Propper et al., 1999). The relative importance of the C-terminus in dimer formation was not confirmed in later deletion studies that showed mutation of both the C- and N-termini of S100A9 did not prevent dimer formation with S100A8 in the human system (Hessian and Fisher, 2001). The crystal structure of S100A8/9 complex has been recently released and is shown in Figure 1.2.

The murine system is often used as a model to evaluate the function of proteins and the results obtained applied to the human system. Comparison of the murine and human homologs of S100A9 has revealed that both murine S100A9 and S100A8 share 59% and 64% nucleotide identity with the human proteins. At the protein level 59% identity is reported, with the most conserved areas being the calcium binding motifs and the most divergent the C-termini (Lagasse and Weissman, 1992). Biochemical analysis of murine S100A9 indicated that it appears to be the homolog of the human protein and is expressed at similar levels to the human protein in murine granulocytes (Nacken et al., 2000).

Phosphorylation of human S100A9 has been reported following ionomycin treatment of both monocytes and neutrophils. The site of this phosphorylation was shown to be the penultimate amino acid in the C-terminus of S100A9 (Edgeworth et al., 1989). Phosphorylation of S100A9 also occurs in response to FMLP and PMA (Bengis-Garber and Gruener, 1993; Guignard et al., 1996). The phosphorylation of murine S100A9 has never been published and indeed the C-terminal phosphorylation site described in the human protein is not conserved in the murine protein (E. McNeill - data not shown).

A

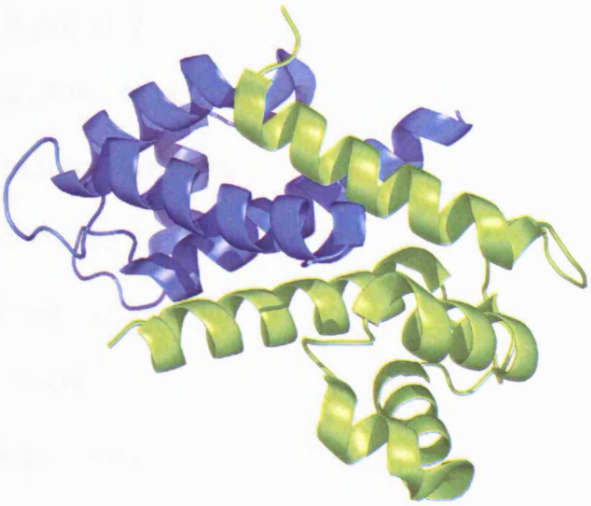

B

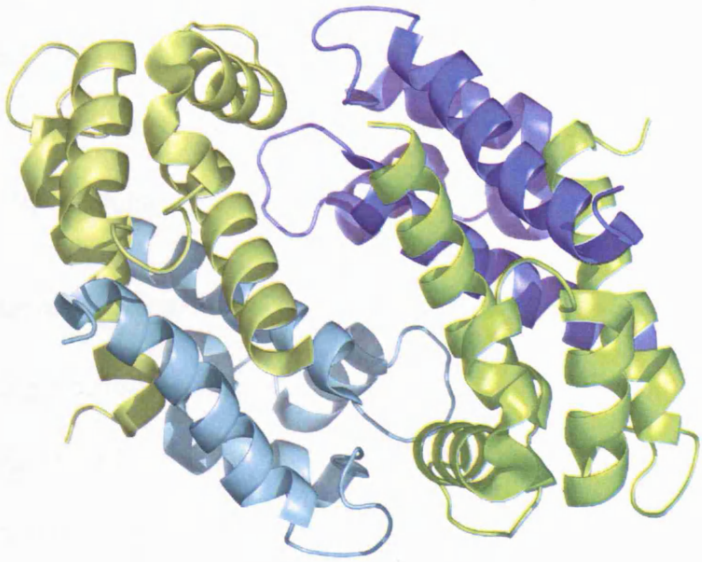

Figure 1.2 Crystal structure of S100A8/9 as a heterotetramer at 1.8A resolution

Data from RCSB protein databank entry IXK4 (http://pdbbeta.rcsb.org/pdb). 1.8Å Structure released 15th October 2005, as yet unpublished. Authors: Brueckner, F.N.A., Skerra, A., Korndoerfer, I.P. Stuctural diagrams produced by Dr Rebecca Kirk (IMP Vienna) using PyMOL software (DeLano, 2004). S100A9 shown in green, S100A8 shown in blue. **A:** S100A8/9 dimer crystalised as a alpha helical heterodimer. The predicted biological entity is of a dimer of dimers **(B)**.

1.2.3 S100A8/9 expression

S100A8/9 is primarily expressed in neutrophils and monocytes. Stratified squamous epithelia of the tongue, oesophagus and buccal cells and cells of the hair follicle also express this protein in healthy individuals (Brandtzaeg et al., 1987; Schmidt et al., 2001; Wilkinson et al., 1988). A more widespread expression profile for the heterodimer occurs during disease, in particular by hyper-proliferative epithelial cells and in squamous cell carcinomas of skin and lung (Wilkinson et al., 1988). Expression by epithelial cells during inflammatory conditions is also frequently reported. Human epithelial keratinocytes have been shown to express S100A8/9 during conditions including psoriasis, lupus erythematosus and atopic dermatitis (Gabrielsen et al., 1986; Kunz et al., 1992; Saintigny et al., 1992). A subset of human macrophages express S100A8/9 in inflammatory and infective conditions such as rheumatoid arthritis and pneumonia (Odink et al., 1987) (Buhling et al., 2000).

1.2.4 Subcellular localisation

In resting neutrophils S100A8/9 has a cytosolic localization and treatment with activating stimuli such as zymosan causes the protein to move to the membrane, illustrated by cell fractionation experiments (Lemarchand et al., 1992). Recent studies have demonstrated the membrane localisation of S100A8/9 to be in detergent insoluble lipid rafts (Nacken et al., 2004). In human monocytes the protein complex translocates completely from the cytosol to the cytoskeletal and vimentin-containing structures following treatment of the cell with elevated calcium concentrations (Roth et al., 1993). This movement occurs in these cells following treatment with the calcium ionophore ionomycin (Burwinkel et al.,

1994). The preferential translocation of phosphorylated S100A9 to the membrane and cytoskeletal fraction of monocytes has been suggested (van den Bos et al., 1996). An association of S100A9 with the microtubule system and the secretion of these proteins under these circumstances are reported (Rammes et al., 1997).

Similarly in keratinocytes expressing S100A8/9, a calcium dependent association with the vimentin cytoskeletal fraction occurs (Goebeler et al., 1995).

1.2.5 S100A8/9 – putative functions

As high extracellular concentrations of S100A8/9 are found in a range of inflammatory conditions, a range of extracellular functions as well as intracellular functions have been proposed. In particular faecal levels of the S100A8/9 complex are used as a non-invasive means of assessing inflammatory bowl disease (Fagerhol, 2000). High elevated serum levels of S100A8/9 complex were first reported in cystic fibrosis patients and the complex at that time was known as the Cystic Fibrosis Antigen (CFA). CFA was thought to be key in the pathogenesis of this disease prior to the identification of a mutation in the cystic fibrosis transmembrane receptor (CFTR), a chloride ion transporter, as being causative in this condition. CFA was eventually identified as being a small calcium binding protein of myeloid origin (Barthe et al., 1991; van Heyningen et al., 1985).

In many cases putative roles for a protein come from observations of diseases in which expression of the protein is absent – effectively human 'knockouts'. No condition of this type has been reported in humans, however, a condition comprising of massive elevations in serum S100A8/9 level has been described – hypercalprotectinaemia (Saito et al., 2002; Sampson et al., 2002).

This condition is associated with serum protein concentrations in the region of 1-6g/L compared to a standard level of less than 1mg/l. The condition manifests with serum zinc levels of 77-200μmol/l compared to basal levels of 11-18μmol/l. Whether the elevated levels of zinc are a cause or effect of the elevated S100A8/9 levels is unclear as the zinc was found bound to the protein complex. The patients suffer from recurrent infections and systemic inflammation, symptoms that can be attributed to elevated zinc levels.

In the following section proposed roles for S100A9 and other S100 proteins that could imply a role in neutrophil function will be discussed in context of an overview of the role of neutrophils in innate immunity. Neutrophil functions are summarised in figure 1.3.

1.3 Innate immunity

In order to survive in an environment with constant exposure to potentially harmful microorganisms, we must have a means to prevent our bodies being invaded to deleterious effect. The body is protected by two arms of the immune system the evolutionarily ancient innate immune system and the more recent adaptive immune system. The innate immune system is the body's first line of defence against pathogens and is responsible for protecting the body against the majority of potentially dangerous microbial insults. The innate immune system consists of both the physical barriers of the epithelial surfaces, that act to stop pathogenic microorganisms adhering to and entering the body, and cell-mediated immunity mediated by phagocytic leukocytes such as macrophages and neutrophils. These cells are capable of recognising pathogens, engulfing and

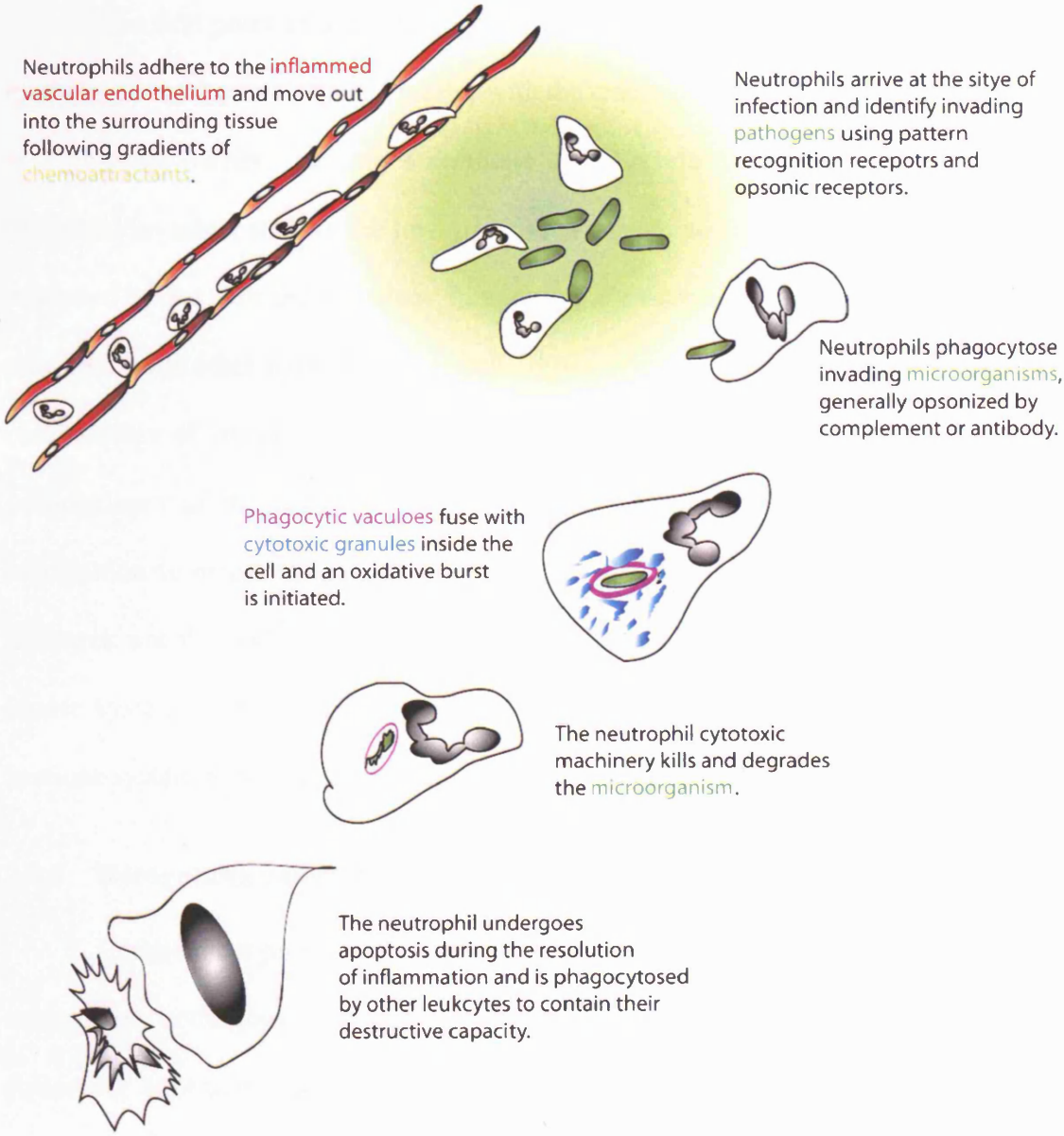

Figure 1.3 General scheme of neutrophil function

destroying them whilst at the same time producing chemical signals to activate the inflammatory response and stimulate the adaptive immune system.

The first point of protection against pathogens is the continuous surface epithelium that forms a physical barrier with the external world. As well as acting as a physical barrier, the body's epithelia act to produce chemical barriers to microbial invasion, such as the low pH of the stomach and antibacterial peptides produced by the skin and intestine. In addition, the normal gut flora compete for nutrients with other pathogenic bacteria, thus preventing their growth. These mechanisms of immunity require no specific recognition of pathogens. The cellular arm of the innate immune system requires a method of pathogen recognition to direct their cytotoxic potential in a focused manner against the pathogen not the body itself. One of the first lines of activation of the cellular innate system is the complement cascade. (Basic core elements of the innate immune system reviewed in (Beutler, 2004; Janeway and Medzhitov, 2002))

1.3.1 Recognising pathogens

Complement proteins circulate the body in blood and tissue fluid. The C3 component undergoes a constant low-rate hydrolysis into C3a and C3b and following adhesion of C3b to a pathogen surface binds to factor B in blood allowing recognition and cleavage by factor D cleavage to form the C3 convertase complex. The C3 converatse converts more C3 into C3a and C3b allowing large quantities of C3b to bind at high density to the microorganism surface allowing recognition by complement receptors on leukocytes. As a result the bacteria are opsonized and can be recognised and phagocytosed by cells of the innate immune system. In addition the complement pathway can also assemble the bactericidal

pore forming complement complex that punctures bacterial membranes, and also produces the anaphylatoxins C3a, C4a and C5a. These attract the cellular component of the innate immune system to the site of infection. (Complement function reviewed in (Fujita, 2002)).

Another way in which cells recognise invading microbes is by ligation of the Toll like receptors (TLRs). This family has been the subject of intense investigation in recent years since their identification. TLRs were identified as mammalian homologs of a drosophila protein crucial in allowing these flies to sense fungi. There are ten TLRs in humans and nine TLRs (along with two additional paralogs) in mice. These cellular receptors are thought to be the major mechanism by which mammals sense microbes. The TLRs act as Pattern Recognition Receptors (PRRs), receptors that recognise conserved Pathogen Associated Molecular Patterns (PAMPs). The identification of TLRs shows that PAMPS are specific molecules that are generally unique to microbes. The first to be identified in humans was TLR4, which recognises LPS, a heat stable bacterial wall component. LPS had been known for more than 100 years as a cause of fever and potentially fatal septic shock. In addition to the TLR family other PRRs such as Mannose Binding Lectin and f-Met-Leu-Phe Receptor (FMLP receptor) recognise terminal mannosyl residues and formylated peptides originating from bacteria. (Pattern recognition reviewed in (Beutler, 2004; Gordon, 2002; Janeway and Medzhitov, 2002))

1.3.2 The leukocytes of the innate immune system

The first cells to be recruited to the site of infection are neutrophils. Neutrophils are short-lived polymorphonuclear leukocytes, also known as

granulocytes. These have a half-life of around 6 hours in the circulation before undergoing apoptosis and are the most abundant leukocyte in blood (although to a lesser degree in mice). Neutrophils are specialized to rapidly take up microbes by phagocytosis. They have an artillery of cytotoxic machinery to kill and degrade the pathogen once it has been phagocytosed. They are capable of producing an oxidative burst and contain numerous granules that contain a host of anti-microbial peptides and protease enzymes. It is the function of these cytotoxic leukocytes that is the principle focus of study in this thesis. (Review of neutrophil biology (Witko-Sarsat et al., 2000).

Another type of leukocyte that is important in the early phase of an innate immune response is the macrophage. Macrophages are a mature differentiated form of monocytes, collectively known as mononuclear phagocytes. Monocytes are formed in the bone marrow and circulate around the body in the blood and become resident macrophages in most tissues. They act as sentinels recognising invading pathogens by opsonic receptors or other pathogen recognition receptors and produce a range of cytokines that attract other members of the innate and adaptive immune system to the affected area.

1.3.3 Neutrophil development

The bone marrow is the principle site for the production of blood cells, termed haematopoiesis. Leukocytes and erythrocytes are derived from multi-potential pluripotent stem cells. Neutrophils arise from these stem cells via the "Common Myeloid Progenitor" (CMP) and "Granulocyte-Monocyte Precursor" (GMP) in a process termed granulopoiesis. Neutrophils are a terminally differentiated cell type and do not under go further cell division. As a result of

their short life span and in order for the body to respond rapidly to an infection, the bone marrow must contain a large reserve of neutrophils to meet the challenge of an acute infection. The granulocyte/macrophage lineage is characterised by the expression of FcγRII/III during development (Myeloid development summarised in (Imhof and Aurrand-Lions, 2004)). *In vitro* Granulocyte-Colony Stimulating Factor (G-CSF) and Granulocyte/Macrophage Stimulating Factor (GM-CSF) have been shown to promote the growth of bone marrow cell colonies containing neutrophils in methylcellulose cultures. During the maturation of neutrophils, the primary granules arise first during the myeloblast to promyelocyte stage. At this point cell division ceases and the secondary and tertiary granules arise. Later markers of neutrophils maturation include lactoferrin and the Gr-1 surface marker. (Neutrophil development reviewed in (Friedman, 2002; Ward et al., 2000; Witko-Sarsat et al., 2000))

The study of granulopoiesis has received interest in recent years in terms of elaborating the transcription factors involved and their activation by factors such as GM-CSF with the objective of understanding the generation of myeloid leukaemias. A scheme of required transcription factors for the production of the GMP shows a role for induction of high levels of PU-1 via a C/EBP dependent or independent pathway. Commitment to the granulocyte lineage requires continued expression of PU-1 and C/EBP along with signalling via the Retinoid acid receptor (reviewed in (Friedman, 2002; Ward et al., 2000)).

The control of neutrophil release from the bone marrow has recently been shown to occur via an axis of increased stimulation of the neutrophil mobilising chemokine receptor CXCR2 and is required to overcome the effects of the bone marrow homing chemokine receptor CXCR4 (Martin et al., 2003a). It is assumed

that via this chemokine-induced signalling, the number of neutrophils circulating in the blood is tightly controlled.

1.3.4 A role for S100A9 in neutrophil development?

The expression of S100A9 in mature human blood neutrophils has been recognised for a number of years, but the precise point at which it arises in neutrophil development is less clear. Initial studies of the expression of S100A9 mRNA by HL-60 cells (a human leukaemic granulocyte progenitor cell-line) showed that S100A9 mRNA was induced when the HL-60 was stimulated to differentiate to either a monocytic or neutrophilic phenotype (Lagasse and Clerc, 1988). This study was extended to look at the expression of S100A8 and S100A9 in murine haematopoiesis. Expression of S100A9 was shown to occur at sites of haematopoiesis in both foetal and adult mice. S100A9 expression was shown to be coincident with expression of the Gr-1 and Mac-1 myeloid markers in both bone marrow, foetal liver and yolk sac at day 11 of gestation (Lagasse and Weissman, 1992). Confirmation of the expression of S100A9 by granulocytes and monocytes and possibly myelo-monocytic precursors was provided by examination of the morphology of bone marrow cells staining positively for S100A8/9 expression (Goebeler et al., 1993). A survey of alveolar, resident peritoneal and thioglycollate-elicited macrophages showed them all to be S100A8/9 negative (Goebeler et al., 1993). This implies the expression of S100A8/9 in the monocyte lineage expression is limited to the non-terminally differentiated cell types.

S100A8/9 dimer has been implicated in modulating the activity of casein kinase I and II. These enzymes phosphorylate topiosomerase I and RNA

polymerases I and II. That S100A8/9 can potentially modulate the activity of parts of the transcriptional machinery could highlight a role for them in the differentiation or commitment of cells to the myeloid lineage (Murao et al., 1989).

1.4 Chemokines and the leukocyte adhesion cascade

The correct, controlled trafficking of leukocytes to the site of an infection is an essential facet of immune system function. When this process becomes uncontrolled pathological inflammatory conditions can develop. In order to perform their key function of protecting the body from infection neutrophils must be able to leave their site of development/circulation and follow signals to wherever an infection is present. These directional signals are provided by chemokines and other chemoattractants, which provide both activating and directional information to leukocytes. To do this they must be able to follow an orchestrated set of signals that direct them to the correct location. If this process fails and the neutrophils do not reach the site of infection, as in the case of disorders such as Leukocyte Adhesion Deficiency 1 (LAD1), then infections are not controlled and can be life-threatening. Similarly if the neutrophils are targeted to the wrong location they have the capacity to cause great damage to the body due to their inflammatory potential. (Neutrophil disorders reviewed (Lakshman and Finn, 2001)).

1.4.1 Chemoattractants and chemotaxis

Chemoattractants can be broadly broken up into 3 distinct groups: 'classical chemokines', other chemoattractant substances produced by the body and substances produced by invading microbes.

Classical chemokines are small (8-10 kDa) constitutive or inducible proteins causing homeostatic lymphocyte trafficking to secondary lymphoid organs or secreted by cells at the site of infection/inflammation respectively. These proteins have defined C-terminal cysteine motifs. They are sub-grouped according to this motif as CXC, CC, C or CX_3C chemokines and bind to CXCR, CCR, XCR and CX_3CR receptors respectively. These are seven-transmembrane spanning G-protein coupled receptors that activate cytosolic calcium elevations through a phospholipase C coupled mechanism. (Classical chemokines reviewed in (Rossi and Zlotnik, 2000)).

The body also produces small protein and lipid mediators that act as chemoattractants for leukocytes. These include C5a, a part of the Complement cascade, which is produced following activation of this protective serum protein mechanism. In addition the lipid Platelet Activating Factor (PAF) produced by activated endothelial cells, and Substance P, produced by sensory neurones also act as non-classical chemoattractants. These non-classical host produced chemoattractants also ligate G-protein coupled seven transmembrane spanning receptors.

The most comprehensively studied chemoattractant produced by invading bacteria is the formylated peptide formyl-methionyl-leucyl-phenylalanine (FMLP). This is a potent chemoattractant for neutrophils and ligates a G-protein coupled seven transmembrane spanning receptor on these cells.

Chemoattractants activate a host of signalling pathways downstream of activation of their receptors. In general these receptors produce a range of biologically active lipid mediators such IP_3 and diacylglycerol (DAG) and products of the enzyme phosphoinositide-3-kinase (PI-3K) (Chemoattractant

signalling in neutrophils reviewed in (Niggli, 2003)). In addition they activate various protein kinase families and small Rho-family GTP-binding proteins. Whilst the role of Rho-family proteins appears to have a clear role in cell morphology changes associated with a migratory phenotype, the role of the lipid mediators is more unclear (reviewed in (Vicente-Manzanares and Sanchez-Madrid, 2004) and (Wu, 2005)). The most perplexing of these is the role of the IP_3 mediated calcium signal. IP_3 is generated by phospholipase C (PLC). Studies of PLCβ2/3 null mice show that these molecules are entirely responsible for chemoattractant induced calcium signalling in murine neutrophils. However, in an *in vivo* model of peritonitis the chemotaxis of the PLCβ2/3 null neutrophils was unimpaired (Li et al., 2000b; Wu et al., 2000). This seems to imply that both the directional and migratory aspects required for chemotaxis do not require this calcium signal. No global elevations or persistent gradients of calcium were found in neutrophils migrating on glass towards an FMLP stimulus, again finding no correlation of calcium signalling with chemotaxis (Laffafian and Hallett, 1995). Indeed the ability of neutrophils to produce a gradient of calcium within the cell, which would be required to provide a directional signal, is questionable given the release of calcium following chemoattractant stimulation has been shown to come from a central store within the cell (Pettit and Hallett, 1998). (The potential role of calcium in chemotaxis is reviewed in (Tian et al., 2004)).

1.4.2 Leukocyte adhesion and migration

In order to circulate around the body in the blood stream in the absence of inflammatory stimuli, neutrophils need to be kept in a non-adhesive state. This circulating pool of neutrophils provides a reservoir of cells for a rapid response to

a danger signal. The neutrophil receives this signal in the post-capillary venules where the slower flow rate allows the cell to interact with the activated endothelium. The process of leukocyte adhesion is summarised in figure 1.4. The interaction of selectins and their glycoprotein ligands mediate the initial tethering and rolling of the neutrophils along the activated endothelium. P-selectin can be rapidly mobilised to the endothelial cell surface and interacts with P-selectin glycoprotein ligand-1 (PSGL-1) expressed on neutrophil microvilli. This interaction is strengthened by the interaction of E-selectin, expressed with slightly less rapid kinetics by the activated endothelium, with PSGL-1. The neutrophils themselves express L-selectin constitutively, and the binding capacity of this ligand is greatly enhanced following leukocyte activation. This molecule interacts with glycoprotein ligands upregulated by the endothelium. These tethering interactions slowdown the neutrophil allowing interaction with activating and directional stimuli such as chemokines and other chemoattractants immobilised on the endothelium (Neutrophil adhesion and activation reviewed in (Ley, 2002; Witko-Sarsat et al., 2000)).

Following selectin binding and chemoattractant exposure neutrophil β2 integrins undergo an increase in binding capacity as a result of "inside-out" signalling that leads to clustering of the integrins and a conformational change to a high-affinity state. This disengagement of the integrin "safety switch" allows a transition to firm interaction with the endothelium. In particular Leukocyte function-associated antigen-1 (LFA-1) (αLβ2 or CD11a/CD18) binds to the inflammation-induced ligand Intercellular adhesion molecule-1 (ICAM-1) or the constitutively expressed ICAM-2. The combination of chemokine activation and

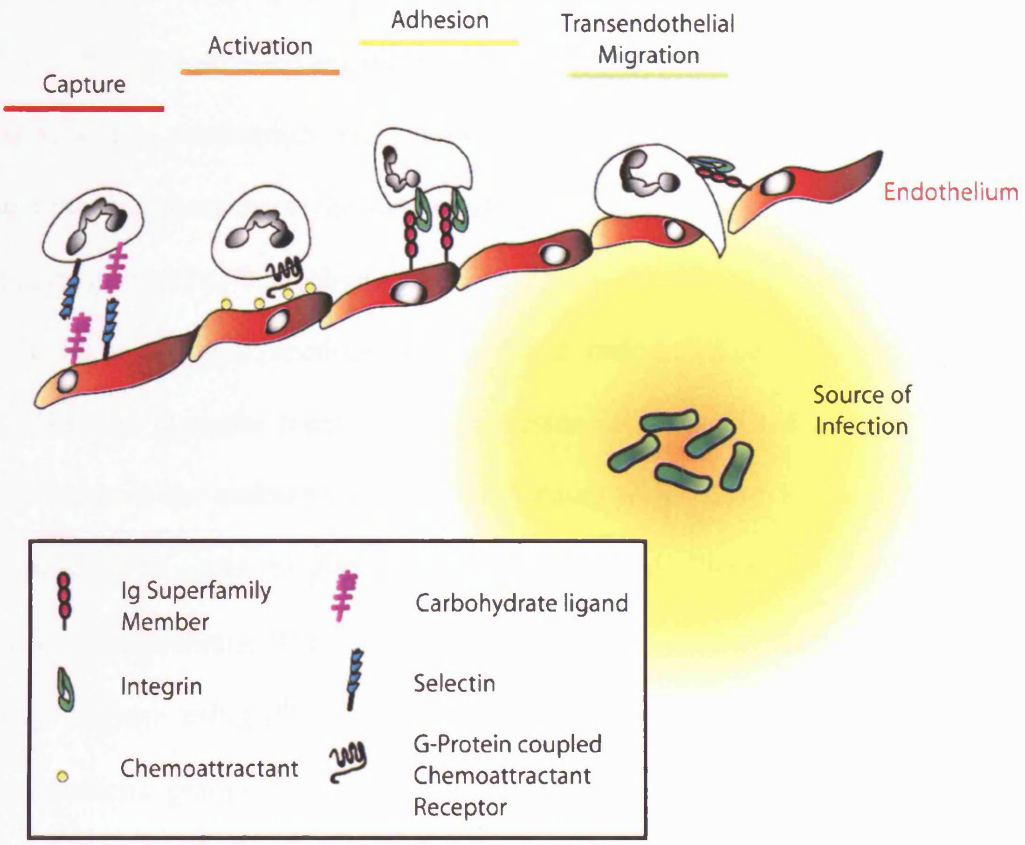

Figure 1.4 Leukocyte adhesion cascade

In order to migrate to the site of infection neutrophils first become tethered to the inflammatory endothelium. The tethering process occurs by binding interaction of selectins with their carbohydrate ligands. This process allows chemokine receptors on the neutrophil surface to bind chemokine immobilised upon the endothelial cells. Downstream signalling pathways from chemokine receptors cause an increase in the affinity and avidity of neutrophil β2 integrins increasing their binding to ICAM molecules allowing firm adhesion and shape change to occur. Neutrophils migrate along the endothelial wall to intracellular junctions where they extravasate using PECAM and JAMs. The cells migrate through the extracellular matrix following chemoattractant gradients by haptotaxis mediated by β1 integrins.

"outside-in" signals from the engaged integrin allows the neutrophils to spread on the vascular wall and gain a motile phenotype.

Having arrested on the vascular endothelium and received activating stimuli, the neutrophils must now extravasate out of the vessel into the surrounding tissues to the origin of the inflammatory stimuli. Neutrophil transmigration has been shown to occur most frequently at discontinuities in the endothelial cell tight junctions. Using Platelet/endothelial cell adhesion molecule-1 (PECAM-1) and/or Junctional cell adhesion molecule (JAM), neutrophils pass out between the endothelial cells with binding to PECAM-1 causing increased expression of $\alpha 6\beta 1$ integrin by the neutrophils and allowing passage across the basement membrane (Dangerfield et al., 2002). Once in the extracellular matrix they migrate using $\beta 1$, $\beta 2$ and $\beta 3$ integrin-ligand interactions to follow the chemotactic gradient to its source by haptotactic movement. (Extravasation reviewed in (Nourshargh and Marelli-Berg, 2005; Weber, 2003)).

1.4.3 The cytoskeleton in leukocyte migration

In order for leukocytes to undergo the rapid shape-changes and movement required for leukocyte recruitment and cytotoxic functions such as phagocytosis, they must be able to intricately re-organise their cytoskeleton. The cytoskeleton is an organised network of polymers consisting of actin microfilaments, microtubules and intermediate filaments. The most stable, un-dynamic of these are the intermediate filaments, which are primarily formed of vimentin in leukocytes. These seem to play a role in cell rigidity and structural integrity rather than in active cellular rearrangement during leukocyte migration (reviewed in (Vicente-Manzanares and Sanchez-Madrid, 2004)).

Microtubules are formed by uni-directional polymerisation, or nucleation, of αβ tubulin heterodimers to form hollow tubes. These tubes are dynamic, their length being controlled by a process of treadmilling. The interaction of dynesin and kinesin motor proteins with the microtubules allows the rapid transport of vesicles around the cell. As well as a role in cell migration, these filaments are also vital in cell division. In the migrating cell the microtubules organise with the microtubule organising centre behind the nucleus away from the direction of migration towards the trailing edge (Vicente-Manzanares and Sanchez-Madrid, 2004).

The cytoskeletal element that appears to have the most extensive role in leukocyte migration is actin. Monomeric actin nucleates to form micro-filaments by treadmilling. An array of proteins modulate this such as the ARP2/3 complex that bind to the filaments promoting further actin binding and conformational changes in the filament. In a polarised migratory leukocyte, rapid actin polymerisation occurs at the lamellipodia in coordination with actomyosin based contraction. Rear detachment of the cell requires actinomyosin contraction in the absence of actin fibre extension. (The involvement of the cytoskeleton in leukocyte migration reviewed in (Pettit and Fay, 1998; Vicente-Manzanares and Sanchez-Madrid, 2004))

1.4.4 S100 protein association with the cytoskeleton

There are numerous reports of different S100 family members interacting with the cytoskeleton, which could translate to playing a role in cell migration in rapidly migrating cells such as the neutrophil. Some association of at least 10 of the 19 family members with the cytoskeleton seems to indicate a possible

conserved role for these proteins in cytoskeletal associated processes (review (Donato, 2001)). However, despite numerous S100 family members having an association with the cytoskeleton, there appears to be no consensus concerning mechanism of action or association with one particular part of the cytoskeleton. Also much of the data comes from *in vitro* biochemical studies, with the proposed functions not being demonstrated *in vivo*. For example both S100B and S100A1 have been described to cause the inhibition of microtubule formation by sequestration of tubulin, and to confer calcium sensitivity to preformed microtubules, yet other members of the family (S100A1, S100A6 and S100A4) apparently modulate tropomyosin activity (reviewed in: (Donato, 1999; Donato, 2001)).

With regard to S100A8/9, much of the evidence presented comes from *in vitro* studies alone or is descriptive rather than mechanistic. S100A8/9 has been shown to translocate to the plasma membrane and vimentin intermediate filaments in monocytes following the elevation of cytosolic calcium (Roth et al., 1993). This translocation is enhanced when S100A9 is phosphorylated (van den Bos et al., 1996), it should be noted that phosphorylation of murine S100A9 has never been reported. Indeed a "Phosphosite" search of the protein sequence for murine S100A9 shows the major human phosphorylation site at the C-terminal of the molecule is not conserved in the murine protein, although other probable phosphorylation sites are found in the primary structure of the protein (E. M^{c}Neill – data not shown). Following phorbol ester stimulation the S100A8/9 complex apparently translocates to microtubules in monocytes and macrophages ((Rammes et al., 1997)). Recent data has also shown that *in vitro* S100A9 is capable of

promoting tubulin polymerisation (Vogl et al., 2004). These putative roles for S100A8/9 could clearly translate to a role in cell migration.

S100A4 is associated with cancer metastasis, with its overexpression promoting metastatic ability in non-metastatic cell-lines (Levett et al., 2002). A transgenic over-expressing S100A4 mouse has also demonstrated a metastasis promoting activity (Ambartsumian et al., 1996). The mechanism of action is still unclear but S100A4 is found associated with myosin II and localises in the lamellipodia of migrating cells (Kim and Helfman, 2003). The ability of S100A4 to promote a migratory/metastatic phenotype can be reversed by co-transfection of S100A1, which has been shown to directly interact with S100A4 *in vivo* (Wang et al., 2005).

In addition to specific evidence of an interaction between S100 proteins and the cytoskeleton, any role of these proteins in calcium signalling or homeostasis could translate to a role in neutrophil motility. Cell motility is intimately linked with calcium signalling, with calcium necessary for both integrin function and for cytoskeletal reorganisation.

1.4.5 S100A8 and S100A9 in cell trafficking

S100 proteins are unusual in having both intracellular and extracellular roles assigned to them. S100A8 and S100A9 have both been described as being potent chemotactic agents for neutrophils being secreted in a novel "tubulin-dependent" process (Rammes et al., 1997; Ryckman et al., 2004). It is claimed non-oxidised recombinant murine S100A8 (also known as CP-10) is chemotactic to neutrophils, causing them to undergo F-actin polymerization and shape changes without de-granulation, calcium flux or oxidase activity (Cornish et al., 1996;

Devery et al., 1994; Lackmann et al., 1992). The chemotactic activity of CP-10 resides in the proteins "hinge-region" (Lackmann et al., 1993). CP-10 was identified as an S100 protein and is now recognised as the murine homolog of S100A8 (Lackmann et al., 1992). An interesting phenomena related to the function of this protein is its regulation by oxidation (Harrison et al., 1999). Upon oxidation, murine S100A8 was inactive in a chemotaxis assay and not able to recruit leukocytes *in vivo*. The chemotactic function of murine S100A8 is purely based on the action of recombinant protein independent of S100A9; S100A8 is induced in the absence of S100A9 in fibroblasts and macrophages (Rahimi et al., 2005; Xu and Geczy, 2000).

Recombinant human S100A8 and S100A9 have been shown to be chemotactic for neutrophils in a Transwell chemotaxis assay and in an *in vivo* air-pouch model of inflammation (Hobbs, 2003; Ryckman et al., 2003b). This activity in the air-pouch model was shown by the Ryckman publication still to be present in the C3H/HeJ endotoxin insensitive mice, showing this activity was not due to LPS contamination of the recombinant proteins but not in the Hobbs study and is therefore controversial. Blocking antibodies against S100A9 reduced infiltration in an LPS-stimulated air-pouch model of inflammation (Vandal et al., 2003). The release of S100A8/9 from neutrophils by a tubulin dependent process upon stimulation with monosodium urate crystals, was shown and hypothesised to provide a mechanism for leukocyte recruitment in gout (Ryckman et al., 2004; Ryckman et al., 2003a). Other than the chemotactic activity of S100A8 and S100A9, S100A7 is chemotactic for lymphocytes and neutrophils using a recombinant protein approach *in vitro* (Jinquan et al., 1996).

If S100A8 and/or S100A9 do indeed act as chemokines, then this would indicate a double role for these proteins in cell motility and chemotaxis, both acting within the cell on the cytoskeleton and as part of the chemical signalling program required for neutrophil recruitment. Another manner in which S100A8/9 may affect leukocyte recruitment is by binding to cell surface glycosaminoglycans on endothelial cells near to the site of inflammation (Robinson et al., 2002). This could provide a mechanism of presenting the S100A8/9 protein to carry out any extracellular roles. The association of the complex bound to the cell surface in proximity to extravasating leukocytes is strongly suggestive of a function in this process (Hessian et al., 1993). Antibodies against a carboxylated *N*-glycan motif present on the surface of endothelial cells, which is shown to bind S100A8/9, reduce the recruitment of neutrophils *in vivo* providing further suggestive evidence of a role for these proteins in leukocyte trafficking (Srikrishna et al., 2001). Treatment of endothelial cells with recombinant S100A9 has also been reported to cause a decrease in monolayer integrity and expression of pro-inflammatory mediators (Viemann et al., 2005). It should be remembered that S100 proteins are calcium binding proteins and the chelation of extracellular calcium causes a decrease in endothelial cell-cell adhesion.

Other than glycans, the Receptor for advanced glycation end-products (RAGE) has been shown to be a receptor for S100 family members including S100A12, S100A1 and S100B. Interaction of these proteins with RAGE regulates neurite out-growth following stimulation of RAGE expressing neurites with recombinant S100 proteins (Huttunen et al., 2000). S100A12 is highly homologous to S100A8 and S100A9 and is abundantly expressed in human neutrophils, but is absent in the murine genome (Fuellen et al., 2003; Fuellen et

al., 2004). S100A12 has been suggested to be central to pro-inflammatory functions mediated by RAGE. *In vitro* S100A12 was shown to cause cellular activation of various leukocytes. In models of colitis and footpad delayed type hypersensitivity a reduced inflammatory infiltrate was seen following treatment with a RAGE blocking antibody (Hofmann et al., 1999). However given the lack of S100A12 in the mouse, the ligand of RAGE in the *in vivo* assays is unclear, but has been postulated to be other S100 family members.

1.5 Neutrophil phagocytosis and microbial killing

Once a neutrophil has responded to a chemotactic stimulus and has arrived at the site of infection, it must then identify the invading microorganism and utilise its cytotoxic killing artillery. Neutrophils recognise pathogens using a variety of surface expressed receptors. Neutrophils predominantly use Fcγ receptors (FcγRIII/CD16 and FcγRII/CD32) or complement receptors (CR1/CD35 and CR3/CD11b/CD18) to recognise antibody or complement opsonized microorganisms. Intracellular signals downstream of phagocytic receptors act in concert with activating signals from chemoattractant receptors (eg FMLP receptor) and pathogen associated microbial-recognition pattern receptors (PAMPs) to cause cytoskeletal reorganisation and engulfment of the opsonized particle. This occurs by either the formation of a phagocytic cup or membrane protrusions that engulf antibody coated particles, or by a 'sinking' of complement opsonized particles into the cell. (Phagocytosis reviewed in (Stuart and Ezekowitz, 2005; Underhill and Ozinsky, 2002)). A small local release of calcium is reported upon complement-opsonized particle attachment followed by a larger global increase in cytosolic concentration resulting from calcium influx

(Dewitt et al., 2003). The global rise in calcium concentration was coincident with liberation of β2 integrin from cytoskeletal restraints, which was shown to be dependent on the activity of the calcium activated protease calpain (Dewitt et al., 2003).

1.5.1 Neutrophil granules

The phagocytosed particle sits in a phagocytic vacuole that undergoes fusion with neutrophil granules. Neutrophils contain several types of granule, the predominant types being the azurophilic and specific granules. The azurophilic, or primary granules contain myeloperoxidase (catalyses hydrogen peroxide mediated oxidation of halides, which are then thought to have anti-microbial activity), neutral proteases (cathepsin G, elastase and proteinase 3), defensins (small antimicrobial peptides) and lysozyme (capable of lysing bacteria) amongst other antimicrobial proteins. The majority of these proteins are maintained in an inactive state by binding to the highly cationic matrix in the acidic pH of these granules. The specific granules contain the greatest amount of lysozyme along with lactoferrin (copper and iron chelator). The membrane of the specific granules contains transmembrane proteins of the NADPH osidase required for oxidative burst formation (Neutrophil granule biology reviewed in (Faurschou and Borregaard, 2003; Witko-Sarsat et al., 2000)).

1.5.2 Neutrophil oxidase activation

The activation of the oxidase is important to host defence against bacteria and fungi. Patients suffering from Chronic Granulomatous Disease (CGD) illustrate this. CGD patients have a genetic mutation in one of the gp ^{PHOX} proteins that make up the NADPH oxidasethat cause the protein to be absent or

non-functional. As a result the patients have an increased susceptibility to infection (Neutrophil disorders reviewed in (Lakshman and Finn, 2001)).

The oxidative burst occurs as a result of activation of the multi-enzyme NADPH oxidase. This machinery consists of the catalytic core, membrane bound flavocytochrome b558, which is a heterodimer of $p22^{PHOX}$ and $gp91^{PHOX}$ proteins. This heterodimer is found in both the plasma membrane and in the membrane of neutrophil specific granules, before becoming incorporated in the wall of phagocytic vacuole upon granule/vesicle fusion. This portion of the oxidase machinery acts as a conduit for electron transfer from cytosolic NADPH to oxygen in the vacuole. To activate this process the flavocytochrome must interact with a complex of cytosolic proteins: $p40^{PHOX}$, $p47^{PHOX}$ and $p67^{PHOX}$. Deficiencies in all of these proteins (except the $p40^{PHOX}$) have been identified as varying causes of CGD. The interaction of the small GTPase Rac is vital in activating this system, with a patient with a dominantly negative mutation in RAC2 having a deficiency in superoxide production. The various components of NADPH oxidase machinery have different roles acting either directly as part of the catalytic machinery, or to target other members of the complex to the correct region (activation of the oxidase machinery reviewed in (Roos et al., 2003; Segal, 2005)):

$gp91^{PHOX}$ supports the electron transport chain in its entirety. The C-terminal region allows NADPH and FAD binding, whilst the N-terminal region is capable of haem binding allowing electron transport across the membrane into the vacuole.

$p22^{PHOX}$ has a high-affinity binding site for $p47^{PHOX}$ and allows stable docking of the cytosolic components with the $gp91^{PHOX}$ subunit.

$p67^{PHOX}$ binds both NADPH and rac and $p47^{PHOX}$ in high concentrations.

$p47^{PHOX}$ is phosphorylated by protein kinases causing a conformational change in the cytosolic complex of ^{PHOX} proteins allowing them to translocate to the membrane. Here it seems to stabilise the association of $p67^{PHOX}$ with the flavocytochrome by interaction with $p22^{PHOX}$.

$p40^{PHOX}$ appears to stabilize the interaction of $p47^{PHOX}$ and $p67^{PHOX}$ in the cytosol. Any other functions of this protein are as yet unclear.

The chemical reaction that occurs to produce superoxide radicals by this complex is essentially:

$$NADPH + 2O_2 \rightarrow NADP^+ + 2O_2^- + H^+$$

The electron transfer into the vacuole occur along the following electron transfer chain:

$$NADPH \rightarrow FAD \rightarrow 2\ Haem \rightarrow 2\ O_2$$

Once formed the superoxide molecule can react with protons, pumped in to the phagolysosome to compensate for the negative charge occurring following the introduction of the electrons, to form hydrogen peroxide. The phagolysosome contains the enzymes myeloperoxidase and catalase following granule fusion, these enzymes use hydrogen peroxide as a substrate either to produce hypochlorous acid or water. It has been reported that the pH of the phagolysosome does fall initially but after only 3 minutes begins to rise to neutral or slightly above. This observation lead to the identification of potassium channels playing a key role in microbial killing because if protons alone were responsible for normalising the electrogenic potential of the NADPH oxidase a more lasting dramatic decrease in pH would be seen. The activation of a potassium current, as a part of charge compensation, into the phagolysosome

prevents the pH dropping. The alterations in pH of the phagocytic vacuole allow the cytotoxic proteins of the azurophilic granules to be released from the granule matrix and the near neutral pH of the vacuole allows the activation of the neutral proteases. This ion flux system is further complicated by the presence of a chloride ion flux that also acts as a form of charge compensation ((Ahluwalia et al., 2004; Reeves et al., 2002; Segal, 2005)).

In recent years there has been some controversy over the relative importance of direct cytotoxic effects of oxidant species and its role in releasing and activation antimicrobial proteins from the fused granules. The importance of myeloperoxidase in antimicrobial killing has been illustrated by an increased susceptibility of MPO deficient mice to yeast infection (Aratani et al., 1999). Neutral protease deficient mice lacking elastase and/or cathepsin G show decreased survival following challenge with *S. aureus* or *C. albicans* (Reeves et al., 2002; Segal, 2005). This indicates that protease activity is necessary for the killing of some microorganisms and that in these cases oxidant species alone are insufficient for this purpose. The elegant proposition of Segal and colleagues is that the oxidase activates ion fluxes in the phagocytic vacuole that form an environment in which the antimicrobial proteins of neutrophil granules are designed to work. This model suggests a complex system of regulation to minimise the potential of these cytotoxic moieties to damage healthy tissue when released from the neutrophil (Segal, 2005).

1.5.3 A role for S100A9 in neutrophil oxidase activation?

There is a body of literature that appears to identify a key role for S100A9 in oxidase activation. It has been published that the S100A8/9 complex in

combination with arachidonic acid can enhance NADPH oxidase activity in a cell-free system of neutrophil membranes and cytosolic NADPH subunits (Doussiere et al., 1999; Doussiere et al., 2002; Kerkhoff et al., 2005). Its ability to do this has been linked to an ability to interact with $p67^{PHOX}$ and Rac-2. A role for arachidonic acid in activation of the oxidase has also been highlighted in a study where phospholipase A2 was deleted from a myeloid cell-line causing inactivation of the oxidase machinery (Dana et al., 1998). The oxidase activity could be restored by introduction of arachidonic acid into the system (Dana et al., 1998). Given the reported properties of S100A9 to bind arachidonic acid (Kerkhoff et al., 1999b; Siegenthaler et al., 1997; Sopalla et al., 2002) it seemed possible that it acted to supply arachidonic acid to the NADPH oxidase. The most recent publication on the phenomenon showed a decreased oxidase activity in NB4 cells (a myeloid progenitor cell-line that can be differentiated to a neutrophil phenotype by retinoic acid) treated with antisense RNA for S100A9 to block its production (Kerkhoff et al., 2005). In addition the kinetics of oxidant production by neutrophils from another independent line of S100A9 null mice were reduced. The mechanism of activity was hypothesised to be that S100A9 supplies arachidonic acid to the NADPH causing a conformational change in the flavocytochrome b558 molecule that then favours NADPH binding.

A more indirect role for the calcium sensor S100 proteins could be in control of oxidase activity via alteration of calcium signalling. Work dissecting calcium signals associated with phagocytosis showed, using oxidant-sensitive zymosan particles, that the activation of the oxidase upon phagocytosis is coincident with a global calcium signal (Dewitt et al., 2003).

1.5.4 S100A9: antimicrobicidal?

The S100A8/9 complex was isolated from human blood leukocytes and used to assess any anti-microbicidal activity of this complex. The complex was found to exhibit microbial growth inhibitory activity at concentrations between 4-128mg/L against *E.coli, Klebseilla sp., S. aureus and S. epidermidis* (Steinbakk et al., 1990). Further investigation revealed the complex also caused growth inhibition of *C. albicans* (Sohnle et al., 1991). This antimicrobial action of the S100A8/9 complex was shown to be zinc reversible by a number of researchers indicating that the ability of the complex to chelate zinc appears to be key (Santhanagopalan et al., 1995; Sohnle et al., 1991; Sohnle et al., 2000).

The ability of the isolated proteins to bind zinc has been implicated as a mechanism for other extracellular functions of S100A8/9. These include a zinc reversible inhibition of matrix metalloproteinases, which are enzymes important in processes such as wound healing, tumourigenesis and inflammation (Isaksen and Fagerhol, 2001). As a factor isolated from rat leukocytes, the complex was shown to have the ability to inhibit the growth of a mouse mammary carcinoma cell line (Yui et al., 1995a). A related growth-inhibitory/apoptosis inducing function on normal fibroblasts was shown to be reversed by elevating zinc levels (Yui et al., 1997; Yui et al., 1995b). The relevance of these zinc related functions is unclear as the level to which the complex has the capability of bind zinc *in vivo* is unclear.

1.6 Aim of this Thesis

To date almost all the evidence for the function of S100A9 comes from *in vitro* and biochemical assays. A mouse model lacking expression of S100A9 was produced by Richard May in this lab previously. Some basic characterisation of the phenotype of these mice has been published recently (Hobbs et al 2003). It is the aim of this project to utilise these mice to test some of the many hypothesised potential roles for S100A9 in neutrophil function. In addition a range of broader *in vivo* assays will be presented looking in a more generalised and unbiased way for a true function of this protein *in vivo*.

CHAPTER 2

2 Materials and Methods

2.1 Materials

2.1.1 Stimulants

Reagent	Supplier	Stock Solution	Storage
FMLP (N-formyl-methionyl-leucyl-phenylalanine)	Sigma	10mM in DMSO	-20°C
Ionomycin	Calbiochem	1mM in DMSO	-20°C
IP_3-AM	Gift from A. Conway and J.Holmes	As supplied	-80°C
KC	Sigma	1mg/ml in PBS	-20°C
MIP-1α	Peprotech EC	10mg/ml in PBS	-20°C
MIP-2	Peprotech EC	0.1mg/ml in PBS	-20°C
Murine IL-1β	Peprotech EC	0.1mg/ml in PBS	-20°C
Murine TNFα	Sigma	10μg/ml in PBS/0.1% BSA	-20°C
PAF	Sigma	1 mg/ml in PBS	-80°C
PdBu (Phorbol-12,13-dibutyrate)	Calbiochem	2mM in DMSO	-20°C
PMA/TPA (Phorbol-12Myristate-13-acetate)	Calbiochem	2mM in DMSO	-20°C
Recombinant Human C5a	Sigma	1mg/ml in PBS	-80°C
Recombinant Murine S100A9	Gift from P. Tessier	As supplied	-80°C
Sodium Arachidonate	Sigma	Single Use	-20°C
Thapsigargin	Calbiochem	2mM in DMSO	-20°C

2.1.2 Inhibitors

Reagent	Supplier	Stock Solution	Storage
2-APB (2-Aminoethyl-diphenylborinate)	Calbiochem	50mM in Ethanol	-20°C
8-Br-cADPR	Sigma	Single use Aliquot	-80°C
BIM	Calbiochem	2mM in DMSO	-20°C
Calphostin C	Calbiochem	1mM in Ethanol	-20°C
DAG Kinase Inhibitor II	Calbiochem	10mM in DMSO	-20°C
ET-18-OCH_3	Calbiochem	5mM in Ethanol	-20°C
ETYA (5,8,11,14-eicosatetraynoic acid)	Sigma	Make fresh	-20°C
OAG (1-oleolyl-2-acyl-sn-glycerol)	Calbiochem	Single Use Aliquot	-20°C
Pertussis Toxin	Calbiochem	100µg/ml in PBS	+4°C
RHC80267	Calbiochem	50mM in DMSO	-20°C
U73122	Calbiochem	Single Use Aliquot	Room Temperature
U73343	Calbiochem	Single Use Aliquot	Room Temperature

2.1.3 Buffers/Serum

Reagent	Supplier
E4	Dulbecco's modified Eagle's medium (In-house – Endotoxin Free)
FACSfix	PBS containing 2% formaldehyde
FACSwash	PBS containing 0.2% bovine serum albumin
FCS	Foetal Calf Serum
HBSS	Hanks Balanced Salt Solution (Gibco-BRL)
HBSS (cation supplemented)	HBSS with 1mM Ca^{2+}, 1mM Mg^{2+} and 10µM Zn^{2+}
HEPES	Gibco-BRL
RPMI	Roswell Park Memorial Institute medium (Gibco-BRL)

2.1.4 Gifts

- DCDHF-coupled Zymosan – Gift from M.B.Hallett, University of Cardiff.
- IP_3-AM – Gift from A. Conway J.B. Holmes, University of Cambridge
- Recombinant Murine S100A9 – Gift from P. Tessier, University of Toronto
- Polyclonal anti murine CXCR2 antibody – Gift from R.M. Strieter UCLA

2.1.5 Cell-lines

$B16_{GALV}$: Sub-strain of Murine Melanoma Cell line, Cancer Research UK Cell-Production Department

3LL: Lewis Lung Carcinoma Cell line, Cancer Research UK Cell-Production Department

E.Coli K12: *Eschericha coli* Gift from J. Edgeworth, St Georges Hospital London

2.1.6 Antibodies

Antibody	Conjugate	Epitope	Species	Supplier
β1 integrin	Biotin	β1 integrin	Rat IgG2a	BD Biosciences
α4 integrin	PE	α4 integrin	Rat IgG2b	BD Biosciences
2B10	None/FITC	S100A9	Rat IgG2a	CRUK
6A4	None	S100A8	Rat IgG2b	CRUK
7/4	PE/none	Neutrophil/monocyte 40kDa protein	Rat IgG2a	Caltag Medsystems

Anti Mouse	HRP	Mouse Ig	Rabbit Polyclonal	DAKO
Anti Rabbit	HRP	Rabbit Ig	Goat Polyclonal	DAKO
Anti Rat	HRP	Rat Ig	Goat Polyclonal	Southern Biotech. Associates
Anti-Rat	Alexa-633	Rat IgG	Goat Polyclonal	Molecular Probes
Anti-Rat	PE	Rat IgG	Goat Polyclonal	BD Biosciences
Anti-Rat	Alexa-488	Rat IgG	Donkey Polyclonal	Molecular Probes
B220 (RA3-6B2)	FITC/CyChrome	CD45 on B cells	Rat IgG2a	BD Biosciences
CD4 (L3T4)	FITC	CD4	Rat IgG2a	BD Biosciences
CD8a (53-6.7)	PE	CD8 α chain	Rat IgG2a	BD Biosciences
F4/80	Biotin/Tri-colour	Macrophage 160kDa glycoprotein	Rat IgG2b	Serotec
FcγRII/III	None	FcγRII/III	Rat IgG2a	BD Biosciences
Gr-1	Biotin/FITC	Ly-6C/G	Rat IgG2b	BD Biosciences
IgG2a	FITC/PE/Biotin	-	Rat IgG2a	BD Biosciences
IP_3 Receptor	None	Pan IP_3 Receptor subtypes	Mouse polyclonal	Chemicon Intl.
Ly-6G	None/FITC	Ly-6G	Rat IgG2a	BD Biosciences
Mac-1	PE/Biotin	CD11b/CD18	Rat IgG2b	BD Biosciences
NH9	None	S100A9	Rabbit Polyclonal	CRUK
Phalloidin	Alexa 488, 547	Actin	(not antibody)	Molecular Probes
PLCβ2	None	PLCβ2	Rabbit Polyclonal	Santa Cruz Biotech
PLCβ3	None	PLCβ3	Mouse Polyclonal	Cell Signalling Tech.
PyLT	None	Control IgG2b	Rat IgG2b	CRUK
Streptavidin	Alexa-633	Biotin	(not antibody)	Molecular Probes

Tubulin	Alexa-547	γ-Tubulin	Mouse	Sigma
Y13	None	Control IgG2a	Rat IgG2a	CRUK

2.2 Methods

2.2.1 Animal husbandry

S100A9 null mice were generated as published previously (Hobbs et al., 2003). Mixed background 129Sv x C57BL/6J transgenic mice derived from two independent embryonic stem cell clones were backcrossed against C57BL/6J mice (CRUK in house stock) for ten generations. Heterozygous and homozygous offspring were identified within each generation using the following genotyping protocol. Wildtype and S100A9 null mice from the same generation of back-cross were compared at each generation, until generation ten when in-house C57BL/6J control mice were used. Mice were maintained in specific-pathogen-free conditions in accordance with UK Home Office guidelines.

2.2.2 Genotyping S100A9 null mice

5mm of tail was cut into an Eppendorf tube and 700µl of tail digestion buffer (50mM Tris pH 8.0, 100mM EDTA, 100mM NaCl, 1% SDS) was added. 25µl of a 10mg/ml Proteinase K solution (Sigma) was added and tubes were incubated at 55°C overnight. 700µl of phenol:chloroform (Phenyl:chloroform:isoamyl alcohol (25:24:1); Sigma) solution was added to the digested tail solution and tubes were vigorously shaken on a bench top shaker for 10min. Tubes were centrifuged in a microfuge at full speed for 10 min. The top layer was transferred into a new tube and DNA was pelleted by centrifugation at

full speed in a microfuge for 15 mins at 4°C. The DNA pellet was then washed with 70% ethanol and allowed to dry prior to being dissolved in 50µl water.

Alternatively, 80µl sodium acetate 3M (Sigma) and 400µl isopropanol were added to 400µl of pre-boiled tail lysate (prepared as above) and gently mixed. The solution was centrifuged at full speed in a microfuge at 4°C and the supernatant removed. The resulting pellet was washed in 500µl ethanol followed by centrifugation at full speed in a microfuge at 4°C. The ethanol was removed and the pellet left to air dry prior to resuspension in 20µl water.

Primers

GF1 – T_m 50.3°C – AACATCTGTGACTCTTTAGCC

GB1 – T_m 50.3°C – CATCTGAGAAGGTGCTTTGTT

GNEO – T_m 56.3°C – ACCGCTTCCTCGTGCTTTACG

PCR Program

5 min - 94°C

REPEAT FOLLOWING FOR 30 CYCLES:

20s - 94°C

30s - 55°C

60s - 72°C

FINISHING:

5 min - 72°C

HOLD - 12°C

PCR Protocol

PCR reactions were set up in PCR plates (Cycleplate 24ET, Strip-ease-8 caps; Robbins Scientific). The PCR reaction mix consisted of: 1µl purified tail DNA, 125ng of each primer, 1.5U Taq Polymerase (Cancer Research UK) and PCR Buffer (1x Thermophilic PCR buffer, 1.5mM $MgCl_2$, 200µM dATP/dGTP/dCTP/dTTP; all Promega) in a final volume of 25µl. PCR programs were run on a Peltier Thermal Cycler PTC-225 (MJ Research).

2.2.3 Agarose gel electrophoresis

Tris-acetate (TAE) buffer

A 50x stock solution was prepared by dissolving 242g Tris base and 57.1ml glacial acetic acid in dH_20 followed by 100ml 0.5M EDTA (pH8.0), with the solution then being made up to 1 litre with dH_2O.

Electrophoresis

TAE buffer containing 1.8% agarose (Life Technologies) was heated in a microwave oven, with intermittent mixing, to dissolve the agarose. The solution was allowed to cool briefly prior to addition of ethidium bromide (4µl/100ml; Sigma) in a fume hood. The solution was then cast in a mould and allowed to set. BlueJuice (Promega) DNA loading dye was added to PCR reaction products at 1:10 dilution. 25µl of each sample was loaded per agarose well and DNA was electrophoresed at 100mV in 1x TAE buffer.

2.2.4 Leukocyte Preparations

Murine bone marrow leukocytes

Murine bone marrow leukocytes were harvested by flushing both femurs and tibiae with HBSS containing 0.2% BSA (or relevant assay buffer) using a needle and 2.5ml syringe. Cell clumps were dispersed by gentle agitation with a plastic pastette prior to passage through a 70μm cell strainer (Falcon). The cells were pelleted by centrifugation at 500 x g for 5 min prior to resuspension in 1ml hypotonic red blood cell lysis solution (0.144M NH_4Cl/0.017M Tris-HCl, pH7.2). Red blood cells were lysed at room temperature for 3 minutes at which time the cells were washed and resuspended in HBSS/assay buffer. This protocol typically yields a population containing 25-35% neutrophils.

Peritoneal leukocytes

3% Thioglycollate (Sigma) solution in PBS was prepared by autoclaving twice and resting for at least one week at 4°C. 0.5ml Thioglycollate was injected ip into the peritoneum. After 6 hours the mice were sacrificed according to Schedule 1 of the Scientific Procedures Act and peritoneal lavage was performed with 5ml PBS/5mM EDTA. The harvested cells were passed through a cell strainer, pelleted by centrifugation at 500 x g for 5min, washed once and resuspended in assay buffer/HBSS. This protocol typically yields a cell preparations containing 60-70% neutrophils.

Human neutrophils

Erythrocytes were sedimented from EDTA-anticoagulated whole blood by addition of Dextran T500 (Amersham Biosciences) to a final concentration of

0.6%. After 45 minutes at room temperature the leukocyte-rich plasma was layered onto a discontinuous gradient of 70% over 80% isotonic Percoll (Amersham Pharmacia Biotech). Following centrifugation at 1137 x g for 15min, the neutrophils were harvested from the interface between the 70% and 80% Percoll. The neutrophils were then washed three times in HBSS/HEPES 20mM. This protocol typically yields a cell population containing 80-90% neutrophils.

2.2.5 RT-PCR

Primers

Primers were designed against the murine cDNA reference sequence for S100A8, S100A9, S100A4, S100A1 and S100Z. For all genes except S100A9 forward and reverse primers were designed to sit in separate exons. All primers were designed to have an annealing temperature of 60°C.

S100A1: **GCCCTTCTGTCGAGAATCTG**

AAGCACGCTAAAGGGGAAAT

S100A4: **TTGTGTCCACCTTCCACAAA**

GCACTATGCTCACAGCCAAC

S100Z: **GCTCAACCACCTTCTTCTGC**

TCTTTATTGGCGTCCAGGTC

S100A9: **ACCTGGACACAAACCAAGGAC**

GCCATTGAGTAAGCCATTCC

S100A8: **GGAAATCACCATGCCCTCTA**

TCCTTGTGGCTGTCTTTGTGT

RNA Isolation

RNA was prepared from $5x10^6$ bone marrow cells using the Promega SV total RNA isolation kit according to the manufacturer's instructions. RNA yield was quantified by diluting the prepared sample 1/100 and measuring the optical density at 260nm and calculated by ratio to an optical density of 1 = 40μg/ml.

RT-PCR

The RT/PLATINUM *Taq* HiFi Mix was used according to the manufacturer's instructions. Briefly, the following reaction mix was prepared in thin walled PCR tubes on ice: 1x Reaction Mix (as supplied), 250ng template RNA, 0.2μM sense primer, 0.2μM anti-sense primer, 1-2μl RT/PLATINUM *Taq* HiFi Mix, water to 50μl. The following thermocycler setup was used as one continuous program for all stages:

cDNA synthesis: 1 cycle of:

50°C for 30 minutes

94°C for 2 minutes

PCR amplification: 35-40 cycles of:

Denature: 94°C for 15 seconds

Anneal: 55°C for 30 seconds

Extend: 68°C for 1 minute

Final Extension: 1 cycle of:

72°C for 10 minutes

12°C to hold.

PCR products were visualised on 1.8% agarose gel as before.

2.2.6 Protein Analysis

Preparation of detergent soluble leukocyte extracts

Cells were suspended at $5x10^7$/ml in ice cold lysis buffer (50mM Tris pH 8.0 containing 1% Triton X-100 (Sigma), 2mM EDTA, 50mM NaCl, 20μg/ml PMSF (Sigma), 1μg/ml aprotinin (Sigma)) and incubated for 30 minutes on ice with intermittent disruption with a 25G needle. The solution was then centrifuged in a microfuge to remove insoluble material and the supernatant decanted and used in assays.

Immunoprecipitation

Aliquots of cell lysate were incubated with 10-20μl/ml mAbs 2B10 or Y13 overnight at 4°C under gentle rotation. The mAbs were precipitated by incubation with 50μl Protein G sepharose slurry (Amersham Pharmacia Biotech) for a further hour. The sepharose was collected by centrifugation and wash by resuspension and re-pelleting in lysis buffer five times. The sepharose was then boiled in SDS-PAGE sample buffer (as below) for 5 min.

SDS PAGE

A polyacrylamide gel composed of a stacking gel layered over a separating gel was formed. The separating gel was made from 375mM Tris, pH8.0, containing acrylamide:bis-acrylamide 37.5:1 solution (Amersham Pharmacia Biotech) to give acrylamide concentrations of 15% for S100 proteins, (6% for IP_3 receptor or PLC), 0.1% SDS, 0.04% ammonium persulphate and 1/5000 TEMED (Sigma). The stacking gel was made of 125mM Tris, pH6.8, with 3% acrylamide, 0.08% bis-acrylamide, 0.1% SDS, 0.04% ammonium

persulphate and 1/5000 TEMED. Proteins for analysis were boiled in sample buffer (125mM Tris, pH6.8, 25% glycerol, 2% SDS, 1% 2-mercaptoethanol, 0.02% bromophenol blue) for 5 minutes. Electrophoresis was performed in an Atto Dual Mini Slab Chamber (Genetic Research Instrumentation Ltd) with electrophoresis buffer (25mM Tris, 192mM glycine, 0.1% SDS) at 100V through the stacking gel and 180V through the separating gel. Rainbow coloured protein standards (Amersham Pharmacia Biotech) were run under identical conditions in the same gel to allow calibration by molecular weight. Samples not analysed by Western blot were visualised using a Silver stain protocol.

Silver stain

Gels were washed twice for 15 minutes in a 50% methanol and 10% acetic acid solution, followed by washing in 10% ethanol and 5% acetic acid solution for five minutes and a final wash in dH_2O. The gels were sensitized in a 20mg/l solution of $Na_2S_2O_4$ for nine minutes. The sensitising solution was exchanged, without washing for a 0.1% solution of $AgNO_3$ in dH_20 to which was added 75µl 37% formaldehye solution per 100ml $AgNO_3$ solution. The gel was incubated for 9 minutes with gentle agitation in the solution prior to a 30 second wash with dH_20. The stain is developed with a solution of 1ml/litre 37% formaldehyde in 0.3% carbonate solution and 1g/litre sodium thiosulphate to the required intensity. The reaction is stopped by replacement of the solution with a 2.5% acetic acid solution.

Western blotting

Following SDS-PAGE, proteins were transferred onto a nitocellulose membrane (Hybond ECL, Amersham Biosciences) at 60V for 50min (S100) or

overnight (PLC/IP_3 Receptor) at 4°C in a Transblot Cell (Bio-Rad) containing transfer buffer (25mM Tris, 192mM glycine, 20% methanol). The transfer was confirmed by staining of the membrane with 0.1% Ponceau S solution (Sigma). Following this step the membrane was blocked with PBS/Tween (PBS containing 0.1% Tween 20 (Sigma)) containing 5% milk powder at 4°C overnight with gentle agitation. After washing three times the membrane was incubated in PBS/Tween with 5% milk and primary antibody for one-two hours or according to manufacturers instructions at room temperature. After washing a further three times in PBS/Tween the HRP-conjugated secondary antibody was applied (according to the manufacturer's instructions) in PBS/Tween with 5% milk for one hour at room temperature. The membrane was washed a final three times and the bound antibody visualised using chemiluminescent substrate (ECL detection reagent; Amersham Biosciences) according to the manufacturer's instructions. Excess substrate was blotted from the membrane onto clean tissue. The membrane was exposed to film (Hyperfilm ECL; Amersham Biosciences) to visualise the protein levels.

2.2.7 Flow Cytometry

FACS staining of leukocyte suspensions

A minimum of $2x10^5$ leukocytes were incubated in 200µl FACSwash containing saturating concentrations of antibody on ice in the dark for 15 minutes. For larger numbers of samples the leukocytes were pelleted in a 96-well plate and resuspended in 50µl of FACSwash containing saturating concentrations of antibody. The cells were washed three times with an excess of FACSwash and

resuspended in 200µl FACSwash (for immediate analysis) or FACSfix (for storage overnight-2 days) and stored in the dark at 4°C.

FACS staining in whole blood

50µl of EDTA-anticoagulated blood was incubated with 50µl of saturating antibody solution in a FACS tube (BD Biosciences) for 30 minutes at room temperature. The samples were washed in FACSwash and erythrocytes were lysed using FACS lysing solution (BD Biosciences) according to the manufacturer's instructions.

Multi-parametric flow cytometry

For multi-parametric flow cytometry the above protocols were followed for each successive layer of antibody. For analysis with directly conjugated antibody combinations all antibodies were incubated simultaneously. For combinations containing un-conjugated or biotinylated antibodies, these antibodies were incubated first followed by fluorochrome conjugated secondary antibody/streptavidin, finally directly conjugated antibodies were applied. Individually stained controls for each fluorochrome were also prepared.

Flow cytometric analysis

Unstained and single-fluorochrome control samples were used to set voltages and compensation for each experiment. The fluorescence intensity of each fluorochrome in each sample was recorded for in excess of 5000 target cells per sample.

Cell sorting

Cells were stained as for flow cytometry and neutrophils (7/4 Hi + Ly-6G/Gr-1 Hi) were sorted using a Mo-Flo cell sorter (Dako Cytomation)

Absolute cell counting

Absolute cell counts were obtained by adding a known quantity of calibration bead (CaliBRITE, BD Biosciences) to a known proportion of total sample. The number of cells and beads were assessed using a flow cytometer and used to calculate the number of cells in the original sample by ratio to the number of beads added.

2.2.8 Leukocyte density analysis

Two-step gradient

Bone marrow leukocytes a Lymphoprep gradient was made by carefully layering 4 ml of 1.077g/ml Lymphoprep (Sigma) on top of 4ml 1.083g/ml Lymphoprep (Sigma). 1ml of bone marrow leukocytes at 2-3x10^7/ml (prepared as described above) in RPMI were then layered on top. Following centrifugation at 700 x g for 30 minutes, the granulocyte-rich band was collected from the Lymphoprep:Lymphoprep interface and the mononuclear cells at the RPMI:Lymphoprep interface.

Continuous Percoll gradient

A 1.097g/ml solution of isotonic Percoll (Amersham Biosciences) in 0.15M NaCl was prepared and used to create a 9-ml self-generating gradient as described by the manufacturer (running conditions: 23° angle-head rotor, 30,000 x

g, 25°C, 12 min). The gradient was calibrated between 1.018 and 1.138g/ml with density marker beads (Amersham Biosciences). Bone marrow leukocytes at $5x10^7$/ml in HBSS were layered onto the preformed gradient at 1 ml/tube and centrifuged at 700 x g at 21°C for 30 minutes. The mean buoyant density of the cellular bands was calculated with density marker bead calibration, and the composition of the bands was determined by flow cytometric analysis.

2.2.9 Measurement of intracellular calcium concentration

Bone marrow leukocytes were prepared in Flux buffer (HBSS: 0.4g/L KCl,0.06g/L KH_2PO_4, 8g/L NaCl, 0.9g/L Na_2HPO_4, 0.35g/L $NaHCO_3$, 1 g/L D-glucose supplemented with 1mM Ca^{2+} and 0.5%BSA) and resuspended at $1x10^7$/ml in 2.5mM Indo-1AM/Pluronic acid 2.5%. The cell suspension was incubated at 30°C for one hour prior to washing in an excess of Flux buffer (30°C). The cells were resuspended at $5x10/^7$/ml in Flux buffer containing mAbs 7/4PE and Ly-6G/Gr-1-FITC for 15 minutes at 30°C. Cells were washed one final time and resuspended at $5x10/^7$/ml and maintained at 30°C prior to use. For inhibitor studies requiring pre-incubation aliquots of cells were separated into tubes with the inhibitor indicated. Fluorescence was monitored using a BD LSR flow cytometer (FL-4 530/30nm BF filter, FL5 424/44 filter, 510LP filter; BD Biosciences). Samples were read at a flow rate of 2000-3000 events/sec and stimulants were added from 100x stock solutions at the indicated time points. Data was analyzed using FlowJo software (TreeStar Inc). Results are represented as the median Indo-1 ratio for 500-700 neutrophils per second.

2.2.10 Confocal microscopy

Ethanol cleaned coverslips were coated in 24 well plates with murine ICAM-1 solution overnight at 4°C and blocked with 2.5% BSA in PBS for one hour at room temperature. Cells were allowed to adhere to the coverslips in cation supplemented HBSS. Adherent cells were fixed with 3% paraformaldehyde in PBS at room temperature for 20mins. The paraformaldehyde solution was replaced with 50mM NH_4Cl in PBS to quench autofluorescence and the coverslips incubated for 10 minutes. The coverslips were washed three times with PBS and incubated in 0.1% Triton X-100 (Sigma) for 4 mins. Coverslips were washed 2 times in PBS followed by three washes with blocking solution (PBS/10% FCS) over five minutes. Primary and secondary antibody solutions were applied sequentially and each incubated for 20/30mins in blocking buffer with 3 washes in PBS between antibody changes. Nuclei were stained using DAPI (Sigma) according to the manufacturer's instructions (Molecular Probes). Coverslips were washed 3 times in water and mounted onto microscope slides using Mowiol (prepared according to the manufacturer's instructions). The images were taken on a Zeiss Laser Scanning Microscope LSM5101.

2.2.11 Adhesion Assay

Fibrinogen (Sigma) was dissolved at 2mg/ml in 0.1M sodium carbonate buffer at 37°C for 30 minutes. 96 well plates (Immulon-1® 96-well plates (Dynatech) were coated with 100µl fibrinogen solution overnight at 4°C. Plates were washed twice with RPMI immediately prior to commencement of the assay. Bone marrow cells were prepared in RPMI as described and incubated at

$5x10^6$/ml in 1μM BCECF-AM (Sigma) at room temperature for 30 minutes. Cells were washed in RPMI and resuspended at $1x10^7$/ml and 50μl of cell suspension applied per well. Stimuli were prepared in RPMI at 2x concentration and 50μl applied to the wells. The plate pulsed was in a centrifuge for 30 seconds and cells left to adhere for 30 minutes. The fluorescence of the well was assessed prior to washing using a Cytofluor multiwell platereader (PerSeptive Biosystems; excitation: 488nm, emission: 530nm). The plate was washed gently and 50μl RPMI added per well and the fluorescence of the well reassessed. The level of adhesion was assessed by calculating the percentage of total fluorescence remaining following the plate wash step.

2.2.12 Migration assay

Migration assays were performed as detailed by Smith et al with minor modifications (Smith et al., 2003). 35 mm glass bottom microwell dishes (MatTek Corp) were coated at 4°C overnight with 200 μl of murine ICAM-1Fc in PBS, then blocked with 2.5% BSA in PBS. Bone marrow cells were prepared in cation supplemented HBSS and $5x10^5$ cells per dish were allowed to migrate for 20 minutes at 37°C before rinsing to removed unattached cells. Images were taken at 5 second intervals using a Nikon Diaphot 300 microscope and AQM2001 Kinetic Acquisition Manager software (Kinetic Imaging Ltd).

2.2.13 Chemotaxis assay

Transwell (Corning) plates with a 3μm pore and 6.5mm diameter insert were pre-incubated with Chemotaxis buffer (HBSS containing 20mM HEPES, 1mM Ca^{2+}, 1mM Mg^{2+}, 10μM Zn^{2+} and 0.1% BSA) at 37°C for one hour. 600μl Chemotaxis buffer containing various chemoattractant stimuli was placed in the

plate wells. The Transwell insert was replaced and $5x10^6$/ml bone marrow leukocytes in 100µl added. The plates were incubated for 2-4 hours at 37°C prior to removal of the insert and removal of the buffer from the lower chamber for analysis. The lower chambers were washed with ice-cold PBS/EDTA (5mM) twice and the recovered cells added to the buffer sample. The harvested cells were pelleted and stained in FACSwash to identify the neutrophils, prior to absolute cell counting by flow cytometry.

2.2.14 Measurement of oxidant production

Luminol enhanced chemiluminescence

This protocol is adapted from (Dahlgren and Karlsson, 1999). Bone marrow leukocytes were suspended at $2x10^7$/ml in RPMI containing luminol at 50µM at 37°C. The cell suspension was applied to a 96-well plate at 200µl per well. Stimulants were added at 10x concentration immediately prior to placing in a heated luminometer (Dynex MLX Luminometer) at 37°C. Readings were taken for the whole plate every 17 seconds. The mean light units produced per sample per time-point were calculated.

DCDHF-coupled zymosan

Zymosan particles were supplied prepared as detailed in (Dewitt et al., 2003). $5x10^5$ bone marrow cells (in 50µl HBSS) were mixed with 50µl zymosan suspension (2mg/ml) and incubated at 37°C with intermittent gentle mixing. Samples taken and washed in ice cold HBSS and resuspended in FACS wash kept at 4°C prior to analysis by flow cytometry. For confocal microscopy cells were

adhered onto fibrinogen coated coverslips and stained as described using the monoclonal anti-S100A9 antibody (2B10).

2.2.15 Bacterial Killing Assays

Human neutrophil assay

Non-pathogenic *E.coli* K12 were grown to log phase in LB broth at 37°C with constant agitation. $2.5x10^6$ human neutrophils in HBSS were mixed with the bacteria at a ratio of 10:1 and 10% human autologous serum in a final volume of 1ml. A control tube of bacteria alone in HBSS containing 10% human serum was also prepared. The samples were incubated at 37°C with constant gentle agitation. Samples were removed at indicated time points and the leukocyte population separated by centrifugation at 200g for 5 minutes. The cell pellet and supernatant samples were diluted in water to lyse the leukocytes and plated onto agarose culture plates at 3 different dilutions in duplicate. Culture plates were incubated overnight and colonies counted.

Murine killing assay

Non-pathogenic *E.coli* K12 were grown to log phase in LB broth at 37°C with constant agitation. $2.5x10^5$ murine peritoneal leukocytes in HBSS were mixed with the bacteria at a ratio of 1:1 with 10% murine serum in a final volume of 1ml. A control tube of bacteria alone in HBSS containing 10% murine serum was also prepared. The samples were incubated at 37°C with constant gentle agitation. Samples were removed at indicated time points and diluted in water to lyse the leukocytes and plated onto agarose culture plates at 3 different dilutions in duplicate. Culture plates were incubated overnight and colonies counted.

2.2.16 Air pouch model of inflammation

The protocol was carried out as described by Tessier et al (Ryckman et al., 2003b). On day 0 and day 3 mice were anaesthetised with halothane and injected sub-cutaneously on the back with 2.5ml of sterile air to generate a dorsal air pouch. On day 6 mice were anaesthetised and 1ml of stimulus injected into the pre-formed pouch. The stimuli were prepared in PBS containing 1mM Ca^{2+}, 1mM Mg^{2+} and 10μM Zn^{2+}. At six hours following stimulation the mice were euthanised by carbon dioxide exposure followed by cervical dislocation. The migrated cells were harvested by flushing the air pouch twice with 2ml of ice-cold PBS containing 5mM EDTA. The cells were counted by flow cytometry. Five mice per time point were analysed.

2.2.17 Peritonitis model

Peritonitis was induced by intraperitoneal injection of 0.5ml sterile thioglycollate (prepared as described previously), TNFα (10ng) or IL-1β (100ng). One hour prior to intraperitoneal injection, opiate analgesia (Temgenic) was dosed to each mouse subcutaneously. At a time point 6 hours following stimulant injection, the mice were euthanised by carbon dioxide exposure and peritoneal cavities were lavaged with 5ml ice-cold PBS containing 5mM EDTA. Leukocytes were stained to identify the myeloid cells and cells were analysed by flow cytometry. Five mice were analysed per genotype for each sample point.

2.2.18 Streptococcus pneumoniae-induced pneumonia

Mice were lightly anaesthetised with 1.5% (v/v) halthane and 50μl PBS containing $1x10^6$ CFUs of *S. pneumoniae* (D39, serotype 2) was then

administered into the nostrils of each mouse as previously described (Kerr et al., 2002). At certain time points mice were sacrificed by cervical dislocation and blood samples taken via cardiac puncture. Lung tissue was removed and homogenised and viable bacterial counts were determined as described by Kerr et al. Four to six mice of each genotype were analysed at each time point.

2.2.19 Wound Healing Assay

Wound healing assays were performed essentially as described in (Reynolds et al., 2005). Female mice were anesthetized and the dorsum shaved then cleaned with alcohol. Two 3-mm full-thickness cutaneous biopsy punch wounds were made either side of the midline of the mouse. Wounds were made maintaining the underlying fascia. The wounded tissue was collected on various days after injury. Tissue was bisected and fixed in 10% formalin for paraffin embedding.

2.2.20 Tumour growth assay

Maintenance of cell-lines

3LL: Maintained in suspension in RPMI (CRUK in-house) supplemented with 5% FCS at 37°C in 5% CO_2. Colonies were split to give colonies containing $5x10^5$ cells/ml three times per week. For tumour growth experiments the cells were harvested and resuspended at $5x10^7$/ml in PBS.

$B16_{GALV}$: Maintained as an adherent colony in E4 (CRUK in-house) supplemented with 10% FCS at 37°C in 5% CO_2. Confluent monolayers were harvested using versene and reseeded at dilution of 1:4 or 1:10. For tumour growth experiments the cells were harvested and resuspended at $2x10^5$/ml in PBS.

In vivo tumour growth assay

Tumour cells were harvested and prepared as above and placed on ice immediately prior to the beginning of the experiment. 100µl of the relevant cell solutions were injected sub-cutaneously into the right flank of each mouse. Tumour size was monitored by measurement of size in two dimensions every 2-3 days for 3-4 weeks until a critical threshold of tumour size was reached ($1.2cm^2$). Mice were euthanised and tumour excised and weighed.

2.2.21 Chemical induced carcinogenesis

Timed breeding was undertaken to provide mice born within a four day window. The backs of all mice were shaved at 7 weeks of age followed by painting of the shaved area with 25µg DMBA in acetone or acetone alone control. The treated skin was painted with 4µg TPA in acetone solution thrice weekly for 15 weeks beginning 1 week after DMBA treatment. The mice were examined weekly and the incidence of benign/non-benign skin tumours noted.

2.2.22 Immunohistochemistry

4µm sections were cut from paraffin-embedded tissues and dewaxed, and endogenous peroxidases blocked. Following rehydration the samples were microwaved for 10min at 700W or treated with 1mg/ml Trypsin (BDH, Merck Eurolab) for 15 minutes at 37°C (mAb 6A4 only). Sections were then stained with rat mAbs 2B10, Y13, 6A4, PyLT or 7/4 at 10µg/ml in Tris buffered saline, pH 7.6 for 40 minutes at room temperature. Biotinylated secondary antibody (rabbit anti-rat, Vector Labs) was applied in a similar manner at 1:100. Finally StreptABC/HRP was used according to the manufacturer's instructions (Dako

cytomation) and the slides were exposed to 3,3'diaminobenzidine for 2-3 minutes. Slides were counterstained with Harris' Haematoxylin.

CHAPTER 3

3 Basic characterisation of S100A9 null neutrophils

3.1 Introduction

The primary site of expression of S100A8/9 is in myeloid cells. In human neutrophils the heterodimer is reported to constitute 40% cytosolic protein (Edgeworth et al., 1991) and S100A9 to constitute 10-20% in murine neutrophils with the dimer presumably constituting 20-40% similarly to the human situation (Nacken et al., 2000). Given this expression pattern a logical place to start an investigation into the function of this protein is by examining the myeloid cells in the S100A9 null animals. By comparing the function of cells that do and do not express S100A9 it is hoped that altered cellular function in the S100A9 null animals will indicate the functional role of the protein. Early reports on the expression of this protein by neutrophils showed it to be expressed during the differentiation of neutrophils to their fully mature form (Lagasse and Clerc, 1988; Lagasse and Weissman, 1992). S100A9 has been shown to interact with casein kinases implicating them in the control of transcriptional machinery giving a mechanism by which they could modulate the differentiation process (Murao et al., 1989). To ascertain whether this protein does indeed have a role in neutrophil development the number of myeloid cells and their expression of surface molecules will be evaluated.

In this laboratory S100A9 null mice were generated using an insertional strategy. A *Lac Z/Neo* cassette was inserted into exon 2 of the murine S100A9

gene immediately after the ATG translational start codon, preventing transcription of the S100A9 gene. ES cell clones in which the targeting strategy had occurred as expected were micro-injected into C57BL/6J blastocysts to create chimaeric mice (Hobbs et al., 2003). This work was carried out in collaboration with Ian Rosewell, Mary Ann Jacobs and Stephen Wilson at Cancer Research UK Clare Hall laboratories. These chimaeric mice were bred with C57BL/6J mice to produce heterozygous mice with a mixed 129Sv/C57BL/6J background. Two independent strains were created from the 2G1 and 2E5 ES cell clones and were maintained independently. The two S100A9 null mouse lines were backcrossed against C57BL/6J mice for 10 generations, at which time they were considered to be wholly C57BL/6J in background. The mice used in the preparation of this thesis are from back-cross generations 5-10. All mice used in the preparation of this thesis were maintained in Specified Pathogen Free conditions.

Work to characterise the S100A9 null mice has been underway for a number of years. The initial observations made on these mice were published in 2003. At that time the mice had been back-crossed for 3-5 generations onto a C57BL/6J background. The initial characterisation of the S100A9 null mice indicated that S100A9 was dispensable for the production of neutrophils and monocytes in mice. Initial characterisation of the S100A9 null mice showed them to be viable, fertile and to live a normal life-span (Hobbs et al., 2003). They displayed normal numbers of circulating leukocytes, which appeared to have normal morphology by electron-microscopy. The most obvious difference between the S100A9 null and wildtype cells was the absence of any S100A8 protein in the S100A9 null animals. Although S100A8 has been shown to be crucial for development, and so is presumably expressed during development in

the S100A9 null animals, it was totally absent from the mature leukocytes. This seems to imply that in the mature animal, in the absence of its heterodimeric binding partner S100A9, S100A8 is totally unstable as has been suggested previously (Hunter and Chazin, 1998). This finding is in conflict to the reported expression of S100A8 in the absence of S100A9 found in some studies indicating that in those studies S100A8 may have another stabilising binding partner (Grimbaldeston et al., 2003; Rahimi et al., 2005). The lack of expression of S100A8 makes the S100A9 null mice effectively S100A8/9 null animals, making interpretation of any phenotype simpler, with the entire heterodimer being absent.

In this section the work contributing to the initial phenotyping of the S100A9 null mice is presented as well as further characterisation of the state of the S100A9 null neutrophils.

3.2 Results

3.2.1 Neutrophil identification

Studies published to date have found no morphological abnormalities in the S100A9 null neutrophils. For comparison a human neutrophil, wildtype and S100A9 null mouse neutrophils stained using the Diff-Quik stain are shown (figure 3.1A-C). Lobed nuclear architecture characteristic of this cell-type is clearly shown by bright purple staining. The cellular morphology in murine and human samples is similar, with the murine cells being smaller in size.

Counting neutrophils identified by nuclear morphology as shown in figure 3.1 is a common way to enumerate experimental samples. However, for most of the work presented in this thesis, flow cytometry was used to identify the neutrophil cell population. Myeloid cells can be discriminated by dual staining the cell

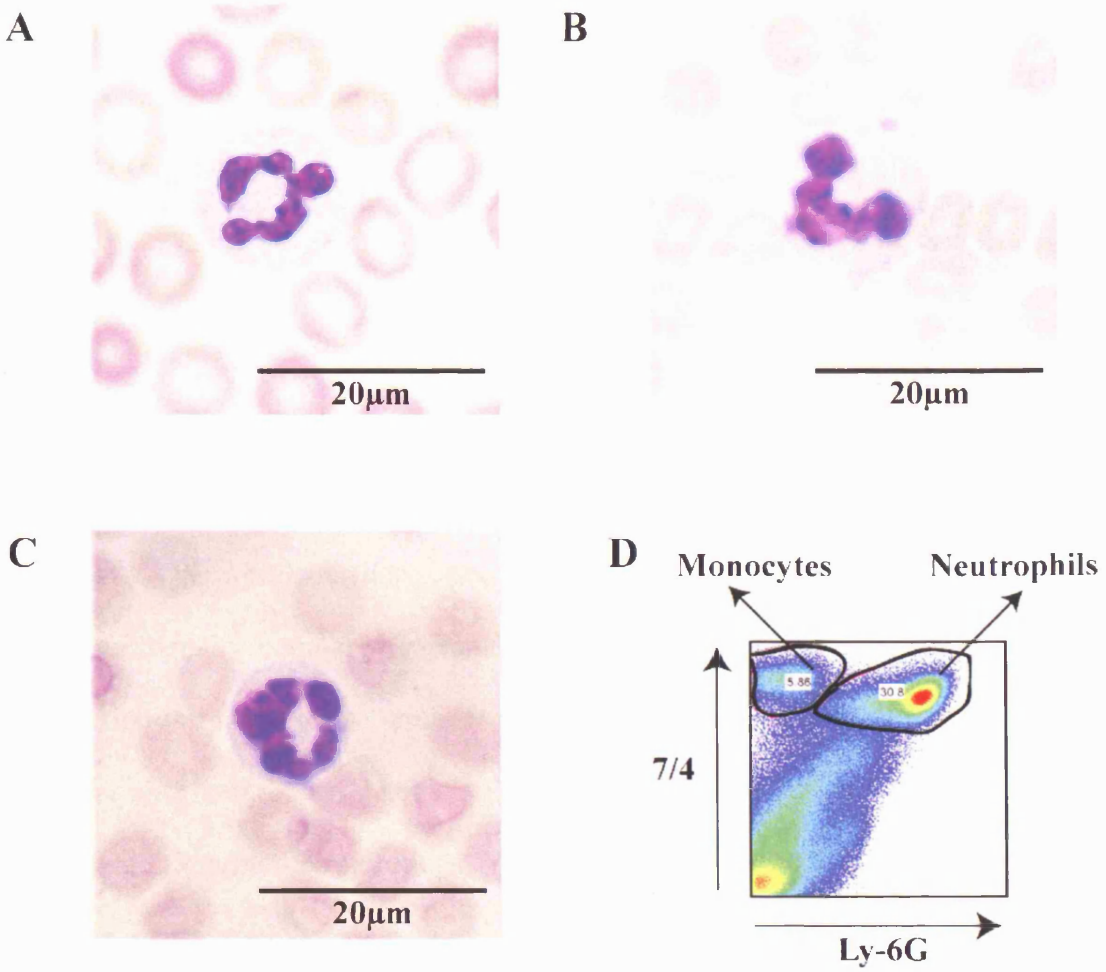

Figure 3.1 Identification of human, mouse and S100A9 null murine neutrophils.

Blood leukocytes were isolated from human, wildtype mice and S100A9 null mice. Blood smears were prepared and the cells fixed briefly in 100% methanol. Leukocyte morphology was visualised using Diff-Quik stain according to the manufacturers instructions. Neutrophils were identified by characteristic lobed nuclear morphology (purple) and are shown to the same scale. **A:** Human blood neutrophil, **B:** wildtype murine neutrophil, **C:** S100A9 null neutrophil. **D:** Bone marrow leukocytes were prepared as described in Material and Methods and double stained with mAbs Ly-6G (FITC) and 7/4 (PE). Neutrophils and monocytes were identified by flow cytometry as indicated.

population with mAbs 7/4 (PE) and Ly-6G (FITC) (figure 3.1D) (Henderson et al., 2003). This staining protocol produces good separation of the monocyte and neutrophil populations, which is particularly useful when using bone marrow samples where the populations are less discrete. The neutrophil population is identified as 7/4 high / Ly-6G high and the monocytes as 7/4 high / Ly-6G negative.

3.2.2 Neutrophil density

One of the first observations of a difference between the wildtype and S100A9 null cells was a difference in partitioning on a two-step Lymphoprep gradient. This protocol allows neutrophils to be enriched according to their increased density compared to mononuclear phagocytes. When a leukocyte suspension is applied to the gradient and centrifuged, the cells separate over the gradient with neutrophils sedimenting at the interface between 1.077g/ml and 1.083g/ml Lymphoprep solutions. While the starting population had equal numbers of neutrophils, when an enriching gradient was performed, the S100A9 null neutrophils were recovered at a lower percentage from the 'neutrophil' band. This observation was first made by Meg Matthies in this lab. Following on this work I repeated the initial experiments with the two-step gradient and observed a higher percentage of neutrophils in the 'monocyte' layer in the S100A9 null samples than in the corresponding wildtype samples (figure 3.2a). Co-ordinately a lower percentage of S100A9 null neutrophils were found in the 'neutrophil' band compared to the wildtype samples. This appeared to indicate that the S100A9 null cells had a lower buoyant density and so were partitioning with the cells of lower density than would be expected. To try and confirm this observation a continuous Percoll gradient approach was undertaken.

Continuous Percoll gradients were formed by ultracentrifugation of a Percoll solution, which causes Percoll particles of different sizes to be separated forming a gradient of density through the tube. The continuous Percoll gradient can be calibrated by inclusion of a range of coloured latex beads of known density in tubes. The position of the bands formed by the different coloured particles within the tube can be measured and used to produce a calibration curve of position of the band in tube relative to buoyant density. Bone marrow samples from wildtype and S100A9 null mice are then applied to the gradients and centrifuged at low speed to allow the cells to separate by density through the tube. The position of the neutrophil rich band and the lymphocyte band were assessed from wildtype and S100A9 null samples. As lymphocytes do not express S100A9 and so would not be expected to be affected by the deletion of this molecule the position of this band acts as an internal control to ensure any differences seen in the position of the neutrophil band are not due to differences in the formation of the gradient. When the position of the lymphocyte band was compared in the different samples it was found to have a buoyant density of 1.0439g/ml in both wildtype and S100A9 null samples. When the neutrophil band was examined it was observed that the S100A9 null neutrophil band showed a consistently lower buoyant density (1.0811g/ml) compared to the wildtype band (1.0836g/ml) (figure 3.2b). The difference was calculated and shown to be significant. The identity of the neutrophil band was confirmed in both wildtype and S100A9 null samples by flow cytometry with a myeloid cell identification antibody cocktail and was shown to contain 80% of the neutrophils (data not shown) loaded onto the gradient.

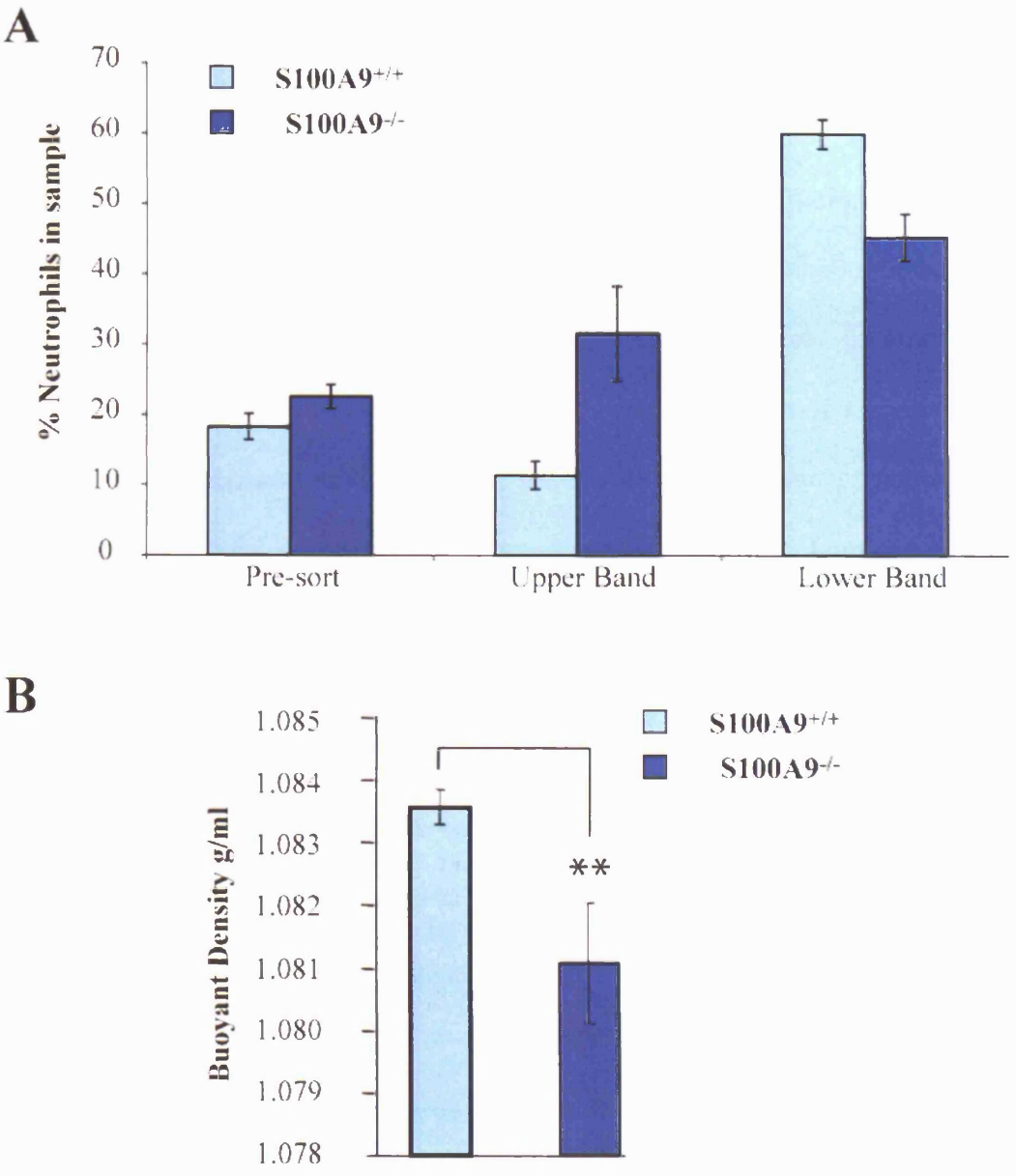

Figure 3.2 Lower density of bone marrow neutrophils from S100A9 null mice

Bone marrow cells were flushed out of femurs and tibias of 6-10 week-old mice. **A**: The cells are applied to a Lymphoprep gradient and cells were recovered cell bands formed at the 1.077g/ml and 1.083g/ml Lymphoprep interfaces. The percentage of neutrophils present before sorting and in each cell band were assessed by flow cytometry. The data shown is the mean +/- standard deviation for 3 independent samples per genotype and representative of 3 experiments. **B**: The cells were applied to a calibrated pre-formed continuous Percoll gradient. A band containing 80% of the neutrophils loaded on to the gradient was significantly less dense in S100A9 null mice. Data, representative of five experiments, are expressed as mean +/- standard deviation. **, P>0.001 using Student's T test.

3.2.3 S100 mRNA expression

The difference in density of the two neutrophil populations seems to indicate that there is not a compensatory up-regulation of proteins to replace the absent S100A8/9 heterodimer. Extensive 2D gel analysis has been performed on the S100A9 null bone marrow cells to identify any up-regulation of compensatory proteins. As published in Hobbs *et al,* proteomic analysis was performed on wildtype and S100A9 null bone marrow samples and no differences in any proteins apart from S100A8 and S100A9 could be detected (Hobbs et al., 2003). A related issue was whether any other S100 family members had increased expression to compensate for the absence of the S100A8/9 heterodimer. To satisfy reviewers comments for the Hobbs *et al* publication, RT-PCR studies were performed. First a literature search was undertaken to identify which family members were reported to be expressed in neutrophils, as 19 S100 family members have been identified to date screening all S100 proteins seemed excessive given no gross differences had been observed at protein level. S100A1 and S100A4 have a more ubiquitous distribution or had been reported in neutrophils respectively (Grigorian et al., 1994). As S100Z, a recently reported human neutrophil protein, was found to have a putative sequence for expression in mouse, this was also tested (Gribenko et al., 2001). To detect mRNA expression of these three S100 proteins RT-PCR was performed. Primers were designed to give a product of between 200 and 400 bp with similar annealing temperatures to allow all samples to be run in the same experiment. As a control for the experiment primers were designed to detect S100A8 and S100A9. For the S100A9 protein primers were designed to look for the 3rd coding exon, as a check

for expression of a truncated mutant, given that S100A9 is targeted with an insertional mutation in these animals. Equal quantities of RNA from wildtype and knockout bone marrow cells were used in each experiment.

The data obtained from these experiments is shown in figure 3.3. Expression of S100A8, S100A9, S100A4 and S100A1 mRNA was detected in the wildtype samples. No expression of S100A9 mRNA was found in the S100A9 null samples as expected. Expression of S100A8, S100A4 and S100A1 did not appear to be altered in the S100A9 null bone marrow samples. No S100Z RNA was detected in either wildtype or S100A9 null bone marrow samples. As no indication of differences in expression was observed, it was decided not to follow this line of investigation any further.

This study could have been extended to test primers for all other family members and to quantify any suspected differences by performing quantitative real-time PCR. The study could also be improved by the inclusion of a control primer pair against a constitutively expressed protein such as GAPDH, to confirm that equal RNA amounts are included in all samples. Any more subtle differences could be more easily picked up in a purified neutrophil population, rather than from whole bone marrow. This data along with the 2D gel analysis and western blotting data for S100A8 appear to confirm that no compensatory upregulation of other proteins has occurred in the S100A9 null animals.

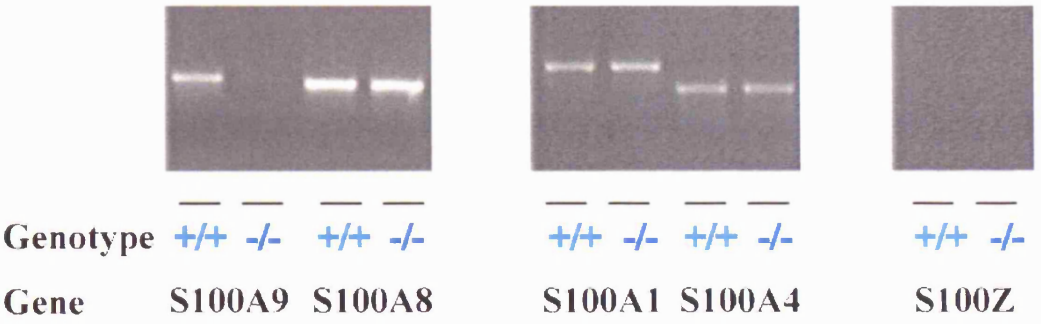

Figure 3.3 Expression of S100 protein mRNA in bone marrow samples from wildtype and S100A9 null mice.

Bone marrow leukocytes were isolated from wildtype and S100A9 null mice. RNA was prepared and reverse transcribed to cDNA. Primers specific to the DNA sequence of various S100 proteins were designed and used in a PCR reaction to form primer specific DNA products. An ethidium bromide-stained 1.8% agarose gel of the PCR products generated is shown. Data is representative of 3 independent experiments.

3.2.4 Leukopoiesis

It has been previously published that leukopoiesis is normal in the S100A9 null mouse (Hobbs et al., 2003). As this data originates from low back-cross mice (generation three), the experiment was repeated on the fully backcrossed (generation ten) mice. This was necessary to confirm that no lesion in leukopoiesis was revealed on the fully C57BL/6J background that may affect the interpretation of both the *in vitro* and *in vivo* data. As many assays are performed in this study using whole bone marrow, it was vital to know that the percentage of neutrophils is the same in both wildtype and S100A9 null samples. Similarly for the *in vivo* assays it must additionally be known that the numbers of circulating neutrophils are the same.

To assess the number of different leukocytes, flow cytometry was performed with antibodies recognising different leukocyte types (figure 3.4a). The number of B cell (B220+), CD4+ and CD8+ positive T cells, neutrophils and monocytes per ml of blood were the same in wildtype and S100A9 null blood samples. When the leukocytes present in bone marrow (number per femur and tibia) were examined, no differences were found in the number of CD4+, CD8+, neutrophils and monocytes. In the experiment represented in figure 3.4a a reduced number of B cells were seen in the S100A9 null mice. This difference was not consistent upon repetition and when subsets of the B220+ population were examined no differences were seen between wildtype and S100A9 null mice (figure 3.4b). This seems to indicate that, as was observed previously, there is no defect in leukopoiesis in the S100A9 null mice.

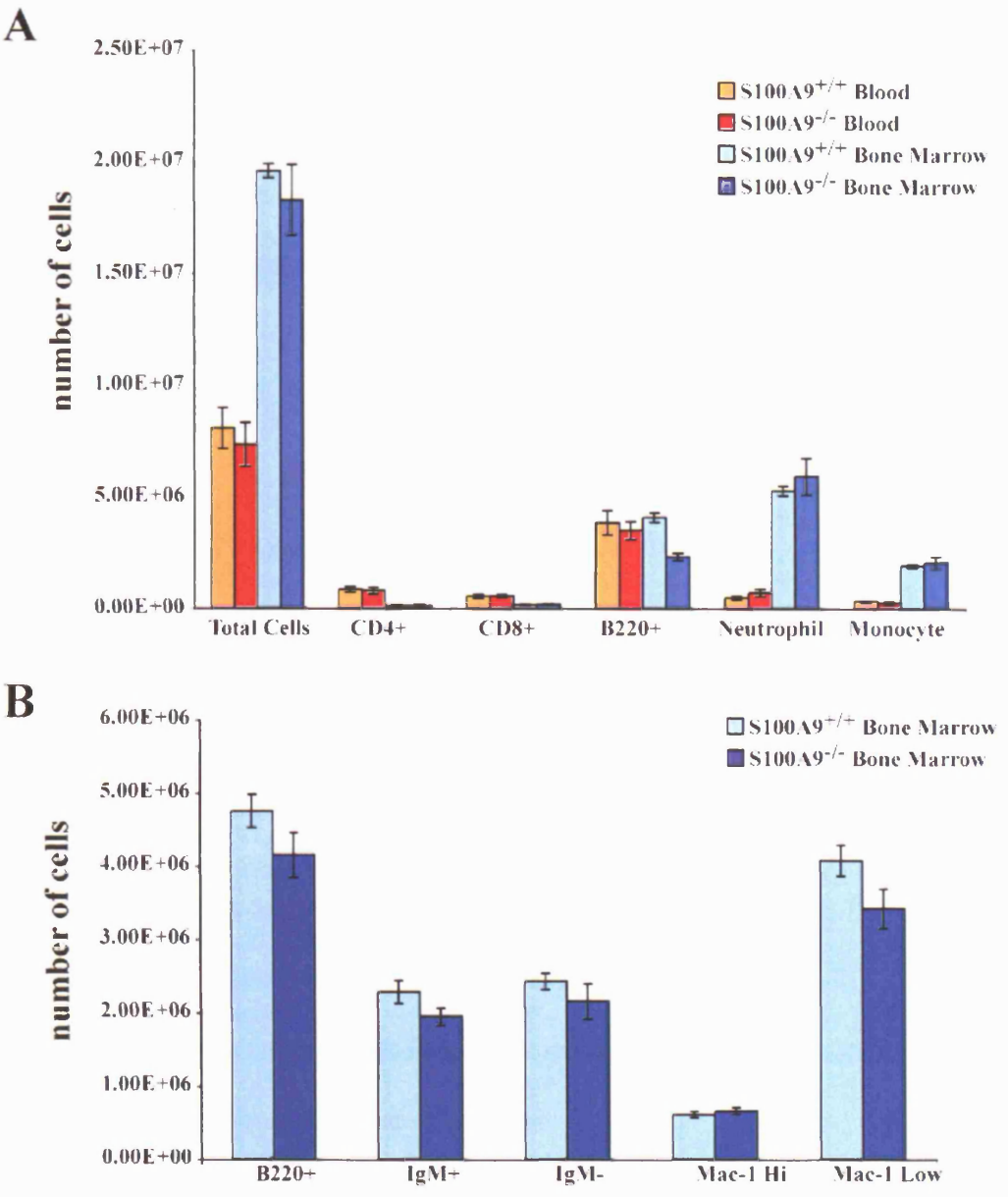

Figure 3.4 Leukopoiesis in wildtype and S100A9 null mice

Leukocytes were isolated from blood (shown as cells/ml) and bone marrow (shown as cells/tibia and femur pooled) of wildtype and S100A9 null mice. Leukocytes were identified and counted by flow cytometry as described in Materials and Methods. Data is from 5 independent samples per genotype and displayed as mean +/- standard error of the mean and representative of 3 experiments.

3.2.5 Myeloid cell development and activation

Having confirmed that the number of myeloid cells is normal in the S100A9 null mice, it was also important to check that the differentiation and activation state of the cells was also normal. Multi-parametric flow cytometry was performed to assess the level of a range of myeloid cell surface molecules on the neutrophils and monocytes in both blood and bone marrow. This was achieved by examining the expression of adhesion molecules L-selectin Mac-1, LFA-1, β1, α4 and the phagocytic receptor FcγRII/III on blood and bone marrow neutrophils (figure 3.5) and monocytes (figure 3.6).

Comparing bone marrow and blood neutrophils, it can be seen that the levels of LFA-1, Mac-1 and L-selectin are higher on the bone marrow neutrophils. The levels of α4 do not appear much higher than background on either bone marrow or blood neutrophils. The levels of FcγRII/III and β1 appear similar on bone marrow or blood neutrophils. The levels of all surface markers studied appeared similar on both blood and bone marrow monocytes.. No differences in expression of any of the six surface markers studied could be detected when S100A9 null mice were compared to wildtype.

This data shows no difference in the differentiation or activation of the S100A9 null myeloid cells compared to the wildtype cells. The increased expression of Mac-1, LFA-1 and L-selectin on bone marrow versus blood neutrophils seems to imply that the bone marrow neutrophils are potentially more adhesive, however the activation state of the integrins are not known. The increased expression could be due to chemokine signalling causing their retention in the bone marrow under normal conditions. The data relating to the up-

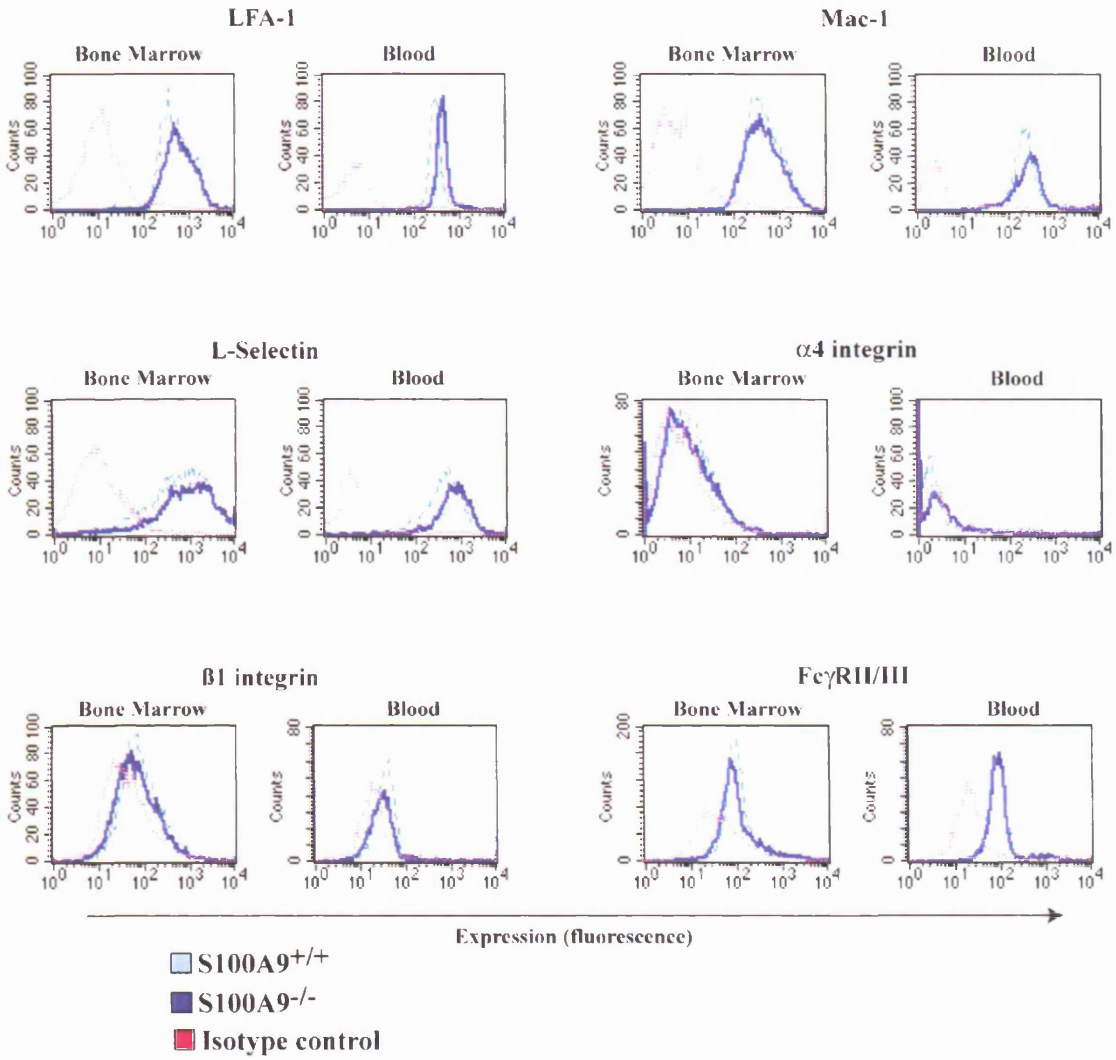

Figure 3.5 Expression of surface markers of differentiation and activation by neutrophils

Neutrophils from blood and bone marrow of wildtype and S100A9 null mice were identified by staining cells with mAbs 7/4 and Ly-6G. The expression of cell surface molecules was determined by flow cytometry after co-labelling cells with a panel of antibodies as described in the Materials and Methods. Data shown is for pooled samples from 5 independent animals per genotype.

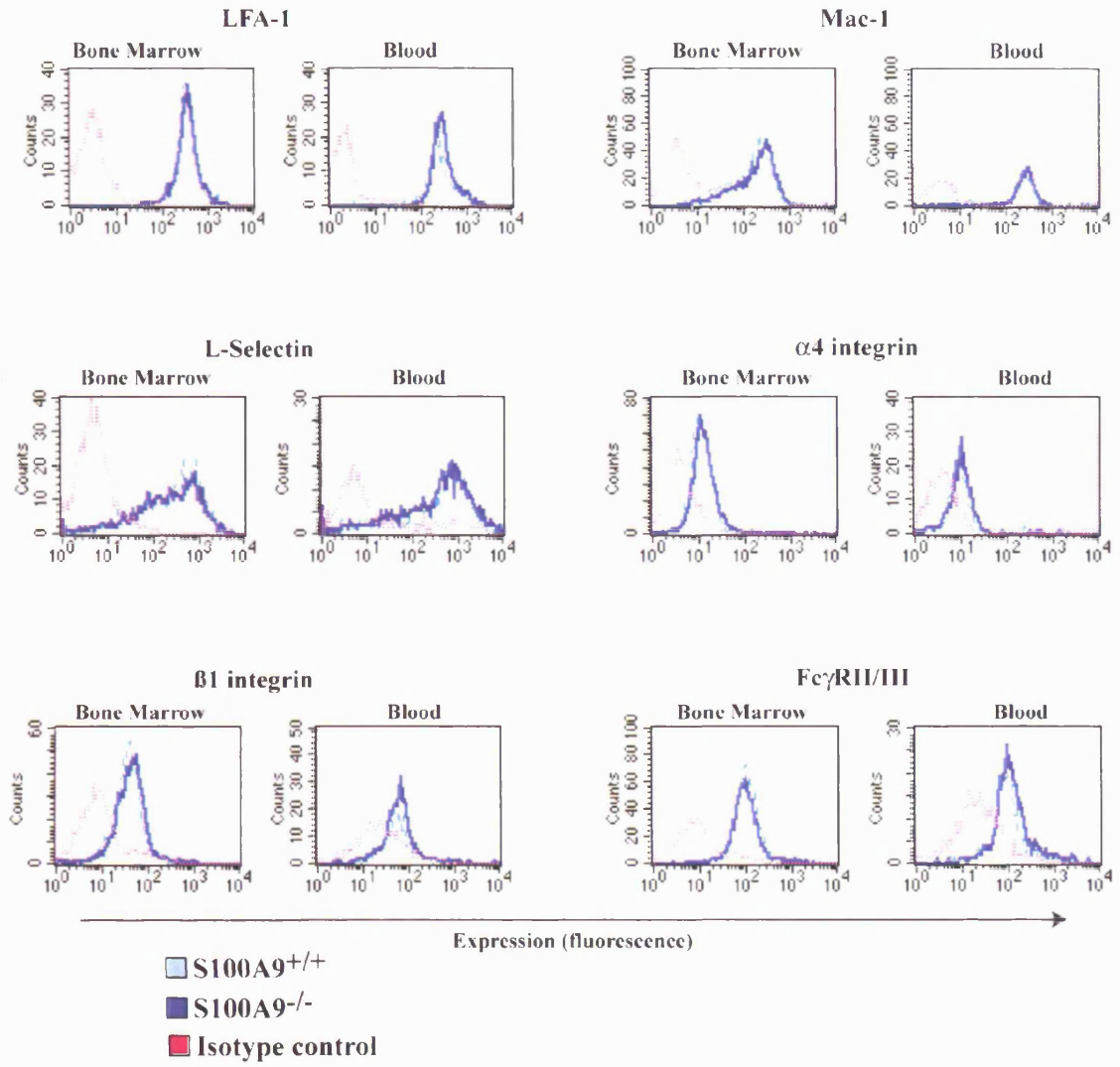

Figure 3.6 Expression of surface markers of differentiation and activation by monocytes

Monocytes from blood and bone marrow of wildtype and S100A9 null mice were identified by staining cells with mAbs 7/4 and Ly-6G. The expression of cell surface molecules was determined by flow cytometry after co-labelling cells with a panel of antibodies as described in the Materials and Methods. Data shown is for pooled samples from 5 independent animals per genotype.

regulation of Mac-1 in response to inflammatory stimuli will be presented later in this thesis.

3.2.6 CXCR4 expression

As a final comparison to confirm that the S100A9 null myeloid cells were maturing normally the expression of CXCR4 was examined on these cells. CXCR4 levels have been reported to be high on bone marrow myeloid cells, acting as a mechanism for their retention at this site until required/mature as the CXCR4 ligand SDF-1 is highly expressed in bone marrow (Martin et al., 2003a). When the mature cells are released from the bone marrow, it is reported that they have a lower CXCR4 level reducing their retention in the bone marrow. Their release is thought to occur via an axis of this change in CXCR4 expression and a concurrent rise in CXCR2 expression allowing the CXCR2 ligands to mediate their entry into the systemic circulation (Martin et al., 2003a).

The expression of CXCR2 is seen to be normal in the S100A9 null bone marrow neutrophils (this data is shown in chapter 4 (figure 4.2b)). The expression of CXCR4 is similar on neutrophils and monocytes from both wildtype and S100A9 null mice in the bone marrow (figure 3.7). The expression of CXCR4 is higher in bone marrow than in the blood on both cell types. The expression of CXCR4 on blood neutrophils is higher than on blood monocytes. No difference in CXCR4 expression on blood myeloid cells is seen between S100A9 null and wildtype mice. These data concerning the number and state of the myeloid cells in blood and bone marrow show that the development and maturation of myeloid cells in the S100A9 null mouse is normal.

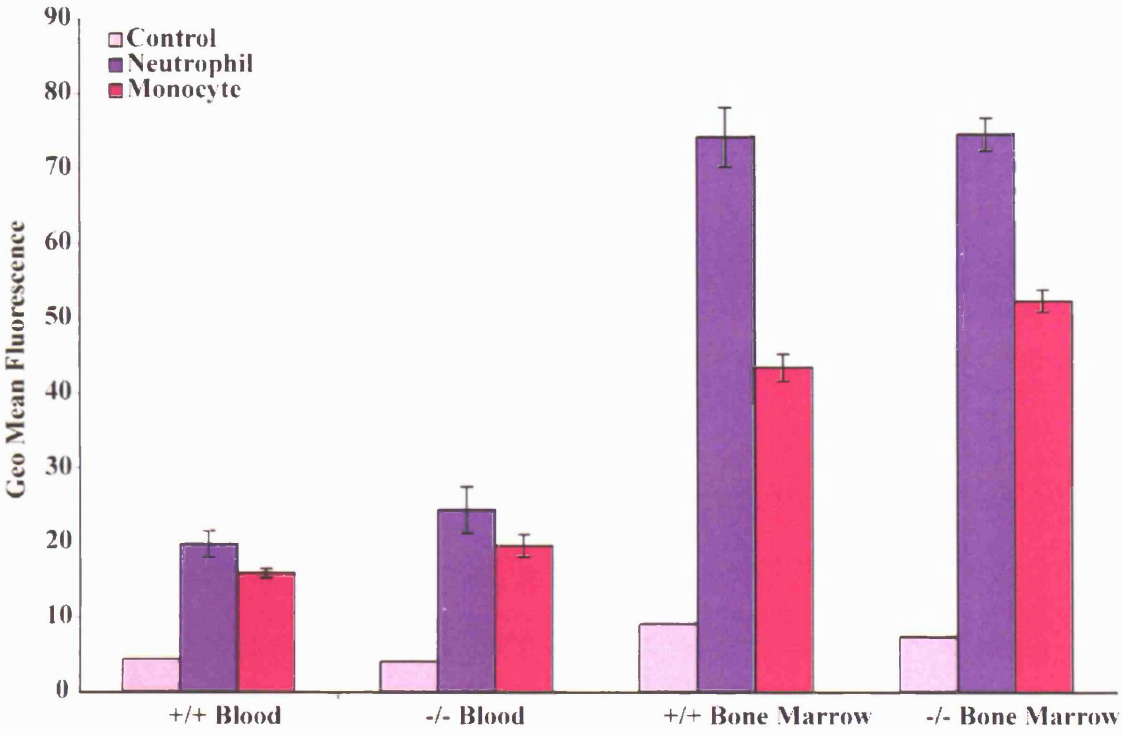

Figure 3.7 Expression of CXCR4 by wildtype and S100A9 null myeloid cells

Myeloid cells from blood and bone marrow of wildtype and S100A9 null mice were identified by staining cells with mAbs 7/4 and Ly-6G, The expression of CXCR4 was determined by co-labelling cells with mAb anti-CXCR4 as described in the materials and methods. Data is shown as mean fluorescence of 5 independent samples per genotype +/- standard deviation.

3.3 Discussion

3.3.1 Compensation

If we consider the work in the context of the other data gained from the characterisation of the S100A9 null mice ((Hobbs et al., 2003)), we have good evidence that the S100A9 null mice show no compensatory upregulation of other proteins. The findings in our original publication that S100A8 is absent in these mice, despite normal levels of message being present, are reflected in the RT-PCR data presented. S100A8 RNA levels are unaltered as would be expected as normal RNA levels were found by RNAse protection previously (Hobbs et al., 2003). S100A8 protein is totally absent in the mature animal, as shown by 2D gel analysis, immunohistochemistry and western blotting. Those experiments showed that when 175 proteins found by 2D gel analysis were compared in S100A9 null and wildtype mice the only proteins altered in expression were S100A8 and S100A9. It was thought that a more subtle alteration in the expression of other leukocyte expressed S100 family members, or a low level expression of a truncated fragment of S100A9 could be occurring. No obvious differences in the RNA levels of the S100 proteins examined were found. Taking all these pieces of data into account along with the altered density of the S100A9 null neutrophils it seems clear that no compensatory changes in protein expression have occurred.

3.3.2 Normal myelopoiesis

The initial characterisation of the S100A9 null mice provides good evidence that S100A9 is not required for the production of normal mature neutrophils or monocytes. The first evidence comes from the normal number of

these myeloid cells being present in blood and bone marrow. This seems to imply that the steady state numbers being produced are normal in the S100A9 null mice. That normal numbers are found in the circulation implies that they are responding normally to signals to retain and release these cells from the bone marrow. A phenotypic study of the myeloid cells shows that the maturation and activation state of these cells is normal given that the expression of various surface markers is normal. Also the levels of CXCR4, a chemokine receptor associated with retention in the bone marrow, are similar on wildtype and S100A9 null cells in blood and bone marrow.

The presence of normal leukopoiesis and the normal differentiation and activation state of the S100A9 null neutrophils shows that S100A9 is dispensable for this process in mice. The absence of S100A8 protein in the mature animal seems to imply that this protein also plays no role in myeloid development in the adult animal. This evidence is partially in conflict with data published for an independent line of S100A9 null mice (Manitz et al., 2003). In the Manitz study no S100A8 protein could be detected by western blot from peripheral blood leukocyte, spleen or bone marrow. However, S100A8 reactivity of bone marrow cells was detected by immunohistochemical means. More robust evidence of the actual presence of S100A8 protein detected by biochemical means at the correct molecular size would be needed to confirm this is indeed S100A8.

It was concluded by Manitz *et al* that there was a shift in the myelomonocytic potential of the S100A9 null bone marrow, however the data presented is unconvincing. Bone marrow cells were cultured in Teflon bags for 4 days and the number of cells expressing surface markers including Gr1 and CD11b were assessed. It was observed in the publication that slight differences in

the cell numbers could be seen. The colony formination by bone marrow cells stimulated with IL-3, GM-CSF, G-CSF or M-CSF was also studied to evaluate the myelomonocytic potential. In this experiment it was again observed that some small variation between the potential of wildtype and S100A9 null cells was seen. Analysis of the data presented for these two experiments does not appear to show any of these differences to be significant, with wildtype and S100A9 samples having overlapping error bars in most cases and no statistical evaluation being performed.

The normal number and developmental status of the S100A9 null neutrophils in blood and bone marrow allows the role of the protein in other neutrophil functions to be investigated, without any observed effects being a possible result of the cells being in a different state. The low number of neutrophils in murine blood, and the limited quantities that can be obtained per animal makes the use of this source impractical for performing further *in vitro* assays. This leaves the more abundant source of neutrophils in the bone marrow as the best to use. Given the difference in density of the S100A9 null neutrophils the use of the simple two-step gradient to enrich the neutrophil population will not be appropriate to use. The process of forming the Percoll gradient is relatively time consuming and there may be different populations of cells contaminating the S100A9 null and wildtype bands given their different densities. As such un-fractionated bone marrow was used in the majority of *in vitro* studies conducted for this publication.

The evidence presented in this section shows no role for S100A9 in the development and maturation of neutrophils or monocytes. Despite the expression

of S100A9 during the development of myeloid cells, as discussed in the introduction, there appears to be no non-redundant role for it in myelopoiesis.

CHAPTER 4

4 Calcium signalling in S100A9 null neutrophils

4.1 Introduction

S100A8/9 are low molecular weight calcium binding proteins of the EF-hand type. Proteins of the S100 family are assumed to be calcium sensor proteins, rather than potent calcium buffering proteins. Upon calcium binding S100 dimers undergo a conformational change exposing a hydrophobic interaction surface, presumably mediating their interaction with target proteins (reviewed in (Marenholz et al., 2004)). Other S100 proteins have been highlighted as having a role in calcium homeostasis. Lack of S100B causes enhanced calcium transients in glial cells, and overexpression of S100A1 causes increased calcium loading of the sarcoplasmic reticulum in cardiomyocytes (Most et al., 2003; Xiong et al., 2000). As calcium binding proteins form part of the cellular calcium signalling machinery it seemed logical to investigate the ability of the S100A9 null neutrophils to transduce a calcium signal.

There is evidence of almost all neutrophil functions being regulated by calcium from phagocytosis and superoxide burst to apoptosis (Reviewed in (Ayub and Hallett, 2004; Dewitt et al., 2003)). One of the most well defined stimuli of calcium signalling in neutrophils is chemoattractant-induced calcium signalling. Despite many years of study the exact mechanism and purpose of the calcium-induced signal is still not fully defined. The calcium response to chemoattractants

provides a simple system to examine whether the S100A9 null neutrophils are capable of normal calcium signalling.

The first point to address when designing a system to analyse calcium signalling in murine neutrophils is the source of the cells. In the mouse only 5% blood leukocytes are neutrophils, and typically only 500-700µl of blood can be obtained from a mouse, however murine bone marrow consists of 25-30% neutrophils. Although these may not be as 'mature' as the circulating blood neutrophils they have been shown to exhibit calcium flux upon chemoattractant stimulation (Hobbs et al., 2003). Using murine bone marrow as a source of neutrophils requires working with a mixed cell population and makes studying the calcium properties of the S100A9 null neutrophils more complicated. The percentage of neutrophils can be enriched in a bone marrow population, but the difference in density of the S100A9 null neutrophils causes differential partitioning of the neutrophils in an enriching gradient as discussed in chapter 3. Traditional studies often rely on using a cuvette based method where the whole population of cells is loaded with a calcium indicator dye and the change in fluorescence of the entire population is monitored. Using whole murine bone marrow as a source of neutrophils makes this approach inappropriate for a number of reasons:

1. The neutrophils make up only 20-30% of the total population and so any difference in response to an 'all-cell' stimulus in the knockout cell population could be masked by the other unaffected cells.

2. Chemokines are a potent stimulus of calcium flux in the neutrophil, and many stimuli of this type are specific for neutrophils alone. The response to these

specific agents may be masked by the majority population, which will remain unresponsive.

To address these issues it was decided to study the neutrophil calcium response by flow cytometry. The murine neutrophil can be readily identified by flow cytometry by dual mAb staining with anti-Ly-6G and 7/4 antibodies (Henderson et al., 2003). Staining the whole population of bone marrow cells with this antibody combination will allow the neutrophils to be identified and analysed in isolation from the rest of the cells, eliminating the problems above.

In comparing a population of cells from two different animals it becomes critically important that no difference in calcium indicator loading affects the results. Although it could be argued that the loading of the two bone marrow populations would be controlled by maintaining equal concentrations of indicator dye and cells, any differences in the state or number of cells could still theoretically lead to differential loading of different batches of cells. The use of a ratiometric calcium indicator dye will remove any problems of differential dye loading, as ratiometric calcium indicator dye gives a measure of calcium concentration within the cell that is largely independent of dye concentration. INDO-1 is excited by UV light to emit fluorescence at 2 different wavelengths dependent on it being in a calcium-bound or calcium-free state (use of ratiometric dyes reviewed in (Hallett et al., 1996; Hallett et al., 1999; Rudolf et al., 2003)). The calcium concentration within the cell is proportional to the ratio of these dye states. By flow cytometry this ratio can be calculated for every cell and as the absolute concentration of dye within each cell does not affect the ratio per se then any small differences in dye loading between wildtype and knockout animal will have no effect. INDO-1 is also particularly useful as it is available as a lipophilic

AM-ester. This allows uptake of the hydrophilic dye by the cell after which it is cleaved by cellular esterases to release the INDO-1 compound (loading AM-esters into neutrophil reviewed in (Hallett et al., 1996; Hallett et al., 1999)).

In this section the basic calcium homeostasis and induced calcium signals in the S100A9 null neutrophils will be examined. In order to assess whether the deletion of S100A9 has had an impact on the calcium signalling potential of the neutrophils it makes sense to look both at their ability to handle calcium and their ability to form a calcium flux in response to physiological stimuli. To examine if the gross manner in which the cell handles calcium is the same in wildtype and S100A9 null cells, the response of the cells to a high level of extracellular calcium entry (using the calcium ionophore ionomycin), the loading of the intracellular stores (by causing emptying of these stores using thapsigargin which inhibits the Ca^{2+}ATPase causing leaching of the calcium into the cytosol) and the refilling mechanism of the intracellular stores by Store Operated Calcium Entry (SOCE) were studied. Should all these parameters appear unaffected, it would be concluded that there was no gross defect in calcium homeostasis in the knockout cells. To test the ability of the cells to mount a calcium response to a physiological stimulus, it was decided to examine the response to chemoattractant stimulation. It has been previously published by this lab that the S100A9 null neutrophils exhibit reduced calcium signalling to sub maximal levels of chemokine stimulation (Hobbs et al., 2003). I have followed up this observation by investigating the response to a range to different chemoattractant stimuli and attempting to elucidate the mechanism of this lesion in the S100A9 null cells.

The aim of this section is to examine the calcium signalling in the S100A9 null neutrophils and to define and describe any lesion as far as possible. Due to

the limitations of using primary murine neutrophils to examine cell signalling my studies to localise the defect to one particular pathway have relied heavily on pharmacological means. The tools available to study calcium signalling in whole cells are limited and due to the 'delicate' nature of the murine neutrophil, invasive means such as micro-injection or DNA construct transfections would not yield definitive results.

4.2 Results

4.2.1 Neutrophil calcium homeostasis

Treatment of the S100A9 null and wildtype neutrophils with the calcium ionophore ionomycin, which causes calcium influx across the plasma membrane, elicited an identical sustained rise in intracellular calcium of similar magnitude and kinetics in both groups (figure 4.1a). That the magnitude of the response is equal in both cell types implies that S100A8/9 is not acting as a major cellular calcium buffer. If an abundant calcium buffer were absent it would be expected that the peak of a response would be much greater, with more of the calcium being available to bind the indicator dye and less binding to endogenous buffers thus higher cytosolic calcium would be registered. This situation is observed in the calbindin D28k (a cellular calcium buffer) knockout animal (Airaksinen et al., 1997). In these animals stimulation of the afferent climbing fibre, a neuronal cell expressing high levels of calbindin D28K, causes a higher transient calcium

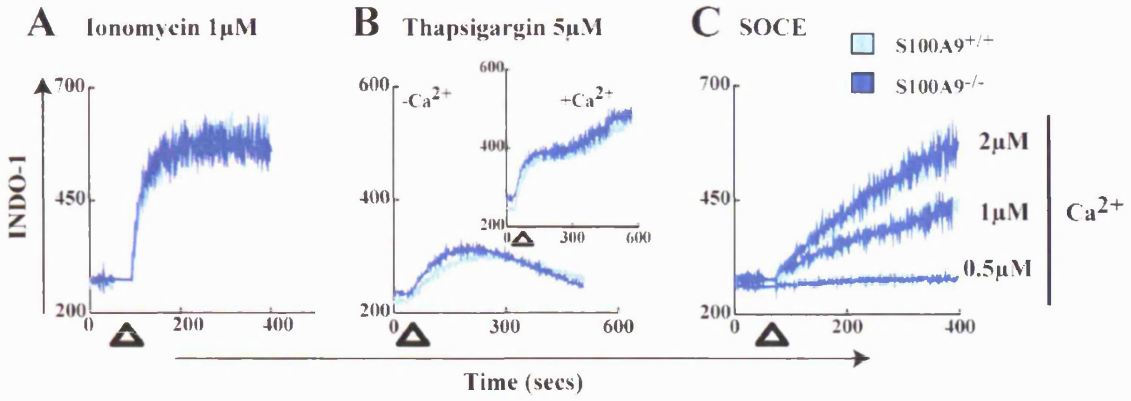

Figure 4.1 Normal calcium homeostasis in S100A9 null neutrophils.

Bone marrow leukocytes were loaded with Indo-1 and were identified by labelling with mAbs 7/4 and Ly-6G. Intracellular calcium concentration was monitored by flow cytometry and was expressed as an arbitrary figure, based on the ratio of Indo-1 fluorescence at 424nm and 530nm. The median response neutrophil Indo-1 ratio of ≈500-700 events is plotted every second. The response to stimulation, in the presence of extracellular calcium, with 1μM ionomycin (A) and 5μM thapsigargin in the presence/absence of extracellular calcium by chelation with EGTA is shown (B and inset). C: Store operated calcium entry is examined by treatment of the neutrophils with 5μM thapsigargin in the absence of extracellular calcium, prior to add-back of calcium at 0.5-2μM. All data representative of 3 or more independent experiments.

spike in heterozygous and null animals compared to wildtype, even though resting calcium levels are normal.

Thapsigargin is an inhibitor of the Ca^{2+} ATPase, an ion channel located on the endoplasmic reticulum, causing emptying of the calcium stores by leakage through this channel. Treatment of the cells with thapsigargin caused a transient increase in cytosolic calcium levels in the absence of extracellular calcium in both wildtype and S100A9 null neutrophils (figure 4.1b). The duration and magnitude of this response gives an indication of the loading of the intracellular stores, which appears equal in wildtype and S100A9 null cells. There was no consistent difference in the S100A9 null and wildtype responses. When the cells were treated with thapsigargin in the presence of extracellular calcium there was a bi-phasic increase in intracellular calcium concentration after which the calcium concentration reached a plateau. This response was similar in wildtype and S100A9 null neutrophils. The second phase of calcium elevation is caused by opening of calcium channels on the cell surface to allow re-filling of the emptying stores. This process is called Store Operated Calcium Entry (SOCE). That the profiles of cytosolic calcium concentration are similar in wildtype and S100A9 null cells implies that the SOCE process is working normally. However this can be more directly assessed by treating the cells with thapsigargin in calcium free buffer to fully empty the calcium stores, then adding back calcium to the buffer and observing the profiles of the response. Figure 4.1c shows that SOCE in the wildtype and S100A9 null cells is identical over a range of extracellular calcium concentrations.

4.2.2 Reduced MIP-2-induced calcium signalling

The wildtype and S100A9 null cells were stimulated with a titration of the neutrophil chemokine MIP-2 in the presence of extracellular calcium, as shown in figure 4.2a. At higher levels of chemokine (10ng/ml) no difference in the magnitude or duration of the calcium response in the wildtype or S100A9 null neutrophils was seen. At lower levels of stimulation (1ng/ml and 0.3ng/ml) there was a decreased calcium flux response in the S100A9 null neutrophils compared to the wildtype cells. This shift in the dose response to MIP-2 could theoretically be explained by a lower expression of the MIP-2 receptor (CXCR2) on the cell surface. To test this possibility bone marrow cells from wildtype and S100A9 null animals were immuno-stained with a polyclonal anti-(murine) CXCR2 antibody (gift from RM Strieter, UCLA) and fluorescent secondary antibody. The cells were then further stained with the mAb 7/4 and IA8 cocktail to identify the neutrophils as before. Flow cytometric analysis of the neutrophil population showed similar expression of CXCR2 on both the wildtype and S100A9 knockout neutrophils (figure 4.2b).

4.2.3 Reduced calcium signalling to a range of chemoattractants

To examine the extent of the lesion in calcium signalling in the S100A9 null neutrophils a range of chemokines were titrated against wildtype and S100A9 null cells. Figure 4.3 shows that titration of the murine chemokine KC, which is also a ligand of CXCR2, showed a similar defect to that seen in response to MIP-2. Similarly to MIP-2, there was no defect in calcium flux response to high levels of KC, but decreased magnitude of the calcium flux response to lower levels of

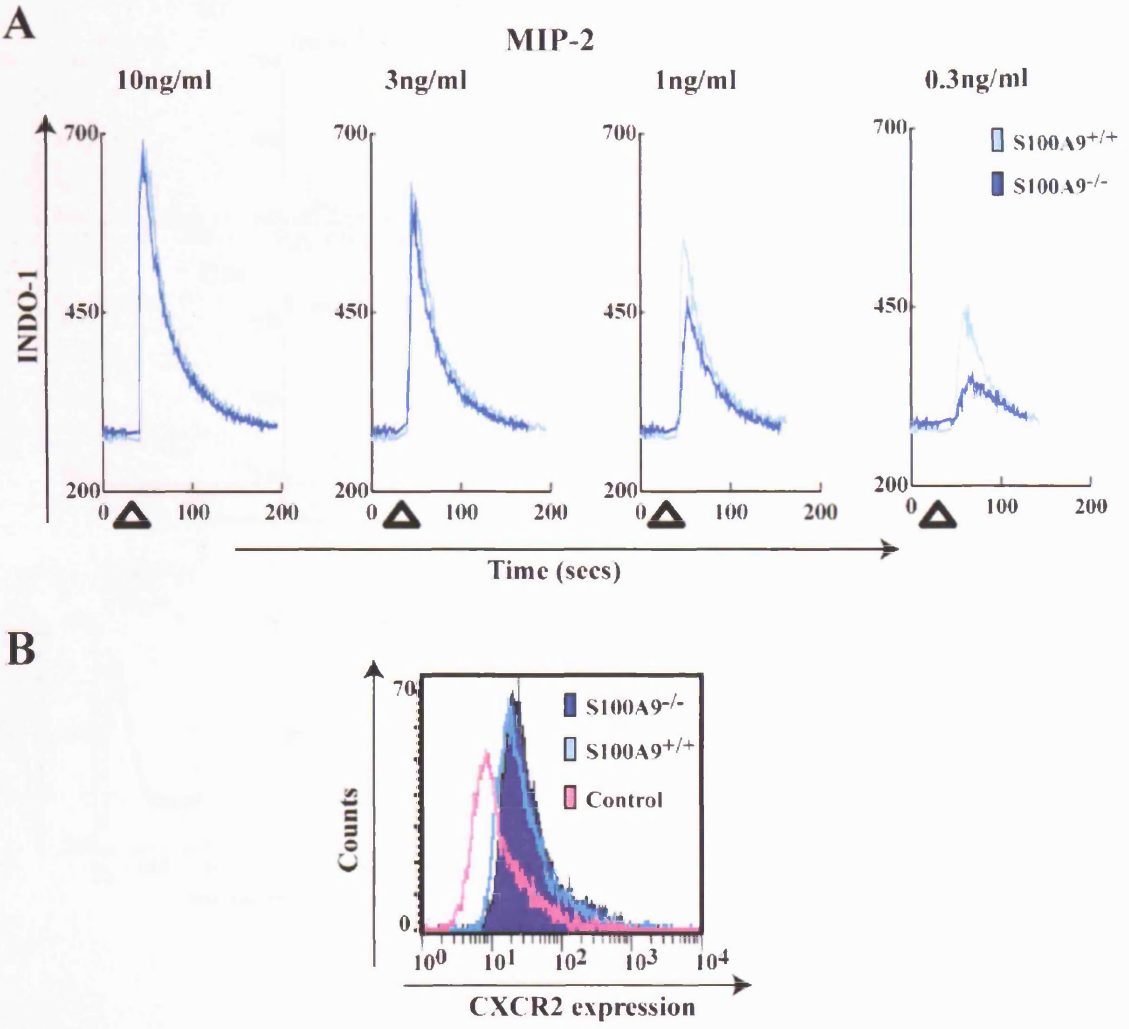

Figure 4.2 Reduced calcium response to MIP-2 but normal CXCR2 expression by S100A9 null neutrophils

Bone marrow leukocytes were loaded with Indo-1 and were identified by labelling with mAbs 7/4 and Ly-6G. Intracellular calcium concentration was monitored by flow cytometry and was expressed as an arbitrary figure, based on the ratio of Indo-1 fluorescence at 424nm and 530nm. The median response neutrophil Indo-1 ratio of ≈500-700 events is plotted every second. A: The response of neutrophils to the chemokine MIP-2. Data representative of 3 independent experiments. B: The cell surface expression of CXCR2 was determined by co-labelling cells with antibody as described in the materials and methods. Flow cytometry data presented for pooled samples of 3 independent mice per genotype.

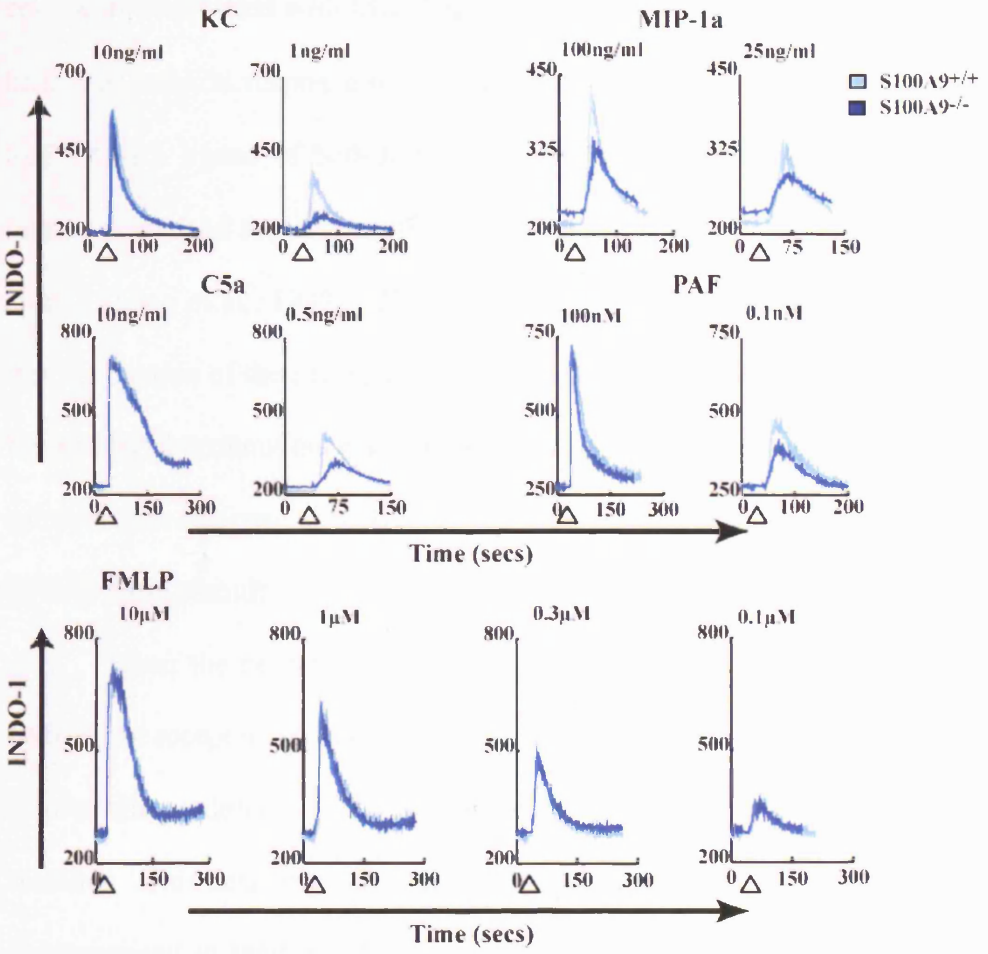

Figure 4.3 Reduced calcium response to the chemoattractants KC, MIP-1α, C5a and PAF but not FMLP in S100A9 null neutrophils.

Bone marrow leukocytes were loaded with Indo-1 and were identified by labelling with mAbs 7/4 and Ly-6G. Intracellular calcium concentration was monitored by flow cytometry and was expressed as an arbitrary figure, based on the ratio of Indo-1 fluorescence at 424nm and 530nm. The median response neutrophil Indo-1 ratio of ≈500-700 events is plotted every second. Neutrophils from wildtype and S100A9 null mice were stimulated with KC, MIP-1α, C5a, PAF and FMLP. Data representative of 3 independent experiments (2 for PAF).

KC in the S100A9 null compared with wildtype cells. When the S100A9 null cells were stimulated with MIP-1α, a decreased calcium flux in the S100A9 null cells was seen in response to all concentrations of this chemokine. Although MIP-1α is a ligand of both the CCR1 and CCR4 chemokine receptors, in the murine neutrophil the calcium flux is elicited by stimulation of the CCR1 receptor alone (Zhang et al., 1999). The chemoattractants PAF and C5a caused calcium flux by ligation of their receptors, PAF receptor and C5a receptor respectively. In the S100A9 knockout out cells, the same pattern was observed of no difference in calcium flux response at high levels of these stimuli, but a defect at lower levels of both these stimuli.

When the neutrophil stimulant FMLP, which stimulates the FMLP and FMLP-like receptors on neutrophils, was applied to the wildtype and S100A9 null neutrophils no defect in calcium flux response was seen at any concentration of stimulus. This data seems to indicate that while the S100A9 null neutrophils are compromised in their ability to produce a calcium flux response to a range of chemoattractant stimuli, this lesion is not a generalised reduced reactivity, but a problem with a specific signalling pathway that is used by some but not all chemoattractants.

4.2.4 Defect in intracellular calcium release

To localise the observed deficiency to a particular pathway, the first step is to study the source of the calcium measured in these responses. The change in cytosolic calcium concentration in response to a chemoattractant stimulus can be made up of calcium from two general sources: intracellular calcium release from the intracellular calcium stores and extracellular calcium entry through calcium channels on the cell surface. To ascertain which calcium source(s) are being used

to form the calcium responses seen in this study, the cells were stimulated with the various chemoattractant stimuli in the presence of extracellular calcium, as before, or in the absence of extracellular calcium (figure 4.4).

When the neutrophils were stimulated with a high concentration of MIP-2 (20ng/ml) the calcium response has a similar magnitude but decreased duration when the cells are stimulated in the absence of extracellular calcium compared with the response in the presence of extracellular calcium. In cells stimulated with a lower dose of MIP-2 (1ng/ml) the response had a similar magnitude and duration in the presence and absence of extracellular calcium and the lesion in the S100A9 null response is evident in both conditions. This implies that the majority of the calcium contributing to this response is coming from the intracellular calcium stores, with a minor component of extracellular calcium entry contributing at high levels of chemokine. Removing extracellular calcium does not reveal a further lesion in S100A9 null neutrophil signalling and does not affect the deficiency seen at the lower level of MIP-2 stimulation. This seems to indicate that the lesion is in intracellular calcium release rather than extracellular calcium entry. Experiments with similar results were performed with C5a as the stimulus. These showed that the majority of the calcium flux response was due to intracellular calcium release, but that the magnitude and duration of the response to a high level of C5a was reduced in the absence of extracellular calcium. In particular the elevated baseline following stimulation with high concentrations of C5a is returned to the pre-stimulation baseline in the absence of extracellular

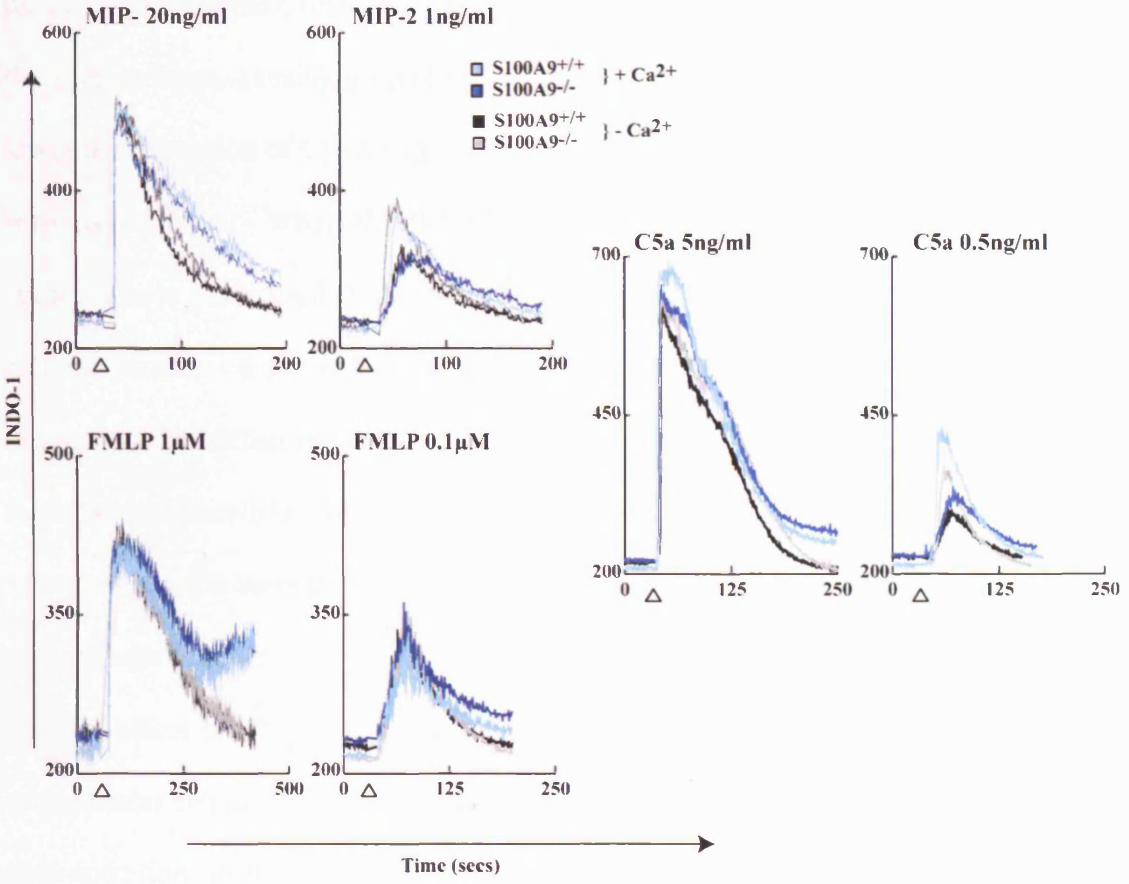

Figure 4.4 The lesion in calcium signalling in S100A9 null neutrophils is in intra-cellular calcium release

Bone marrow leukocytes were loaded with Indo-1 and were identified by labelling with mAbs 7/4 and Ly-6G. Intracellular calcium concentration was monitored by flow cytometry and was expressed as an arbitrary figure, based on the ratio of Indo-1 fluorescence at 424nm and 530nm. The median response neutrophil Indo-1 ratio of ≈500-700 events is plotted every second. Neutrophils from S100A9 null and wildtype mice were stimulated with MIP-2, C5a and FMLP in the presence and absence of extracellular calcium (calcium removed by chelation with EGTA). Data representative of 3 independent experiments.

calcium. This seems to imply that extracellular calcium entry plays a small role in the rapid calcium peak seen and that after this initial reaction calcium channels on the surface open, causing a sustained elevation in intracellular calcium. At the lower concentration of C5a a slight decrease in the magnitude and duration of the response is seen. When the difference between wildtype and S100A9 null neutrophils is considered in this experiment, no effect of removing extracellular calcium is seen on the relative differences between the 2 groups. This again implies that the defect in the S100A9 null cells is in intracellular calcium release, rather than extracellular calcium entry.

When the response to FMLP is studied in the presence and absence of extracellular calcium, it is seen that at high concentrations of FMLP (10μM) there is little effect on the magnitude of the initial calcium peak of removing the extracellular calcium. However, there is a sustained increase in cytosolic calcium concentration following the initial calcium flux peak and this sustained concentration of calcium is not seen when the extracellular calcium is chelated. At lower levels of calcium there is no effect on the magnitude of the response and only a slight affect on the duration of the response is evident. This data indicates that similarly to C5a, extracellular calcium entry pathways are activated in response to FMLP, that allow a sustained elevation of intracellular calcium concentration following the initial peak of the response. When the wildtype and knockout cells are compared it is seen that removing the extracellular calcium does not reveal a lesion in the calcium flux response in the S100A9 null cells. This shows that enhanced extracellular calcium entry is not compensating for the intracellular calcium release deficiency seen in the other responses in the S100A9 null cells. To elucidate the intracellular calcium release pathway compromised in

the S100A9 null cells, a pharmacological study comparing the effect of different agents on the FMLP and MIP-2 responses in the wildtype and S100A9 null neutrophils was undertaken.

4.2.5 Signalling via a G-protein coupled pathway

Previous studies on signalling by FMLP and IL-8 (human homolog of MIP-2) have shown these proteins to signal by G-protein coupled pathways (Jiang et al., 1996; Schorr et al., 1999). To confirm that both the MIP-2- and FMLP-induced calcium flux responses occur via a G-protein coupled receptor pathway in this system, the cells were pre-incubated in the presence of pertussis toxin (figure 4.5). This toxin blocks most G-protein activity. When the responses to MIP-2 and FMLP were compared to responses observed in the presence of PTX it was seen that the magnitude of the responses was reduced in both wildtype and S100A9 null cells. A long incubation with PTX of 90 minutes at 37°C was required to allow this relatively non-cell permeable toxin to pass into the cells.

To confirm if the G protein-coupled calcium release pathways were broadly normal in these cells, they were treated with AlF_4^- (figure 4.5). This moiety non-specifically activates G-proteins. AlF_4^- had a lag time of around 5 mins and caused a bi-phasic increase in calcium concentration with an early small increase in calcium concentration and a later further, more marked, increase in calcium concentration. This response was similar in wildtype and S100A9 null cells.

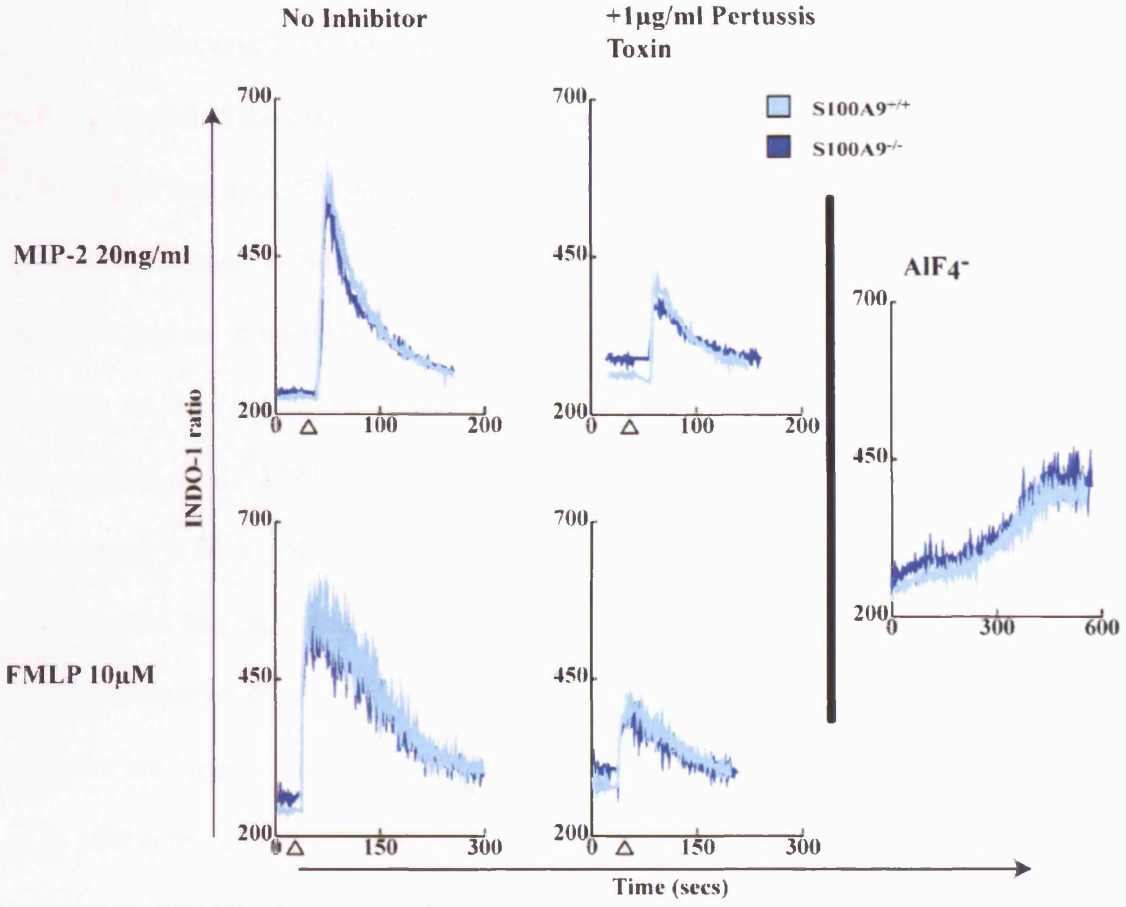

Figure 4.5 Function of G-proteins in S100A9 null and wildtype neutrophils

Bone marrow leukocytes were loaded with Indo-1 and were identified by labelling with mAbs 7/4 and Ly-6G. Intracellular calcium concentration was monitored by flow cytometry and was expressed as an arbitrary figure, based on the ratio of Indo-1 fluorescence at 424nm and 530nm. The median response neutrophil Indo-1 ratio of ≈500-700 events is plotted every second. The bone marrow leukocytes were pre-incubated with 1µg/ml pertussis toxin for 90 minutes at 37°C prior to stimulation with MIP-2 or FMLP. In addition the cells were stimulated with a solution of AlF_4^- (due to the lag in initiation of a calcium signal data is shown from the initiation of the signal at 5 minutes post-stimulation). Data shown was obtained in duplicate in 2 independent experiments.

4.2.6 IP_3 mediated calcium release pathway

As discussed in the Introduction, the IP_3-mediated calcium release pathway is one of the major calcium release pathways in non-excitable cells. The most potent and specific pharmacological inhibitor of the IP_3 receptor, a ligand gated ion-channel, is heparin. Unfortunately heparin is not a cell-permeable inhibitor and so is unsuitable for use in this system. A relatively new tool for looking at IP_3 receptor activity is 2-aminoethoxydiphenylborate (2-APB) (Maruyama et al., 1997). In its effects on intra-cellular calcium release, this compound is a highly selective inhibitor of this receptor. More recent investigation has indicated that it has a broader range of activity than originally thought (Bootman et al., 2002; Peppiatt et al., 2003). The 'other' functions of this inhibitor are largely related to its effects on extracellular calcium entry pathways or to effects on mitochondria following prolonged exposure. As we are primarily looking at intracellular calcium release, 2-APB will act selectively to inhibit the IP_3 receptor in this context. In order to more easily interpret any differential effects of 2-APB on the S100A9 neutrophils, the effect of the inhibitor was examined at a dose of chemoattractant that gave equal calcium flux responses in wildtype and S100A9 null neutrophils. It was seen that applying 50μM 2-APB to the cells at the beginning of an experiment caused a large decrease in the MIP-2-induced calcium flux response in the S100A9 null cells and had only minimal effects on the wildtype cells (figure 4.6a). Other repetitions of this experiment have shown that the wildtype response can also be inhibited so is not resistant to the effects of 2-APB. That inhibition of the IP_3 receptor has a greater effect on

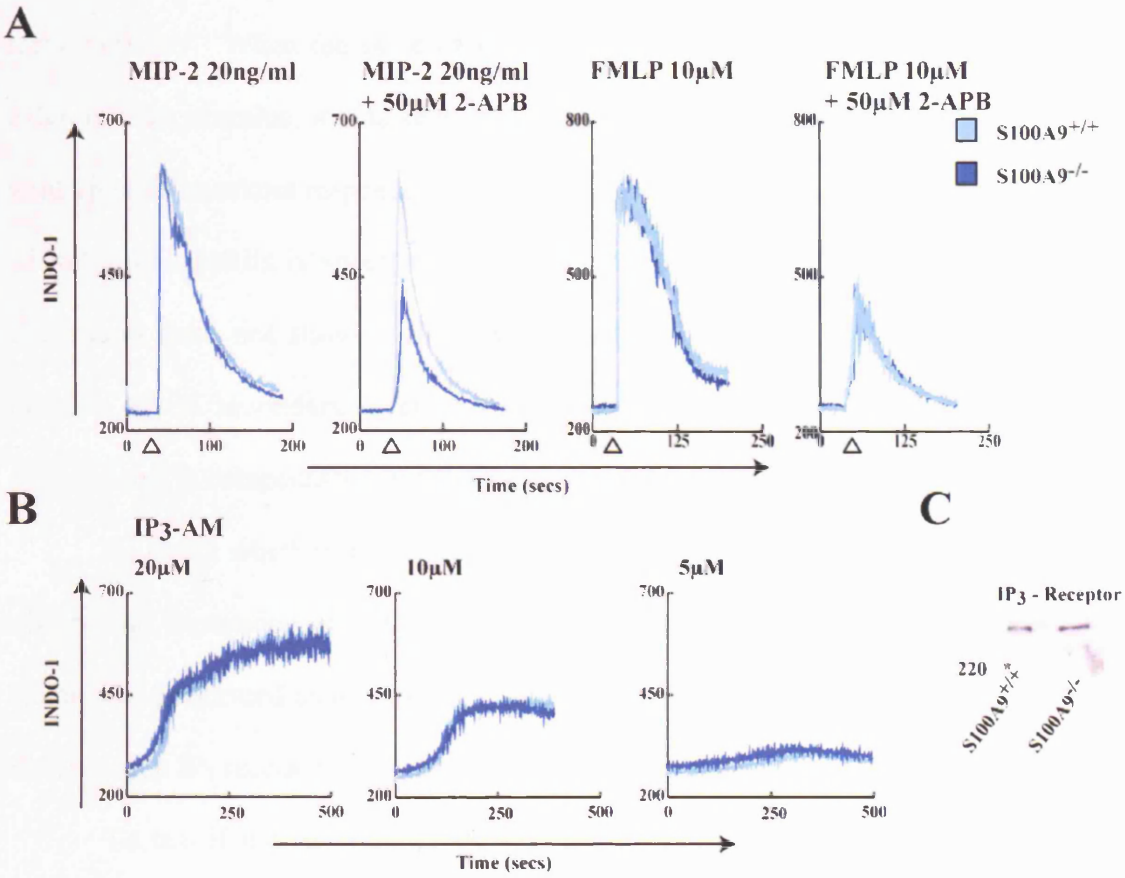

Figure 4.6 Function of the IP_3 receptor in wildtype and S100A9 null neutrophils

Bone marrow leukocytes were loaded with Indo-1 and were identified by labelling with mAbs 7/4 and Ly-6G. Intracellular calcium concentration was monitored by flow cytometry and was expressed as an arbitrary figure, based on the ratio of Indo-1 fluorescence at 424nm and 530nm. The median response neutrophil Indo-1 ratio of ≈500-700 events is plotted every second. A: Cells were exposed to 2-APB (50µM) at time zero prior to stimulation with chemoattractant at the indicated time. B: Cells were incubated with a titration of IP_3-AM for ten minutes prior to observation of the Indo-1 signal for the time period shown. C: The expression of the IP_3-receptor was examined by western blot analysis of neutrophil lysate as described in the materials and methods. Calcium data shown is representative of 3 independent experiments.

the S100A9 null cells could imply that the lesion in MIP-2 signalling is in the same pathway. When the same experiment was conducted using FMLP as the calcium flux stimulus, it was seen that 2-APB had the same effect on both the wildtype and knockout response. This gives further evidence that the lesion in the S100A9 neutrophils is specific to some but not all stimuli. That the 2-APB compound does not show a differential effect on the FMLP response could indicate that a secondary calcium release pathway is being activated by this stimulus that is compensating for the lesion in the S100A9 cells.

To check whether the possible lesion in the IP_3 pathway could be down to differential expression of this receptor, western blotting of a neutrophil protein lysate was performed using a pan-IP_3 receptor antibody. This revealed no gross difference in IP_3 receptor expression as shown in figure 4.6c.

To test if the function of the IP_3 receptors was grossly normal a small amount of a cell-permeable IP_3-ester was obtained. Stimulating the IP_3 receptor with IP_3 itself is not possible in this system as IP_3 would not pass through the membrane, and is an exceedingly labile substance. The IP_3-ester is more stable and passes through the membrane. The ester group is then removed in the cytosol and IP_3 is released intracellularly (Peppiatt et al., 2003). This was applied to the cells at various concentrations. It was found to have a lag period of 5 mins before any activity was seen, presumably the time taken to pass into the cell and be cleaved. The IP_3 ester caused a sustained rise in cytosolic calcium concentration at the higher doses tested (figure 4.6b). No difference in calcium release following stimulation with the IP_3 ester was seen when wildtype and S100A9 null neutrophils were compared. This implies that the overall ability of the receptor to be activated by its ligand is normal and that S100A8/9 does not play a constitutive

role in controlling the function of this receptor. It is of interest that a small EF-hand protein (CaBP-1) has been reported to interact the IP_3 receptor. The evidence was provided by alterations in the effect of IP_3-AM in the presence and absence of the overexpressed CaBP-1 protein (Kasri et al., 2004). We do not observe an effect of lack of S100A9 in this similar system but this does not absolutely rule out a selective interaction with the IP_3 receptor upon stimulation by some but not all chemoattractants.

4.2.7 A physical association with the IP_3 receptor

There is growing evidence that small calcium binding proteins of the EF-hand type are capable of interacting with the IP_3 channel and modulating its activity either positively or negatively ((Kasri et al., 2004; Yang et al., 2002)). S100A1, another family member, is reported to interact directly with the ryanodine receptor and modulate its function upon binding ((Most et al., 2003; Treves et al., 1997)). Given this information it seems reasonable to hypothesise that S100A8/9 could be acting in this pathway by interacting with the IP_3 receptor.

In order to investigate this possibility an immunoprecipitation protocol was devised. A monoclonal anti-S100A9 antibody, 2B10, was shown to pull-down S100A9 from a bone marrow lysate, along with its heterodimeric binding partner S100A8. Figure 4.7 illustrates a silver stained gel showing 2 bands of approx 14 and 8 kDa pulled down by 2B10 in wildtype lysate, these bands are absent in the S100A9 null lysate control and from a control immunoprecipitation

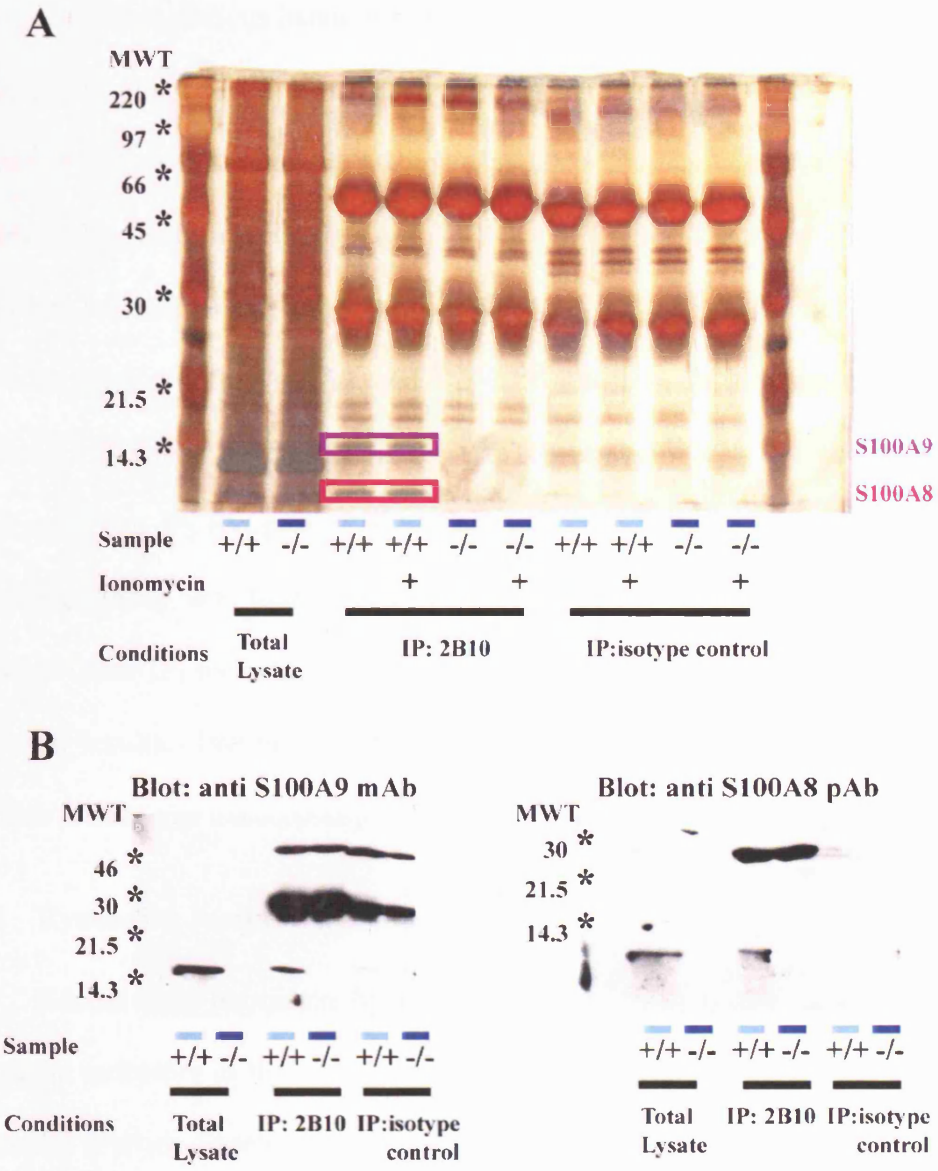

Figure 4.7 Immunoprecipitation of S100A9

Protein lysates were made from bone marrow samples from wildtype and S100A9 null mice. The samples were incubated with 20-30µg/ml of mAb 2B10, to precipitate S100A9, or an isotype control antibody. Antibody bound proteins were isolated using Protein G coupled sparse. Bound proteins were removed from the sparse by boiling the sample in SDS-PAGE gel loading buffer. A: Samples were run on a 15% SDS-PAGE gel and visualised using a silver-stain protocol. B: Western blotting was performed on IP samples using mAb anti-S100A9 (2B10) and polyclonal anti-S100A8 (NH9) antibody.

with a non-specific isotype control antibody in the wildtype and S100A9 null lysates. No other obvious bands are seem in the 2B10 immunoprecipitation in the presence or absence of elevated cytosolic calcium (following ionomycin treatment) that are not present in isotype of S100A9 null controls. To confirm the 14 and 8 kDa bands are S100A8 and S100A9 as expected western blotting was performed with 2B10 and a rabbit polyclonal anti-S100A8 antibody (NH9). As shown in figure 4.7b S100A9 and S100A8 were pulled down by 2B10 as expected. Western blotting with the pan IP_3 receptor did not produce any evidence of the IP_3 receptor co-precipitating with S100A8/9; however, the IP_3 receptor antibody was found not to give consistently clear results by western blotting. Other IP_3 receptor antibodies were also evaluated and also found not to give clear results. Immunoprecipitation with a panel of IP_3 receptor antibodies was also found to be unsuccessful.

4.2.8 Ryanodine receptor signalling

Recent data published by Partida-Sanchez *et al* showed a role for the ryanodine receptors in the FMLP-induced calcium flux response in the murine neutrophil (Partida-Sanchez et al., 2001). In this publication the CD38 molecule was deleted in mice. CD38 is an ecto-enzyme that catalyses the production of cADPR from NAD and facilitates its transport into the cell. cADPR is a ligand for the ryanodine receptor which is a ligand gated ion channel located on the intracellular stores. In the CD38 knockout neutrophils the response to FMLP was shown to have a slightly reduced maximum and no secondary peak of calcium. Although the profiles of the calcium response in this study are different to those found in the published study (namely no secondary peak of calcium is seen on stimulation of the bone marrow neutrophils with FMLP in this study), it seems

possible that this second pathway of calcium release activated by FMLP and apparently not other chemoattractants might act as a compensatory pathway in the S100A9 null neutrophils.

To test this hypothesis the cells were incubated with 50-100μM 8-Br-cADPR, a cell-permeable inhibitor of the ryanodine receptor, in conditions similar to those published using this compound (Partida-Sanchez et al., 2001). When a range of FMLP concentrations were used to stimulate wildtype and S100A9 null neutrophils in the presence and absence of 8-Br-cADPR at 50μM, no effect on the magnitude or duration of the response was seen in either group (figure 4.8). A similar result was found when the experiment was repeated using MIP-2 as a stimulant. The experiment was also attempted using Ruthenium Red, another inhibitor of the ryanodine receptor, and no effect could be seen in this system (data not shown).

As a control for the presence of the ryanodine receptor in this system ryanodine was used to treat the cells. Ryanodine activates the ryanodine receptor at low concentrations and inhibits its function at higher concentrations but this compound is poorly cell-permeable. No effect of ryanodine was seen in this system over a range of doses (data not shown), although it is unclear if this is due to the moiety not passing the cell membrane or to absence of the receptor.

Assuming that the 8-Br-cADPR compound was used at an appropriate concentration, it does not appear that the ryanodine receptor pathway is acting as a compensatory calcium release pathway in these cells. These results could be

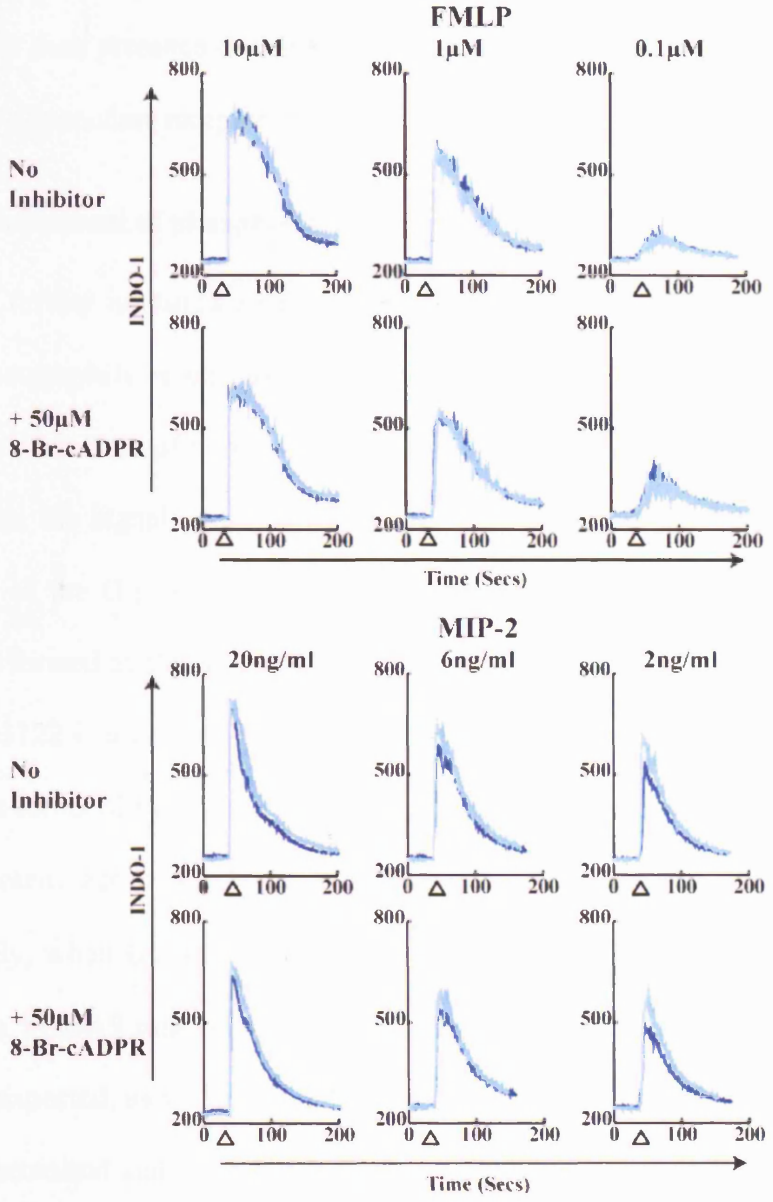

Figure 4.8 No involvement of 8-Br-cADPR signalling in FMLP or MIP-2 induced signalling

Bone marrow leukocytes were loaded with Indo-1 and were identified by labelling with mAbs 7/4 and Ly-6G. Intracellular calcium concentration was monitored by flow cytometry and was expressed as an arbitrary figure, based on the ratio of Indo-1 fluorescence at 424nm and 530nm. The median response neutrophil Indo-1 ratio of ≈500-700 events is plotted every second. Cells were preincubated for in excess of 15 minutes with 50µM 8-Br-cADPR prior to stimulation with a titration of MIP-2 or FMLP. Data shown is representative of 3 independent experiments.

improved by the use of cell permeable activator of the ryanodine receptor to demonstrate their presence or that the inhibitor, used as described, can inhibit the receptor in a ryanodine receptor expressing cell type.

4.2.9 Involvement of phospholipase C

To further investigate whether the lesion in the MIP-2 signalling in the S100A9 neutrophils is due to an abnormality in the IP_3-mediated signalling pathway, an inhibitor of phospholipase C (PLC) was used. As discussed in the Introduction the signalling downstream of chemoattractant receptors involves activation of the G-protein operated phospholipase C. IP_3 and diacylglycerol (DAG) are formed by the action of PLC on the lipid precursor PIP2.

U73122 is a cell-permeable inhibitor of PLC. Its relative specificity for the various forms of PLC is not completely clear, but there is evidence that it has a more potent action on PLCβ2 than other isoforms (Hou et al., 2004). Surprisingly, when U73122-treated cells were stimulated with either MIP-2 or FMLP, the S100A9 null cells showed less inhibition by U73122 (figure 4.9a). This is unexpected, as so far the calcium signalling in the S100A9 null cells has been compromised and no lesion in FMLP signalling has been observed. With the inhibition of the IP_3 receptor having a greater affect on the S100A9 null cells, the implication is that this pathway is possibly compromised in these cells. It is also surprising that the inhibitor reveals a lesion in the FMLP response in the knockout cells as inhibition using the 2-APB compound had not revealed any disparity between wildtype and S100A9 null cells. A higher 10μM dose of U73122 completely inhibits the response to MIP-2 and FMLP in both wildtype

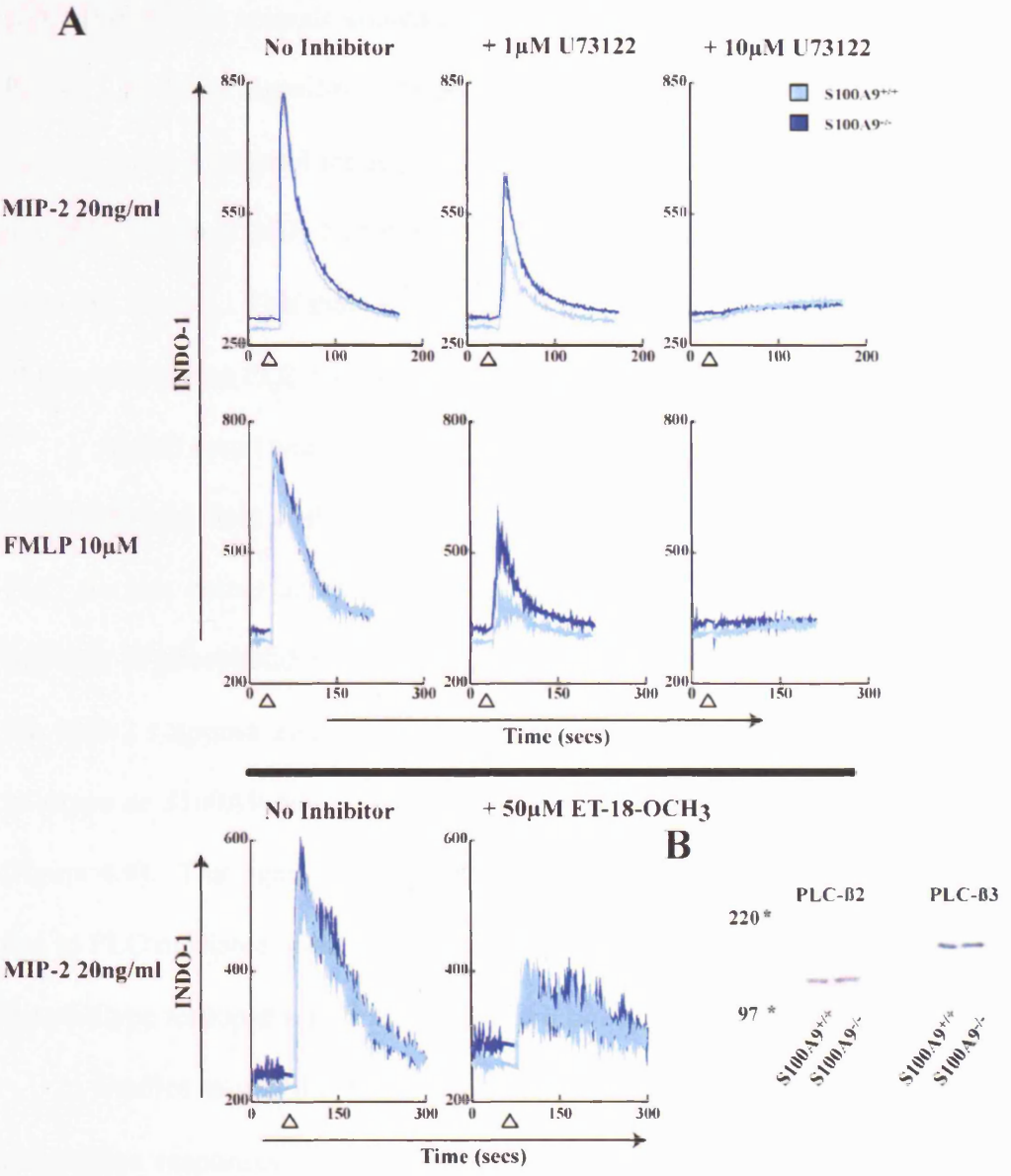

Figure 4.9 Involvement of PLC in neutrophil chemoattractant induced calcium signalling

Bone marrow leukocytes were loaded with Indo-1 and were identified by labelling with mAbs 7/4 and Ly-6G. Intracellular calcium concentration was monitored by flow cytometry and was expressed as an arbitrary figure, based on the ratio of Indo-1 fluorescence at 424nm and 530nm. The median response neutrophil Indo-1 ratio of ≈500-700 events is plotted every second. A: Cells were preincubated for ≥ 15 minutes with 1-10μM U73122 or 50μM ET-18OCH_3 prior to stimulation with MIP-2 or FMLP. Data shown is representative of 3 independent experiments. B: The expression of the PLCβ2 and PLCβ3 isoforms was examined by western blot analysis of neutrophil lysates as described in the Materials and Methods.

and S100A9 null animals showing again that both responses are dependent on PLC-IP_3 mediated signalling. An inactive analog of U73122 (U73343) was used in this system to control for any PLC independent effects and was found to have no effect on either MIP-2 or FMLP signalling in wildtype or S100A9 null cells (data not shown). This indicates the effect seen is presumably due to the effects of this inhibitor on PLC function.

As this result was quite surprising it was decided to repeat the experiment with other inhibitors of PLC. Unfortunately the other published inhibitors of PI-PLC are less potent and less specific than U73122. ET-18-OCH_3 is another inhibitor of phosphatidylinositol PLC and this compound did show inhibition of the MIP-2 response after a long incubation. No differential inhibition of the wildtype or S100A9 null response was seen, with both being strongly inhibited (figure 4.9). This again shows that the MIP-2 response appears to be primarily due to PLC mediated signalling. It does not provide any further insight into why the wildtype response was more strongly inhibited by U73122.

Studies using the PLCβ2/3 knockout mice have shown that several chemokine responses (FMLP, MIP-1α and IL-8) are entirely dependent on signalling via a combination of these molecules in the murine neutrophil (Li et al., 2000b). Studies using the single PLCβ2 or PLCβ3 animals show that both these molecules contribute to different degrees in the signalling by chemokines (Jiang et al., 1997; Li et al., 2000b). These experiments showed that PLCβ2 was the predominant isoform involved in murine chemoattractant calcium signalling, but that PLCβ3 also performed a minor role and could compensate to some degree for the absence of PLCβ2. Given the recent data that U73122 may have a different potency against PLCβ2 and PLCβ3 ((Hou et al., 2004)), it could be argued that

the S100A9 knockout animals have compensated for a lesion in this signalling pathway by using a different PLCβ family member. If this member were less affected by U73122 than the isoform used in the wildtype cells (ie PLCβ3 versus PLCβ2) then the U73122 phenotype could be explained. To test for any compensation by upregulation or downregulation of the PLCβ family, the levels of PLCβ2 and PLCβ3 were studied by western blotting of a neutrophil lysate as before. This experiment found no apparent difference in the expression levels of either isoform when wildtype and S100A9 null neutrophils were compared (figure 4.9b).

As PLCβ2 and PLCβ3 are activated by G-proteins rather than phosphorylation, this makes detecting the level of activation of these PLC isoforms more difficult than studying the phosphorylation activated forms (reviewed in (Rhee, 2001; Williams, 1999)). Differences in phosphorylation state can be evaluated by immunoprecipitation and phospho-blotting, or by the use of phosphorylation specific antibodies. The PLCβ family are thought to be modulated, rather than activated, by phosphorylation, but the precise site involved is unclear (reviewed in(Rhee and Bae, 1997)). Attempts to immunoprecipitate the PLCβ2 and PLCβ3 proteins from the wildtype and S100A9 neutrophil lysates were unsuccessful, so any difference in phosphorylation as a cause for the differences in wildtype versus S100A9 signalling could not be evaluated.

The only way to test the activity of these PLCβ isoforms is to measure the level of IP_3 produced in response to the stimuli. This, unfortunately, is not an easy process. A commercially available kit (Amersham) allows the levels of IP_3 in a sample to be measured using a competitive radio-ligand binding assay to an engineered IP_3 binding protein. The kit was used in conjunction with an

immunomagnetic sorted 98% pure neutrophil (Ly-6G positive) population but failed to detect any IP_3 in the neutrophil samples, despite using very high cell numbers (> $1x10^7$/sample) and inhibiting the degradation of IP_3 by including LiCl in the stimulation buffer. Data provided with the kit for the production of IP_3 by neutrophils from rabbit shows that the amount of IP_3 produced following IL-8 stimulation is very low. This would imply that the problem with my assay may have been that the levels extracted were below the limits of detection of the kit, particularly as all other parameters and standards were within expected limits.

4.2.10 Involvement of DAG

Data considered so far seems to implicate PLC as a possible site for the lesion in the S100A9 null neutrophils. Attempts to evaluate the function of PLC with respect to IP_3 production have been exhausted but PLC also produces DAG. DAG is itself a bioactive moiety, activating PKC and PKC-independent targets as well as acting as an activator of extracellular calcium entry via DAG-operated calcium channels (Brose et al., 2004; Hardie, 2003; Spassova et al., 2004). If we hypothesise that PLC function is somehow altered in the S100A9 null cells then it follows that DAG production is also affected.

To investigate any role for altered DAG production in this system the metabolism of DAG was blocked by using the DAG Kinase Inhibitor II (R59949). Preincubating the cells with this compound prior to stimulation with MIP-2 showed little effect of the inhibitor on the wildtype response at low or high concentrations (figure 4.10). However, the S100A9 null neutrophils showed a considerable inhibition of the MIP-2-induced calcium flux with both the magnitude and duration of the response being reduced. When the calcium flux response to FMLP was evaluated in the presence and absence of R59949, little

effect of the inhibitor was seen on either the wildtype or S100A9 null neutrophil response (figure 4.10).

Studies with another inhibitor of DAG metabolism RHC80267, an inhibitor of DAG lipase, did not reveal any inhibition of either the MIP-2 or FMLP response in wildtype or S100A9 null neutrophils (figure 4.10). This could imply that either R59949 is having an effect other than its effect on DAG metabolism, or that DAG metabolism occurs primarily via the DAG kinase route in neutrophils.

These data show that increased DAG levels have a greater inhibitory effect in the S100A9 null cells. These data are also interesting as they show that affecting DAG levels seems to inhibit MIP-2 signalling but have no effect on FMLP signalling. To confirm that the effect is due to an effect of DAG itself rather than an unexpected effect of the R59949, a cell permeable DAG analogue was used to see if it has a similar effect.

OAG is a cell permeable DAG mimetic, which can be used to mimic the effects of DAG on the cells without the need to affect the entire DAG metabolic cycle. Cells were pre-treated with 100μM OAG, then stimulated with MIP-2 or FMLP as before (figure 4.11). When the effect of OAG on the MIP-2 induced calcium flux was considered it was seen that some effect of the OAG was seen on the wildtype response, but a much more pronounced reduction of the MIP-2

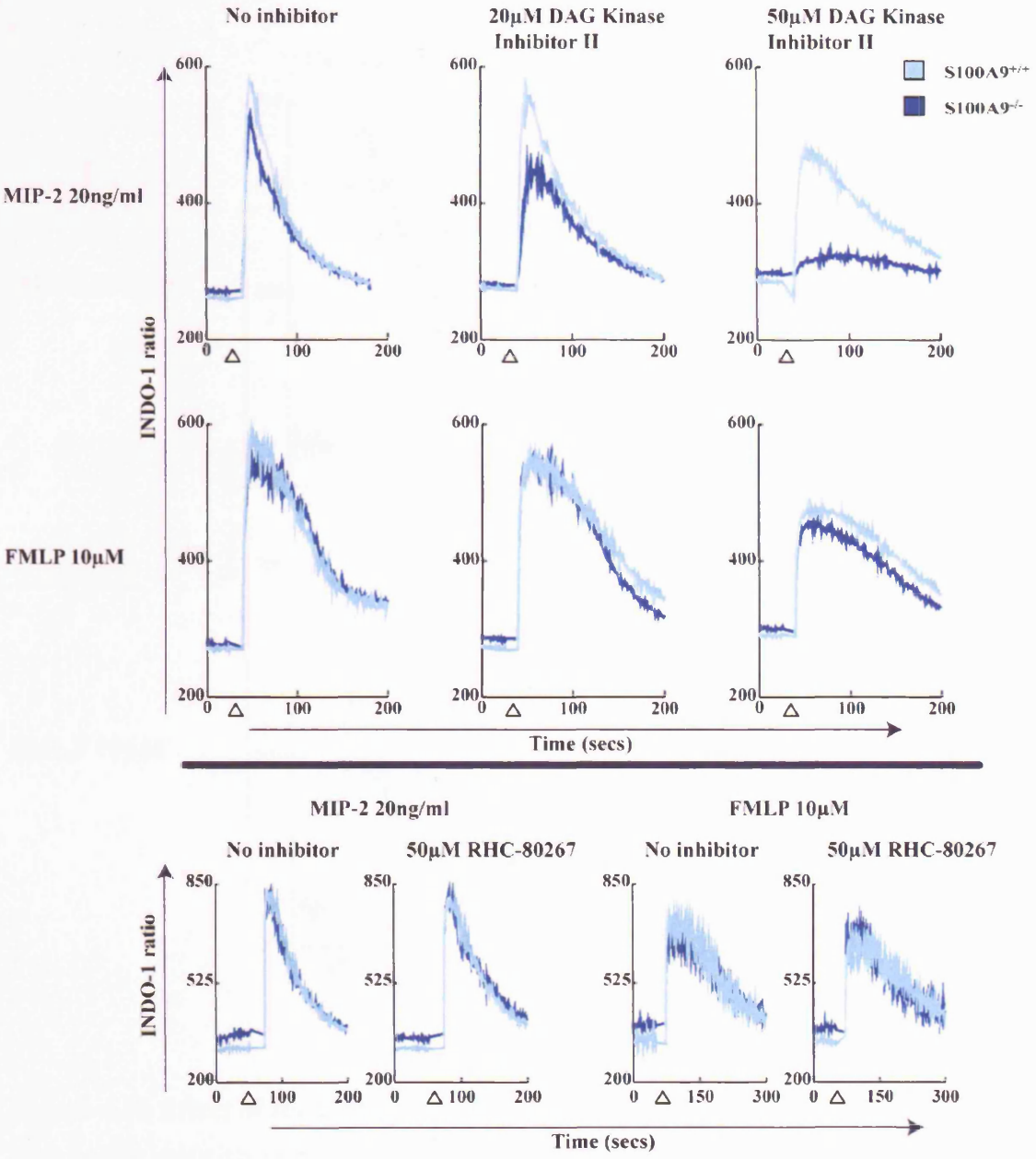

Figure 4.10 Effect of alteration of DAG metabolism on neutrophil calcium signalling

Bone marrow leukocytes were loaded with Indo-1 and were identified by labelling with mAbs 7/4 and Ly-6G. Intracellular calcium concentration was monitored by flow cytometry and was expressed as an arbitrary figure, based on the ratio of Indo-1 fluorescence at 424nm and 530nm. The median response neutrophil Indo-1 ratio of ≈500-700 events is plotted every second. Cells were preincubated for in excess of 15 minutes with 20-50µM DAG Kinase Inhibitor II or RHC-80267 (an inhibitor of DAG lipase) prior to stimulation with MIP-2 or FMLP. Data shown is representative of 3 independent experiments.

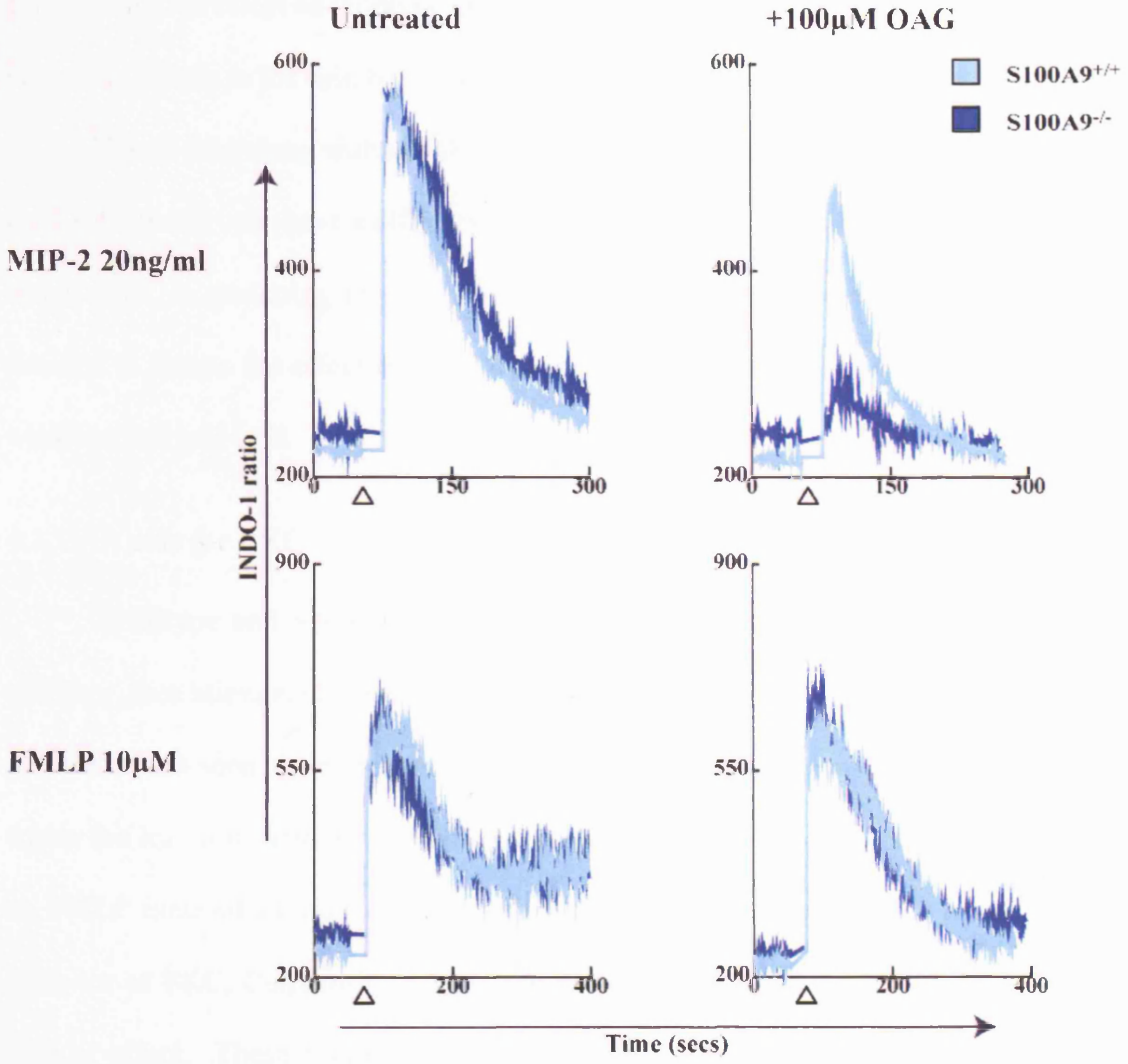

Figure 4.11 Effect of the DAG analog OAG on neutrophil calcium signalling

Bone marrow leukocytes were loaded with Indo-1 and were identified by labelling with mAbs 7/4 and Ly-6G. Intracellular calcium concentration was monitored by flow cytometry and was expressed as an arbitrary figure, based on the ratio of Indo-1 fluorescence at 424nm and 530nm. The median response neutrophil Indo-1 ratio of ≈500-700 events is plotted every second. Cells were preincubated for ≥ 15 minutes with 100µM OAG prior to stimulation with MIP-2 or FMLP. Data shown is representative of 3 independent experiments.

response in the S100A9 null cells was seen. When the FMLP response was considered little effect on wildtype or S100A9 null cells was seen. DAG can have numerous effects in the cell, but a major one of these is to activate PKC.

These data along with the DAG kinase inhibitor data seem to indicate that the S100A9 null cells have a different response to an elevation of DAG levels. To test if PKC is mediating this effect of DAG in the S100A9 null cells, it was decided to assess the effect of PKC inhibition on the calcium signalling in the wildtype and null cells.

4.2.11 A role for PKC

Wildtype and S100A9 null cells were preincubated with BIM, a PKC inhibitor, then stimulated with FMLP and MIP-2 (figure 4.12). No effect of PKC inhibition was seen on the response to MIP-2 at maximal responses or at levels where the lesion in S100A9 signalling was evident. No effect of BIM was seen on FMLP induced calcium flux in either wildtype or knockout cells. Another inhibitor of PKC, Calphostin C, was also tested in the experiment, with similar lack of effect. These results show that inhibition of PKC does not rescue the lesion in the S100A9 null cells. While the knockout cells have a different response to DAG signalling an altered response to PKC is not the cause of the lesion seen in MIP-2 signalling.

4.2.12 Another hypothesis: arachidonic acid

S100A8/9 has been implicated as a major arachidonic acid (AA) binding protein in neutrophils (Kerkhoff et al., 1999b; Klempt et al., 1997; Roulin et al., 1999; Siegenthaler et al., 1997; Sopalla et al., 2002). Arachidonic acid has also

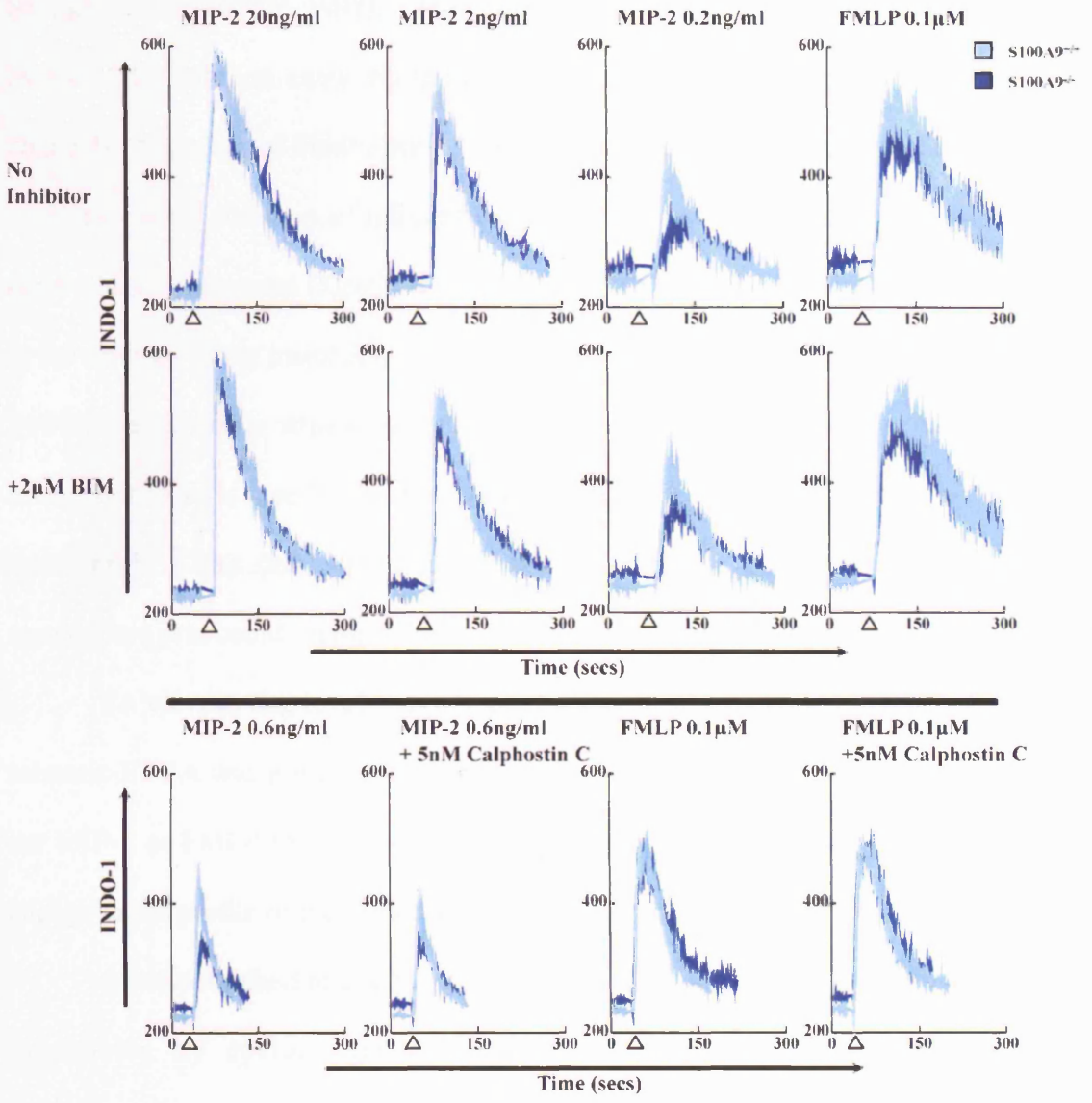

Figure 4.12 Effect of inhibition of PKC on neutrophil calcium signalling

Bone marrow leukocytes were loaded with Indo-1 and were identified by labelling with mAbs 7/4 and Ly-6G. Intracellular calcium concentration was monitored by flow cytometry and was expressed as an arbitrary figure, based on the ratio of Indo-1 fluorescence at 424nm and 530nm. The median response neutrophil Indo-1 ratio of ≈500-700 events is plotted every second. Cells were preincubated for in excess of 15 minutes with 2μM BIM or Calphostin C prior to stimulation with a titration of MIP-2 or FMLP. Data shown is representative of 3 independent experiments.

been shown to affect calcium signalling (Mignen and Shuttleworth, 2000; Striggow and Ehrlich, 1997). Arachidonic acid has been shown to mediate extracellular calcium entry via the arachidonic acid activated calcium (ARC) channels (Mignen and Shuttleworth, 2000). It has been shown that arachidonic acid can cause inhibition of intracellular calcium release via the IP_3 receptor in cerebellum microsomes (Striggow and Ehrlich, 1997). It could be speculated that in the absence of the major AA binding capacity, more free AA is available in the S100A9 neutrophils which could cause an increase in the cytosolic calcium concentration as is seen by the increased basal calcium levels in the S100A9 null neutrophils. The data showing that the IP_3 receptor can be inhibited by arachidonic acid could supply a direct route of affecting calcium signalling.

To elevate the levels of AA in the neutrophils, the arachidonic acid mimetic ETYA was pre-incubated with the cells. When the effect of ETYA on the MIP-2 or FMLP response is considered it can be seen that ETYA causes no change to the profile of the responses (figure 4.13).

Another method of altering the AA metabolism in the cells is to inhibit the breakdown by cyclooxygenase enzymes to form prostanoid/leukotriene derivatives. This can be done by treating the cells with indomethacin. When the cells were treated with indomethacin no effect on the response to MIP-2 or FMLP could be seen (figure 4.13).

Neutrophils were stimulated with arachidonic acid in the presence and absence of extracellular calcium (figure 4.14). In the presence of extracellular calcium a robust spike of calcium was seen. This appeared to be of similar magnitude and duration in the wildtype and S100A9 null cells. In the absence of

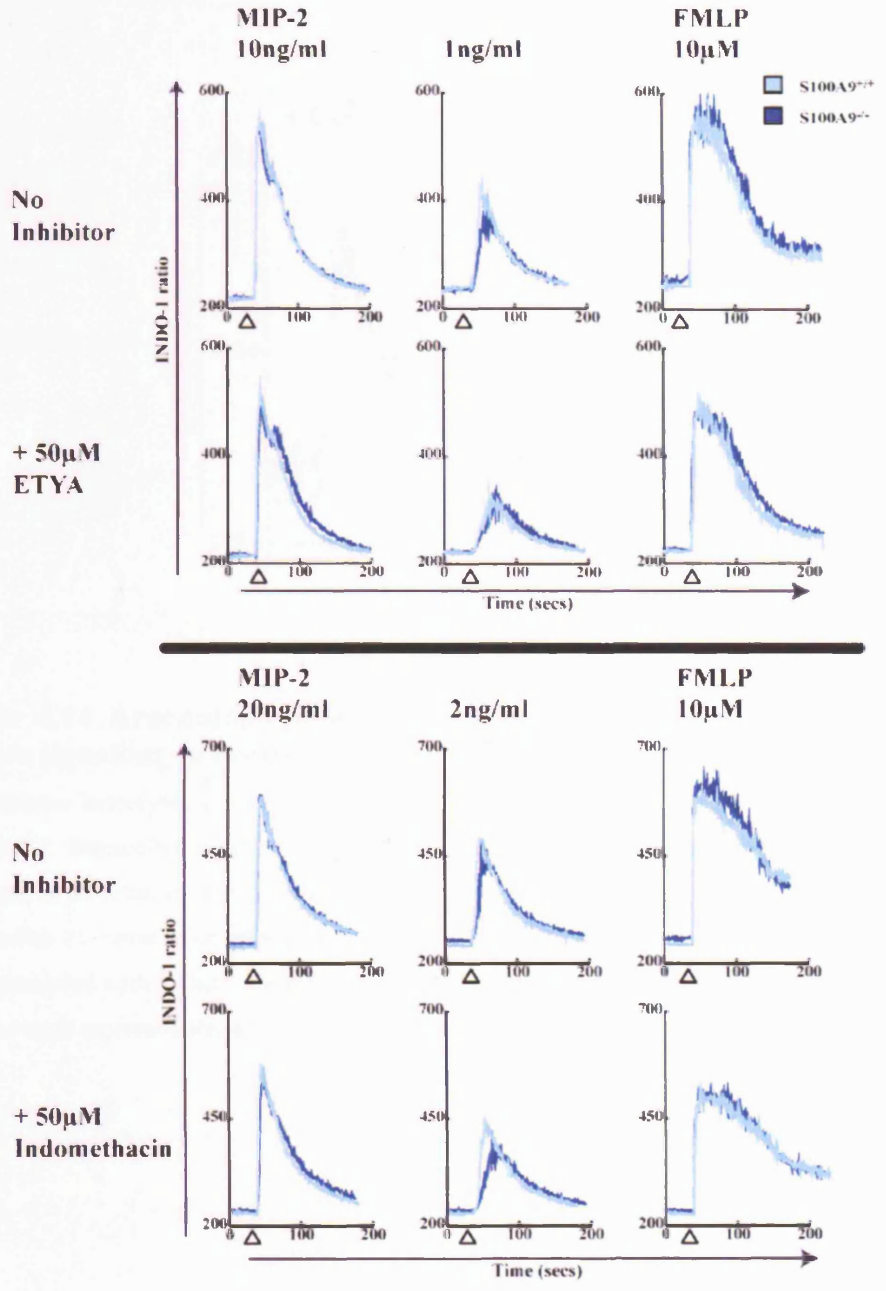

Figure 4.13 Effect of alteration of Arachidonic Acid metabolism on neutrophil calcium signalling

Bone marrow leukocytes were loaded with Indo-1 and were identified by labelling with mAbs 7/4 and Ly-6G. Intracellular calcium concentration was monitored by flow cytometry and was expressed as an arbitrary figure, based on the ratio of Indo-1 fluorescence at 424nm and 530nm. The median response neutrophil Indo-1 ratio of ≈500-700 events is plotted every second. Cells were preincubated for in excess of 15 minutes with 50μM ETYA or Indomethacin prior to stimulation with a titration of MIP-2 or FMLP. Data shown is representative of 3 (2 for Indomethacin) independent experiments.

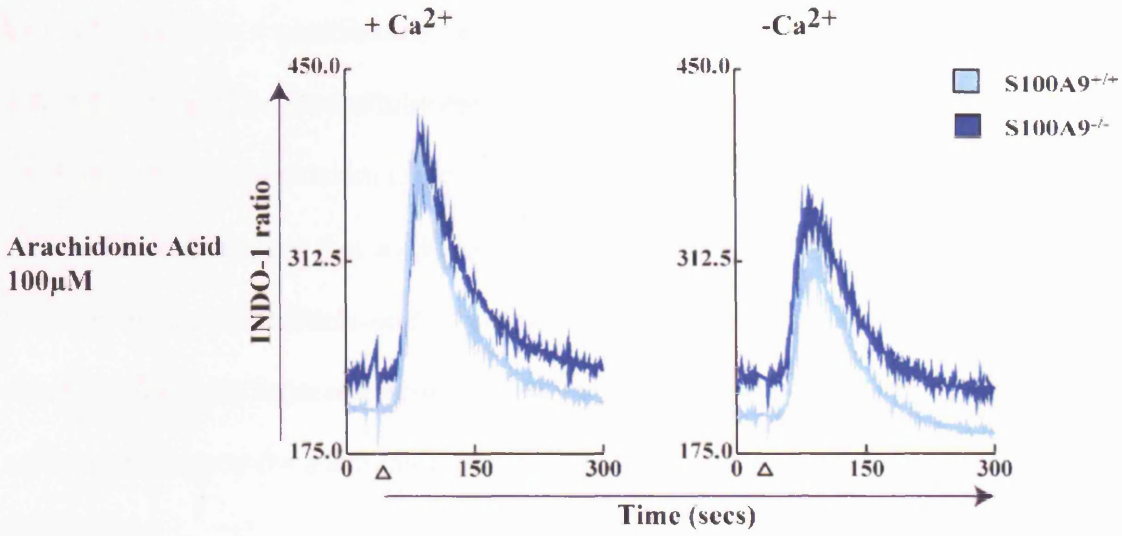

Figure 4.14 Arachidonic acid stimulates intracellular and extracellular calcium signalling in neutrophils

Bone marrow leukocytes were loaded with Indo-1 and were identified by labelling with mAbs 7/4 and Ly-6G. Intracellular calcium concentration was monitored by flow cytometry and was expressed as an arbitrary figure, based on the ratio of Indo-1 fluorescence at 424nm and 530nm. The median response neutrophil Indo-1 ratio of ≈500-700 events is plotted every second. Cells were stimulated with 100µM arachidonic acid in the presence or absence of extracellular calcium. Data shown is representative of 2 independent experiments.

extracellular calcium the magnitude of the AA induced calcium flux was reduced in both wildtype and S100A9 null animals to an equal degree. This data shows that AA can cause a combination of extracellular calcium entry and intracellular calcium release. The intracellular calcium release seems to be independent of the need for extracellular calcium entry.

These data show that arachidonic acid can stimulate calcium signalling but attempts to alter arachidonic acid levels in the neutrophils have only minor effects on chemoattractant induced calcium signalling. This data does not provide robust evidence to support the arachidonic acid theory.

4.3 Discussion

4.3.1 Calcium Homeostasis

The results obtained in this study do not indicate any abnormalities in the basic homeostatic calcium parameters in the S100A9 null neutrophils. Most interestingly despite the abundance of the dimer in neutrophils there was no obvious effect on the calcium buffering potential of the cells, with the magnitude of the ionomycin response being identical in S100A9 null and wildtype neutrophils. Indeed preliminary experiments carried out by S. Bolsover (University College London) to directly measure the calcium buffering potential of the two cell types revealed no significant decrease in calcium buffering potential. When calbindin D28k, a highly abundant neuronal calcium buffering protein, was deleted in mice the magnitude of synaptically induced calcium transients was enhanced by 80% in the mutant mice (Airaksinen et al., 1997). Calbindin D28k, like S100A8/9, is startlingly abundant, being 15% of total cellular protein in mature Purkinje cells ((Baimbridge et al., 1982)), and it is this

parallel of high expression levels that lead to the assumption that the S100A8/9 dimer must be a major neutrophil cytosolic calcium binding protein. The evidence from this study fits with the idea that the S100 family act as calcium sensor proteins transducing a signal.

Normal loading of the internal calcium stores in the S100A9 null cells is also another key observation of normal calcium homeostasis in these cells. In the cardiomyocytes of S100A1 overexpressing transgenic mice the sarcoplasmic reticulum, a major calcium storage structure in excitable cells, has increased calcium content (Most et al., 2003). In light of this data it was important to observe if the loading of the neutrophil internal stores was affected in the S100A9 null mice. Having established no deficiency or enhancement of ER calcium loading it was then logical to evaluate the refilling of these stores. The precise mechanism of store operated calcium entry (SOCE) is unclear, but depletion of the intracellular stores causes opening of calcium channels on the surface, either by direct coupling of the stores to these channels or by production of an intracellular messenger. By studying the effects of thapsigargin in the presence of calcium and the store operated calcium entry profiles for the S100A9 null and wildtype neutrophils it was seen that this process is unaffected by the absence of S100A9.

The one aspect of calcium homeostasis that has not been examined in this study is the elevated baseline calcium as described previously (Hobbs et al., 2003). This apparent increased calcium level in the unstimulated S100A9 null neutrophils is still evident in this current study. It has been difficult to define and investigate its significance due to the size of the difference involved. This increase in calcium under basal conditions was not explained by enhanced release

from intracellular stores or alteration in SOCE. The buffering of acute elevations in cytosolic calcium seems to indicate no profound affect on the ability of the cell to buffer calcium. A source of intracellular calcium buffering and release not explored in this study are the mitochondria (reviewed in (Duchen, 1999; Rizzuto et al., 2004)). These are able to both take up and release calcium in the cell and could in theory act as a broad compensatory pathway for a lack of calcium buffering potential. Whether this would allow the cell however to have perfectly identical calcium kinetics in wildtype and S100A9 null cells as seen in this study is unclear. Any differences in the number or function of the mitochondria could be detected by flow cytometry using mitotracker dyes to assess the number of mitochondria present and the ratiometric dye JC-1, that changes fluorescence relative to the membrane potential of the mitochondria, to assess their function.

4.3.2 Lesion in chemoattractant-induced calcium flux

Having established that calcium homeostasis as explored in the S100A9 null cells was normal, the next stage was to examine and confirm the published deficiency in chemokine-induced calcium signalling in the S100A9 null mice (Hobbs et al., 2003). In this study the lesion was shown to be present in the calcium response to a broad range of chemoattractants, chemokines of the CCR and CXCR type and other chemoattractants such as C5a and PAF. The lesion was localised to intracellular calcium release. Rather than being a generalised deficiency in all chemoattractant induced calcium signalling the absence of any lesion in the response to FMLP indicated that a specific intracellular release mechanism used by some but not all chemoattractants was affected in the S100A9 null mice. To dissect the lesion, a model system of comparing MIP-2 and FMLP

mediated signalling was used. Figure 4.15 summarises the generally accepted scheme of chemoattractant signalling.

The calcium signalling induced in neutrophils by these two mediators has been studied in various ways. The signalling by FMLP and IL-8 (the human homolog of MIP-2) was pertussis toxin sensitive as shown by others (Jiang et al., 1996; Schorr et al., 1999). The signalling by MIP-2 and FMLP was not completely abolished by PTX in this study. This was likely to be due to difficulty in loading the cells with PTX, which usually requires an incubation of several hours to be fully effective. As neutrophils have a short life-span, much longer incubation times were not feasible. Pertussis toxin is a bacterial toxin that modifies a set of G-protein α subunits belonging to the Gi and Go classes (but not the Gq, Gs or G_{12} classes), preventing receptor coupling to these G-proteins. G-proteins consist of three stably associated subunits α, β and γ. Interaction of a G-protein and an activated receptor causes exchange of the GDP bound to the α subunit for GTP. The GTP bound α subunit can then disassociate from the βγ dimer. Both the α and βγ subunits subsequently transduce the signal into the cell. PLCβ can be activated by either αi or by α or βγ subunit of the Gq pathway (reviewed in (Neves et al., 2002)). The sensitivity of CXCR1/2 and FMLP receptor signalling to PTX shows coupling to the Gi pathway (Jiang et al., 1996; Wu et al., 1993).

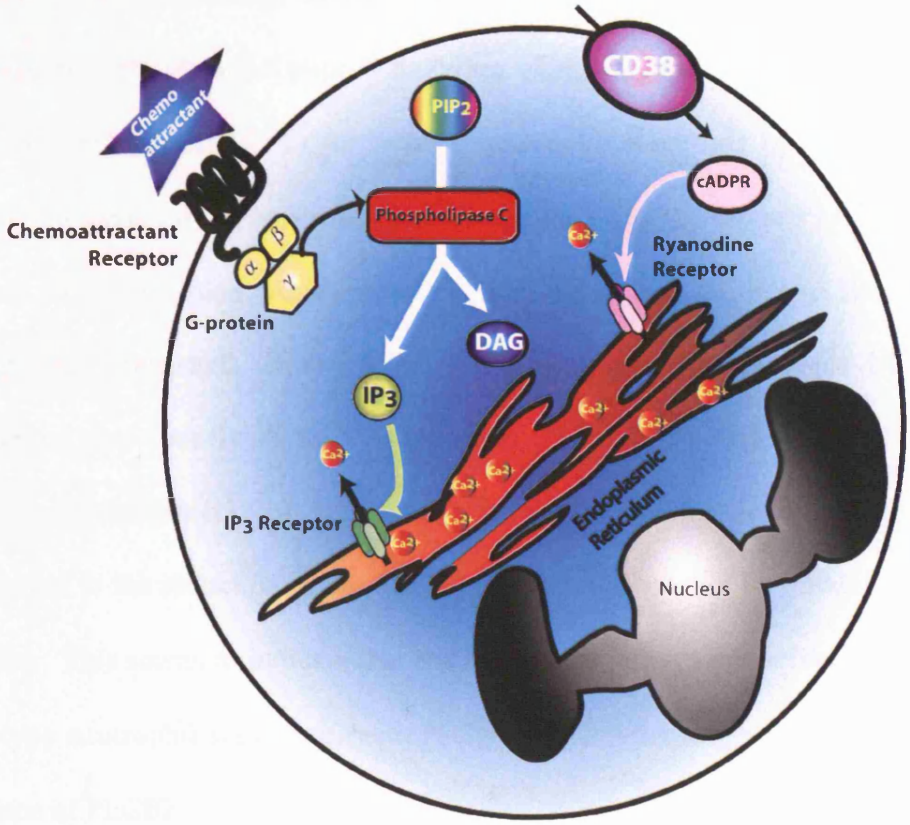

Figure 4.15 General scheme of chemoattractant calcium signalling

When chemoattractants such as MIP-2 or FMLP ligate their seven transmembrane spanning receptors activation of G-proteins occurs. This causes activation of PLC, PLCβ2/3 in murine neutrophils. The hydrolysis of the membrane lipid PIP2 to form IP_3 and DAG then occurs. IP_3 acts to ligate the IP_3 receptor on the intracellular calcium stores triggering the release of calcium into the cytosol. In addition to this standard mechanism FMLP has been shown to activate CD38, a surface membrane ecto-enzyme that catalyses the formation and subsequent transport of cADPR into the cell. This molecule can ligate the ryanodine receptor that also sits in the membrane of the intracellular stores and cause release of calcium into the cytosol.

Members of the Gi class of G-protein can transduce a signal using both the α and βγ subunits (reviewed in (Neves et al., 2002)). The α subunit does not activate calcium signalling, but the βγ subunit released by receptor interaction can directly activate phospholipase C enzymes of the β class. In mice lacking the haematopoietic specific PLCβ2 isoform neutrophil signalling by both IL-8 and FMLP was reduced, but not abolished (Jiang et al., 1997). When PLCβ2/PLCβ3 double knockout mice were studied, signalling to both IL-8 and FMLP was completely abolished, showing the intracellular calcium release by these mediators was entirely PLCβ2/3 dependent (Li et al., 2000b). In PLCβ3 null animals the reduction in calcium flux following FMLP stimulation was minimal compared to the reduction in the PLCβ2 and double knockout animals (Li et al., 2000b). This seems to indicate that the PLCβ2 isoform is the default isoform in wildtype neutrophil signalling, with PLCβ3 playing a compensatory role in the absence of PLCβ2.

The data obtained from the wildtype neutrophils seems to indicate that both MIP-2 and FMLP use pertussis toxin sensitive PLCβ to hydrolyse PIP2 to produce IP_3 mediated calcium flux in neutrophils. The MIP-2 induced calcium flux was shown to be sensitive to elevation of intracellular DAG levels by inhibiting DAG kinase or applying the DAG mimetic OAG. The FMLP induced calcium response was unaffected by increasing DAG levels. Both pathways were shown to be unaffected by inhibition of PKC signalling, a primary effector of DAG. No role for ryanodine receptor mediated calcium release was shown in either response in the conditions used for this study. Similarly there was little effect of altering arachidonic acid metabolism on the MIP-2 or FMLP induced calcium flux. This shows a picture where the basic calcium release pathways

used by both CXCR2 and the FMLP receptor are similar but that the regulation of these pathways is different.

4.3.3 Differential regulation of intracellular calcium release

In the S100A9 null neutrophils the signalling by MIP-2 and FMLP appeared to be via PLC and the IP_3 receptor, as both are sensitive to 2-APB and U73122. Additionally the MIP-2 response was sensitive to inhibition by increased DAG levels or OAG. The interesting observation is that the S100A9 null cells were far more sensitive to inhibition by 2-APB and the DAG kinase inhibitor. The increased efficacy of the 2-APB compound on MIP-2 signalling in the S100A9 null neutrophils seems to imply that the PLC-IP_3 pathway is working less efficiently. The data from the U73122 compound seems to indicate the opposite, showing that the wildtype MIP-2 response is more compromised. There a few possible explanations for this. The compound may have greater efficacy against one PLC family member than another, which seems to be indicated in the literature (Hou et al., 2004). Here greater potency of the inhibitor against PLCβ2 than PLCβ3 is shown in a cell-free system where the ability of U73122 to inhibit the hydrolysis of PIP2 by recombinant PLCβ isoforms is tested (Hou et al., 2004). This could imply that in the S100A9 null cells the signalling is coupled to PLCβ3 in preference to PLCβ2 thus being more resistant to inhibition by U73122. What is more puzzling about the U73122 data is that it shows a differential effect in wildtype and S100A9 null signalling induced by FMLP, a response that is unaffected in the S100A9 null mice in all other conditions tested. Attempts to confirm this data with other inhibitors of PLC were unsuccessful. That the effect produced by this inhibitor does not mirror the lesion seen in the S100A9 null mice

could imply that its lack of potency against the S100A9 null neutrophils is not directly related to the lesion described so far.

One recent paper of interest that may provide a mechanism to identify whether the lesion in calcium signalling is at or above the level of PLC activity concerns a novel real-time IP_3 sensor (Sugimoto et al., 2004). This system uses an engineered protein identical to the PH domain of PLC with a fluorescent indicator attached. The binding of IP_3 to the probe displaces the fluorophore and its fluorescence is decreased. The probe is cell-permeable due to the inclusion of an arginine-rich tag. The probe was capable of detecting IP_3 production in the DT-40 B cell-line in response to B cell receptor stimulation. This system should be usable by flow cytometry and would thus be suitable to study the production of IP_3 in neutrophils.

4.3.4 Theories for the mechanism of action of S100A9

The two most attractive explanations for the calcium signalling lesion in the S100A9 null neutrophils, given the existing literature, are an effect of altered arachidonic acid availability and a direct interaction of S100A9 with the IP_3 receptor. The data presented here does not validate either hypothesis. The lack of any effect of the arachidonic acid mimetic or of indomethacin gives no evidence for arachidonic acid mediators playing any role in regulating chemoattractant-induced calcium flux in neutrophils. The evidence for a direct interaction of S100A9 with the IP_3 receptor is less robustly ruled out.

Although the data from the IP_3 ester shows no constitutive effect of S100A9 in calcium release from the internal stores, it could be that S100A9 is only recruited to the receptor upon defined stimuli, thus accounting for the lack of lesion when the cells are stimulated with IP_3 directly. There are several studies

documenting protein ligands for the IP_3 receptor that can enhance or inhibit its activity. The prototypical protein of this type is calmodulin (CaM), a highly abundant ubiquitous four-EF-hand-containing intracellular protein. The calcium-unbound apo-CaM form has been shown to inhibit IP_3 binding to the IP_3 Receptor. In its calcium-bound state, Ca-CaM facilitates the calcium-mediated inactivation of the receptor (reviewed in (Nadif Kasri et al., 2002; Roderick and Bootman, 2003)).

More recent studies have demonstrated a modulatory effect of CaBP1 on IP_3 receptor activation. Two contrasting studies have demonstrated both a positive (Yang et al., 2002) and negative role (Kasri et al., 2004) for this protein on IP_3 receptor activity. In the paper by Kasri *et al* the inhibitory role of overexpressed CaBP1 in COS-7 cells on the activity of the IP_3 receptor following stimulation with IP_3-ester was used as proof of concept. In the other report CaBP1 was shown to interact directly in a calcium dependent manner with the IP_3 receptor both in transfected systems and in rat brain extracts by co-immunoprecipitation (Yang et al., 2002). In that study the presence of CaBP1 was associated with Xenopus IP_3 receptor opening measured by individual channel patch clamping.

Hypothesis of an interaction of S100A9 with the IP_3 receptor requires some proof of a physical interaction between the IP_3 receptor and S100A9. Attempts to gain this evidence were unsuccessful due to the limitations of the available antibodies. A biochemical system, such as a yeast two-hybrid screen or co-precipitation of tagged proteins could be used to look for a direct *in vitro* interaction of the proteins. Such attempts are warranted given the evidence from the study of S100A1. This member of the S100 family has been shown to interact

with both ryanodine receptors type I and II (Most et al., 2003; Treves et al., 1997). Furthermore studies with S100A1 overexpressing transgenic mice, or S100A1 overexpressing cardiomyocytes *in vitro*, demonstrate an increase in calcium release from the sacroplasmic reticulum following cell stimulation (Most et al., 2004; Most et al., 2003). More tantalizingly the S100A1 knockout mice show a slight impairment of calcium release from cardiomyocytes following β1 adrenoceptor stimulation (Du et al., 2002) that is reminiscent of the magnitude of effect seen in the S100A9 null calcium responses. Although in two very different cell systems, the principle of the interaction of an S100 protein with an intracellular ligand gated ion channel causing enhancement of calcium release following receptor stimulation could be a conserved role for these proteins.

4.3.5 A role for DAG kinase in chemoattractant signalling?

The evidence presented here seems to imply a strong modulatory role for DAG in MIP-2-induced calcium signalling. That this effect is manifested only when DAG kinase, rather than DAG lipase, is inhibited indicates that this molecule is of greater importance in this role. Given that inhibition of PKC has shown little effect on chemokine stimulation in this model, it is possible that DAG is exerting its effect through other downstream mediators. Interestingly a very recent publication has highlighted a modulatory role for DAG in IP_3 mediated signalling (Hisatsune et al., 2005). In this system addition of the DAG mimetic OAG caused increased IP_3-dependent calcium oscillations in various cell types. Elevation of endogenous DAG levels by inhibition of DAG lipase caused an increased calcium response to low levels of agonist stimulation. Whilst this effect is the opposite of that seen in this system, where DAG is inhibitory, it does provide proof of concept for non-PKC mediated modulation of calcium signalling

by DAG. Whether the effect of DAG on chemoattractant signalling is the site of the lesion in the S100A9 null neutrophils or whether DAG plays a modulatory role in the same pathway is unclear. The DAG kinase α enzymes contain EF-hand motifs that when bound to calcium have been shown to cause translocation to the membrane and increased kinase activity (reviewed in (Luo et al., 2004b)). Regulation of this molecule by calcium provides a mechanism by which a calcium-binding protein such as S100A9 could modulate the activity of this enzyme.

CHAPTER 5

5 Adhesion and migration of S100A9 null neutrophils

5.1 Introduction

The primary role for the neutrophil is as a first line of defence against invading pathogens. To perform this activity they must be able to move rapidly out of systemic circulation, following a series of directional signals to arrive at the site of the infection. It has already been shown that the S100A9 null neutrophils have a deficiency in their ability to produce a calcium signal in response to many chemoattractant stimuli. It seems possible that this deficiency could impair their ability to become activated by and respond to these stimuli both in *in vitro* and *in vivo* situations. As well as a role in chemoattractant signalling, S100A9 could play other roles in the calcium-dependent process of adhesion and migration.

The complex nature of leukocyte recruitment to the site of inflammation *in vivo* requires the neutrophil to respond appropriately to a concert of activating and directional signals. Individual steps of this process can be modelled *in vitro* with the phases of adhesion, chemotactic movement and migratory ability and morphology being studied separately. Adhesion can be quantified by assessing the ability of neutrophils to bind to immobilised integrin ligands in response to activating stimuli. PMA or chemoattractants cause cellular activation and result in "inside-out" integrin activation causing adhesion. Divalent cations activate by binding directly to β2 integrin, acting as a model of "outside-in" signalling.

Assessment of the directional movement of cells towards a chemoattractant stimuli can be undertaken using a range of different methods. The most simple of these is the Transwell™ system where cells are placed in a well separated from a chemoattractant stimulus by a polycarbonate filter of varying pore size to allow specific subsets of cells to migrate through. This assay is relatively easy to perform and provides a gross indication as to whether the cells are being activated by the chemoattractant stimulus. The assay can be extended to investigate the process further by coating the filter with specific integrin ligands or an endothelial cell layer should any interesting phenomena be observed.

The ability of the cells to migrate normally on integrin ligands can be evaluated by allowing the cells to attach and migrate on the LFA-1 ligand ICAM-1, where leukocytes undergo seemingly random migration in physiological salt solution in the presence of divalent cations (magnesium and calcium). The speed and directionality of the migration can be assessed by video microscopy along with any obvious abnormalities in cell morphology. A normal migrating cell exhibits an elongated polarised morphology having a narrow un-attached uropod at the trailing edge and a fan-shaped attached lamellipodia towards the direction of movement. Microscopical studies of the migrating cell can be made to examine the organisation of cytoskeletal and signalling molecules.

In this section any role for S100A8/9 in cell adhesion and migration is examined using both *in vitro* and *in vivo* methods.

5.2 Results

5.2.1 Integrin mediated adhesion

The function of cell surface integrins can be studied using an adhesion assay. This entails activating the cells, or the integrin directly, and monitoring the ability of the cells to bind a suitable integrin ligand. In this study the binding of the β2 integrin Mac-1 to its ligand fibrinogen is used as a model. To assess cell adhesion resulting from an increase in Mac-1 avidity, PdBu was used to stimulate bone marrow cells (figure 5.1). Over a titration range of PdBu an increase in adhesion to fibrinogen was observed between 0.04μM and 1μM. No significant difference between wildtype and S100A9 null cells was seen. To test the ability of Mac-1 to mediate adhesion following an increase in affinity the cells were stimulated with a titration of the divalent cation Mn^{2+}. Mn^{2+} was shown to cause an increase in cell adhesion to fibrinogen. The level of adhesion stimulated in the wildtype and S100A9 null cells showed no significant difference with ~40% of the bone marrow cells adhering in both populations in response to 500μM Mn^{2+}.

5.2.2 Mac-1 up-regulation

In addition to changes in affinity and avidity Mac-1 expression levels are increased in response to neutrophil activating stimuli. This gives an indication of the activation state of the neutrophil and its ability to become activated by pro-inflammatory stimuli. In this study increased surface expression of Mac-1 was detected by performing three-colour flow cytometry to identify the neutrophils in a mixed bone marrow cell population and by studying the expression of Mac-1 on those neutrophils using a monoclonal anti-Mac-1 antibody. A range of chemoattractants that were used in the calcium signalling studies were used to

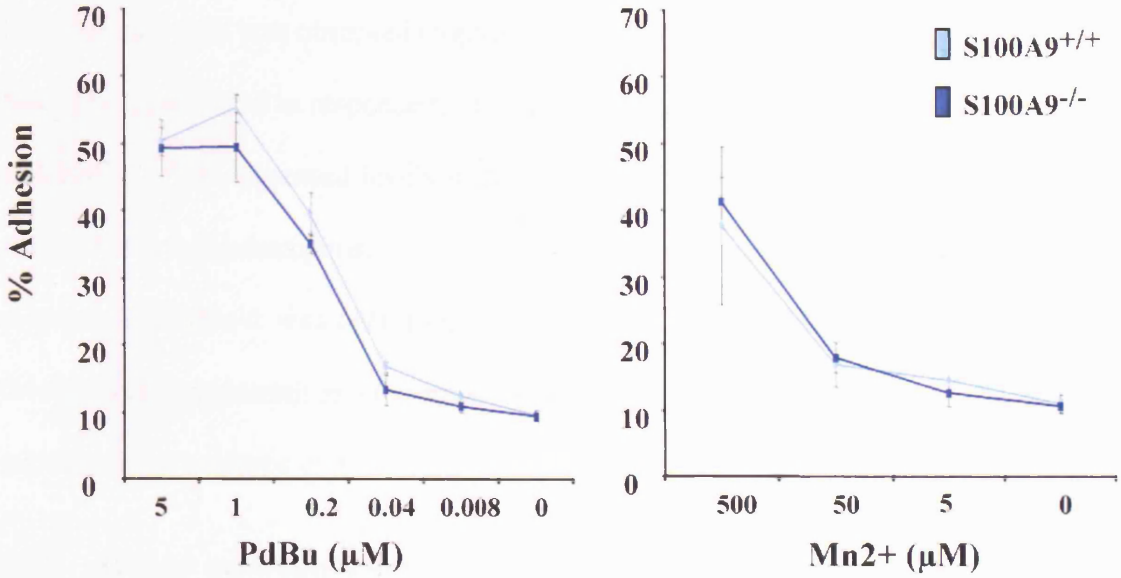

Figure 5.1 Integrin-mediated adhesion of bone marrow leukocytes stimulated by inside-out and outside-in signalling

Bone marrow cells were flushed out of femurs and tibias of 6-10 week-old mice. The cells were loaded with the fluorescent dye BCECF for 30 minutes at 37°C. The cells were then applied to a fibrinogen coated 96 well plate in the presence of a titration of PdBu or Mn^{2+}. The plate was centrifuged briefly and the cells left to adhere at room temperature for 30 minutes. At the end of the experiment unadhered cells were removed by gentle washing and the cell-associated fluorescence of each well was assessed using a plate-reading Cyto-Fluor. The percentage of adhesion for each samples was calculated by comparing the fluorescence of each well before and after the unattached cells had been removed. The experiment was performed in triplicate and the data shown is representative of 3 independent experiments. The mean values +/- standard deviation for the triplicates are shown.

stimulate the neutrophils at concentrations that gave maximal calcium responses or sub-maximal concentrations where a deficiency in the calcium response of the S100A9 null cells was observed (figure 5.2). Increased cell-surface expression of Mac-1 was observed in response to the higher concentrations of C5a, MIP-2, KC and FMLP. The increased levels of Mac-1 expression were similar in wildtype and S100A9 null neutrophils. At the lower concentrations of chemoattractant, up-regulation of Mac-1 was only seen in response to FMLP, C5a and MIP-2. At these lower concentrations of stimulation there was still no difference in Mac-1 expression by wildtype or S100A9 null neutrophils.

5.2.3 S100A9 neutrophils can polarise and migrate on ICAM-1

The morphology of migrating neutrophils was examined to look for any defects in this process. Preliminary studies observed cells from whole bone marrow attaching and migrating on ICAM-1 coated coverslips in a similar assay to that published by this lab for human T cells (Smith et al., 2003). Bone marrow cells were allowed to attach to the coverslips for 15mins in normal HBSS containing calcium and magnesium, unattached cells were removed by gentle rinsing. The cells were filmed using time-lapse light microscopy with images being taken at 10 second intervals. The neutrophils were identified as rapidly migrating cells with a large lamellapodia and small uropod. Neutrophils were observed to attach and rapidly migrate at a similar speed. No consistent abnormalities in the morphology of the S100A9 null population were observed (figure 5.3). A population of large flattened cells adhere to the ICAM-1 coated cover slips. These were assumed to be macrophage or monocyte-like cells and appeared similar in both cell populations. These cells attached, flattened and underwent membrane ruffling during the course of the experiment. No difference

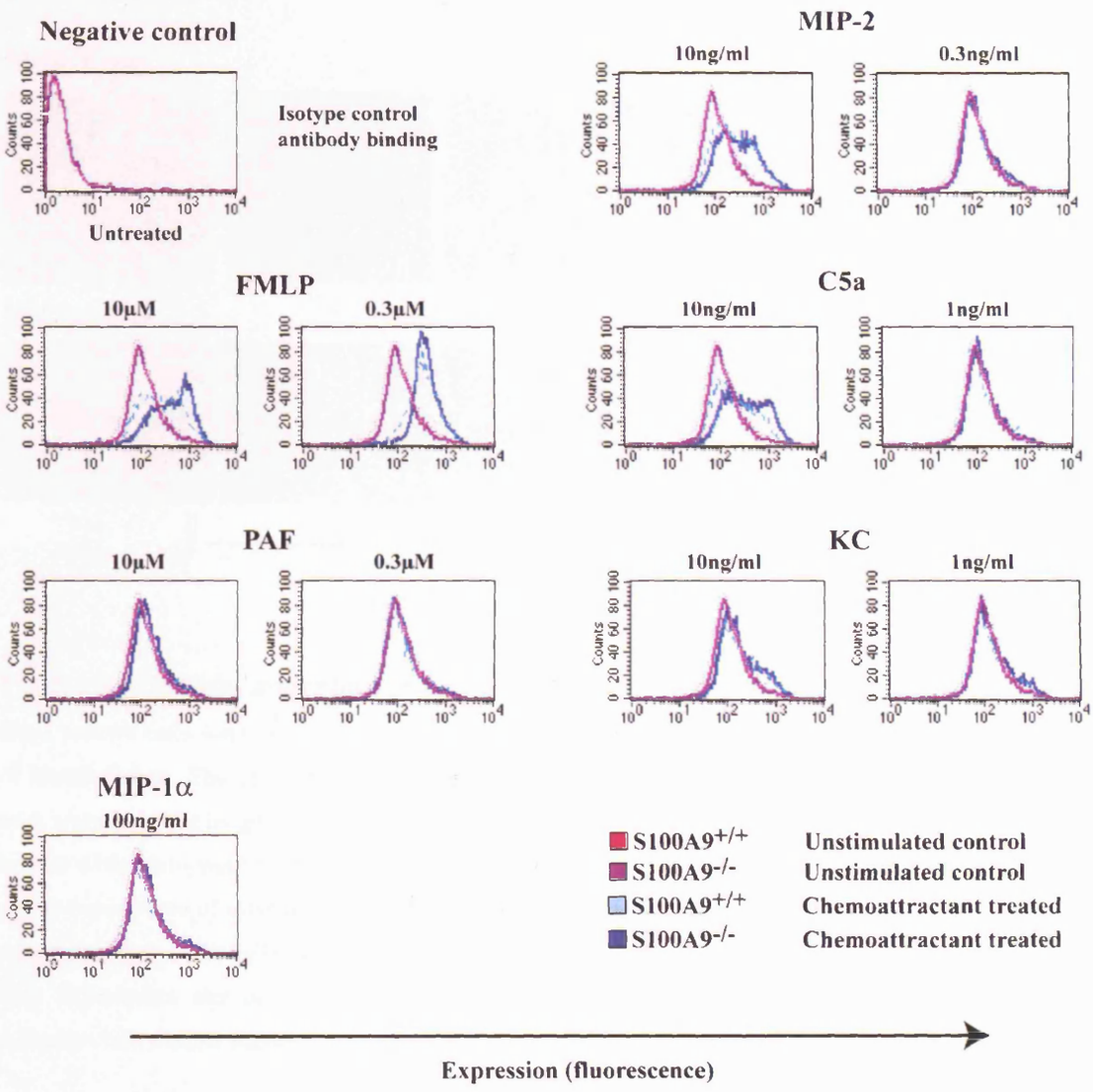

Figure 5.2 Chemoattractant-induced Mac-1 up-regulation on neutrophils

Neutrophils from bone marrow of wildtype and S100A9 null mice were identified by staining cells with mAbs 7/4 and Ly-6G. The expression of Mac-1 was determined by flow cytometry after co-labelling cells with a monoclonal Mac-1 antibody as described in the Materials and Methods. Data shown is for pooled samples from 3 independent animals per genotype and is representative of 3 independent experiments.

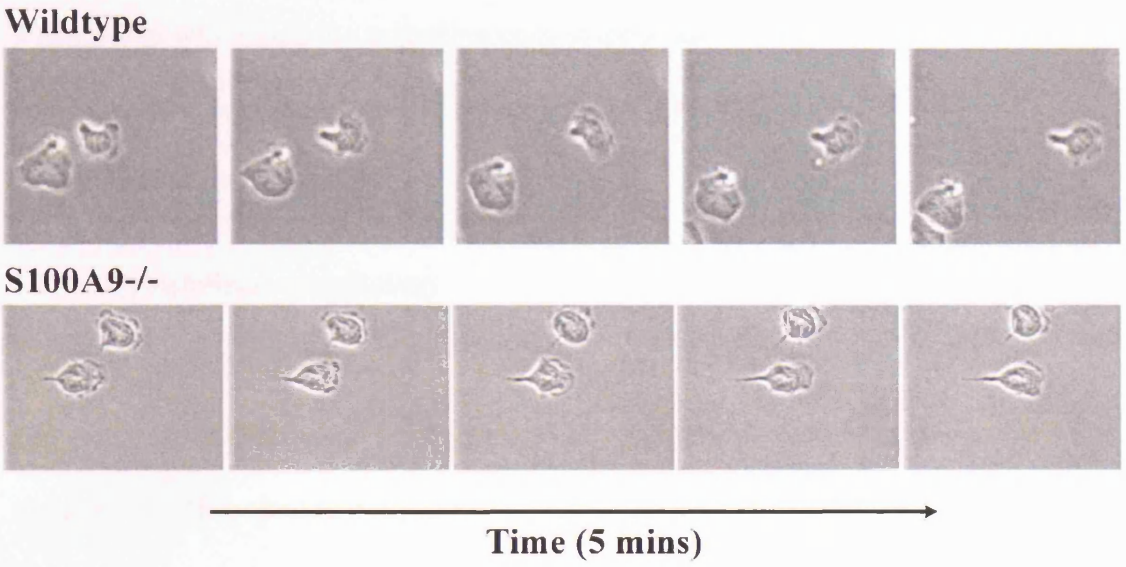

Figure 5.3 Normal migration of S100A9 null neutrophils on ICAM-1

Bone marrow cells were prepared and applied to ICAM-1 coated coverslips mounted in the bottom of Matek dishes. The cells were left to adhere at 37°C for 15minutes. After this time unadhered cells were removed by gently washing the dishes. A representative field of view was selected and images of the cells were taken at 10 second intervals using a light microscope and used to compile a time-lapse video of their behaviour. Images shown are images of individual cells taken at one-minute intervals. The cells shown are representative of more than 30 cells observed per genotype. This experiment was performed in collaboration with Dr Andrew Smith of the Leukocyte Adhesion Lab, Cancer Research UK.

in the behaviour of the wildtype or S100A9 null cells was seen following the addition of LPS, FMLP or MIP-2 during the assay (preliminary, data not shown). When PdBu was added the migrating cells stopped and spread. No difference in this response was observed comparing wildtype and S100A9 null cells. (preliminary, data not shown).

5.2.4 Cytoskeletal morphology

In a migrating leukocyte a highly organised cytoskeletal system is formed and maintained (reviewed in (Pettit and Fay, 1998; Vicente-Manzanares and Sanchez-Madrid, 2004; Wu, 2005)). Interference with this system using pharmacological agents such as cytochalasin D causes the cells to stop migrating or to migrate with compromised morphology. Calcium has been shown to be vital in forming and maintaining this cytoskeletal machinery. It was decided to examine the cytoskeleton of the S100A9 null neutrophils to look for any abnormalities in their morphology.

Wildtype and S100A9 null neutrophils were adhered to ICAM-1 coated coverslips under similar conditions to the migration assay. The adhered cells were stained with anti-tubulin antibodies and phalloidin to visualise the microtubule and actin networks respectively. The neutrophils were identified by lobed nuclear morphology, with nuclei being visualised using DAPI. Figure 5.4 shows a polarised actin distribution in the polarised neutrophil. Polarised actin networks were observed in both wildtype and S100A9 null cells. An organised microtubule cytoskeleton was observed in both wildtype and S100A9 null cells. This shows that the ability of the neutrophils to form a polarised cytoskeletal system while migrating on ICAM-1 is not grossly compromised. Attempts to stain the intermediate filaments using anti-vimentin antibodies were unsuccessful.

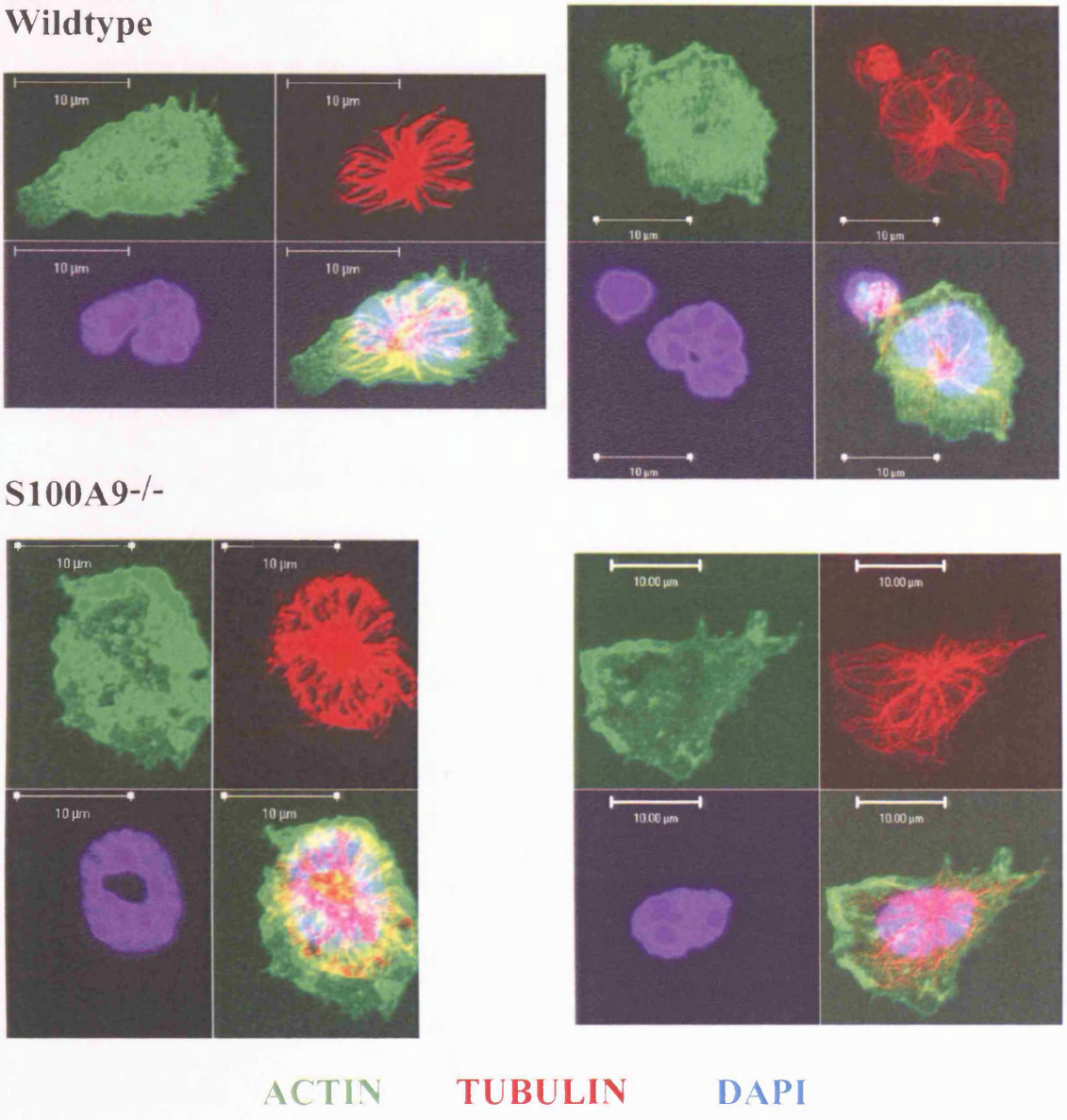

Figure 5.4 Morphology of the actin and microtubule cytoskeleton in wildtype and S100A9 null neutrophils

Bone marrow leukocytes were prepared and allowed to adhere to ICAM-1 coated coverslips for 30min at 37°C. Unattached cells were removed by washing and fixed using 3% formaldehyde followed by quenching of cellular auto-fluorescence using ammonium chloride. The cells were permeabilised using 1% Triton and incubated with directly conjugated Alexa 488-phalloidin to visualise the actin cytoskeleton (shown in green), Alexa 567-anti-tubulin antibody (shown in red) and DAPI to visualise nuclear morphology (shown in blue). Serial sections throughout the cell were imaged using a confocal microscope and compiled together to form a composite image. Cells shown are representative of the total population observed in 2 independent experiments.

5.2.5 S100A9 localization

While looking at the cytoskeletal system of the bone marrow leukocytes any co-localization of the S100A9 protein with any particular cellular compartment was examined. A monoclonal anti-S100A9 antibody directly conjugated to Alexa-488 was used. The specificity of this antibody was confirmed by the absence of staining in the S100A9 null bone marrow cells and also by the presence of staining only in myeloid cells (identified by morphology) in the wildtype samples. In the adherent cells the distribution of S100A9 appeared to both cytosolic and membranous (figure 5.5). Co-staining with anti-tubulin antibody to identify the microtubules revealed no co-localization with S100A9. When the cells were stained with phalloidin and the anti-S100A9 antibody some co-localization was seen, with areas of high actin expression often showing intense S100A9 staining (figure 5.6). However, not all the S100A9 staining was co-incident with actin staining and *vice versa*, indeed S100A9 seemed to be excluded from some actin rich areas. The significance of this limited co-localization is unclear, and it should be remembered that S100A9 is an abundant protein. To look for any alteration of the distribution of S100A9 upon cell stimulation, the adhered cells were treated with ionomycin, LPS, PdBu, MIP-2 and FMLP (preliminary, data not shown). More flattened cells were observed following PdBu treatment, but no change in the distribution of S100A9 was seen following any stimuli (data not shown).

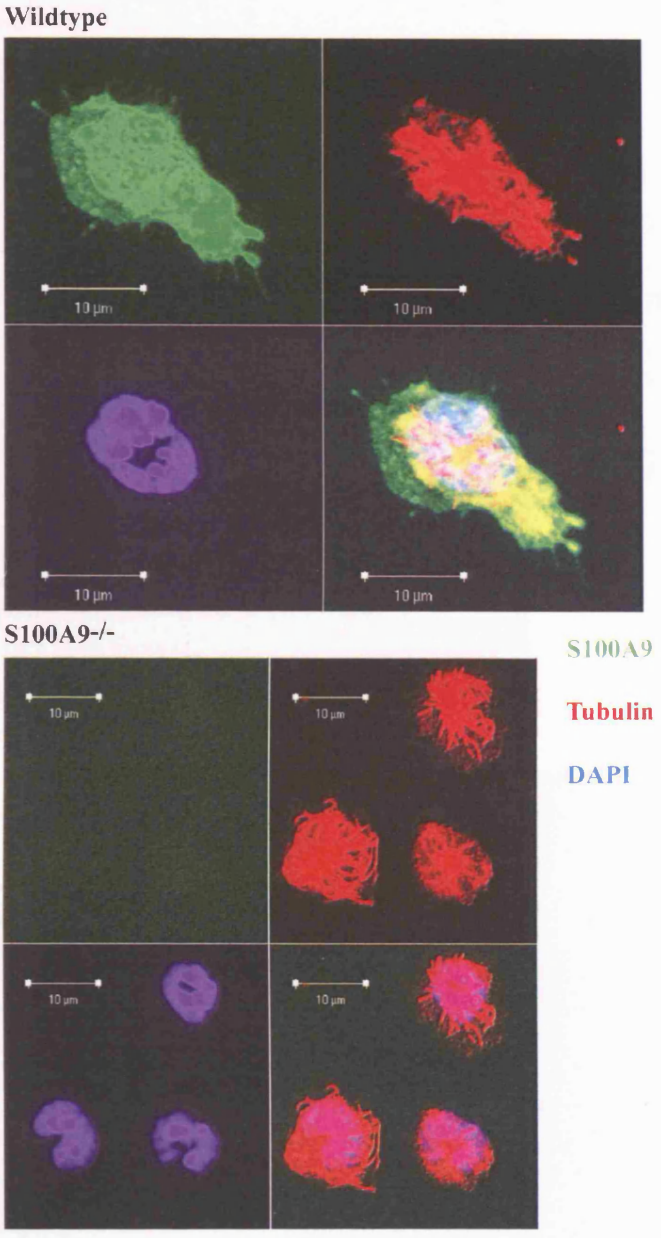

Figure 5.5 No co-localization of S100A9 with micro-tubules

Bone marrow leukocytes were prepared and allowed to adhere to ICAM-1 coated coverslips for 30min at 37°C. Unattached cells were removed by washing and fixed using 3% formaldehyde followed by quenching of cellular auto-fluorescence using ammonium chloride. The cells were permeabilised using 1% Triton and incubated with directly conjugated anti-S100A9 antibody Alexa 488-2B10 (shown in green), Alexa 567-anti-tubulin antibody (shown in red) and DAPI to visualise nuclear morphology (shown in blue). Serial sections throughout the cell were imaged using a confocal microscope and compiled together to form a composite image. Cells shown are representative of the total population observed in 2 independent experiments.

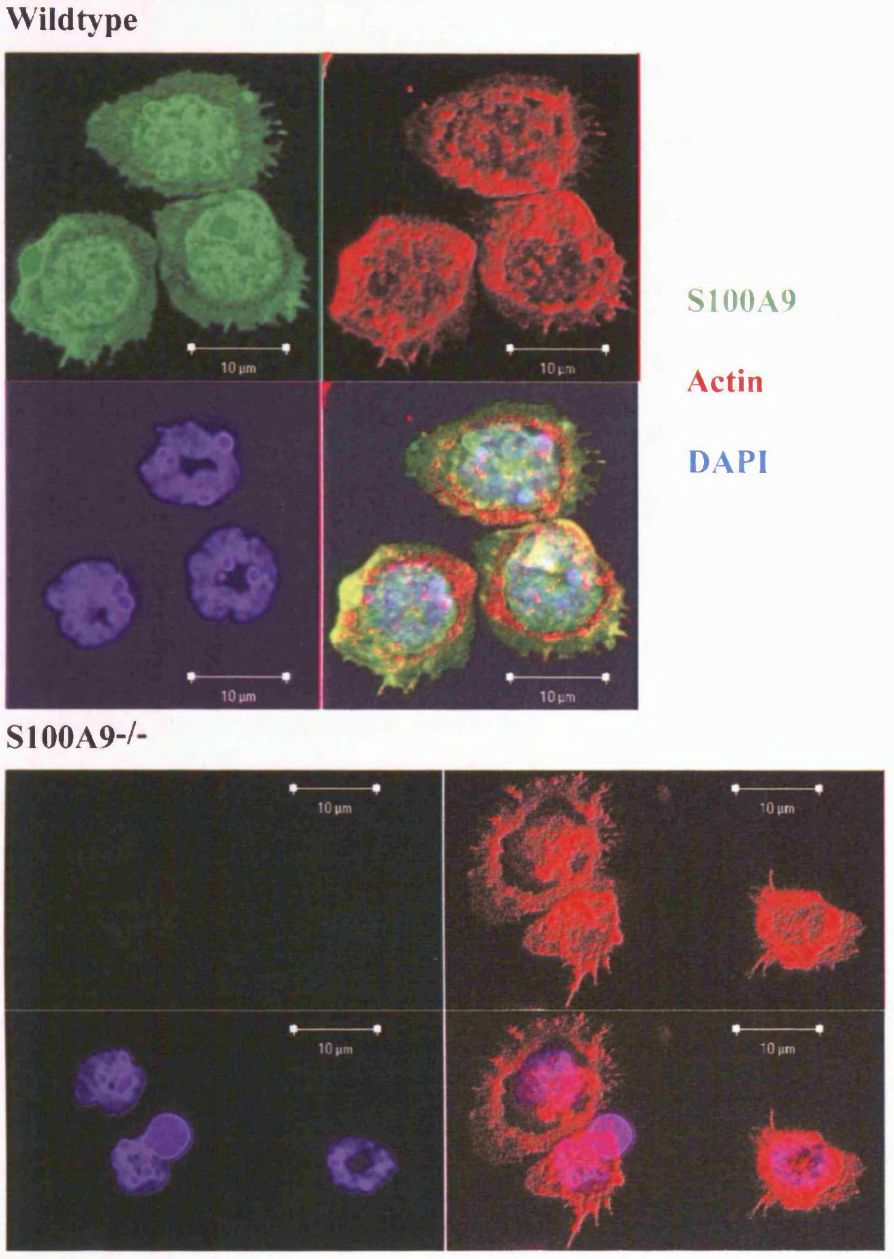

Figure 5.6 Limited co-localisation of S100A9 with actin in neutrophils

Bone marrow leukocytes were prepared and allowed to adhere to ICAM-1 coated coverslips for 30min at 37°C. Unattached cells were removed by washing and fixed using 3% formaldehyde followed by quenching of cellular auto-fluorescence using ammonium chloride. The cells were permeabilised using 1% Triton and incubated with directly conjugated anti-S100A9 antibody Alexa 488-2B10 (shown in green), Alexa 567-phalloidin to visualise the actin cytoskeleton (shown in red) and DAPI to visualise nuclear morphology (shown in blue). Serial sections throughout the cell were imaged using a confocal microscope and compiled together to form a composite image. Cells shown are representative of the total population observed in 2 independent experiments.

5.2.6 An *in vitro* model of chemotaxis

To combine the previous experiments and further test if the S100A9 null neutrophils are compromised in their ability to respond normally to chemoattractant stimuli, given their decreased calcium flux response, an *in vitro* chemotaxis assay was performed. In this experiment a Transwell system is set up with the cells in normal media placed in a plastic insert separated by a 3μm pore filter from a well containing media and a chemoattractant stimulus. In this assay the panel of chemoattractants tested in the Mac-1 upregulation studies was again tested. To ensure that the migrating bone marrow cells were indeed neutrophils, the harvested cells were stained with the 7/4 and Ly-6G antibody cocktail and were confirmed to be neutrophils (data not shown). The number of cells migrating towards a chemoattractant stimulus was enumerated by performing an absolute cell count by flow cytometry.

No significant difference in random, unstimulated migration of the cells was observed between wildtype and S100A9 null populations (figure 5.7). Migration of the neutrophils to MIP-2, FMLP and KC was seen at both concentrations studied (figure 5.7). In the case of MIP-2 and KC the highest level of migration correlated with the higher level of chemokine. In the case of FMLP the lower concentration tested showed the greater migration presumably showing that 10μM is above the maximal concentration, as chemoattractants show a bell-shaped curve of sensitivity of chemoattractants. When the number of cells migrating to the three stimuli are compared no significant differences in the number of wildtype or S100A9 null cells migrating is seen (as indicated by the overlapping error bars).

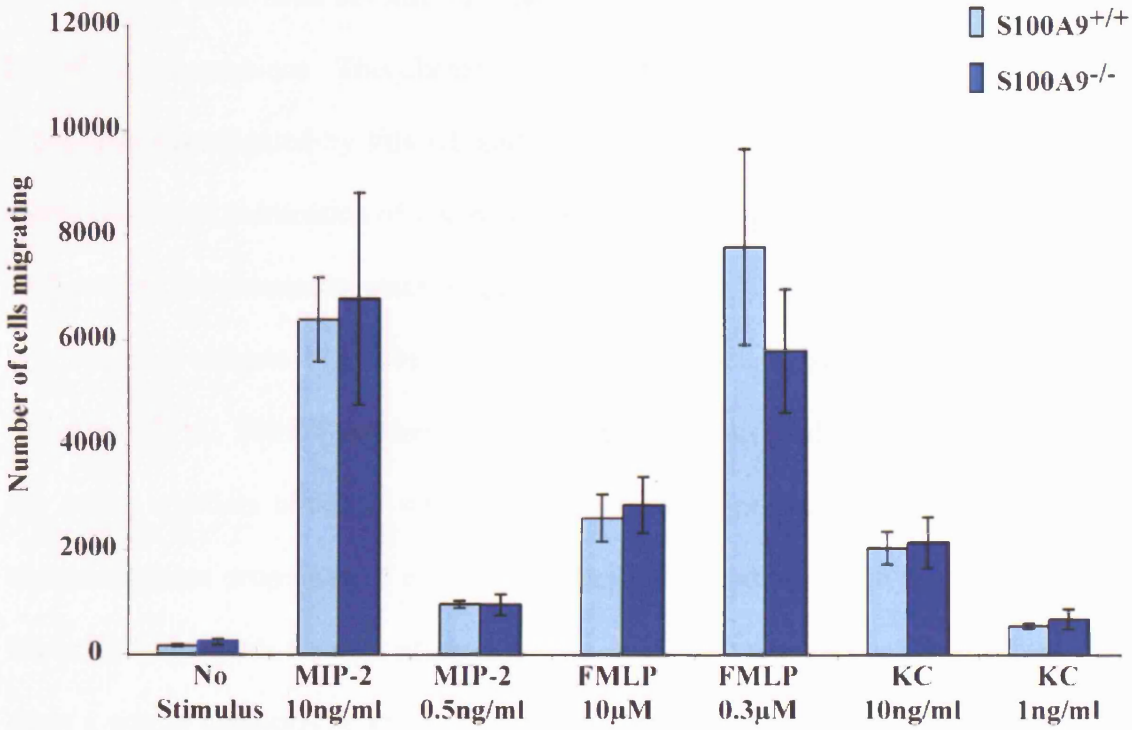

Figure 5.7 Normal *in vitro* chemotaxis of S100A9 null neutrophils

Migration of bone marrow neutrophils in a Transwell chemotaxis assay in response to the chemoattractants was assessed. Cells were allowed to migrate for 2 hours, then cells in the bottom well were stained with mAbs 7/4 and Ly-6G. The number of migrated neutrophils was determined by flow cytometry. Data are expressed as the mean of 3 independent samples per genotype +/- standard deviation. Data is representative of 3 experiments.

5.2.7 S100A9 as a chemokine

There have been several publications indicating a role for S100A8 and S100A9 as chemokines. This chemoattractive effect of murine S100A9 has been previously investigated by this lab and could not be confirmed (Hobbs, 2003). Given the recent publication of several papers by the group of P. Tessier, showing evidence of the chemoattractant properties of human S100A9 it was decided to briefly re-investigate this role using a sample of their recombinant S100A9 (Ryckman et al., 2004; Ryckman et al., 2003a; Ryckman et al., 2003b). One of the major artefacts obtained when using a recombinant protein to investigate chemoattractant properties of a protein is the contamination of the protein with bacterial by-products from its production. Bacterial contaminants can themselves exert a potent chemotactic effect *in vivo*. The Ryckman *et al* paper states that their protein has a low level of endotoxin contamination (Ryckman et al., 2003b). Tests in this laboratory using the limulus amoebocyte assay showed the samples sent to us contained in excess of 1ng/μg protein (E. M^{c}Neill – data not shown).

LPS, a major component of bacterial endotoxin, does not exert a chemoattractive effect *in vitro* so although the proteins were contaminated any chemoattractant effect of the S100A9 proteins in the Transwell assay could be an indication of their activity. When the S100A9 protein was compared to PBS alone control no chemoattractant effect of the protein could be seen at 1nM or 1μM concentrations (figure 5.8). As a positive control C5a was included in the assay and was shown to be highly chemoattractive. These results were in conflict to the published data using the S100A9 protein by Ryckman et al.

To examine the chemoattractive potential of an LPS contaminated protein *in vivo* it is not appropriate to use a normal LPS-sensitive mouse as the LPS will

exert a potent chemoattractive effect itself. We repeated the published air pouch model of *in vivo* chemotaxis in the C3H/HeJ LPS-insensitive mice and the control LPS-sensitive strain C3H/HeN (Ryckman et al., 2003b). The S100A9 sample exerted a chemoattractive effect in the C3H/HeN mice, but showed no chemoattractive potential above the dose of LPS equivalent to the contamination of the protein in the C3H/HeJ mice, indicating that the chemoattractive effect seen was likely to be due to the LPS contamination of this protein (figure 5.8). This is again in conflict with the published data. Similar to previous finding by this lab (Hobbs, 2003) I found no evidence that S100A9 acts as a chemokine either *in vitro* or *in vivo*.

5.2.8 *In vivo* migration studies

The *in vitro* chemotaxis assay provides some evidence that the ability of the S100A9 null neutrophils to chemotax is not severely affected. However, the process of deforming through a plastic filter to move towards a chemoattractant in media does not fully replicate the process of responding to a proinflammatory agent *in vivo*. While the *in vitro* assay is useful in allowing the assessment of the response of the neutrophils to a specific chemotactic agent it is more important to know if the cells can perform normally under physiological conditions. To test this a model of peritonitis was used, where inflammation was initiated in the peritoneum with thioglycollate, IL-1β or TNFα. To respond to the stimuli the neutrophils need to adhere to the inflamed endothelium, extravasate out through the vessel wall, pass through the basement membrane and migrate through the tissue into the peritoneum. Thioglycollate-induced peritonitis has been performed using S100A9 null mice at backcross generation five (Hobbs et al., 2003). These experiments did not show any affect of S100A9 deletion on the ability of the

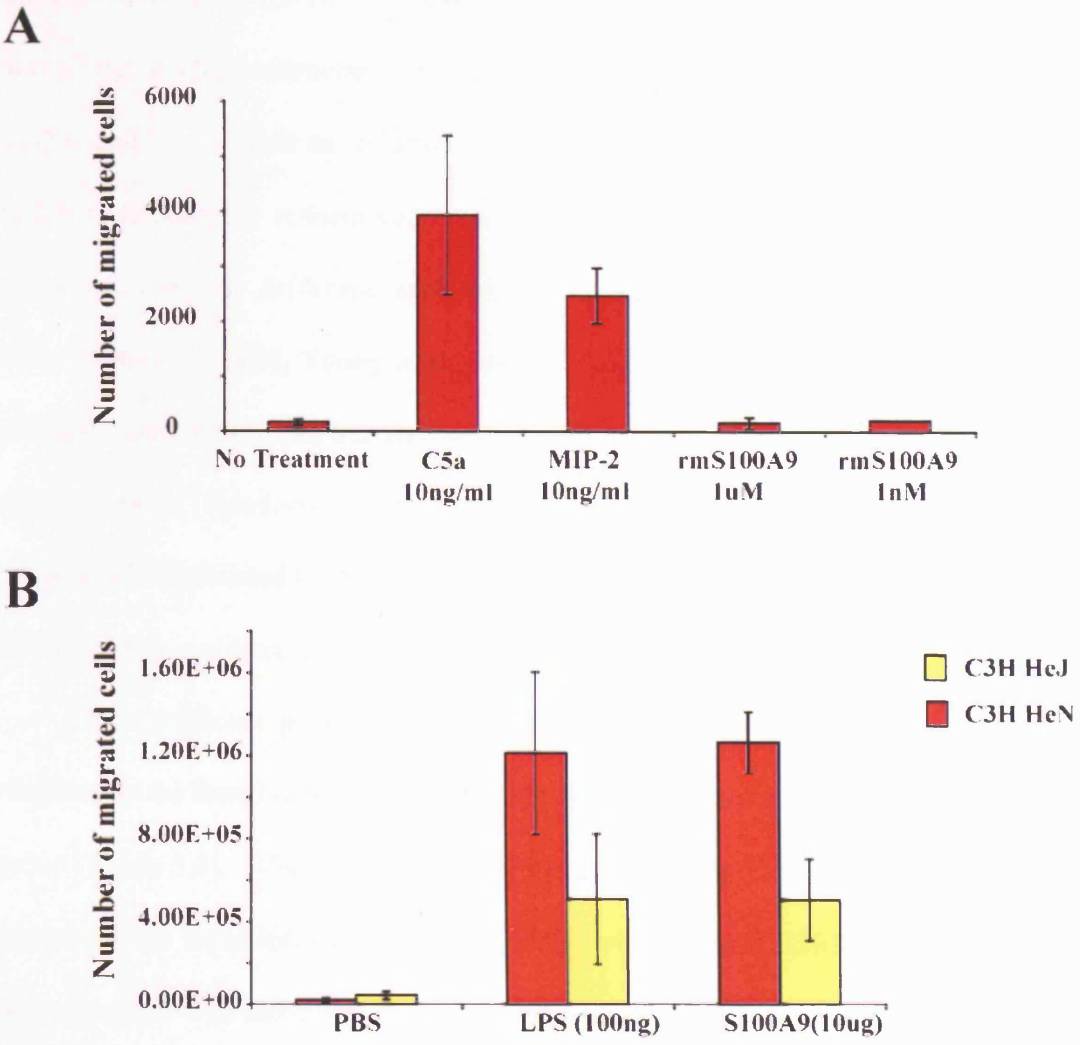

Figure 5.8 Effect of recombinant murine S100A9 on *in vitro* and *in vivo* neutrophil migration

A: Migration of bone marrow neutrophils in a Transwell chemotaxis assay in response to the S100A9 and chemoattractants C5a and MIP-2 was assessed. Cells were allowed to migrate for 2 hours, then cells in the bottom well were stained with mAbs 7/4 and Ly-6G. The number of migrated neutrophils was determined by flow cytometry. The experiment shown was performed in triplicate with data displayed as mean +/- standard deviation.

B: Air-pouches were formed on the back of mice by repeated injection of sterile air. S100A9, LPS or PBS, prepared using endotoxin free reagents, were injected into the air pouches and the cellular infiltrate was recovered by lavage with EDTA containing PBS at 6 hours post-injection. The recovered cells were stained with mAbs 7/4 and Gr-1 and quantified using flow cytometry. Data shown is the mean +/- standard error of the mean for 5 mice per time point.

neutrophils to respond in this model. However, as the mice are now fully backcrossed onto a C57BL/6J background and the cells show a defect in calcium signalling to chemoattractant stimuli, *in vivo* migration was examined further. TNFα and IL-1β elicit an inflammatory reaction by stimulating endothelial and resident leukocytes respectively and have been shown to caused neutrophil extravasation via different mechanisms ((Dahlgren and Karlsson, 1999; Thompson et al., 2001; Young et al., 2002)). A six hour time point was chosen as previous work by this lab has shown significant peritoneal myeloid cells influx at this time point (Henderson et al., 2003). At this time the mice are culled and the elicited cells harvested by peritoneal lavage. Any mice showing significant blood in the peritoneum were discarded.

A significant influx of both neutrophils and monocytes was found in response to the thioglycollate, TNFα and IL-1β stimuli, but not in the PBS control group (figure 5.9). When the numbers of neutrophils migrating to all stimuli were compared, no significant difference between wildtype and S100A9 null groups was observed. The same was also observed when the numbers of monocytes were assessed. This finding is in keeping with the previous work with the S100A9 null mice where thioglycollate alone was used as a stimulus ((Hobbs et al., 2003; Manitz et al., 2003)). No effect on the influx of other leukocytes was found in these previous studies, and as no defect in the initial myeloid cell influx was seen it was decided not to extend these experiments to perform a full time course of leukocyte recruitment.

This work finds no role for S100A9 in leukocyte migration either *in vitro* or *in vivo* either by affecting the function of the neutrophils themselves or by acting as an *in vivo* chemoattractant. This work also casts doubt on the published

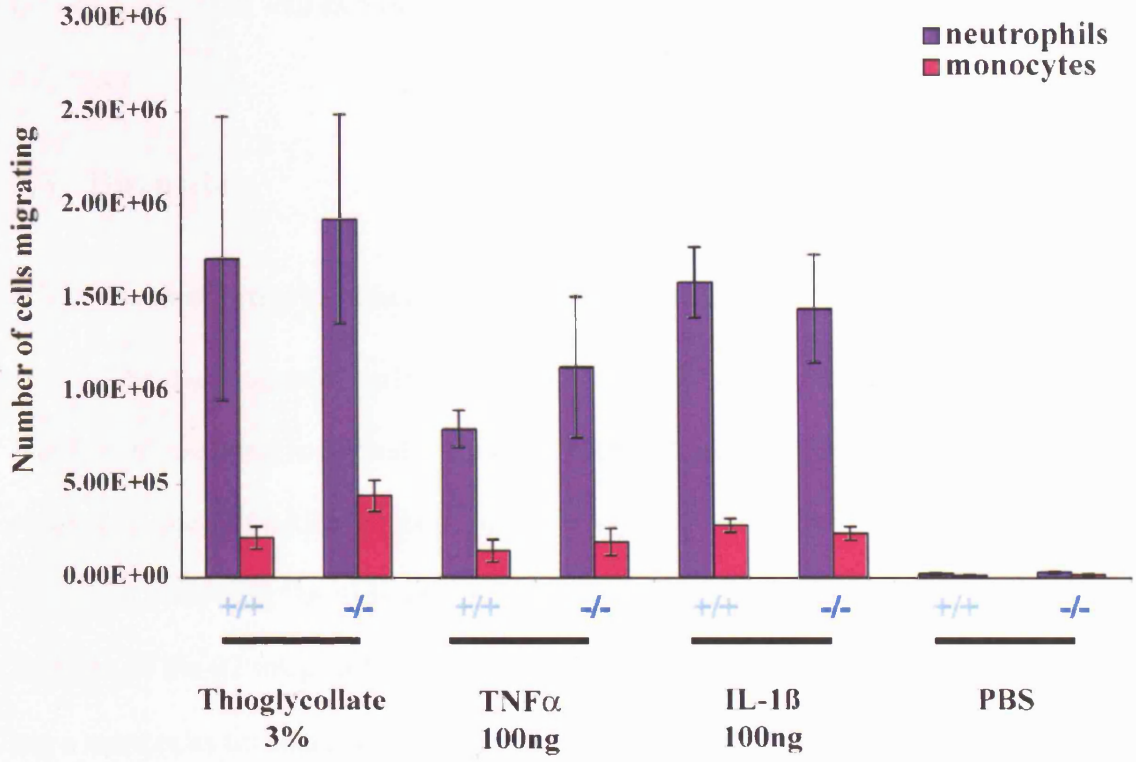

Figure 5.9 *In vivo* migration of myeloid cells into the peritoneum in response to inflammatory stimuli

Leukocyte recruitment into the peritoneum was initiated by intra-peritoneal injection of inflammatory stimuli thioglycollate, TNFα, IL-1β and PBS control. Six hours post injection the mice are culled and the recruited cells harvested by peritoneal lavage with PBS/EDTA. The cells were stained with mAbs 7/4 and Ly-6G and quantified by flow cytometry.

reports of chemoattractant properties for both S100A8 and S100A9. This would include S100A8 as well as S100A9 as both proteins are missing from the S100A9 null mice.

5.3 Discussion

5.3.1 Normal Integrin Function in S100A9 null mice

The data presented earlier in this thesis has shown that the expression of a number of integrins is normal on the S100A9 null cells. Further experiments show that the S100A9 null bone marrow cells demonstrate normal integrin activation following "outside in" and "inside out" stimulation showing that the function of the β2 integrin Mac-1 is broadly normal. Preliminary experiments to use a more relevant chemokine stimuli in this assay showed no obvious difference in activity in the S100A9 null cells. However as only 25-35% of the total cells studied in these experiments are neutrophils it is hard to assess any subtle effects. To extend this part of the study a method of isolating a pure population of neutrophils would be required.

Another manner in which the activity of integrin is enhanced in the neutrophil is the upregulation of the surface expression of Mac-1. In this study upregulation of Mac-1 was seen in response to MIP-2, C5a and FMLP. S100A9 appears to be dispensable for this function. No manifestation of the decreased chemoattractant sensitivity of the S100A9 null neutrophils in the calcium flux assay was seen. It was noted that the concentrations at which the Mac-1 up-regulation was seen were above the levels at which the deficiency in calcium signalling is seen. This data shows that although the Ca^{2+} signalling properties of

the S100A9 null cell are compromised, the cells can be activated by chemoattractants.

5.3.2 Migration and Morphology of S100A9 null neutrophils

Using a model of *in vitro* migration it has been demonstrated that murine bone marrow neutrophils can polarise and migrate on murine-ICAM-1 coated coverslips with no additional activating stimuli. This random migration on ICAM-1 has been recently described in this lab for human T cells (Smith et al., 2003). In the T cell situation, no autocrine secretion of chemokine could be found to provide a directional stimuli for this migration. The migratory pattern was therefore assumed to be truly random, or perhaps following undetectable gradients of ICAM-1 formed during the coverslip coating process. Neutrophils are more sensitive than T cells to signals such as LPS and the products of apoptosis, that do not activate T cells and further investigation and validation of this model would be required to elucidate the migratory stimuli the cells may be following. It should be noted that significant variation between preparations was observed for both wildtype and S100A9 null cells, perhaps a facet of how easily these cells can be activated. However, it could be seen that the S100A9 null neutrophils were as capable of attaching and migrating with a similar morphology to the wildtype neutrophils. No gross difference in their speed or directionality could be seen although it was hard to judge absolutely due to the intra-preparation differences.

As a preliminary study of the migratory capacity of these cells, it can be concluded that S100A9 is dispensable for normal migration of murine neutrophils on ICAM-1. In studies on human T cells, profound morphological effects of pharmacological inhibition of various parts of the cytoskeleton are seen (Smith et

al., 2003). None of these morphologies were present in the S100A9 null neutrophils, implying no gross failure of the cytoskeleton.

Further investigation of these features led to the examination of the cytoskeletal by confocal microscopy. Firstly no difference in the formation of microtubule networks in the S100A9 null or wildtype neutrophils could be seen. Similarly no gross abnormalities in the actin cytoskeleton could be seen. This was expected given the normal migratory phenotype of the cells in the video-microscopy experiments. Further to this, the localization of the S100A9 protein was examined in the wildtype neutrophils. It was assumed that all the S100A9 bright cells were neutrophils. No S100A9 dim cells, that would be assumed to be monocytes, were observed. This led to the interesting observation that the S100A9 positive cells seemed to exhibit two markedly different morphologies, either polarised and migrating or rounded adhered cells, similar to those seen in the video-microscopy experiments. Attempts to confirm that both these populations were Ly6G positive, ie neutrophils, were unfortunately unsuccessful. It might be interesting to see if these two morphologically different groups represent different maturation states of the murine neutrophil. It should be pointed out that no differences in the proportion of the different cell types were observed between S100A9 null and wildtype samples.

In terms of cytoskeletal networks it has been reported that S100A9 co-localises with micro-tubules in human macrophages(Rammes et al., 1997). No observation of a similar feature was seen in murine bone marrow cells. Secondly, although staining for vimentin was unsuccessful the S100A9 staining itself did not appear to form any fibrous structure, arguing against any interaction with the intermediate filaments as has been shown in previous reports (Burwinkel et al.,

1994; Roth et al., 1993). No evidence of the "polarised micro-filament network" that has been reported in another line of S100A9 null mice was seen in these experiments (Manitz et al., 2003). As with the migration assays the observation of several separate neutrophil preparations is required due to the variation in the morphology of the cells between different preparations. In this study some co-localisation of S100A9 with the actin cytoskeleton could be seen. This possible interaction requires further investigation as the sheer abundance of this protein in the cells makes observation of some irrelevant co-localisation likely. It can be said with some certainty that no obvious association of S100A9 with larger cellular structures, such as the nucleus, mitochondria, granules, or endoplasmic reticulum, is obvious under any of the stimuli tested. Staining the two cell populations with probes to identify cellular compartments, such as the endoplasmic reticulum, to observe any altered structure could be an interesting extension to this work.

5.3.3 No role of S100A9 in neutrophil chemotaxis

It has been reported by another group working with an independently derived line of S100A9 null mice that the neutrophils in those mice demonstrate a higher basal migration *in vitro* across Bend5 brain endothelial cells and a decreased migration in response to recombinant human IL-8 or LTB4 (Manitz et al., 2003). This difference was apparently significant. No assessment of the quality of the data can be made as the error bars are absent from the graph shown (Manitz et al., 2003). In addition, the migration of the S100A9 null cells in a 3D collagen matrix was quantified and the S100A9 null cells were deemed to have significantly higher migration rate, velocity of migration and distance of migration (Manitz et al., 2003). The degree to which the error bars overlap in the

data presented in this paper make it highly surprising that the differences are significant and the statistical tests used to evaluate the data are not stated.

It has been previously described by this laboratory that the bone marrow neutrophils from both our S100A9 null mouse lines demonstrate normal chemotaxis to the murine homolog of IL-8 (MIP-2), exhibiting a normal bell-shaped curve of sensitivity to this mediator (Hobbs et al., 2003). To extend the *in vitro* chemotaxis studies, I have used the stimuli to which the S100A9 null mice exhibited a decreased sensitivity in the calcium flux experiments. Due to constraints of reagents, full dose response curves were not performed for all these mediators, but a high and low dose from the titration range calcium assay were used. No deficiencies in the response of the S100A9 null cells were seen. Thus we see no defect in *in vitro* chemotaxis to a range of stimuli.

It is unclear why we obtain different results using cells from our S100A9 null mice to those published for the other S100A9 null mice although, however, no significant differences in myeloid recruitment in an *in vivo* model of peritonitis are seen in either mouse line. This may be the most enlightening data regarding any role for S100A9 in cell migration. Specific differences in the preparation of the cells may cause the differences between the results obtained by independent groups. Differences in genetic background may also play a role in the disparity as our mice are fully back-crossed onto a C57BL/6J strain, whilst the other mice are on a mixed 129/C57BL/6J background and may demonstrate increased variation. Differences in the precise model of *in vitro* migration used may also be an explanation for the different results obtained.

This difference in migratory ability is not the only data I have produced that is in direct conflict with published roles for these proteins. There is a

significant body of work that proposes S100A9 to be a potent chemokine in mouse. Using samples from the authors of that work we were unable to demonstrate any chemotactic activity more than could be assigned to contaminating LPS. An explanation might be the chemotactic activity of the protein samples was destroyed in the transport process. However, previous exhaustive examination of recombinant S100A9 in this lab has failed to show any chemotactic activity other than due to contaminating endotoxin (Hobbs, 2003). The levels of S100A9 required to produce the chemotactic effect are more than a thousand fold lower than the peak concentrations reported in an inflammatory site (Roth et al., 2003). It would be interesting to perform the model of urate crystal-induced neutrophil influx into the air pouch, that has been shown to be S100A9 dependent, in the S100A9 null mice to observe if S100A9 truly participates in this model (Ryckman et al., 2003a).

Final evidence for the function of S100A9 being dispensable in the process of leukocyte adhesion and migration comes from an *in vivo* model of leukocyte migration. Normal myeloid cell recruitment into the peritoneum was observed following stimulation by thioglycollate, TNFα and IL-1β. These stimuli have been previously shown to cause leukocyte recruitment dependent on different integrin family members (Thompson et al., 2001; Young et al., 2002). The lack of any lesion in the S100A9 null mice in recruitment to any of these stimuli seems to imply a relatively broad lack of requirement for S100A9 in neutrophil recruitment. This data is in accordance with results published for the independent strain of S100A9 mice in which no defect in *in vivo* migration was seen (Manitz et al., 2003).

The studies presented in this chapter could be extended to involve more in depth analysis of chemokine-induced adhesion and further investigation of the speed and morphology of the S100A9 neutrophils. However given the lack of any *in vivo* phenotype resulting from the loss of S100A9, it seems unlikely any gross abnormality will be found. This implies that the calcium signalling deficiency in the S100A9 null neutrophils, as shown in chapter 4, does not affect normal migration. The role of the affected calcium signal may be critical to a process independent of leukocyte recruitment. Indeed PLCβ2/3 null neutrophils, that produce no calcium flux in response to chemokine stimulation, show normal leukocyte migration (Li et al., 2000b). This indicates that the calcium signal is dispensable for leukocyte migration.

In conclusion, despite the published data that neutrophils from another strain of S100A9 null mice show abnormalities in leukocyte migration due to a hyper-polarised micro-filament system (Manitz et al., 2003) and that S100A9 is reported to be a potent chemokine *in vivo* (Ryckman et al., 2003b), I find S100A9 to be totally dispensable for normal leukocyte adhesion and migration in the models tested to date.

CHAPTER 6

6 Cytotoxic activity of S100A9 null neutrophils

6.1 Introduction

The role of the neutrophil within the body is to combat infection. So far it has been shown that, in the S100A9 null mice, the neutrophils have a defect in chemokine-induced calcium signalling, yet are able to respond normally to a chemotactic stimuli *in vitro* and *in vivo*. Therefore we assume that they are largely able to arrive normally at the site of infection. To examine any further role for S100A9 in the neutrophil other functions relating to their cytotoxic abilities were investigated.

As has been discussed in the introduction there is a body of evidence that suggests a role for S100A8/9 in the formation of the oxidase machinery. The complex co-precipitated with components of the NADPH oxidase machinery and was able to activate the oxidase machinery in a cell-free system (Doussiere et al., 2002; Kerkhoff et al., 2005). Most recently it has been shown that the independent line of S100A9 null mice showed decreased superoxide formation in response to PMA stimulation(Kerkhoff et al., 2005). It has already been demonstrated that our line of S100A9 null mice are capable of normal phagocytosis of *E. coli* and that they are capable of forming an oxidative burst in response to PMA (Hobbs et al., 2003). In this experiment the kinetics of the superoxide burst was not assessed. The fluorescence of dihydrorhodamine, an oxidant sensitive dye, was tested by flow cytometry following a set time interval. Given that the published effect of S100A9 deletion on oxidant production

appeared to be a subtle decrease in the reaction kinetics a more full exploration of this phenomenon was required.

Along with the oxidase, granule fusion and trafficking are vital aspects of the neutrophil killing mechanism (reviewed in (Faurschou and Borregaard, 2003)). Studying the ability of the S100A9 neutrophils to kill bacteria would provide a test of how the whole neutrophil cytotoxic machinery is working. However the best test for neutrophil function is an *in vivo* bacterial infection, this will test all aspects of neutrophil function from their ability to adhere and migrate to phagocytosis and killing of invading microorganisms.

Streptococcus pneumoniae is a Gram positive human pathogen that is the fifth leading cause of death worldwide (reviewed in (Kadioglu and Andrew, 2004)). This bacterium is responsible for 40-50% of community-acquired pneumonia and 20% of meningitis cases in the UK. As such the pathogenesis of this disease is widely studied and the murine model well characterised. To test the function of the neutrophils in the S100A9 null mice, we require an infection in which the innate immune system plays an important role in its control. In pneumococcal lung disease the bacteria are thought to be primarily opsonized by complement (reviewed in (Kadioglu and Andrew, 2004)). Following opsonization the bacteria are phagocytosed and killed by neutrophils recruited to the lung by resident macrophages following release of TNFα and IL-8. The initial phase of control of infection is highly dependent on the adequate function of neutrophils.

6.2 Results

6.2.1 Kinetics of superoxide formation

In the Hobbs *et al* publication, the production of an oxidative burst by the S100A9 null neutrophils was examined. In that study the production of the oxidative burst was assessed by flow cytometry, with the change in fluorescence of dihydrorhodamine assessed after stimulation of the cells with PdBu (Hobbs et al., 2003). While this experiment shows that the S100A9 null neutrophils are capable of forming a similar oxidative burst, it did not give any data on the kinetics of the response. The kinetics of oxidant production by neutrophils can be assessed using a number of different assays. The most simple to perform is enhanced chemiluminescence monitored using luminol. This substance is freely diffusible through neutrophils and emits a photon of light when it comes into contact with oxidants (discussed in (Dahlgren and Karlsson, 1999)). The photons of light produced over time can be monitored in a plate-reading luminometer. Being freely diffusible, luminol measures the production of oxidants inside the cell as well as any released oxidants. Other methods of measuring superoxide burst such as cytochrome c reduction rely on the release of oxidant species by the cells as they are not cell permeable agents. When wildtype and S100A9 null bone marrow preparations were stimulated with PMA, an increase in Relative Light Units (RLU) occurred over time in both wildtype and S100A9 samples (figure 6.1). When the kinetics of this response was plotted, the two groups had overlapping error bars and thus had similar kinetics. A similar result was obtained when the experiment was repeated using the cytochrome c reduction test (preliminary, data not shown).

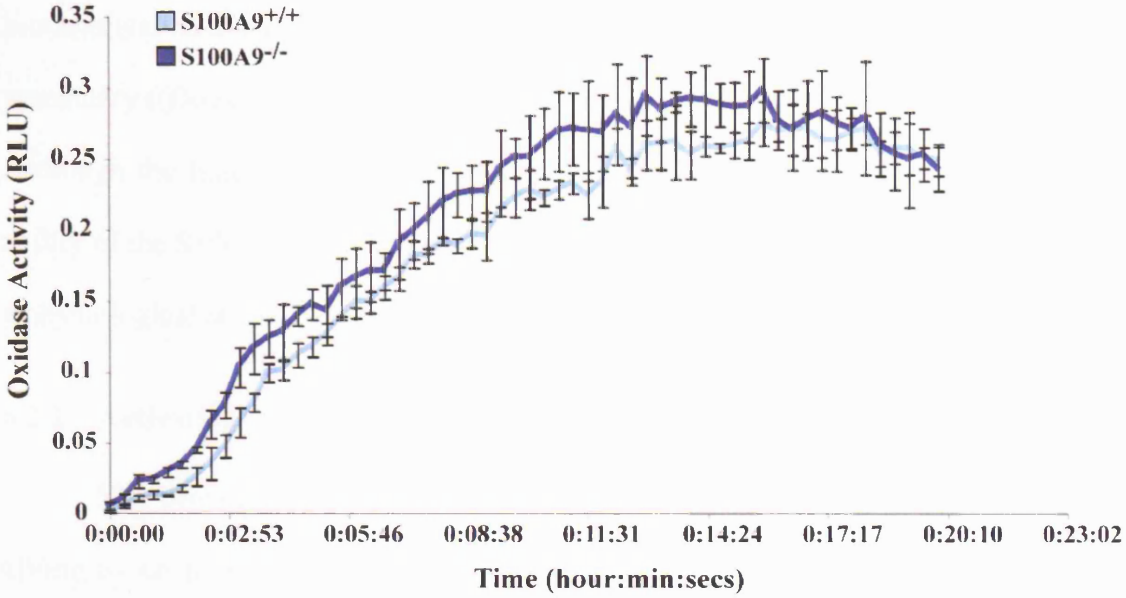

Figure 6.1 Production of oxidant species by wildtype and S100A9 null bone marrow cells in response to PMA

Bone marrow leukocytes were applied to a 96-well plate in luminol supplemented HBSS. The cells were stimulated with PMA and immediately placed in a plate-reading luminometer. The production of oxidants was measured as the production of photons of light by the luminol solution. The plate was read every 17 seconds over a period of twenty minutes. The experiment was performed in duplicate with 3 independent samples per genotype. Data is shown as mean values +/- standard deviation and is representative of 3 experiments.

These data show that the S100A9 null neutrophils are not compromised in their ability to produce an oxidative burst. This conflicts with the published biochemical data that speculates a crucial role for S100A9 in the function of this machinery ((Doussiere et al., 1999; Doussiere et al., 2002; Kerkhoff et al., 2005)). Although the fundamental function of the oxidase machinery is unaffected, the ability of the S100A9 null neutrophils to produce an oxidative burst in response to a physiological stimulus, such as a bacterium, has not been assessed.

6.2.2 Activation of oxidative burst following phagocytosis

The principal role of the oxidative burst is to participate in microbial killing by neutrophils as discussed in the Introduction. Despite the controversy over the mechanism of this function, be it as a direct cytotoxic moiety or as part of a process of protease activation via internal ion flux, its requirement for neutrophil cytotoxicity is clear (reviewed in (Segal, 2005)). Having observed that the S100A9 neutrophils are capable of forming an oxidative burst, it next seemed logical to examine if the cells could perform this function normally following a physiological stimulus.

To carry out this experiment, opsonized dichlorodihydrofluorescein- (DCDHF) coupled zymosan particles were obtained (a kind gift from MB Hallett). As DCDHF becomes fluorescent upon oxidation, the coupled particles act to indicate if the oxidase is activated upon phagocytosis of the particles (preparation and use of particles detailed in (Dewitt et al., 2003)). To monitor this process neutrophils were mixed with the zymosan particles at 37°C with samples being taken at regular intervals. The uptake and oxidation of the particles was monitored by flow cytometry, with the neutrophils being identified using a myeloid cell identification antibody cocktail. The increase in DCDHF

fluorescence over time is plotted in figure 6.2. No difference in the increase in geometric mean fluorescence over time is seen between the S100A9 null and wildtype neutrophils indicating that phagocytosis and oxidation of the particles is normal in the S100A9 null neutrophils.

The localisation of the S100A9 protein in the neutrophils following phagocytosis was examined by staining with the anti-S100A9 monoclonal antibody. The S100A9 protein was seen to be excluded from the phagocytic vacuole, containing the green zymosan particles, and to have a cytosolic distribution (figure 6.2).

6.2.3 *In vitro* bacterial killing

Previous work published with the S100A9 null mice highlighted a lack of defect in the ability of neutrophils to phagocytose bacteria (Hobbs et al., 2003). Work presented in this thesis has shown that the mice are also able to activate the oxidase machinery normally upon phagocytosis. The next step in examining the ability of the S100A9 neutrophils to act normally in their anti-microbial role was to examine their ability to kill micro-organisms.

Initially a protocol using human neutrophils was undertaken. Human neutrophils were isolated from fresh human blood. Neutrophils and bacteria were mixed at a 1:10 ratio. At set time points samples from the experimental tubes were taken and spun to pellet the cells. The cell pellet and supernatant were diluted in water and vortexed to lyse the leukocytes. The supernatant and cell associated samples combine to give the total remaining viable bacteria, and separately give an idea of whether uptake of the bacteria by the neutrophils is occurring (figure 6.3). It could be seen that over time the bacteria alone increased in number in a linear fashion. For the first 30 minutes the number of bacteria in

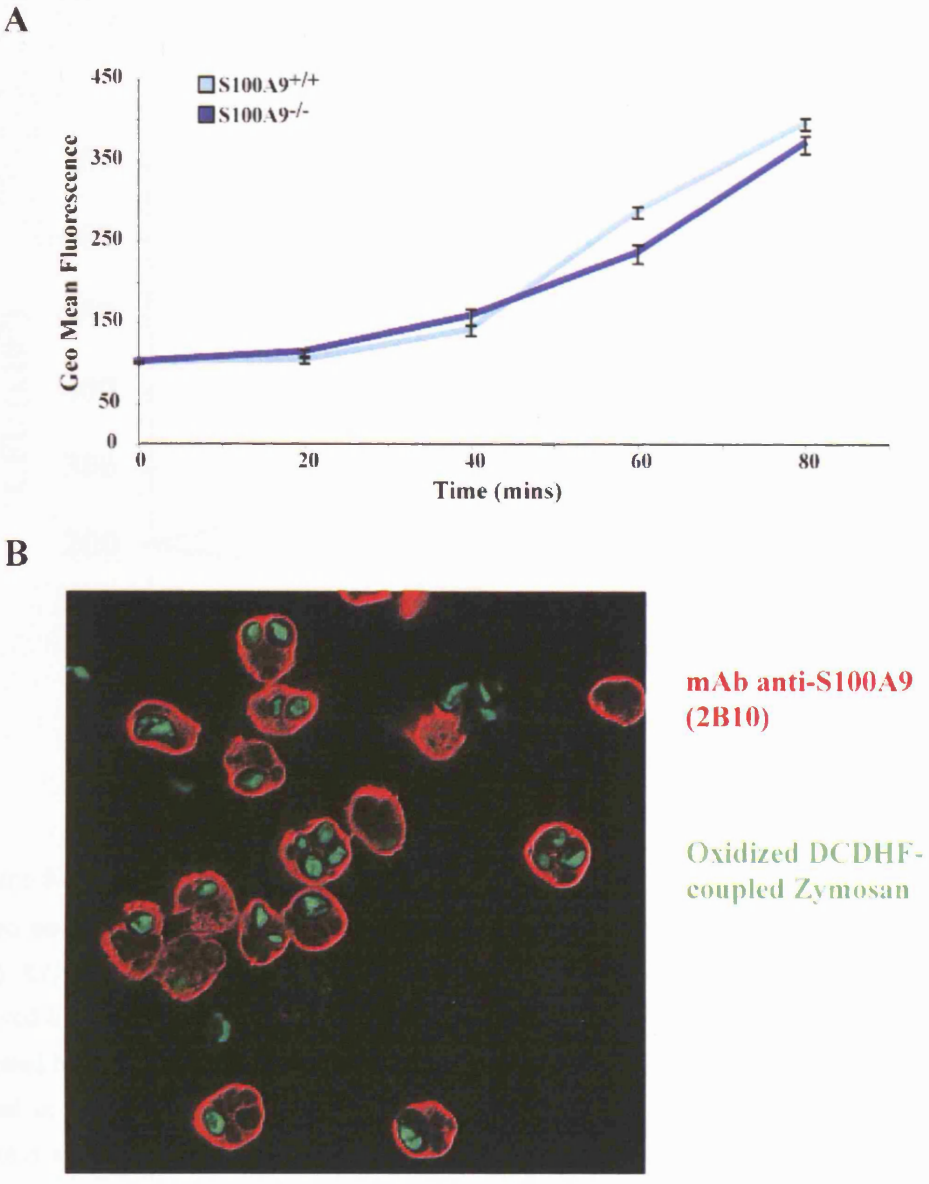

Figure 6.2 Activation of the NADPH oxidase machinery upon phagocytosis of DCDHF-coupled zymosan particles

A: Bone leukocytes were prepared and mixed with iC3b-opsonized DCDHF-coupled zymosan particles. The cells were subjected to intermittent gentle mixing and samples were removed for flow cytometric analysis at 20 minute intervals. The sample aliquots were stained with mAbs 7/4 and Gr-1 to identify the neutrophils and the level of DCDHF fluorescence of these cells assessed by flow cytometry.

B: Aliquots of zymosan containing neutrophils were adhered onto fibrinogen coated coverslips. The cells were fixed, permeabilised and stained with mAb anti-S100A9 (2B10) and an Alexa-547 conjugated secondary antibody. Serial sections throughout the cell were imaged using a confocal microscope and compiled together to form a composite image. S100A9 is shown in red and the oxidised zymosan particles shown in green. The images shown are representative of the whole population.

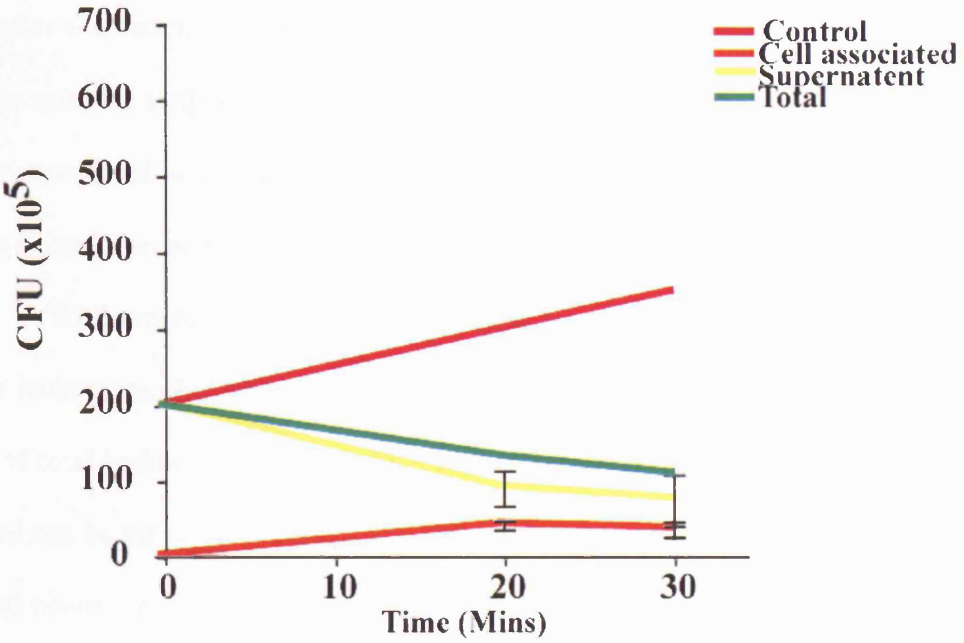

Figure 6.3 Bacterial killing by human neutrophils

Human neutrophils were isolated from blood using a Ficoll gradient. The cells were mixed with *E.coli K12* at a ratio of 10:1 in the presence of heat-inactivated human serum. Aliquots were removed from the reaction mixture at the time points indicated. The leukocyte population was separated by centrifugation of the samples at 200g. The cell pellet and supernatant samples were diluted in water to lyse the leukocytes and plated onto agarose culture plates at 3 different dilutions in duplicate. The plates were incubated over night at 37°C and the number of CFUs counted. The data shown are mean values +/- standard deviation.

the cell associated fraction increased and the number of bacteria in the supernatant decreased. The total number of viable bacteria recovered from the experimental samples was much lower than the number of bacteria recovered from the bacteria-alone samples at these time points. Comparing the number of viable bacteria in the presence of neutrophils compared to the growth of the bacteria alone at any time point it can be seen that bacteria killing has occurred.

While mature neutrophils are abundant in human blood, being 30-40% of total leukocytes, they are relatively scarce in murine blood, accounting for only 3-5% of total leukocytes (figure 3.3). Given that only a few hundred microlitres of blood can be taken from a mouse by terminal cardiac puncture, the use of murine blood neutrophils did not seem a viable approach. Trial experiments using whole bone marrow preparations proved unsuccessful, as the immature neutrophils were unable to kill. In modifying the human killing assay protocol it was decided that it was unnecessary to split the samples into supernatant and cell associated bacteria as the total number recovered gives an indication of whether killing has occurred. Looking at published protocols for murine neutrophil killing assays it was decided to use elicited peritoneal neutrophils as a source of 'mature' neutrophils (Roes et al., 2003). These cells are elicited by intra-peritoneal injection of thioglycollate, with the cells being harvested 6 hours later. At this time point neutrophils are the most abundant leukocyte population in the peritoneal lavage sample. As in the published method the unfractionated peritoneal population was used (Roes et al., 2003). Following 20min incubation with bacteria, killing was observed in wildtype and S100A9 null groups (figure 6.4). No significant difference in the ability of the wildtype and S100A9 null cells to kill the *E. coli* K12 was seen.

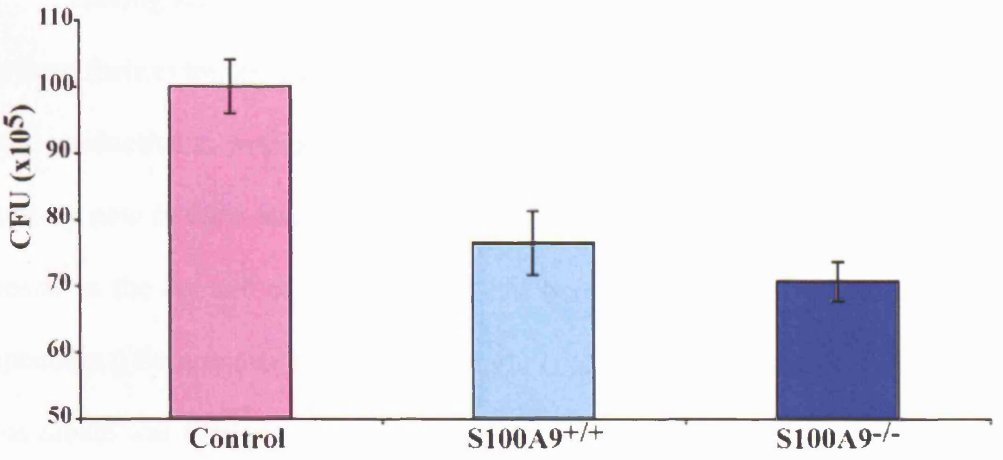

Figure 6.4 No difference in bacterial killing by wildtype of S100A9 null phagocytes

Mature peritoneal phagocytes were elicited following 6 hours of thioglycollate stimulation and recovered by peritoneal lavage. The cells were mixed with *E.coli K12* at a ratio of 1:1 in the presence of heat-inactivated human serum. Aliquots were removed from the reaction mixture at the time points indicated. The samples were diluted in water to lyse the leukocytes and plated onto agarose culture plates at 3 different dilutions in duplicate. The plates were incubated over night at 37°C and the number of CFUs counted. The experiment was performed with triplicate samples. The data shown are mean values +/- standard deviation and representative of 2 experiments.

6.2.4 *In vivo Streptococcus pneumoniae* infection

Having seen that in general the ability of the S100A9 null neutrophils to perform their cytotoxic function appeared normal, it was decided that it might be more productive to evaluate an *in vivo* model of infection rather than continue to work-up new *in vitro* tests. A model of *Streptococcus pneumoniae* infection was chosen as the control of this infection has been shown to be highly neutrophil dependent ((Bergeron et al., 1998; Kadioglu et al., 2000; Takashima et al., 1997)). This model was carried out in collaboration with A. Kadioglu at the University of Leicester. In this model the bacteria are administered via intra-nasal injection. The progression of the disease is followed by harvest of blood and lungs at 24 hourly intervals over the course of a 72-hour experiment. A C57BL/6J mouse generally becomes ill in the first 24 hours showing a peak of bacteria in the lungs, and possibly a low level of bacteria in the blood. By 48 hours the mice are expected the begin to resolve the infection with any bacteria in blood being cleared and a reduction lung infection, this resolution of the infection continues with the mice clearing the infection by 72 hours.

This infection model has been carried out several times over the course of back-crossing the S100A9 null mice onto the C57BL/6J genetic background at generations three, five and ten. The S100A9 null mice are derived from a chimaeric mouse of C57BL/6J and 129 strains. In all experiments the S100A9 null mice were compared to wildtype mice from the same generation of back-cross. Confirmation of any difference between S100A9 null and wildtype mice was required in high back-cross mice.

At back cross generation 5 the S100A9 null mice were shown to be much more susceptible to the *Streptococcus pneumoniae* infection (figure 6.5). The

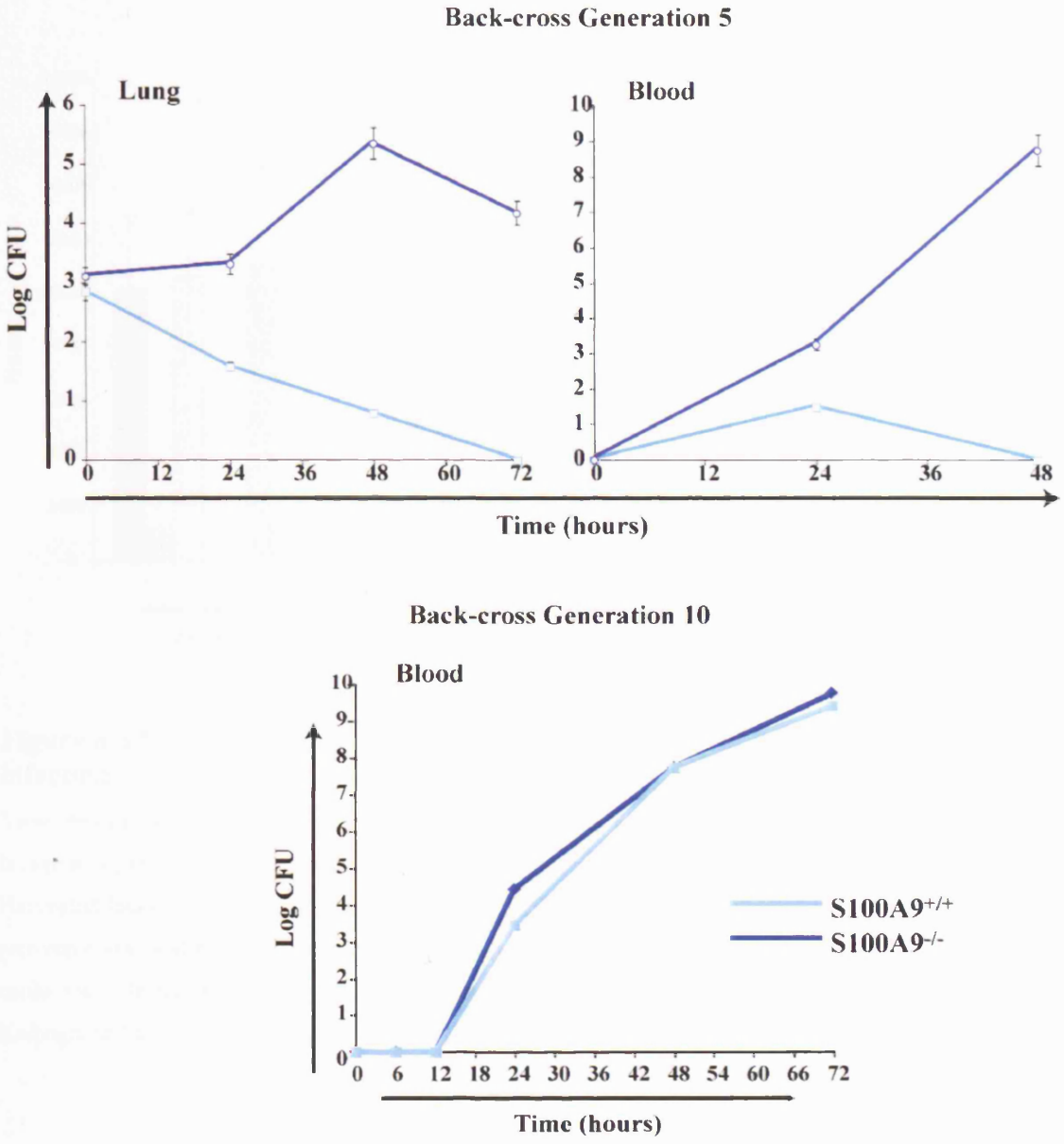

Figure 6.5 Time course of *S. pneumoniae* infection in wildtype and S100A9 null mice

S. pneumoniae were instilled into the lungs of mice by intra-nasal inoculation. At the time points indicated blood was taken by terminal cardiac puncture and the lungs were removed and homogenized. Samples from blood and lung were plated onto blood supplemented agar plates and incubated over night at 37°C. The number of colony forming units was assessed in duplicate. Data from generation 5 back-crossed S100A9 null mice for blood and lung infection levels. Data from generation 10 back-crossed mice for blood infection levels. These experiments were performed by Dr Aras Kadioglu at the University of Leicester. The data is shown as mean values +/- standard error of the mean.

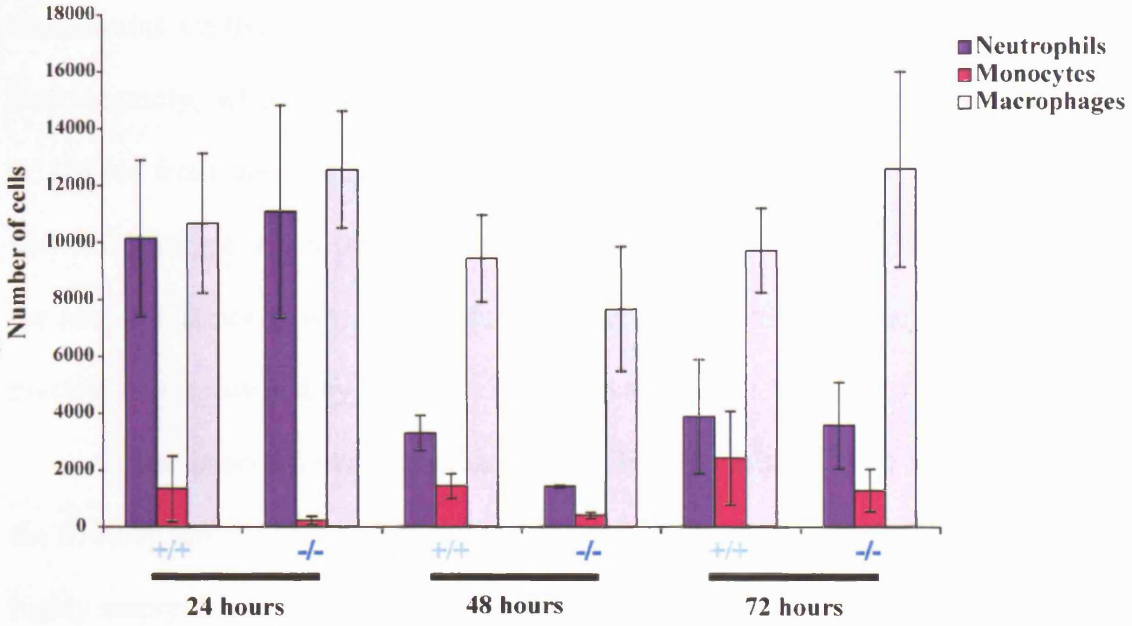

Figure 6.6 Myeloid cell influx into the lung during *Streptococcus pnuemoniae* infection

S.pneumoniae were instilled into the lungs of mice by intra-nasal inoculation. Broncho-alveolar lavage was performed on euthanised mice using PBS at the time points indicated post inoculation. Harvested leukocytes were stained with mAbs 7/4, Ly-6G and anti-F4:80 and the number of cells recovered assessed by flow cytometry. Data is shown as the mean value +/- standard error of the mean for 3-5mice per group. This experiment was performed in collaboration with Dr Aras Kadioglu at The University of Leicester.

S100A9 null mice had higher numbers of bacteria in the lungs and blood at late time points. When back-cross generation 10 mice were compared against commercial C57BL/6J mice this pattern was maintained (data not shown). Unfortunately, when compared in a subsequent experiment against in-house C57BL/6J from the colony with which they were back-crossed, no difference between wildtype and S100A9 null mice was seen in either bacterial numbers in the lungs (data not shown – unavailable at this time) or blood in the number of myeloid cells recovered by broncho-alveolar lavage (figure 6.5 and 6.6).

It was observed over the generations of back-crossing that the response of the S100A9 null to the bacterial infection remained constant, with the mice being highly susceptible to the infection and showing significant septicaemia. When the response of the 'wildtype' mice was evaluated over the generations, it was seen that the mice became more susceptible as they were back-crossed with the in-house C57BL/6J strain (data not shown). This is not what would be expected, given that the mice were being back-crossed away from the susceptible 129 genetic back-ground to the supposedly resistant 'C57BL/6J' background. It appears that the in-house C57BL/6J colony, being a closed colony for 8 years and hence around 20-30 generations, has undergone significant genetic drift away from the original C57BL/6J background. It is highly unfortunate that this genetic drift is manifested as an increase in their susceptibility to this particular infection. The earlier data seems to suggest a defect in the ability of the S100A9 null mice to control this infection, but this lesion is not evident on the current infection-susceptible background. It seems possible that the lack of S100A9 does indeed compromise the ability of the mice to control an infection, but this can be neither confirmed nor a mechanism evaluated on a genetic background where the mice

succumb to the infection readily. At this stage it must be concluded that on the current susceptible genetic background the S100A9 null mice are not further compromised in their response to pneumococcal infection.

6.3 Discussion

The evidence presented in this chapter appears to show no deficiency in the ability of neutrophils to form an oxidative burst in the absence of S100A9. This conflicts with the evidence published that hypothesises a critical role for the S100A8/9 complex in the activation of the NADPH oxidase machinery (Doussiere et al., 1999; Doussiere et al., 2002; Kerkhoff et al., 2005). In addition the ability of the cells to form an oxidative burst in response to phagocytosis of an opsonized particle shows no requirement for the S100A8/9 dimer in coordinated activation of the oxidase machinery. This appears to rule out a direct role in the oxidase machinery or an indirect role in controlling the signalling required for the oxidase burst to happen following phagocytosis. The difference found between our data and that already published might be due to differences in the precise protocol used or method of isolation and handling of the neutrophils. However it should be noted that only one piece of data published to date shows a deficiency in oxidase activity in S100A9 null neutrophils and this deficiency appears to be relatively subtle (Kerkhoff et al., 2005). The published biochemical studies may show a co-incidental effect of the isolated protein that is not physiologically relevant.

The *in vitro* killing assays using murine leukocytes were challenging and time-consuming to design and undertake successfully. Although the level of killing seen was not very high this data demonstrates that in the conditions used

the S100A9 null mice were capable of killing bacteria. When published data from murine killing assays are studied carefully, it can be seen that the observed level of killing is of a similar order to that presented here (Roes et al., 2003). Our protocol could possibly be improved by opsonising the bacteria with C3bi or serum from mice inoculated with the target pathogen. Should these improvements allow more efficient killing, then testing the ability of the neutrophils to kill a panel of different micro-organisms could be undertaken. However, challenging the S100A9 null mice with pathogens *in vivo* is likely to be the most efficient means of identifying any lesion in the function of the S100A9 null neutrophils. Should a lesion to a particular pathogen be seen then the kinetics of the myeloid response can be studied to ascertain if recruitment or function of the neutrophils is compromised. From this data, *in vitro* stimuli relevant to the pathogen could be dissected to define the role of S100A9 in neutrophil function.

CHAPTER SEVEN

7 Wound healing and carcinogenesis in S100A9 null mice

7.1 Introduction

So far the study of the S100A9 null mouse has concentrated on the examination of myeloid cell functions. This is logical given the great abundance of the protein in these cells. However, other than the defect in calcium signalling no clear consistent phenotype has been found either *in vitro* or, perhaps more importantly, *in vivo*. It seemed reasonable under these conditions to take another approach in looking for the function of this protein. Other than the expression of S100A9 in myeloid cells, another site for expression of this protein is in keratinocytes of the wounded epithelium (Li et al., 2000a; Thorey et al., 2001). As well as a potential role in keratinocytes, neutrophils have also been indicated to modulate the healing process (reviewed in (Martin, 1997; Schaffer and Nanney, 1996; Singer and Clark, 1999)). As such it seemed a reasonable hypothesis that the deletion of S100A9 may affect the process of wound healing. Another strongly suggestive function for S100 protein is in the pathogenesis of cancer. The S100A4 null mice have an increased prevalence of cancer and a decreased engraftment of an injected syngeneic tumour cells (C'Naaman et al., 2004; Grum-Schwensen et al., 2005). These conflicting data make hypothesis of a mechanism of action for S100A4 in cancer biology difficult, but clearly demonstrate alterations to this pathological condition in the absence of an S100 protein.

7.1.1 S100 proteins in the skin

The expression of S100 in the skin has largely focussed on the comparison of expression patterns in normal and diseased epidermis. Whilst S100A10 and S100A11 are expressed in normal skin by basal and supra-basal keratinocytes, others are upregulated in inflammatory conditions (reviewed in (Eckert et al., 2004)). S100A7 has been identified as an anti-microbial protein in human skin and to be secreted on the human body surface (Glaser et al., 2005). Secretion of S100A7 from cultured keratinocytes in response to bacterial or pro-inflammatory challenge has been shown and purified S100A7 from human skin has anti-microbial activity against *E.coli* (Glaser et al., 2005). This anti-microbial activity was reversed by increased zinc levels indicating the activity of S100A7 may be to bind zinc which is required for bacterial growth (Glaser et al., 2005). In an assay of bacterial growth on human skin, use of an anti-S100A7 antibody allowed increased bacterial growth compared to isotype control (Glaser et al., 2005). S100A2 is expressed by normal human keratinocytes under basal conditions and has a nuclear distribution (Zhang et al., 2002). Under oxidative stress S100A2 translocates to the cytosol and this phenomenon could be reproduced using ionomycin to elevate intracellular calcium (Zhang et al., 2002). S100A8 is reported to be induced in murine keratinocytes by treatment with UVA (Grimbaldeston et al., 2003). The induction was shown to be a response to oxidant stress. Co-ordinate induction of S100A9 was not seen in that study. S100A8 and S100A9 are overexpressed in psoriasis, an inflammatory skin condition, along with S100A7 (Broome et al., 2003).

7.1.2 The wound healing process

Wound healing is a highly orchestrated and organised process. The morphology of the healing skin is summarised in figure 7.1. As a crucial part of the immune defence, the skin acts as the most important epithelial barrier between the body and the outside pathogen filled world. The healing process has three over-lapping phases: inflammation, tissue formation and tissue remodelling. The immediate issue in wound healing is to prevent haemorrhage from damaged vessels by formation of a clot through the action of platelet and clotting factors. The disruption to the blood vessels in the skin allows the passage of blood leukocytes into the zone of damage. These early arriving leukocytes along with resident cells at the site of injury produce pro-inflammatory stimuli to hasten the entry of leukocytes into the wound (reviewed in (Martin, 1997; Santoro and Gaudino, 2005; Schaffer and Nanney, 1996; Singer and Clark, 1999)).

Leukocytes play a key role in this early phase of healing. Neutrophils are responsible for removing foreign particles, bacteria and fibrin matrix from the site of the wound, but are not essential for the healing process to occur. Neutrophils are later removed from the wound by resident macrophages or by their passage into the debris of the forming scab. The neutrophilic infiltration lasts only for the first 3-4 days of the wound healing process unless infections occurs, in which case continued neutrophil infiltration into the wound retards the healing process (Dovi et al., 2003; Martin et al., 2003b).

Monocytes and resident macrophages play a key role at the interface of inflammation and the repair stages. Monocytes are recruited to the site of the wound where they mature into tissue macrophages. Macrophages, as well as playing a role in clearing the wound of apoptotic neutrophils and other debris,

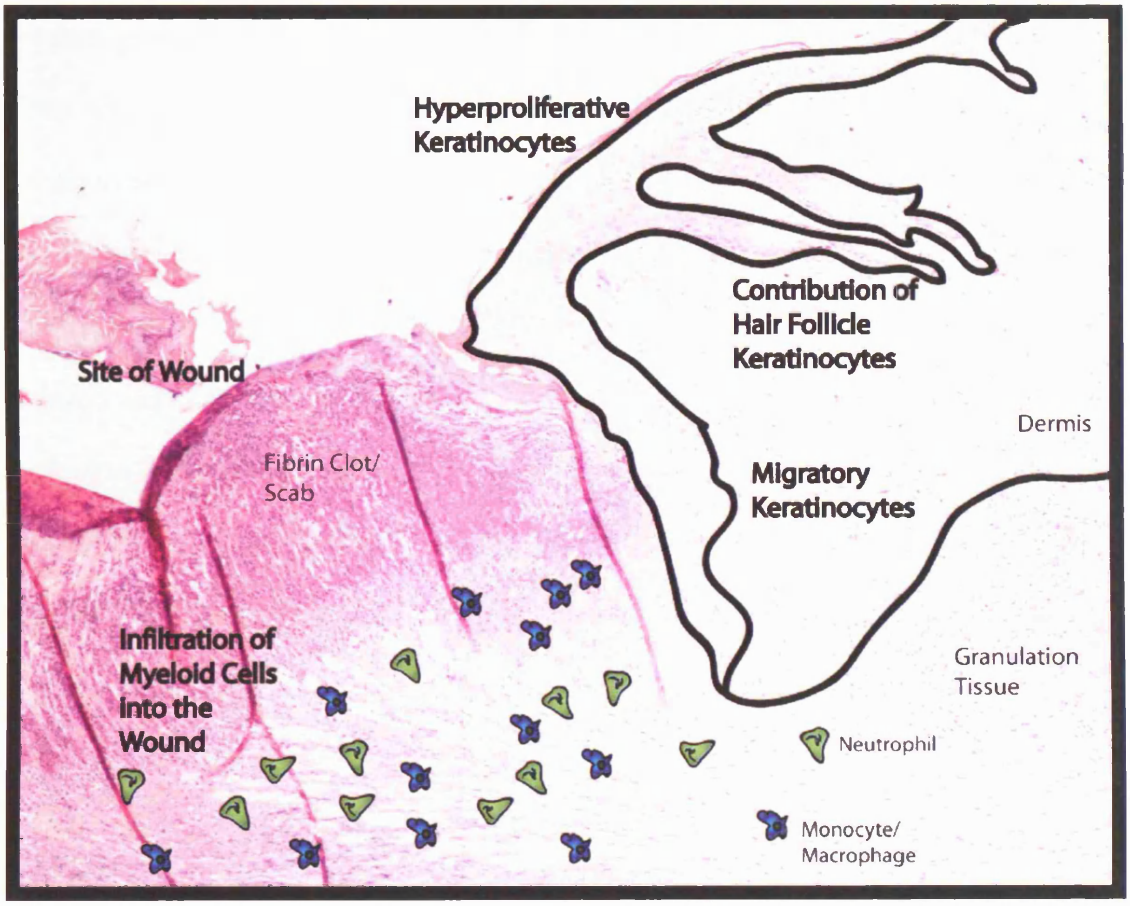

Figure 7.1 Architecture of the healing epithelium

During the healing process the migratory keratinocytes bisect the wound to reform the epithelial barrier. Behind these cells keratinocytes of the epithelium and adjacent hair follicles become hyperproliferative. Initially a fibrin clot fills the wound. Over time this the clot is replaced by granulation tissue and shed as a scab. Myeloid cells infiltrate the fibrin clot and granulation tissue to protect against infection and also provide cytokine signals to activate local fibroblasts and to initiate angiogenesis.

also secrete a host of cytokines and growth factors such TGF-α, TGF-β (Transforming growth factors) and EGF (Epidermal growth factor). They also produce potent tissue degrading and re-modelling enzymes such as collagenase. They also produce IL-1 that activates further production of tissue degrading collagenase by fibroblasts. The crucial role for macrophages in the wound healing process has been demonstrated by macrophage depletion experiments. These result in retarded fibroblast proliferation and wound fibrosis resulting in delayed and abnormal wound healing. When similar experiments are carried out to deplete neutrophil numbers, no effect on un-infected wounds is seen, implying that the role of neutrophils in the wound is to control infection (Dovi et al., 2003; Martin et al., 2003b) and that they have no role in the healing process (wound healing reviewed in (Martin, 1997; Santoro and Gaudino, 2005; Schaffer and Nanney, 1996; Singer and Clark, 1999)).

The second overlapping process of epithelialization begins within hours of the wound occurring. The epithelial cells (keratinocytes) undergo a dramatic phenotypic change. They reduce their attachment to surrounding cells by contraction of intracellular tonofilaments, degrade intra-cellular desmosomes and form a polarised action cytoskeleton and alter their integrin expression, allowing them to become migratory. The migratory keratinocytes bisect the wound dividing healthy tissue from wound debris in an integrin dependent process. One-two days after the migratory keratinocytes begin to bisect the wound, the keratinocytes at the wound edge begin to proliferate responding to local growth factors such are IGF and KGF (Insulin-like and Keratinocyte growth factors) initially released from fibroblasts and laterally as part of an autocrine signalling loop. As the re-epithelialization process completes, the re-expression of normal

basement membrane proteins occurs in an ordered zip-like fashion. Binding of the migratory keratinocytes to the new basement membrane returns them to a normal phenotype and marks reformation of the continuous epithelial barrier (reviewed in (Martin, 1997; Santoro and Gaudino, 2005; Schaffer and Nanney, 1996; Singer and Clark, 1999)).

Whilst the epithelial barrier is restored, extensive granulation tissue is formed to fill the void left by the wound. Granulation tissue results from the proliferation of fibroblasts and the deposition of collagen, allowing macrophages to move further into the wound space and supporting angiogenesis. Once sufficient granulation tissue has been formed to support the re-establishment of the epithelial barrier, the fibroblasts within the wound transform to a contractile myo-fibroblastic phenotype. Their tight interaction with the cell-matrix and the formation of large cytoplasmic actin bundles enables them to contract the wound. The scar tissue is gradually remodelled following contraction over a longer period of weeks as normal skin architecture reasserts itself as far as possible from the edges of the wound. However skin scars are estimated to gain only 70% of the tensile strength of normal skin (reviewed in (Martin, 1997; Santoro and Gaudino, 2005; Schaffer and Nanney, 1996; Singer and Clark, 1999)).

7.1.3 S100 proteins and cancer

A common feature of many S100 family members is their dysregulation in cancer (reviewed in (Donato, 2001; Emberley et al., 2004)). A potential *in vivo* role for S100 proteins in cancer has been highlighted recently in S100A4 transgenic mice (Ambartsumian et al., 2001; C'Naaman et al., 2004; Grum-Schwensen et al., 2005). In these studies mice over-expressing S100A4 demonstrated that this protein does not have tumourigenic potential *per se*, rather

the metastatic potential of tumours in susceptible strains is increased (reviewed in (Helfman et al., 2005)). A possible role in angiogenesis is also indicated from the presence of haemagiomas in aged S100A4 overexpressing mice (Ambartsumian et al., 2001). In the S100A4 null mice there is a higher incidence of spontaneous tumour formation possibly related to destabilisation of p53 in these mice (C'Naaman et al., 2004). Additionally engraftment of syngeneic tumours in the S100A4 null mice is delayed or reduced demonstrating a role for S100A4 produced by stromal fibroblasts in the support of tumour growth (Grum-Schwensen et al., 2005).

S100A9 is dysregulated in squamous cell carcinoma following UVB irradiation and in esophageal squamous cell carcinoma (Dazard et al., 2003; Luo et al., 2004a). S100A8/9 expression has been highlighted in keratinocytes and infiltrating leukocytes in a skin carcinogenesis model in mice (Gebhardt et al., 2002). They were identified as being targets for the glucocorticoid sensitive c-fos pathway activated during TPA treatment. S100A9 have been associated with other aspects of keratinocyte biology, being up-regulated during wound healing (Thorey et al., 2001). Here expression was associated with the hyper-proliferative population of keratinocytes at the wound edge. The expression of S100A9 correlated with proliferation rather than an inflammatory stimulus as expression by keratinocytes was also shown in activin over-expressing mice that exhibit enhanced keratinocyte proliferation in the absence of inflammation (Thorey et al., 2001).

7.1.4 Skin carcinogenesis

To address a potential role for S100A9 in tumourigenesis a multi-stage skin carcinogenesis protocol was undertaken (the protocol and typical molecular

events associated with progression of this model are outlined in figure 7.2). The basis of this protocol is the application of a subthreshold dose of a carcinogen (initiation) followed by successive applications of a non-carcinogenic promotor (promotion). 7,12-dimethylbenz(a)anthracene (DMBA) is a potent carcinogen and causes an irreversible initiation event. The initiation of skin-tumours has been linked to the ability of agents such as DMBA to bind covalently to DNA and the mutagenic activity of this compound. Activation of the H-ras gene is frequently reported in mouse skin early in the carcinogenesis protocol and is considered a likely cause of the initiating event. The promotion phase, using TPA in this case, is initially reversible with benign papillomas arising that can undergo regression. The production of papillomas is followed by the formation of squamous cell carcinomas. In the absence of the initiation phase application of TPA alone typically does not cause tumour formation, not being inherently carcinogenic. The tumour promoting agents do not bind DNA and are not mutagenic, but are capable of causing epigenetic changes (such as down regulation of anti-oxidant enzymes and glucocorticoid receptors), inflammation and epidermal hyperplasia. The key aspect of the promotion phase is the selective and specific expansion of initiated cells through hyperplasia into papillomas. The progression phase of skin carcinogenesis is characterized by high levels of genetic instability and chromosomal alterations (reviewed in (Slaga et al., 1996)). Loss of p53 is reported in skin carcinomas, but not in the benign papillomas and is strongly associated with malignant progression. The final phase of progression is the formation of aggressive carcinomas with metastatic potential (skin tumourigenesis model reviewed in (Slaga et al., 1996; Zoumpourlis et al., 2003)).

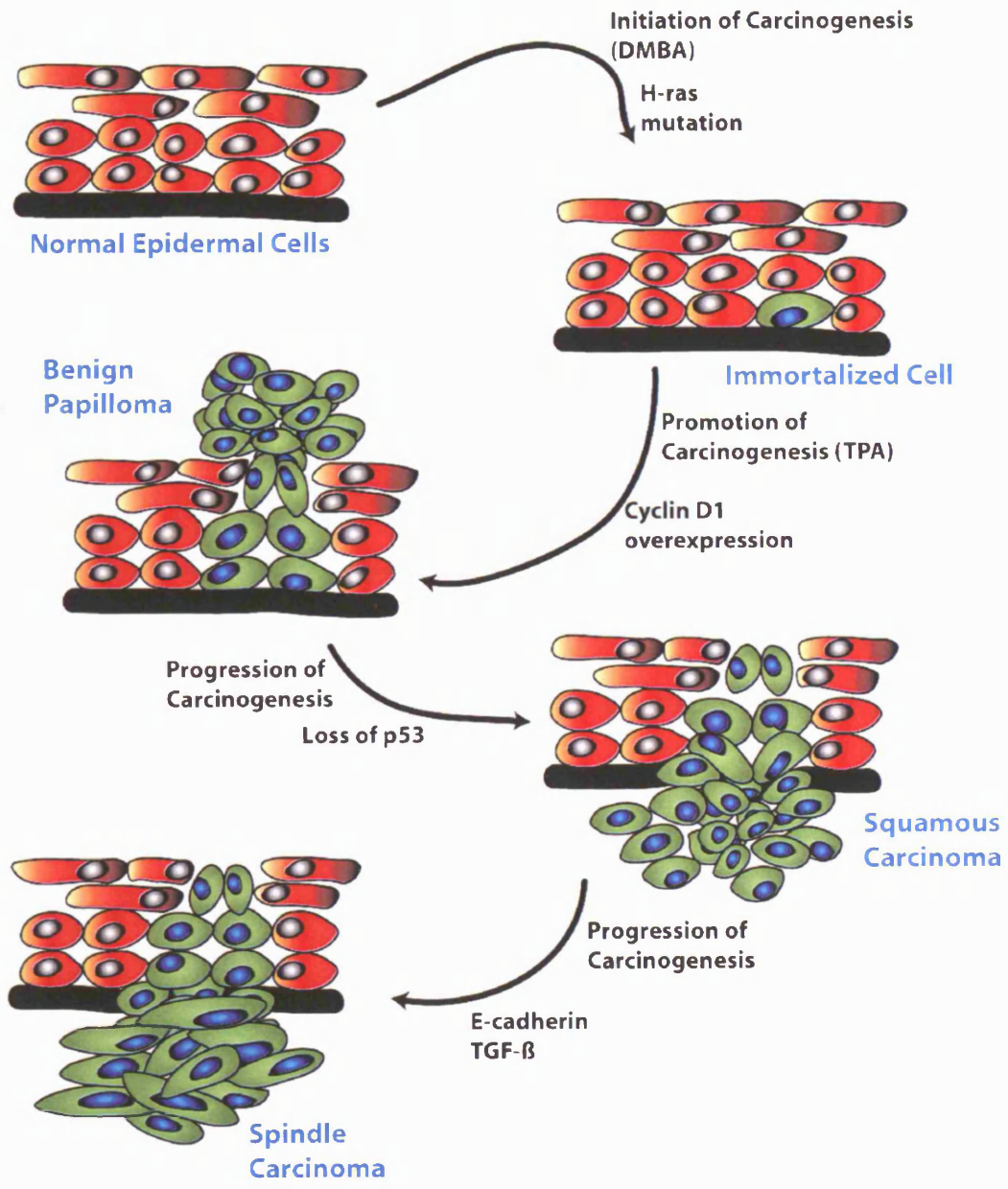

Figure 7.2 Mechanism of chemical induced carcinogenesis in mouse

Adapted from (Zoumpourlis et al., 2003). The initiation and promotion of chemical induced carcinogenesis is shown along with molecules typically altered during progression.

This model is highly interesting to consider in the S100A9 null mice. Aside from any role for S100A9 in the transformation of the keratinocytes recent studies have highlighted a key role for the immune system in modulation of tumour formation. Mice over-expressing IL-1α, a proinflammatory cytokine, under control of a keratinocyte specific promoter, are shown to be resistant to skin papilloma formation in the DMBA/TPA carcinogenesis protocol (Murphy et al., 2003). Crossing these mice onto a RAG deficient background, in which the adaptive immune system is absent, did not alter this phenotype (Murphy et al., 2003). This provides evidence for a role of the innate immune system in skin carcinogenesis. TNFα null mice have also been shown to be resistant to papilloma formation and more advanced carcinoma formation in the DMBA/TPA protocol (Moore et al., 1999). In these mice the inflammation seen during the tumour promotion phase in response to TPA treatment is reduced and the heavy neutrophil and eosinophil infiltration seen in the wildtype animals is absent (Moore et al., 1999). A similar protection from tumour formation is seen in TNF receptor knockout animals, where levels of GM-CSF and matrix-metalloproteinases were reduced (Arnott et al., 2004). Treatment with a TNFα blocking antibody is similarly protective (Scott et al., 2003). The use of MMP9 null mice has demonstrated that this molecule plays a role in tumour progression in the multi-stage carcinogenesis protocol (Coussens et al., 2000). The use of bone-marrow chimaeric mice to re-introduce MMP9 in the bone marrow compartment alone removes the protection of MMP9 deletion, demonstrating a role for bone marrow derived leukocytes in pathogenesis in this model (Coussens et al., 2000). A more speculative role for neutrophils in tumour biology comes from studies using the Mutatect cell line, which acts as a reporter system for

genetic instability and forms subcutaneous tumours in mice. In this system expression of IL-8 correlated with increased neutrophil influx and an increase in genetic instability in the tumour cells (Haqqani et al., 2000).

Differences in susceptibility in female and male mice are not without precedence, with MMP8 (collagenase 2) null mice showing an increased tumour incidence in male mice alone (Balbin et al., 2003). This effect could be reversed by transplantation of neutrophils from wildtype mice, showing that production MMP8 by neutrophils is protective in a model of multi-stage skin carcinogenesis (Balbin et al., 2003).

These data show the importance of inflammation and the innate immune system in carcinogenesis, although the potential role played may be complex.

7.2 Results

7.2.1 Wound healing assay

A wound healing assay was performed in wildtype and S100A9 null mice. A 3mm biopsy punch was used to make a pair of wounds through the skin on the back of the mice. To reduce the possibility of damaging the underlying tissue of the body cavity, the skin on the back was gently stretched away from the anaesthetised mice positioned on one side. This allowed the punch to be made cleanly through the skin alone, with no damage to the underlying tissues. Mice were sacrificed at four and seven days post wounding, with fresh wounds made post-mortem as a zero time point.

Sections cut through the midpoint of the wounds were stained with Haematoxylin and Eosin to visualise the morphology of the skin (figure 7.3). Low magnification images were taken of all the wounds and were used to assess

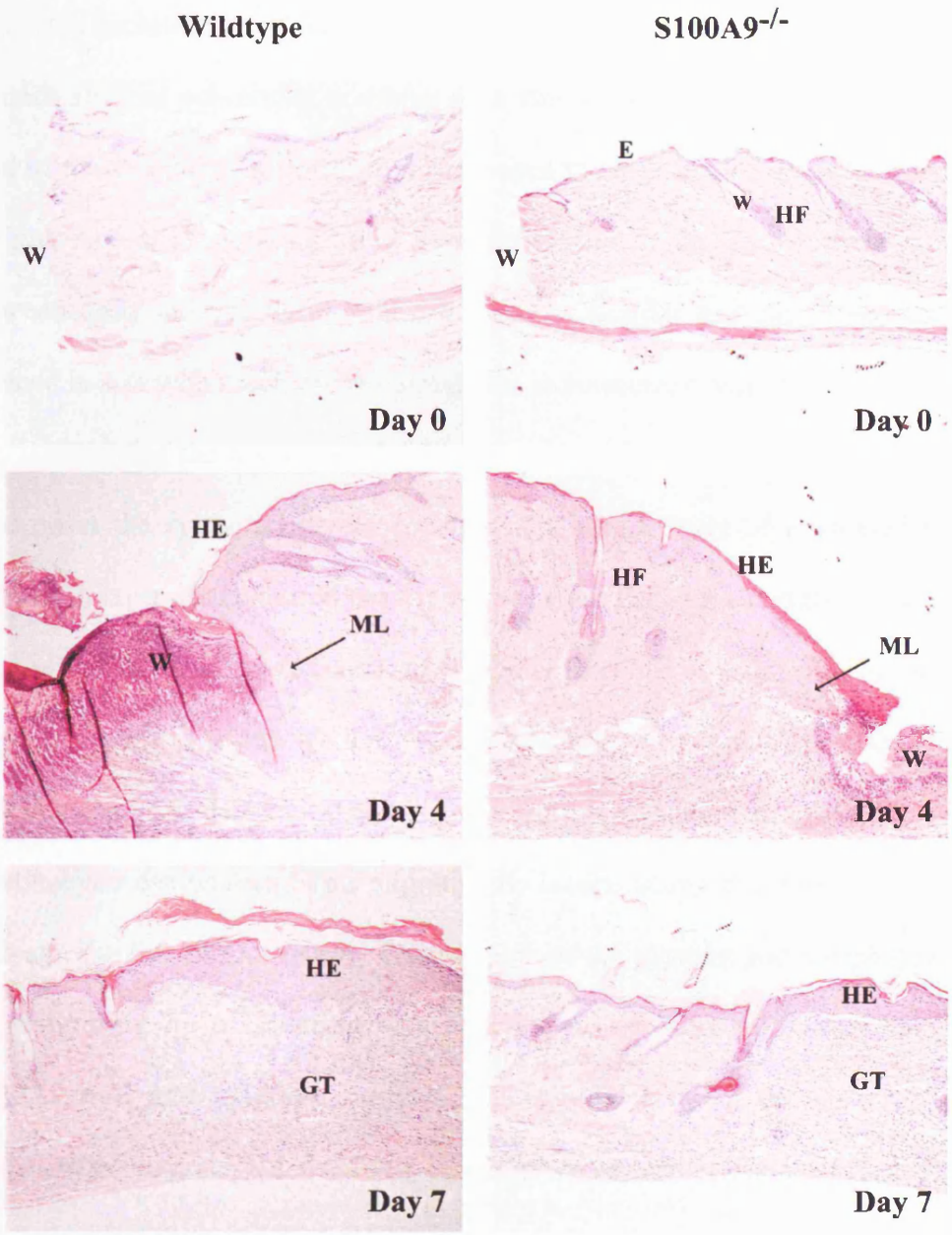

Figure 7.3 Wound healing assay in wildtype and S100A9 null mice

Full thickness skin wounds were formed using a 3mm biopsy punch in duplicate on wildtype and S100A9 null mice to give wounds at day 4 and 7 at the point of experiment termination. The skin time zero wounds were formed post-mortem and the individual wounds excised and fixed. The wounds were bisected and embedded in paraffin blocks. Sections were cut and stained with Haematoxylin and Eosin to visualise morphology. HF: Hair Follicle, E: Epithelium, W: Wound, HE: Hyperproliferative Epithelium, GT: Granulation Tissue, ML: Migrating Lip. Sections shown are representative of 3 duplicate wounds per genotype. Immunohistochemistry was performed by George Elia at Cancer Research UK.

the degree of healing at the difference time point. At day zero a clean break in the organised architecture of the skin could be seen. At day 4 post wounding the wounds showed substantial scabbing with fibrous granulation tissue filling the void of the wound. The epithelium had begun to close in all samples, shown by the presence of a migrating lip of keratinocytes beginning to bisect the wound between dead and live tissue. At day 7 all the wounds had closed and greatly reduced in size with much of the normal skin architecture restored.

Studying the histology of the healing wound we can see that at the zero time point the epithelial layers consists of a single layer of nucleated cells, covered in layer of anucleated heavily fibrous cells, called the cornified envelope. The surface of the skin is interrupted at regular intervals by hair follicles. It is in bulbous structures within the hair follicle that many of the skin stem cells exist (not shown). On day 4 post-wounding an organised population of migrating keratinocytes can be seen. This migrating lip bisects neatly between debris of the scab and the live fibrous tissue. Examination of the location and morphology of this migrating lip of keratinocytes revealed no obvious difference between S100A9 null and wildtype samples. This indicates that the speed of the epithelialization process and activity of this group of cells appears unaffected. At this time point, dramatic thickening of the epithelium behind the migrating lip can be observed. This hyper-proliferative population is located at the wound edge and behind, again the size and morphology of this population appears unaffected. By day 7 post wounding, the keratinocytes have fully re-established the epithelial barrier in all samples. The wound has also contracted significantly and the breadth of the wound is shown by the thickened layer of keratinocytes at the site

of the wound. In most cases the scab over the wounded area had been shed by this time.

7.2.2 Neutrophil influx into the wounded epithelium

Neutrophils act in the wounded epithelium primarily to control any infection, but their persistent presence can retard wound healing. The influx of myeloid cells into the skin was assessed by immunohistochemistry, using the 7/4 antibody (figure 7.4). When examining skin samples, it is necessary to take into account that any apparent positive staining of the hair shaft, cornified layer and scab may be artefact. In the day zero skin samples, no infiltration of myeloid cells into the skin could be seen, this was expected as neutrophils and monocytes are not resident in the skin. As would be expected from the literature on wound healing, infiltrating myeloid cells were seen in the wound in the day 4 post wounding sample. These cells could be seen around what appear to vascular structures at the base of the skin in both S100A9 null and wildtype samples. Myeloid cells that had migrated into the skin were observed in both S100A9 null and wildtype samples. When the day 7 samples were examined no infiltration of myeloid cells was observed. No difference in the myeloid cell influx into the wildtype and S100A9 null wounds could be seen.

Figure 7.4 Myeloid Cell influx into the wounded epithelium

Full thickness skin wounds were formed using a 3mm biopsy punch in duplicate on wildtype and S100A9 null mice to give wounds at day 4 and 7 at the point of experiment termination. The time zero skin wounds were formed post-mortem and the individual wounds excised and fixed. The wounds were bisected and embedded in paraffin blocks. Day 4 skin sections were cut and stained with mAb 7/4 to identify myeloid cells. HF: Hair Follicle, W: Wound, HE: Hyperproliferative Epithelium. Immunohistochemistry was performed by George Elia at Cancer Research UK.

7.2.3 Expression of S100A8 and S100A9 in the wounded epithelium

Gene array data has previously identified S100A8 and S100A9 as being up-regulated during the wounding process (Li et al., 2000a). This could be due to the influx of myeloid cells that express high levels of these proteins during this process. More careful studies on keratinocytes alone have shown that these cells begin to express S100A8 and S100A9 in response to wounding stimuli (Thorey et al., 2001). To confirm any expression of S100A8 and S100A9 in the murine epithelium sections from all time points were stained with monoclonal anti-S100A8 (6A4 – IgG2b) and monoclonal anti-S100A9 (2B10 – IgG2b) antibodies and relevant isotype controls (PyLT – IgG2b and Y13 – IgG2a) (figures 7.5 and 7.6).

No expression of S100A8 or S100A9 was seen at any time point in the S100A9 null samples. No expression of S100A8 or S100A9 was seen in the normal unwounded epithelium. On day 4 post wounding staining for both S100A8 and S100A9 could be seen in a defined population of keratinocytes located at edge of the wound in the wildtype samples (figure 7.5 and 7.6). No staining was seen in the migrating lip. The population of keratinocytes expressing the proteins is a portion of the hyperproliferative epithelium situated at the wound edge. In addition to this expression of S100A8 and S100A9 small positively stained cells within the dermis and granulation tissue could be seen. It would be assumed that these are infiltrating neutrophils or monocytes, although to confirm this co-staining sections with anti-S100 antibodies and other leukocyte marker antibodies would be required. By day 7, when the wounds had contracted significantly and the epithelial barrier completely reformed, the defined population of S100A8/9 positive keratinocytes could no longer be seen, instead a

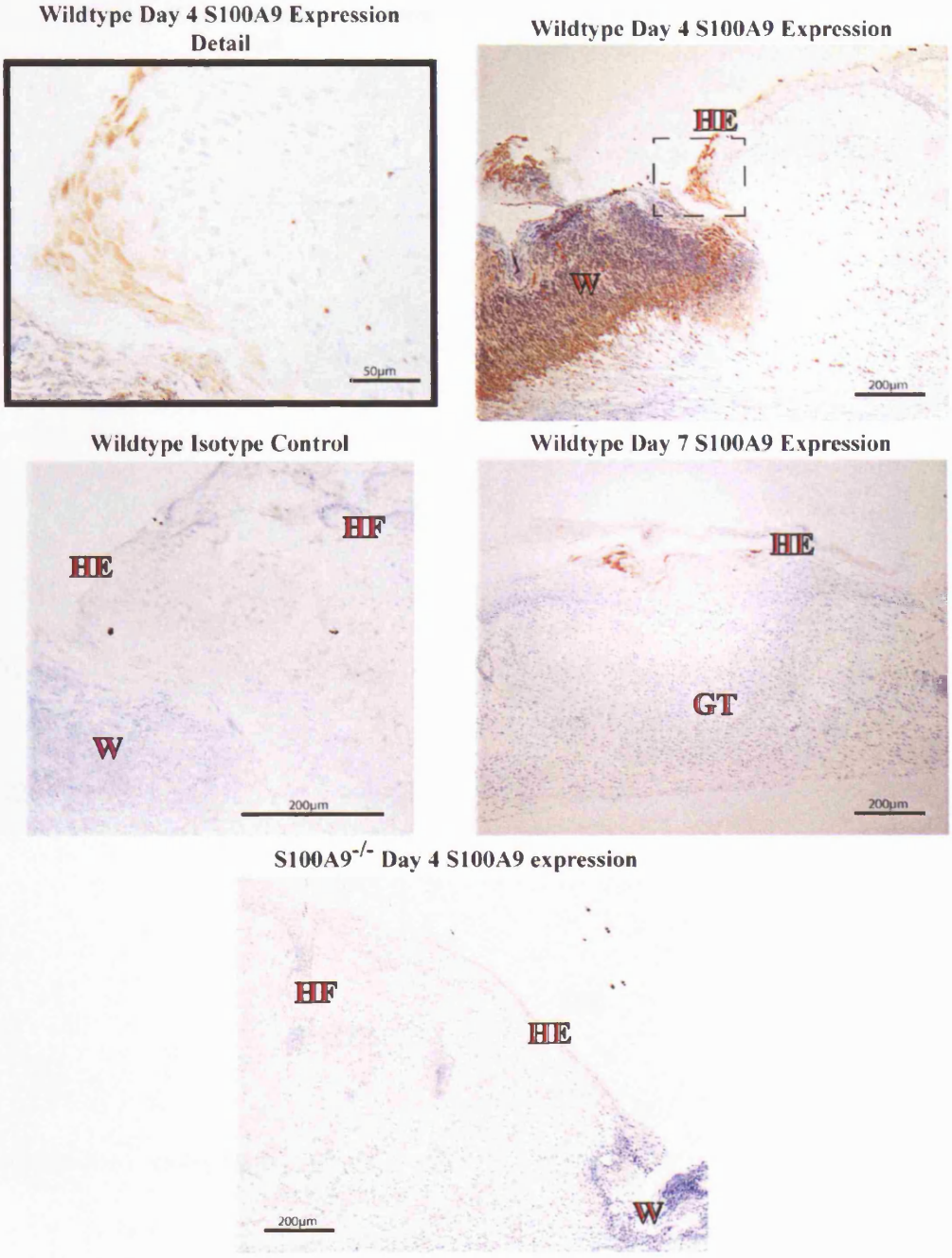

Figure 7.5 Expression of S100A9 in the wounded epithelium

Full thickness skin wounds were formed using a 3mm biopsy punch in duplicate on wildtype and S100A9 null mice to give wounds at day 4 and 7 at the point of experiment termination. The time zero skin wounds were formed post-mortem and the individual wounds excised and fixed. The wounds were bisected and embedded in paraffin blocks. Sections were cut and stained with mAb 2B10 to identify S100A9 or isotype control mAb Y13. HF: Hair Follicle, E: Epithelium, W: Wound, HE: Hyperproliferative Epithelium, GT: Granulation Tissue. Immunohistochemistry was performed by George Elia at Cancer Research UK.

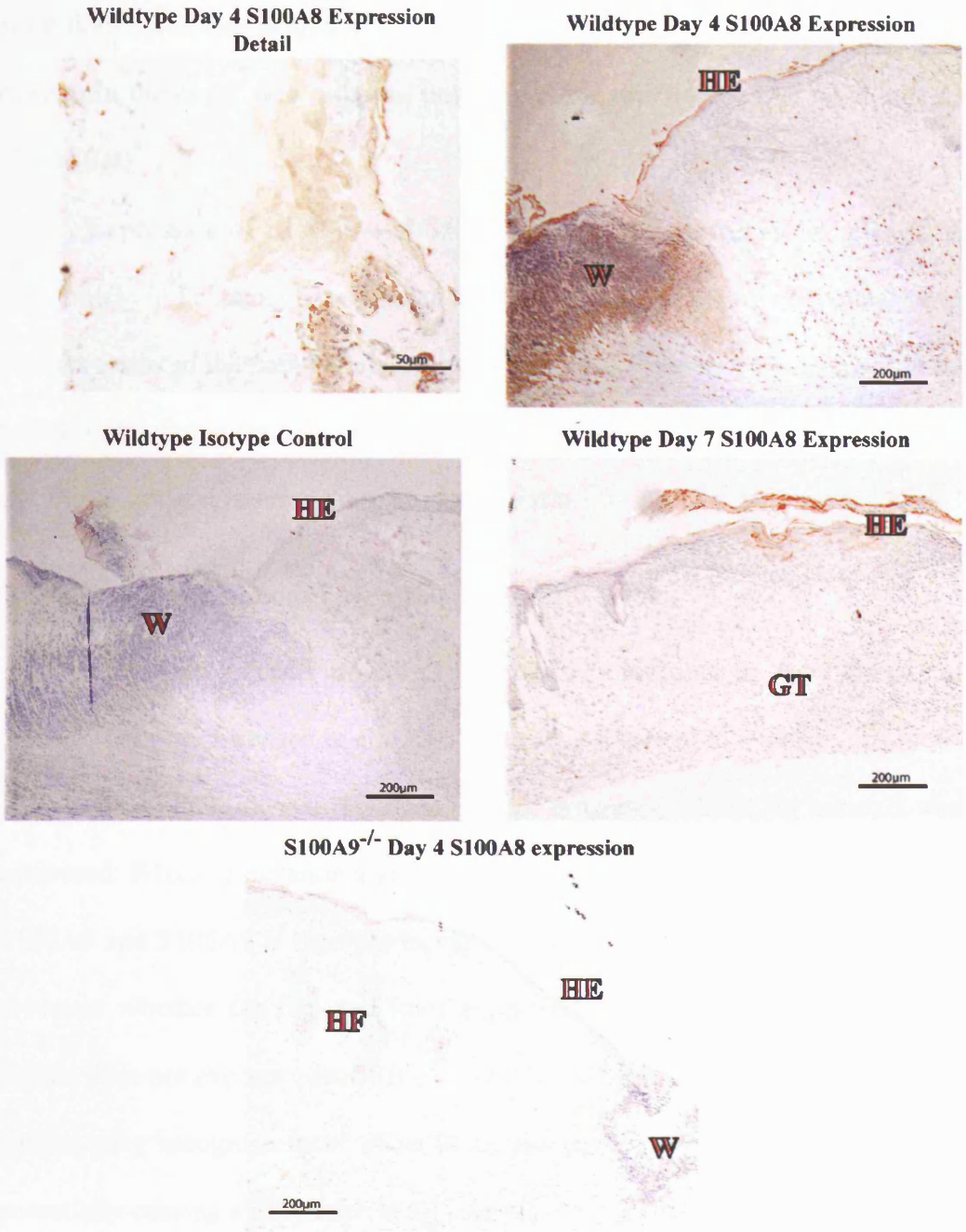

Figure 7.6 Expression of S100A8 in the wounded epithelium

Full thickness skin wounds were formed using a 3mm biopsy punch in duplicate on wildtype and S100A9 null mice to give wounds at day 4 and 7 at the point of experiment termination. The time zero wounds skin were formed post-mortem and the individual wounds excised and fixed. The wounds were bisected and embedded in paraffin blocks. Sections were cut and stained with mAb 6A4 to identify S100A8 or isotype control mAb PyLT. HF: Hair Follicle, E: Epithelium, W: Wound, HE: Hyperproliferative Epithelium, GT: Granulation Tissue. Immunohistochemistry was performed by George Elia at Cancer Research UK.

small number of isolated S100A8/9 expressing cells could be seen within the keratinocytes at the wound site. None of the small S100 positive cells were evident in the day 7 skin samples, nor were there any 7/4 positive myeloid cells (figure 7.4)

Expression of S100A8 and S100A9 has been reported in the cells of the hair follicle in humans. Examination of the hair follicles shows no expression of these proteins in the hair follicle in the mouse or in the stem cells resident in the hair follicle. Some staining of the hair itself is seen, but as this is also seen in the isotype controls, it is assumed to be non-specific.

7.2.4 Syngeneic tumour engraftment model

Given the reduced growth of injected tumours cells in the S100A4 null mouse ((Grum-Schwensen et al., 2005)), it seemed logical to evaluate this model in the S100A9 null mouse. Two cell lines of syngeneic C57BL/6J tumours were examined: $B16_{GALV}$ melanoma and 3LL Lewis Lung Carcinoma. Expression of S100A8 and S100A9 is reported in various cancers and it was first important to ascertain whether the two cell lines expressed either protein. As the mature animal does not express either S100A8 or S100A9, it is possible that the immune system may recognise these proteins as antigens in the S100A9 null mouse, potentially causing a difference in tumour growth due that is not due to a function of S100A9 *per se*. Western blotting of a lysate produced from the B16 GALV and 3LL cell lines did not show any expression of S100A9 or S100A8 (data not shown). Similarly a lysate produced from a B16 tumour grown in the S100A9 null animal did not show any S100A8 or S100A9 expression (data not shown).

When the growth of the 3LL and $B16_{GALV}$ tumours was monitored by measurement of tumour size no difference in the kinetics of growth of either

tumour was observed when the S100A9 null and wildtype mice were compared (figure 7.7). The mass of the tumours was also assessed at the end point of the experiment. The end point was taken as the time when the first tumour passed the critical size threshold at which point the experiment was terminated and all the tumours from both S100A9 null and wildtype groups were weighed. There was no difference in the mass of either 3LL or $B16_{GALV}$ tumours when S100A9 null and wildtype tumours were compared. In addition to measurement of the tumour size the mice were examined for any obvious metastatic spread or other abnormalities. No obvious metastasis or other sign of ill health was found in the mice (data not shown).

The number of lymphocytes present in the tumour-draining lymph nodes was assessed at the end of the experiment as an indication of immune activation in the mice (figure 7.8). No difference in the lymphocyte populations was seen when S100A9 null and wildtype mice were compared. The extent of angiogenesis supporting the tumour growth was assessed by eye and no gross difference in the extent of vessel growth was seen when S100A9 null and wildtype mice were compared (figure 7.9).

This data seems to indicate that unlike S100A4, S100A9 has no role in support or retardation of tumour growth in this model. This may be correct as the only stromal tissue likely to express S100A9 would be infiltrating neutrophils. Preliminary histochemistry performed on the 3LL tumour samples revealed only a low level of neutrophil infiltration and no expression of S100A8 or S100A9 by other cells at the site of tumour (data not shown).

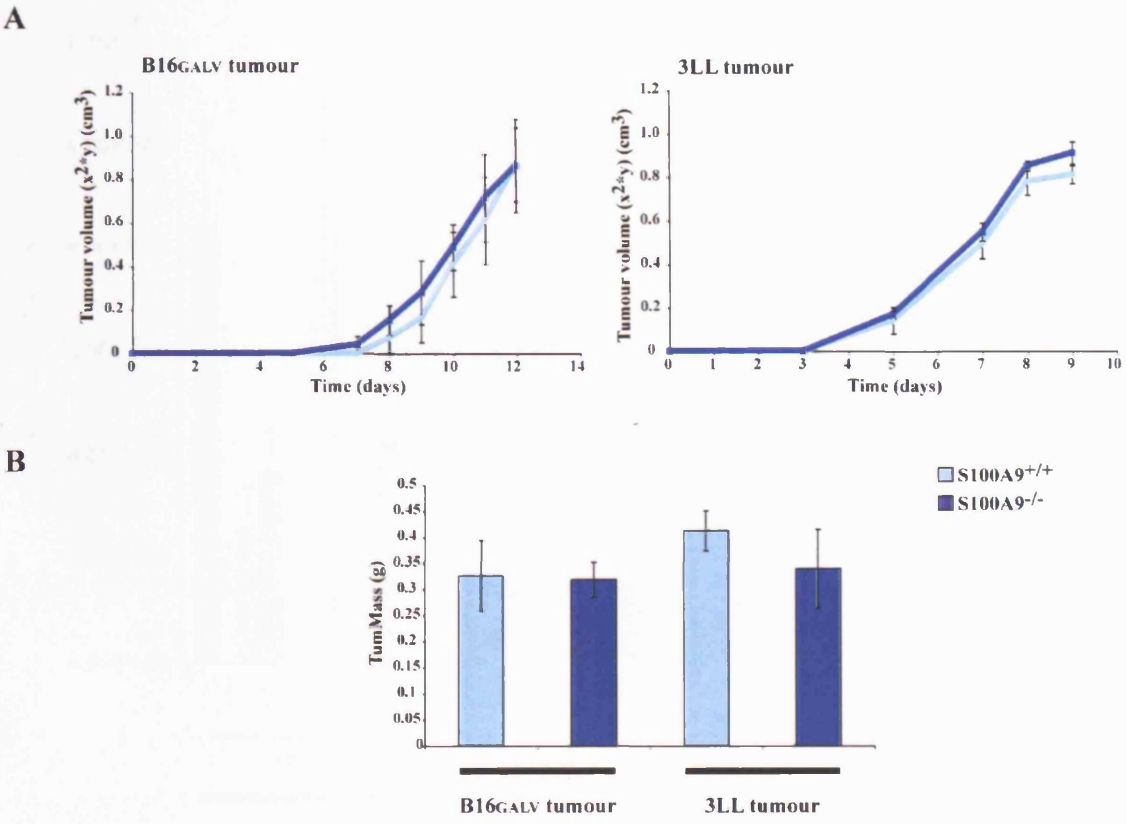

Figure 7.7 Growth of syngeneic tumours in wildtype and S100A9 null mice

$B16_{GALV}$ or 3LL cells were cultured and injected sub-cutaneously into the right flank of anaesthetized mice. Tumour growth was followed by measurement of the tumours in two dimensions every two days. All mice were culled once tumour size reached the legal limit and the tumours were excised. A: Tumour progression monitored by measurement of tumour size. B: Tumour growth assessed as tumour mass at the end-point of the experiment. Data shown as mean value +/- standard error of the mean for groups of 7 animals per genotype. The experiment was performed 3 times.

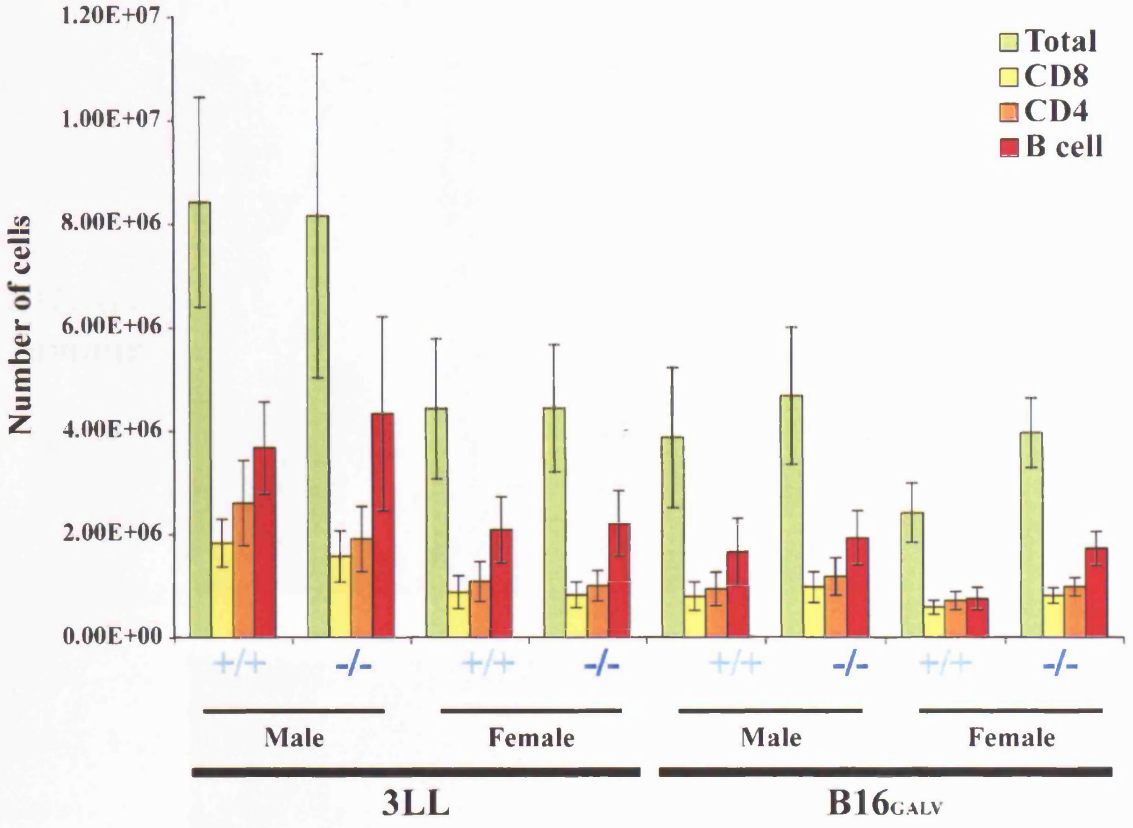

Figure 7.8 Lymphocyte numbers in the tumour-draining lymph nodes

$B16_{GALV}$ or 3LL cells were cultured and injected sub-cutaneously into the right flank of anaesthetized mice. All mice were culled once a single tumour reached the legal limit and the tumours were excised. The inguinal lymph nodes were removed at the end of the experiment and mechanically disrupted. The resulting cell suspension was labelled with antibodies recognising B220 (B cells), CD4 and CD8 (T cells). The number of cells was assessed by flow cytometry. Data shown is the mean +/- standard error of the mean for 5-7 animals per group.

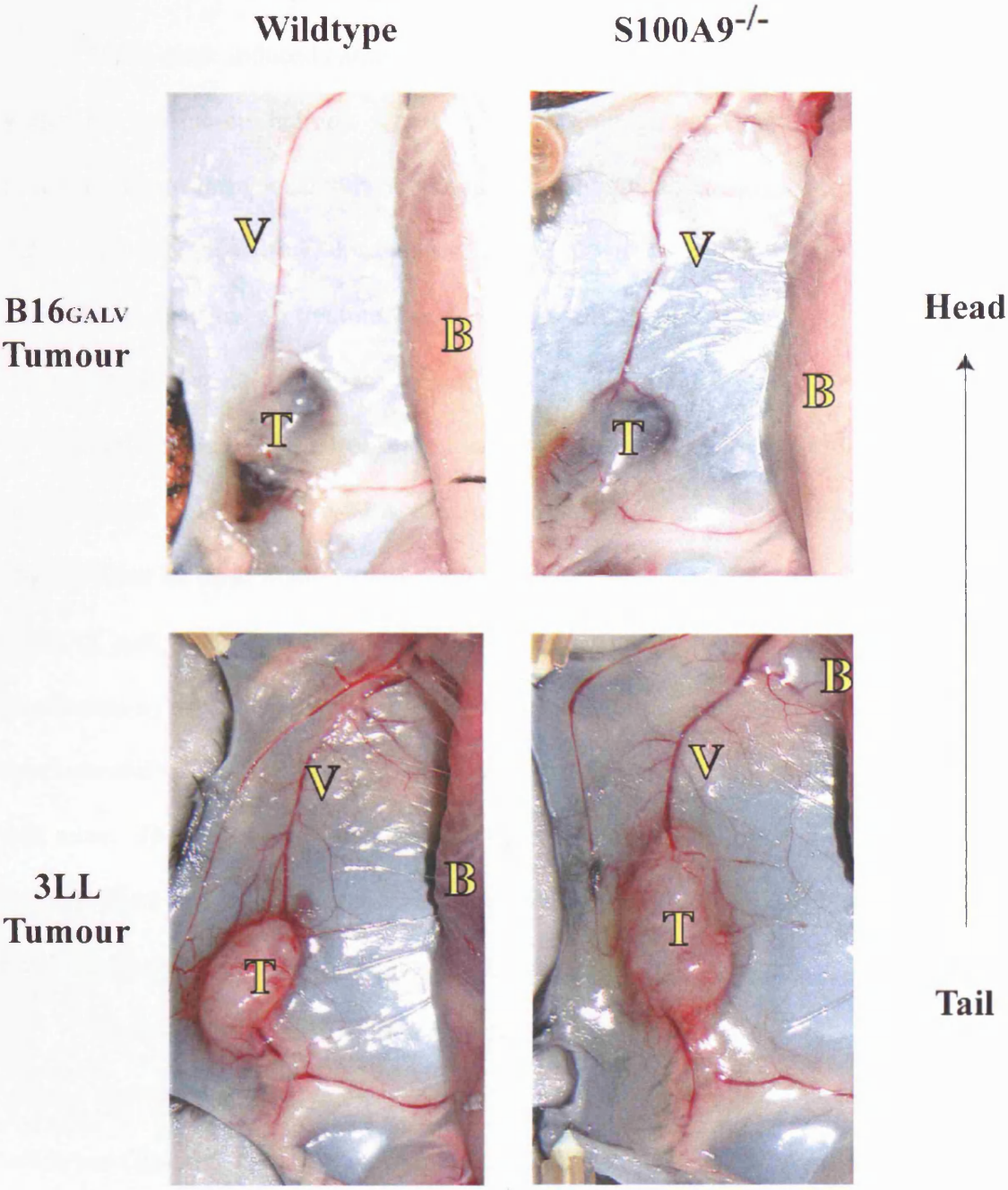

Figure 7.9 Tumour induced angiogenesis

$B16_{GALV}$ or 3LL cells were cultured and injected sub-cutaneously into the right flank of anaesthetized mice. All mice were culled once tumour size reached the legal limit and the tumours were excised. The growth of blood vessels supplying the tumours was assessed visually. T: Tumour, B: Body cavity, V: Vessel. Representative images of mice from each group are shown, with 5-7 animals per group. The experiment was repeated 3 times.

7.2.5 Skin carcinogenesis in S100A9 null mice

Multi-stage induced carcinogenesis promotes the immortalization of cells within the murine epithelium. These cells form benign papillomas that can in time progress to form squamous or spindle cell carcinomas as illustrated in figure 7.2. At the time of writing, this experiment is in progress and so data up to week 18 is shown. Following treatment with DMBA, the tumour initiating agent, the mice are treated weekly with TPA to promote carcinogenesis.

Papillomas were first observed in the female wildtype and S100A9 null mice around week 8 of the TPA tumour promotion phase. Papillomas arose slightly later in both male groups (around week 11). By week 13 all female S100A9 null mice had papillomas, with all wildtype female mice having papillomas by week 15. Time to 50% of the female mice having papillomas was approximately 2 weeks earlier (week 8.5 compared to week 10.5) in the S100A9 null mice. The incidence of papillomas in the male mice was lower with 50% of male S100A9 null mice having tumours by week 7.5 and the wildtype mice not reaching that level by week 18 (figure 7.10).

Observing the mean number of papilloma per mouse in the different groups showed that the female knockout mice had more papillomas than the wildtypes (figure 7.11). The mean number of papillomas present in the S100A9 null mice was significantly different from the wildtype mice at various time points as shown in figure 7.11. At maximum the female S100A9 null group had 3-4 times as many papillomas as the wildtype group. The male mice have a lower number of papillomas to date. The mean number of papillomas is elevated in the male S100A9 null group as in the female group and was also significant at certain time-points. By week 16 the first transformed skin carcinoma had arisen in the

female S100A9 null group. A more comprehensive statistical evaluation will be performed later in the experiment when an 'area under curve' analysis will be performed and used to assess any significant differences (using a Mann-Whitney test) between wildtype and S100A9 null mice over the duration of the experiment.

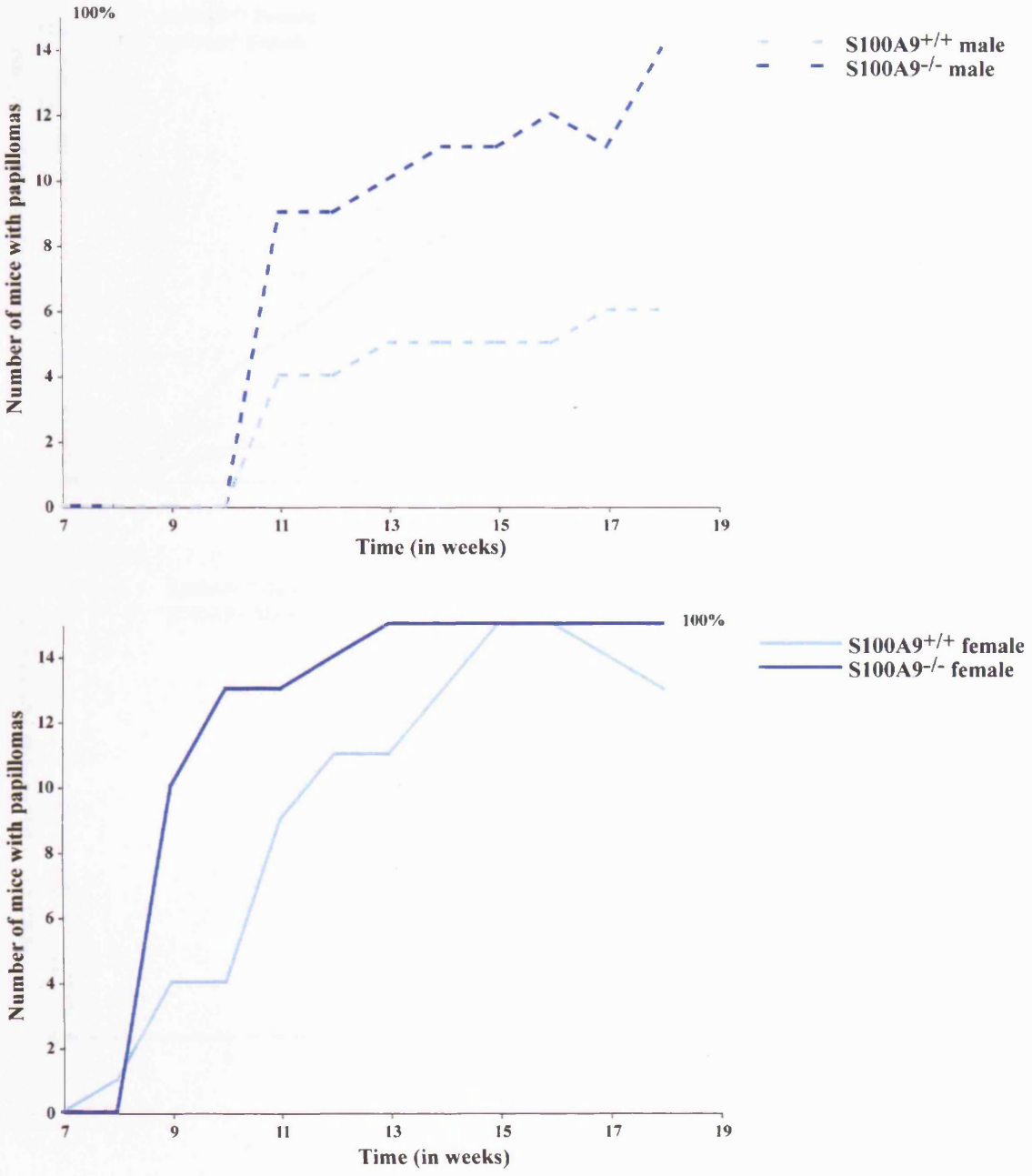

Figure 7.10 Chemical induced carcinogenesis – Papilloma incidence

The backs of mice were shaved and painted with DMBA at the 8 weeks of age. TPA was applied topically to the shaved area weekly for 15 weeks. The development of papillomas was recorded weekly. The incidence of papillomas per group is shown.

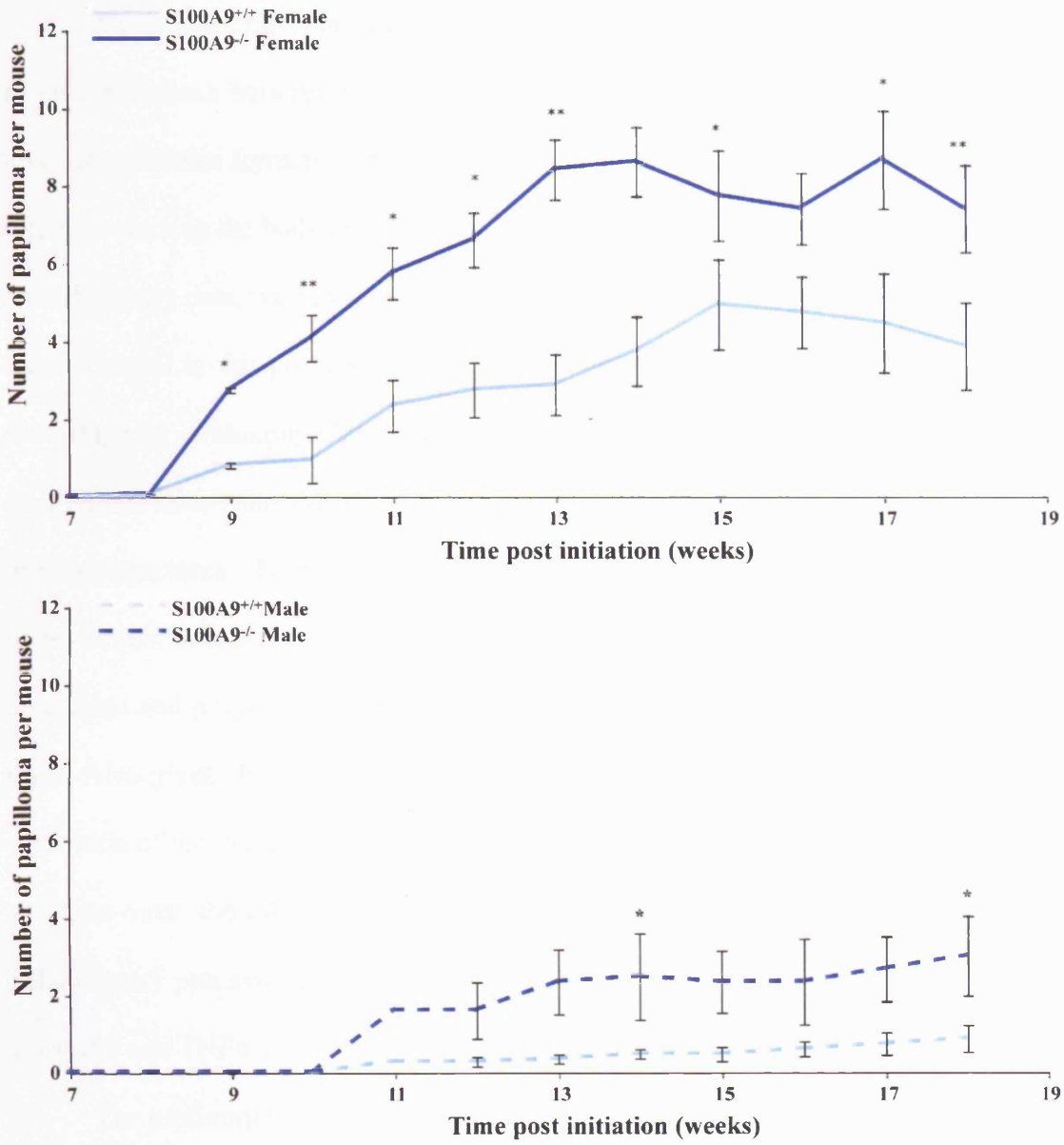

Figure 7.11 Chemical induced carcinogenesis – Papilloma multiplicity

The backs of mice were shaved and painted with DMBA at the 8 weeks of age. TPA was applied topically to the shaved area weekly for 15 weeks. The development of papillomas was recorded weekly. Data shown is mean values per group of 15 mice +/- standard error of the mean. Significance between wildtype and S100A9 null data at each time point was assessed using a Student's T-Test: * $P<0.05$; ** $P<0.01$.

7.3 Discussion

The evidence presented here gives the most promising data to date for an *in vivo* difference between the S100A9 null and wildtype mice. The enhanced level of papilloma formation in the S100A9 null mice could indicate a regulatory role in protecting the body in this model of skin carcinogenesis. In the absence of histochemistry data, we can speculate that this may be an as yet undefined role for the neutrophil in this process, or a role for this protein in the keratinocyte. The first stage in evaluating this model will be to study the morphology of the papillomas/carcinomas arising and assessing cellular proliferation and apoptosis in these structures. To dissect a role for S100A9 immunohistochemistry should be performed to look for expression of S100A8 and S100A9 during the initiation, promotion and progression phases of the experiment in initiated and uninitiated skin. Also given the prominent modulatory role of leukocytes in this process, evaluation of the presence of lymphocytes and myeloid cells in S100A9 null and wildtype mice should be made. To evaluate a role for these proteins in the inflammatory processes linked to tumour promotion, levels of key mediators such as MMP9 and TNFα could be made using a gene array or by RT-PCR.

The preliminary wound healing data does not show a role for S100A9 in wound closure. This does not rule out a role for this protein, either in neutrophils or keratinocytes, in protection of the wound site from microbial attack. Keratinocytes are known to produce a range of anti-microbicidal proteins thus participating in the innate host defence during this vulnerable time. S100A7 is secreted and possibly plays a role of this type (Glaser et al., 2005). Another family of mediators that are expressed in the hyper-proliferative epithelium are anti-oxidant enzymes. Increased expression of these enzymes (including haem-

oxygenase 1, catalase and superoxide dismutase) occurs within the first 3 days of injury and declines by day 7, a similar pattern to that seen for S100A9 (Hanselmann et al., 2001; Steiling et al., 1999). Given that the other major site of expression of these proteins is in the neutrophil, a cell that is exposed to high levels of oxidant, and indeed produces large quantities of oxidant, this could imply some role for this protein in the response to oxidants.

An extension of this study would be to see if the S100A8/9 expressing keratinocyte population is proliferating, this could provide some insight into the role of S100A9. Work previously published has indicated that the expression of S100A9 in the wounded epithelium may be linked to hyper-proliferation rather than an inflammatory response, demonstrated by expression in hyperproliferative keratinocytes of the non-inflamed epithelium of activin over expressing mice (Thorey et al., 2001). Examination of earlier time points may also give interesting information as to the time period over which S100A9 protein is induced. The time-points examined so far do not reveal the kinetics of S100A9 expression and the expression seen at day 4 could be at either the beginning or end of this process, given that little expression remains at day 7.

CHAPTER 8

8 General discussion

One feature of S100A8/9 that has been of abiding interest to leukocyte biologists is the abundance of this protein in neutrophils. That this protein can be entirely deleted and the cells are able to perform their fundamental roles apparently normally is surprising. To date in this study and in the previous publication (Hobbs et al., 2003) the ability of the neutrophils to develop, mature, adhere, migrate, chemotax, phagocytose, produce an oxidative burst, kill bacteria and apoptose has been shown to be broadly normal in the assays tested. This seems to be in conflict with the published literature on this protein that has speculated key roles for this protein in most neutrophil functions. The published chemoattractant properties of S100A8/9 (Ryckman et al., 2003b) could not be reproduced in this work and no defect in migration in a model of peritonitis could be seen. The antimicrobicidal properties of S100A8/9 (Sohnle et al., 2000; Steinbakk et al., 1990) are not evident in the *in vivo* model of *Streptococcus pneumoniae* infection or the *in vitro* killing assay. The reported association of S100A8/9 with the cytoskeleton (Burwinkel et al., 1994; Roth et al., 1993) could not be seen in murine neutrophils and no defect in cytoskeleton function relating to cell migration or phagocytosis has been detected to date (this study and (Hobbs et al., 2003)). Given that the potential functions outlined in the literature have not yielded a clear neutrophil phenotype in the mice to date other than a calcium signalling defect, it seems future studies should concentrate on less biased *in vivo*

models of general innate immune function. The lack of correlation between functions ascribed to recombinant proteins and real *in vivo* functions underlines the necessity of *in vivo* functional studies.

8.1.1 Differences in phenotype between S100A9 null mouse strains

The differences in phenotype of our S100A9 null mice and the Manitz *et al* strain of S100A9 null are perplexing. To date no gross phenotype for these mice have been published. All differences in the function of the S100A9 null neutrophils have been relatively subtle and little difference in any *in vivo* model has been shown (Hobbs et al., 2003; Manitz et al., 2003). The only reported *in vivo* lesion is the preliminary observation of decreased neutrophil recruitment to the site of wound healing in the independent strain of S100A9 null mice (Vogl et al., 2004). The mechanism of this phenotype is unclear and is not reproducible in our line of S100A9 null mice (see Chapter 7). The mechanism published implicates the phosphorylation of S100A9 by the MAP kinase p38 and the polymerisation of the S100A8/9 dimer and interaction with microfilaments (Vogl et al., 2004). The published human S100A9 data shows a role for phosphorylation of S100A9 causing its translocation to microfilaments after which cell migration is enhanced (Kerkhoff et al., 1999a). This explanation is not fully satisfactory as phosphorylation of murine S100A9 has never been demonstrated and the mechanistic data presented shows biochemical studies using human S100A9 and in this instance a correlation in the activity of the human and murine protein cannot be assumed. Indeed the only confirmed phosphorylation site in the human S100A9 protein (Edgeworth et al., 1989) is not conserved in the murine homolog (E. M^{c}Neill - data not shown). To confirm this phenomenon in murine

neutrophils, evidence for any phosphorylation of this protein, and in particular, in this model, would have to be obtained.

To further consider reasons for the different data reported for the two S100A9 null mice strains it should be pointed out that the mice have been produced using different targeting strategies. Rather than an insertional strategy (Hobbs et al., 2003), the second strain of mice was produced using a deletional strategy (Manitz et al., 2003). It is possible that, given the different targeting strategies, effects on the transcription of other proteins has been affected, although in our extensive investigation we have found no evidence for this (Hobbs et al., 2003). Also the mice presented in this study are fully back-crossed onto a C57BL/6J background and the back-cross status of the Manitz *et al* mice is unclear in their publication. Having mice on a mixed background can increase the variation between mice as they may not all exhibit the same level of C57BL/6J or SvJ background and these two strains exhibit different responses in various models. It could also be that differences in the technique used to isolate neutrophils by the different groups may have lead to differences in the activation state of the cells. Given the ease with which this cell type can be activated by bacterial products and mechanical stimulation, differences in how the cells are handled maybe masking/revealing differences in the biology of these cells or leading to false results.

8.1.2 S100A9 and calcium signalling

The data presented in this thesis indicates that specific calcium signalling pathways are altered in the absence of S100A9 (see chapter 3). The significance of the lesion with regard to physiological levels of chemoattractant stimulation is

unclear. The relationship between the levels of chemoattractant used here and the levels found *in vivo* are difficult to interpret as chemoattractants are presented on glycoasminoglycans *in vivo* rather than in a soluble state. It may be that the sub-maximal levels at which the lesion is seen in the *in vitro* assays presented here indicate that calcium signalling is profoundly affected in the absence of S100A9 *in vivo*. While not appearing a profound lesion *in vitro*, this deficiency could give a clue to the fundamental role of this protein family. That this lesion bears some similarity to the subtle alterations in calcium signalling seen in the S100A1 null mice (Du et al., 2002) could indicate that the role of these proteins is in the fine tuning of cellular calcium responses. I have already outlined in chapter 3 that key extensions of this work are to find exactly the point in the IP_3-mediated pathway that is compromised in S100A9 null mice. A piece of evidence needed is to find out if the levels of IP_3 are normal in these mice, which would allow the lesion to be placed prior to or after phospholipase C activation. Another key experiment is to look further for any direct interaction of S100A9 with the IP_3 receptor or any other part of the calcium signalling machinery under various conditions, in a similar manner to the reported interaction of S100A1 with the ryanodine receptor (Du et al., 2002; Most et al., 2003).

8.1.3 *In vivo* infection studies

It seems perplexing that given the abundance of these proteins, we can detect no consistent obvious defect in neutrophil function. Although the results from the *Streptococcus pneumoniae* infection study are tantalising, currently we can demonstrate no effect of the lack of S100A9 on the progress of this infection. There are several neutrophil functions, such as production of cytokines and de-granulation, which we have not yet analysed. However, given that in a model of

infection no gross phenotype can be seen implies no critical non-redundant un-compensated role for S100A9 in neutrophil function. To extend the study of the S100A9 mice with respect to neutrophil function, developing further *in vitro* assays seems unlikely to be a productive avenue until an *in vivo* effect of deletion of this protein can be successfully documented. Challenging these mice with other pathogens and assessing the progress of the infection is likely to be the most productive way forward. This may yield a defined pathogenic stimulus that will reveal the function of this protein in neutrophils. The function that is defective *in vivo* can be dissected by directed *in vivo* and *in vitro* experiments. Until that time, the limits imposed by the difficulty of working with primary murine neutrophils in a mixed bone marrow cell population are too great.

The work presented in this thesis almost entirely deals with the functioning of the innate immune system. The innate immune system plays a role initiating the function of the adaptive immune system through the production of cytokines and the presentation of processed antigen. The delayed-type hypersensitivity reaction tests the function of the adaptive immune system to respond to immunization with antigen. Mice are inoculated with antigen and adjuvant, and following a lag period the lymph nodes are removed, disaggregated and put into culture. The cultures are then restimulated with the antigen and the local lymph node APCs present the antigen to the resident lymphocyes and the degree of proliferation induced in assessed. Preliminary experiments using this protocol have shown no difference in the response to ovalbumin immunization to date, but require further investigation to confirm this (E. M^{c}Neill – data not shown).

8.1.4 Carcinogenesis

The data produced by the carcinogenesis study provides the most exciting *in vivo* phenotype to date. This model seems to show a real difference in the formation of benign papillomas. There are two possible sites at which S100A9 deletion could be playing a role, both in keratinocyte function or in innate immune function. There is evidence for upregulation of S100A9 in the skin carcinogenesis model (Gebhardt et al., 2002) and in this study we have also seen expression by the hyperproliferative keratinocyte population during wound healing as has been reported previously (Thorey et al., 2001). Inflammation and the innate immune system have been shown to play a crucial role in the promotion phase of this model (Moore et al., 1999; Murphy et al., 2003). If it is an alteration in the function of neutrophils that is responsible for this phenotype this will provide the first evidence of a specific role for this leukocyte subset in skin carcinogenesis. To define the phenotype we see in this model the first task will be will be key to perform histology to look for expression of S100A9 by both keratinocytes and cells of the innate immune system in the affected area in wildtype mice. Histology will also provide the opportunity to look for gross changes in the S100A9 null mice such as altered leukocyte infiltration or epithelial morphology.

Additional experiments could include examination of cytokine production such as TNFα that are central to the inflammatory component of the promotion phase (Moore et al., 1999). Examination of the keratinocytes could include measurements of proliferation using BrdU or Ki67. Should any differences be seen in the incidence of carcinomas in the S100A9 null mice, this can be further investigated using a complete carcinogenesis protocol that consists of repeated

treatment with the initiating agent DMBA and does not include a promotion phase. To absolutely confirm a role for either the keratinocytes or neutrophils bone marrow chimearas could be produced to replace the immune system in an S100A9 null animal with wildtype cells and *vice versa*. Once the cell type/s affected by the deletion of S100A9 have been identified then further investigation of the mechanism of action of S100A9 in induced skin carcinogenesis should be carried out. If a role for the immune system is highlighted the role of the adaptive immune system can be assessed by observing papilloma formation in lymphocyte deficicent S100A9 null RAG-2 null animals. To further characterise any role for neutrophils in the wildtype and S100A9 null situation neutrophils could be depleted during the experiment by repeated injection of a neutrophil-depleting antibody such as RB6.

8.1.5 Chronic inflammation

High levels of S100A8/9 are reported in chronic inflammatory conditions such as rheumatoid arthritis (Odink et al., 1987) and inflammatory bowel disease (Fagerhol, 2000). Inflammatory bowel disease can be modelled in mice using a model of TNBS-induced colitis. This causes inflammation in colon similar to that seen in ulcerative colitis. Rheumatoid arthritis can be modelled using a collagen-induced arthritis protocol, although this would require the mice to be bred onto a susceptible background, such as the CBA strain. Studying these conditions in the S100A9 null mice may give some indication if S100A9 plays a role in the pathogenesis of inflammatory conditions or whether the levels seem are simply a marker of myeloid cell based inflammation in these conditions.

8.1.6 Compensation

Whilst the function of S100A9 in neutrophil function may not have been revealed by the assays performed to date another less appealing prospect is that the neutrophils have managed to compensate for the lack of this protein. Although no alterations in protein expression levels has been seen they may have compensated in a manner that does not require altered protein expression. It may be that the alterations in calcium signalling and altered basal calcium levels are all that remains of the effect of deletion of S100A9 on calcium homeostasis and signalling. If this in indeed that case, then a conditional S100A9 knockout mouse, for example produced using the Cre-Lox system, would allow cells to develop normally and undergo deletion of the protein in mature cells. Such a model would reduce the likelihood of any compensation occurring during cell development and allow the function of S100A9 to be reassessed. These experiments would need to be performed using a conditional knockout animal as, even with the advent of siRNA and primary leukocyte transfection strategies, knockdown of S100A9 in primary neutrophils would be problematic. Neutrophils have a short half-life and as a terminally differentiated cell type do not divide and cannot be maintained in culture. The only available cell-lines are leukaemic progenitor cell lines that require differentiation to a neutrophil-like phenotype. These lines then stop dividing and develop the short life span associated with neutrophils. This makes any deletion of S100A9 in a relevant cell or cell-line difficult.

8.1.7 Conclusions

To date it can be concluded from the studies of the S100A9 null mice that S100A8/9 appears to play a redundant role in neutrophil development and many aspects of their function. The complex appears to play a non-redundant role in

intracellular calcium release in response to some but not all chemoattractant signalling. S100A9 null neutrophils show reduced calcium signalling in response to MIP-2 but not FMLP. This deficiency appears to be in the IP_3-mediated calcium release pathway. S100A8/9 plays a non-redundant role in a model of skin carcinogenesis with S100A9 null mice showing increased rate and incidence papilloma formation and increased tumour multiplicity.

9 References

Ahluwalia, J., A. Tinker, L.H. Clapp, M.R. Duchen, A.Y. Abramov, S. Pope, M. Nobles, and A.W. Segal. 2004. The large-conductance Ca2+-activated K+ channel is essential for innate immunity. *Nature*. 427:853-8.

Airaksinen, M.S., J. Eilers, O. Garaschuk, H. Thoenen, A. Konnerth, and M. Meyer. 1997. Ataxia and altered dendritic calcium signaling in mice carrying a targeted null mutation of the calbindin D28k gene. *Proc Natl Acad Sci U S A*. 94:1488-93.

Ambartsumian, N., J. Klingelhofer, M. Grigorian, C. Christensen, M. Kriajevska, E. Tulchinsky, G. Georgiev, V. Berezin, E. Bock, J. Rygaard, R. Cao, Y. Cao, and E. Lukanidin. 2001. The metastasis-associated Mts1(S100A4) protein could act as an angiogenic factor. *Oncogene*. 20:4685-95.

Ambartsumian, N.S., M.S. Grigorian, I.F. Larsen, O. Karlstrom, N. Sidenius, J. Rygaard, G. Georgiev, and E. Lukanidin. 1996. Metastasis of mammary carcinomas in GRS/A hybrid mice transgenic for the mts1 gene. *Oncogene*. 13:1621-30.

Aratani, Y., H. Koyama, S. Nyui, K. Suzuki, F. Kura, and N. Maeda. 1999. Severe impairment in early host defense against Candida albicans in mice deficient in myeloperoxidase. *Infect Immun*. 67:1828-36.

Arnott, C.H., K.A. Scott, R.J. Moore, S.C. Robinson, R.G. Thompson, and F.R. Balkwill. 2004. Expression of both TNF-alpha receptor subtypes is essential for optimal skin tumour development. *Oncogene*. 23:1902-10.

Ayub, K., and M.B. Hallett. 2004. Ca2+ influx shutdown during neutrophil apoptosis: importance and possible mechanism. *Immunology*. 111:8-12.

Baimbridge, K.G., J.J. Miller, and C.O. Parkes. 1982. Calcium-binding protein distribution in the rat brain. *Brain Res*. 239:519-25.

Balbin, M., A. Fueyo, A.M. Tester, A.M. Pendas, A.S. Pitiot, A. Astudillo, C.M. Overall, S.D. Shapiro, and C. Lopez-Otin. 2003. Loss of collagenase-2 confers increased skin tumor susceptibility to male mice. *Nat Genet*. 35:252-7.

Barthe, C., C. Figarella, J. Carrere, and O. Guy-Crotte. 1991. Identification of 'cystic fibrosis protein' as a complex of two calcium-binding proteins present in human cells of myeloid origin. *Biochim Biophys Acta*. 1096:175-7.

Bengis-Garber, C., and N. Gruener. 1993. Calcium-binding myeloid protein (P8,14) is phosphorylated in fMet-Leu-Phe-stimulated neutrophils. *J Leukoc Biol*. 54:114-8.

Bergeron, Y., N. Ouellet, A.M. Deslauriers, M. Simard, M. Olivier, and M.G. Bergeron. 1998. Cytokine kinetics and other host factors in response to pneumococcal pulmonary infection in mice. *Infect Immun*. 66:912-22.

Berridge, M.J. 2002. The endoplasmic reticulum: a multifunctional signaling organelle. *Cell Calcium*. 32:235-49.

Berridge, M.J., M.D. Bootman, and H.L. Roderick. 2003. Calcium signalling: dynamics, homeostasis and remodelling. *Nat Rev Mol Cell Biol*. 4:517-29.

Berridge, M.J., P. Lipp, and M.D. Bootman. 2000. The versatility and universality of calcium signalling. *Nat Rev Mol Cell Biol*. 1:11-21.

Beutler, B. 2004. Innate immunity: an overview. *Mol Immunol*. 40:845-59.

Bhattacharya, S., C.G. Bunick, and W.J. Chazin. 2004. Target selectivity in EF-hand calcium binding proteins. *Biochim Biophys Acta*. 1742:69-79.

Bootman, M.D., T.J. Collins, L. Mackenzie, H.L. Roderick, M.J. Berridge, and C.M. Peppiatt. 2002. 2-aminoethoxydiphenyl borate (2-APB) is a reliable blocker of store-operated Ca2+ entry but an inconsistent inhibitor of InsP3-induced Ca2+ release. *Faseb J.* 16:1145-50.

Brandtzaeg, P., I. Dale, and M.K. Fagerhol. 1987. Distribution of a formalin-resistant myelomonocytic antigen (L1) in human tissues. II. Normal and aberrant occurrence in various epithelia. *Am J Clin Pathol.* 87:700-7.

Broome, A.M., D. Ryan, and R.L. Eckert. 2003. S100 protein subcellular localization during epidermal differentiation and psoriasis. *J Histochem Cytochem.* 51:675-85.

Brose, N., A. Betz, and H. Wegmeyer. 2004. Divergent and convergent signaling by the diacylglycerol second messenger pathway in mammals. *Curr Opin Neurobiol.* 14:328-40.

Buhling, F., A. Ittenson, D. Kaiser, G. Tholert, B. Hoffmann, D. Reinhold, S. Ansorge, and T. Welte. 2000. MRP8/MRP14, CD11b and HLA-DR expression of alveolar macrophages in pneumonia. *Immunol Lett.* 71:185-90.

Burwinkel, F., J. Roth, M. Goebeler, U. Bitter, V. Wrocklage, E. Vollmer, A. Roessner, C. Sorg, and W. Bocker. 1994. Ultrastructural localization of the S-100-like proteins MRP8 and MRP14 in monocytes is calcium-dependent. *Histochemistry.* 101:113-20.

C'Naaman, E.L., B. Grum-Schwensen, A. Mansouri, M. Grigorian, E. Santoni-Rugiu, T. Hansen, M. Kriajevska, B.W. Schafer, C.W. Heizmann, E. Lukanidin, and N. Ambartsumian. 2004. Cancer predisposition in mice deficient for the metastasis-associated Mts1(S100A4) gene. *Oncogene.* 23:3670-80.

Cornish, C.J., J.M. Devery, P. Poronnik, M. Lackmann, D.I. Cook, and C.L. Geczy. 1996. S100 protein CP-10 stimulates myeloid cell chemotaxis without activation. *J Cell Physiol.* 166:427-37.

Coussens, L.M., C.L. Tinkle, D. Hanahan, and Z. Werb. 2000. MMP-9 supplied by bone marrow-derived cells contributes to skin carcinogenesis. *Cell.* 103:481-90.

Dahlgren, C., and A. Karlsson. 1999. Respiratory burst in human neutrophils. *J Immunol Methods.* 232:3-14.

Dana, R., T.L. Leto, H.L. Malech, and R. Levy. 1998. Essential requirement of cytosolic phospholipase A2 for activation of the phagocyte NADPH oxidase. *J Biol Chem.* 273:441-5.

Dangerfield, J., K.Y. Larbi, M.T. Huang, A. Dewar, and S. Nourshargh. 2002. PECAM-1 (CD31) homophilic interaction up-regulates alpha6beta1 on transmigrated neutrophils in vivo and plays a functional role in the ability of alpha6 integrins to mediate leukocyte migration through the perivascular basement membrane. *J Exp Med.* 196:1201-11.

Dazard, J.E., H. Gal, N. Amariglio, G. Rechavi, E. Domany, and D. Givol. 2003. Genome-wide comparison of human keratinocyte and squamous cell carcinoma responses to UVB irradiation: implications for skin and epithelial cancer. *Oncogene.* 22:2993-3006.

DeLano, W.L. 2004. The PyMOL Molecular Graphics System, San Carlos, CA.

Devery, J.M., N.J. King, and C.L. Geczy. 1994. Acute inflammatory activity of the S100 protein CP-10. Activation of neutrophils in vivo and in vitro. *J Immunol.* 152:1888-97.

Dewitt, S., I. Laffafian, and M.B. Hallett. 2003. Phagosomal oxidative activity during beta2 integrin (CR3)-mediated phagocytosis by neutrophils is triggered

by a non-restricted Ca2+ signal: Ca2+ controls time not space. *J Cell Sci.* 116:2857-65.

Donato, R. 1999. Functional roles of S100 proteins, calcium-binding proteins of the EF-hand type. *Biochim Biophys Acta.* 1450:191-231.

Donato, R. 2001. S100: a multigenic family of calcium-modulated proteins of the EF-hand type with intracellular and extracellular functional roles. *Int J Biochem Cell Biol.* 33:637-68.

Doussiere, J., F. Bouzidi, A. Poinas, J. Gaillard, and P.V. Vignais. 1999. Kinetic study of the activation of the neutrophil NADPH oxidase by arachidonic acid. Antagonistic effects of arachidonic acid and phenylarsine oxide. *Biochemistry.* 38:16394-406.

Doussiere, J., F. Bouzidi, and P.V. Vignais. 2002. The S100A8/A9 protein as a partner for the cytosolic factors of NADPH oxidase activation in neutrophils. *Eur J Biochem.* 269:3246-55.

Dovi, J.V., L.K. He, and L.A. DiPietro. 2003. Accelerated wound closure in neutrophil-depleted mice. *J Leukoc Biol.* 73:448-55.

Du, X.J., T.J. Cole, N. Tenis, X.M. Gao, F. Kontgen, B.E. Kemp, and J. Heierhorst. 2002. Impaired cardiac contractility response to hemodynamic stress in S100A1-deficient mice. *Mol Cell Biol.* 22:2821-9.

Duchen, M.R. 1999. Contributions of mitochondria to animal physiology: from homeostatic sensor to calcium signalling and cell death. *J Physiol.* 516 (Pt 1):1-17.

Dyck, R.H., Bogoch, II, A. Marks, N.R. Melvin, and G.C. Teskey. 2002. Enhanced epileptogenesis in S100B knockout mice. *Brain Res Mol Brain Res.* 106:22-9.

Eckert, R.L., A.M. Broome, M. Ruse, N. Robinson, D. Ryan, and K. Lee. 2004. S100 proteins in the epidermis. *J Invest Dermatol.* 123:23-33.

Edgeworth, J., P. Freemont, and N. Hogg. 1989. Ionomycin-regulated phosphorylation of the myeloid calcium-binding protein p14. *Nature.* 342:189-92.

Edgeworth, J., M. Gorman, R. Bennett, P. Freemont, and N. Hogg. 1991. Identification of p8,14 as a highly abundant heterodimeric calcium binding protein complex of myeloid cells. *J Biol Chem.* 266:7706-13.

Emberley, E.D., L.C. Murphy, and P.H. Watson. 2004. S100 proteins and their influence on pro-survival pathways in cancer. *Biochem Cell Biol.* 82:508-15.

Fagerhol, M.K. 2000. Calprotectin, a faecal marker of organic gastrointestinal abnormality. *Lancet.* 356:1783-4.

Faurschou, M., and N. Borregaard. 2003. Neutrophil granules and secretory vesicles in inflammation. *Microbes Infect.* 5:1317-27.

Friedman, A.D. 2002. Transcriptional regulation of granulocyte and monocyte development. *Oncogene.* 21:3377-90.

Fuellen, G., D. Foell, W. Nacken, C. Sorg, and C. Kerkhoff. 2003. Absence of S100A12 in mouse: implications for RAGE-S100A12 interaction. *Trends Immunol.* 24:622-4.

Fuellen, G., W. Nacken, C. Sorg, and C. Kerkhoff. 2004. Computational searches for missing orthologs: the case of S100A12 in mice. *Omics.* 8:334-40.

Fujita, T. 2002. Evolution of the lectin-complement pathway and its role in innate immunity. *Nat Rev Immunol.* 2:346-53.

Gabrielsen, T.O., I. Dale, P. Brandtzaeg, P.S. Hoel, M.K. Fagerhol, T.E. Larsen, and P.O. Thune. 1986. Epidermal and dermal distribution of a myelomonocytic

antigen (L1) shared by epithelial cells in various inflammatory skin diseases. *J Am Acad Dermatol.* 15:173-9.

Gebhardt, C., U. Breitenbach, J.P. Tuckermann, B.T. Dittrich, K.H. Richter, and P. Angel. 2002. Calgranulins S100A8 and S100A9 are negatively regulated by glucocorticoids in a c-Fos-dependent manner and overexpressed throughout skin carcinogenesis. *Oncogene.* 21:4266-76.

Gimona, M., Z. Lando, Y. Dolginov, J. Vandekerckhove, R. Kobayashi, A. Sobieszek, and D.M. Helfman. 1997. Ca2+-dependent interaction of S100A2 with muscle and nonmuscle tropomyosins. *J Cell Sci.* 110 (Pt 5):611-21.

Glaser, R., J. Harder, H. Lange, J. Bartels, E. Christophers, and J.M. Schroder. 2005. Antimicrobial psoriasin (S100A7) protects human skin from Escherichia coli infection. *Nat Immunol.* 6:57-64.

Goebeler, M., J. Roth, U. Henseleit, C. Sunderkotter, and C. Sorg. 1993. Expression and complex assembly of calcium-binding proteins MRP8 and MRP14 during differentiation of murine myelomonocytic cells. *J Leukoc Biol.* 53:11-8.

Goebeler, M., J. Roth, C. van den Bos, G. Ader, and C. Sorg. 1995. Increase of calcium levels in epithelial cells induces translocation of calcium-binding proteins migration inhibitory factor-related protein 8 (MRP8) and MRP14 to keratin intermediate filaments. *Biochem J.* 309 (Pt 2):419-24.

Gordon, S. 2002. Pattern recognition receptors: doubling up for the innate immune response. *Cell.* 111:927-30.

Gribenko, A.V., J.E. Hopper, and G.I. Makhatadze. 2001. Molecular characterization and tissue distribution of a novel member of the S100 family of EF-hand proteins. *Biochemistry.* 40:15538-48.

Grigorian, M., E. Tulchinsky, O. Burrone, S. Tarabykina, G. Georgiev, and E. Lukanidin. 1994. Modulation of mts1 expression in mouse and human normal and tumor cells. *Electrophoresis*. 15:463-8.

Grimbaldeston, M.A., C.L. Geczy, N. Tedla, J.J. Finlay-Jones, and P.H. Hart. 2003. S100A8 induction in keratinocytes by ultraviolet A irradiation is dependent on reactive oxygen intermediates. *J Invest Dermatol*. 121:1168-74.

Grum-Schwensen, B., J. Klingelhofer, C.H. Berg, C. El-Naaman, M. Grigorian, E. Lukanidin, and N. Ambartsumian. 2005. Suppression of tumor development and metastasis formation in mice lacking the S100A4(mts1) gene. *Cancer Res*. 65:3772-80.

Guignard, F., J. Mauel, and M. Markert. 1996. Phosphorylation of myeloid-related proteins MRP-14 and MRP-8 during human neutrophil activation. *Eur J Biochem*. 241:265-71.

Hallett, M.B., E.V. Davies, and E.J. Pettit. 1996. Fluorescent Methods for Measuring and Imaging Cytosolic Free Ca2+ in Neutrophils. *Methods*. 9:591-606.

Hallett, M.B., R. Hodges, M. Cadman, H. Blanchfield, S. Dewitt, E.J. Pettit, I. Laffafian, and E.V. Davies. 1999. Techniques for measuring and manipulating free Ca2+ in the cytosol and organelles of neutrophils. *J Immunol Methods*. 232:77-88.

Hanselmann, C., C. Mauch, and S. Werner. 2001. Haem oxygenase-1: a novel player in cutaneous wound repair and psoriasis? *Biochem J*. 353:459-66.

Haqqani, A.S., J.K. Sandhu, and H.C. Birnboim. 2000. Expression of interleukin-8 promotes neutrophil infiltration and genetic instability in mutatect tumors. *Neoplasia*. 2:561-8.

Hardie, R.C. 2003. Regulation of TRP channels via lipid second messengers. *Annu Rev Physiol.* 65:735-59.

Harrison, C.A., M.J. Raftery, J. Walsh, P. Alewood, S.E. Iismaa, S. Thliveris, and C.L. Geczy. 1999. Oxidation regulates the inflammatory properties of the murine S100 protein S100A8. *J Biol Chem.* 274:8561-9.

Helfman, D.M., E.J. Kim, E. Lukanidin, and M. Grigorian. 2005. The metastasis associated protein S100A4: role in tumour progression and metastasis. *Br J Cancer.* 92:1955-8.

Henderson, R.B., J.A. Hobbs, M. Mathies, and N. Hogg. 2003. Rapid recruitment of inflammatory monocytes is independent of neutrophil migration. *Blood.* 102:328-35.

Hessian, P.A., J. Edgeworth, and N. Hogg. 1993. MRP-8 and MRP-14, two abundant Ca(2+)-binding proteins of neutrophils and monocytes. *J Leukoc Biol.* 53:197-204.

Hessian, P.A., and L. Fisher. 2001. The heterodimeric complex of MRP-8 (S100A8) and MRP-14 (S100A9). Antibody recognition, epitope definition and the implications for structure. *Eur J Biochem.* 268:353-63.

Hisatsune, C., K. Nakamura, Y. Kuroda, T. Nakamura, and K. Mikoshiba. 2005. Amplification of Ca2+ signaling by diacylglycerol-mediated inositol 1,4,5-trisphosphate production. *J Biol Chem.* 280:11723-30.

Hobbs, J.A., R. May, K. Tanousis, E. McNeill, M. Mathies, C. Gebhardt, R. Henderson, M.J. Robinson, and N. Hogg. 2003. Myeloid cell function in MRP-14 (S100A9) null mice. *Mol Cell Biol.* 23:2564-76.

Hobbs, J.A.R. 2003. *In vitro* and *in vivo* functions of MRP-14. *In* UCL Department of Immunology and Molecular Pathology. University of London, London. 260.

Hofmann, M.A., S. Drury, C. Fu, W. Qu, A. Taguchi, Y. Lu, C. Avila, N. Kambham, A. Bierhaus, P. Nawroth, M.F. Neurath, T. Slattery, D. Beach, J. McClary, M. Nagashima, J. Morser, D. Stern, and A.M. Schmidt. 1999. RAGE mediates a novel proinflammatory axis: a central cell surface receptor for S100/calgranulin polypeptides. *Cell.* 97:889-901.

Hou, C., T. Kirchner, M. Singer, M. Matheis, D. Argentieri, and D. Cavender. 2004. In vivo activity of a phospholipase C inhibitor, 1-(6-((17beta-3-methoxyestra-1,3,5(10)-trien-17-yl)amino)hexyl)-1H-pyrrole -2,5-dione (U73122), in acute and chronic inflammatory reactions. *J Pharmacol Exp Ther.* 309:697-704.

Hunter, M.J., and W.J. Chazin. 1998. High level expression and dimer characterization of the S100 EF-hand proteins, migration inhibitory factor-related proteins 8 and 14. *J Biol Chem.* 273:12427-35.

Huttunen, H.J., J. Kuja-Panula, G. Sorci, A.L. Agneletti, R. Donato, and H. Rauvala. 2000. Coregulation of neurite outgrowth and cell survival by amphoterin and S100 proteins through receptor for advanced glycation end products (RAGE) activation. *J Biol Chem.* 275:40096-105.

Ikura, M. 1996. Calcium binding and conformational response in EF-hand proteins. *Trends Biochem Sci.* 21:14-7.

Imhof, B.A., and M. Aurrand-Lions. 2004. Adhesion mechanisms regulating the migration of monocytes. *Nat Rev Immunol.* 4:432-44.

Isaksen, B., and M.K. Fagerhol. 2001. Calprotectin inhibits matrix metalloproteinases by sequestration of zinc. *Mol Pathol.* 54:289-92.

Janeway, C.A., Jr., and R. Medzhitov. 2002. Innate immune recognition. *Annu Rev Immunol.* 20:197-216.

Jiang, H., Y. Kuang, Y. Wu, A. Smrcka, M.I. Simon, and D. Wu. 1996. Pertussis toxin-sensitive activation of phospholipase C by the C5a and fMet-Leu-Phe receptors. *J Biol Chem.* 271:13430-4.

Jiang, H., Y. Kuang, Y. Wu, W. Xie, M.I. Simon, and D. Wu. 1997. Roles of phospholipase C beta2 in chemoattractant-elicited responses. *Proc Natl Acad Sci U S A.* 94:7971-5.

Jinquan, T., H. Vorum, C.G. Larsen, P. Madsen, H.H. Rasmussen, B. Gesser, M. Etzerodt, B. Honore, J.E. Celis, and K. Thestrup-Pedersen. 1996. Psoriasin: a novel chemotactic protein. *J Invest Dermatol.* 107:5-10.

Kadioglu, A., and P.W. Andrew. 2004. The innate immune response to pneumococcal lung infection: the untold story. *Trends Immunol.* 25:143-9.

Kadioglu, A., N.A. Gingles, K. Grattan, A. Kerr, T.J. Mitchell, and P.W. Andrew. 2000. Host cellular immune response to pneumococcal lung infection in mice. *Infect Immun.* 68:492-501.

Kasri, N.N., A.M. Holmes, G. Bultynck, J.B. Parys, M.D. Bootman, K. Rietdorf, L. Missiaen, F. McDonald, H. De Smedt, S.J. Conway, A.B. Holmes, M.J. Berridge, and H.L. Roderick. 2004. Regulation of InsP3 receptor activity by neuronal Ca2+-binding proteins. *Embo J.* 23:312-21.

Kerkhoff, C., I. Eue, and C. Sorg. 1999a. The regulatory role of MRP8 (S100A8) and MRP14 (S100A9) in the transendothelial migration of human leukocytes. *Pathobiology.* 67:230-2.

Kerkhoff, C., M. Klempt, V. Kaever, and C. Sorg. 1999b. The two calcium-binding proteins, S100A8 and S100A9, are involved in the metabolism of arachidonic acid in human neutrophils. *J Biol Chem.* 274:32672-9.

Kerkhoff, C., W. Nacken, M. Benedyk, M.C. Dagher, C. Sopalla, and J. Doussiere. 2005. The arachidonic acid-binding protein S100A8/A9 promotes

NADPH oxidase activation by interaction with p67phox and Rac-2. *Faseb J.* 19:467-9.

Kerkhoff, C., C. Sorg, N.N. Tandon, and W. Nacken. 2001. Interaction of S100A8/S100A9-arachidonic acid complexes with the scavenger receptor CD36 may facilitate fatty acid uptake by endothelial cells. *Biochemistry.* 40:241-8.

Kerr, A.R., J.J. Irvine, J.J. Search, N.A. Gingles, A. Kadioglu, P.W. Andrew, W.L. McPheat, C.G. Booth, and T.J. Mitchell. 2002. Role of inflammatory mediators in resistance and susceptibility to pneumococcal infection. *Infect Immun.* 70:1547-57.

Kim, E.J., and D.M. Helfman. 2003. Characterization of the metastasis-associated protein, S100A4. Roles of calcium binding and dimerization in cellular localization and interaction with myosin. *J Biol Chem.* 278:30063-73.

Klempt, M., H. Melkonyan, W. Nacken, D. Wiesmann, U. Holtkemper, and C. Sorg. 1997. The heterodimer of the Ca2+-binding proteins MRP8 and MRP14 binds to arachidonic acid. *FEBS Lett.* 408:81-4.

Komada, T., R. Araki, K. Nakatani, I. Yada, M. Naka, and T. Tanaka. 1996. Novel specific chemtactic receptor for S100L protein on guinea pig eosinophils. *Biochem Biophys Res Commun.* 220:871-4.

Kunz, M., J. Roth, C. Sorg, and G. Kolde. 1992. Epidermal expression of the calcium binding surface antigen 27E10 in inflammatory skin diseases. *Arch Dermatol Res.* 284:386-90.

Lackmann, M., C.J. Cornish, R.J. Simpson, R.L. Moritz, and C.L. Geczy. 1992. Purification and structural analysis of a murine chemotactic cytokine (CP-10) with sequence homology to S100 proteins. *J Biol Chem.* 267:7499-504.

Lackmann, M., P. Rajasekariah, S.E. Iismaa, G. Jones, C.J. Cornish, S. Hu, R.J. Simpson, R.L. Moritz, and C.L. Geczy. 1993. Identification of a chemotactic domain of the pro-inflammatory S100 protein CP-10. *J Immunol.* 150:2981-91.

Laffafian, I., and M.B. Hallett. 1995. Does cytosolic free Ca2+ signal neutrophil chemotaxis in response to formylated chemotactic peptide? *J Cell Sci.* 108 (Pt 10):3199-205.

Lagasse, E., and R.G. Clerc. 1988. Cloning and expression of two human genes encoding calcium-binding proteins that are regulated during myeloid differentiation. *Mol Cell Biol.* 8:2402-10.

Lagasse, E., and I.L. Weissman. 1992. Mouse MRP8 and MRP14, two intracellular calcium-binding proteins associated with the development of the myeloid lineage. *Blood.* 79:1907-15.

Lakshman, R., and A. Finn. 2001. Neutrophil disorders and their management. *J Clin Pathol.* 54:7-19.

Lemarchand, P., M. Vaglio, J. Mauel, and M. Markert. 1992. Translocation of a small cytosolic calcium-binding protein (MRP-8) to plasma membrane correlates with human neutrophil activation. *J Biol Chem.* 267:19379-82.

Levett, D., P.A. Flecknell, P.S. Rudland, R. Barraclough, D.E. Neal, J.K. Mellon, and B.R. Davies. 2002. Transfection of S100A4 produces metastatic variants of an orthotopic model of bladder cancer. *Am J Pathol.* 160:693-700.

Lewit-Bentley, A., and S. Rety. 2000. EF-hand calcium-binding proteins. *Curr Opin Struct Biol.* 10:637-43.

Ley, K. 2002. Integration of inflammatory signals by rolling neutrophils. *Immunol Rev.* 186:8-18.

Li, X., S. Mohan, W. Gu, N. Miyakoshi, and D.J. Baylink. 2000a. Differential protein profile in the ear-punched tissue of regeneration and non-regeneration

strains of mice: a novel approach to explore the candidate genes for soft-tissue regeneration. *Biochim Biophys Acta.* 1524:102-9.

Li, Z., H. Jiang, W. Xie, Z. Zhang, A.V. Smrcka, and D. Wu. 2000b. Roles of PLC-beta2 and -beta3 and PI3Kgamma in chemoattractant-mediated signal transduction. *Science.* 287:1046-9.

Luo, A., J. Kong, G. Hu, C.C. Liew, M. Xiong, X. Wang, J. Ji, T. Wang, H. Zhi, M. Wu, and Z. Liu. 2004a. Discovery of Ca2+-relevant and differentiation-associated genes downregulated in esophageal squamous cell carcinoma using cDNA microarray. *Oncogene.* 23:1291-9.

Luo, B., D.S. Regier, S.M. Prescott, and M.K. Topham. 2004b. Diacylglycerol kinases. *Cell Signal.* 16:983-9.

Manitz, M.P., B. Horst, S. Seeliger, A. Strey, B.V. Skryabin, M. Gunzer, W. Frings, F. Schonlau, J. Roth, C. Sorg, and W. Nacken. 2003. Loss of S100A9 (MRP14) results in reduced interleukin-8-induced CD11b surface expression, a polarized microfilament system, and diminished responsiveness to chemoattractants in vitro. *Mol Cell Biol.* 23:1034-43.

Mannan, A.U., G. Nica, K. Nayernia, C. Mueller, and W. Engel. 2003. Calgizarrin like gene (Cal) deficient mice undergo normal spermatogenesis. *Mol Reprod Dev.* 66:431-8.

Marenholz, I., C.W. Heizmann, and G. Fritz. 2004. S100 proteins in mouse and man: from evolution to function and pathology (including an update of the nomenclature). *Biochem Biophys Res Commun.* 322:1111-22.

Martin, C., P.C. Burdon, G. Bridger, J.C. Gutierrez-Ramos, T.J. Williams, and S.M. Rankin. 2003a. Chemokines acting via CXCR2 and CXCR4 control the release of neutrophils from the bone marrow and their return following senescence. *Immunity.* 19:583-93.

Martin, P. 1997. Wound healing--aiming for perfect skin regeneration. *Science.* 276:75-81.

Martin, P., D. D'Souza, J. Martin, R. Grose, L. Cooper, R. Maki, and S.R. McKercher. 2003b. Wound healing in the PU.1 null mouse--tissue repair is not dependent on inflammatory cells. *Curr Biol.* 13:1122-8.

Maruyama, T., T. Kanaji, S. Nakade, T. Kanno, and K. Mikoshiba. 1997. 2APB, 2-aminoethoxydiphenyl borate, a membrane-penetrable modulator of Ins(1,4,5)P3-induced Ca2+ release. *J Biochem (Tokyo).* 122:498-505.

Mignen, O., and T.J. Shuttleworth. 2000. I(ARC), a novel arachidonate-regulated, noncapacitative Ca(2+) entry channel. *J Biol Chem.* 275:9114-9.

Moore, R.J., D.M. Owens, G. Stamp, C. Arnott, F. Burke, N. East, H. Holdsworth, L. Turner, B. Rollins, M. Pasparakis, G. Kollias, and F. Balkwill. 1999. Mice deficient in tumor necrosis factor-alpha are resistant to skin carcinogenesis. *Nat Med.* 5:828-31.

Most, P., S.T. Pleger, M. Volkers, B. Heidt, M. Boerries, D. Weichenhan, E. Loffler, P.M. Janssen, A.D. Eckhart, J. Martini, M.L. Williams, H.A. Katus, A. Remppis, and W.J. Koch. 2004. Cardiac adenoviral S100A1 gene delivery rescues failing myocardium. *J Clin Invest.* 114:1550-63.

Most, P., A. Remppis, S.T. Pleger, E. Loffler, P. Ehlermann, J. Bernotat, C. Kleuss, J. Heierhorst, P. Ruiz, H. Witt, P. Karczewski, L. Mao, H.A. Rockman, S.J. Duncan, H.A. Katus, and W.J. Koch. 2003. Transgenic overexpression of the Ca2+-binding protein S100A1 in the heart leads to increased in vivo myocardial contractile performance. *J Biol Chem.* 278:33809-17.

Mouta Carreira, C., T.M. LaVallee, F. Tarantini, A. Jackson, J.T. Lathrop, B. Hampton, W.H. Burgess, and T. Maciag. 1998. S100A13 is involved in the regulation of fibroblast growth factor-1 and p40 synaptotagmin-1 release in vitro. *J Biol Chem.* 273:22224-31.

Murao, S., F.R. Collart, and E. Huberman. 1989. A protein containing the cystic fibrosis antigen is an inhibitor of protein kinases. *J Biol Chem.* 264:8356-60.

Murphy, J.E., R.E. Morales, J. Scott, and T.S. Kupper. 2003. IL-1 alpha, innate immunity, and skin carcinogenesis: the effect of constitutive expression of IL-1 alpha in epidermis on chemical carcinogenesis. *J Immunol.* 170:5697-703.

Nacken, W., C. Sopalla, C. Propper, C. Sorg, and C. Kerkhoff. 2000. Biochemical characterization of the murine S100A9 (MRP14) protein suggests that it is functionally equivalent to its human counterpart despite its low degree of sequence homology. *Eur J Biochem.* 267:560-5.

Nacken, W., C. Sorg, and C. Kerkhoff. 2004. The myeloid expressed EF-hand proteins display a diverse pattern of lipid raft association. *FEBS Lett.* 572:289-93.

Nadif Kasri, N., G. Bultynck, I. Sienaert, G. Callewaert, C. Erneux, L. Missiaen, J.B. Parys, and H. De Smedt. 2002. The role of calmodulin for inositol 1,4,5-trisphosphate receptor function. *Biochim Biophys Acta.* 1600:19-31.

Neves, S.R., P.T. Ram, and R. Iyengar. 2002. G protein pathways. *Science.* 296:1636-9.

Niggli, V. 2003. Signaling to migration in neutrophils: importance of localized pathways. *Int J Biochem Cell Biol.* 35:1619-38.

Nishiyama, H., T. Knopfel, S. Endo, and S. Itohara. 2002. Glial protein S100B modulates long-term neuronal synaptic plasticity. *Proc Natl Acad Sci U S A.* 99:4037-42.

Nourshargh, S., and F.M. Marelli-Berg. 2005. Transmigration through venular walls: a key regulator of leukocyte phenotype and function. *Trends Immunol.* 26:157-65.

Odink, K., N. Cerletti, J. Bruggen, R.G. Clerc, L. Tarcsay, G. Zwadlo, G. Gerhards, R. Schlegel, and C. Sorg. 1987. Two calcium-binding proteins in infiltrate macrophages of rheumatoid arthritis. *Nature*. 330:80-2.

Partida-Sanchez, S., D.A. Cockayne, S. Monard, E.L. Jacobson, N. Oppenheimer, B. Garvy, K. Kusser, S. Goodrich, M. Howard, A. Harmsen, T.D. Randall, and F.E. Lund. 2001. Cyclic ADP-ribose production by CD38 regulates intracellular calcium release, extracellular calcium influx and chemotaxis in neutrophils and is required for bacterial clearance in vivo. *Nat Med.* 7:1209-16.

Passey, R.J., E. Williams, A.M. Lichanska, C. Wells, S. Hu, C.L. Geczy, M.H. Little, and D.A. Hume. 1999. A null mutation in the inflammation-associated S100 protein S100A8 causes early resorption of the mouse embryo. *J Immunol.* 163:2209-16.

Peppiatt, C.M., T.J. Collins, L. Mackenzie, S.J. Conway, A.B. Holmes, M.D. Bootman, M.J. Berridge, J.T. Seo, and H.L. Roderick. 2003. 2-Aminoethoxydiphenyl borate (2-APB) antagonises inositol 1,4,5-trisphosphate-induced calcium release, inhibits calcium pumps and has a use-dependent and slowly reversible action on store-operated calcium entry channels. *Cell Calcium*. 34:97-108.

Pettit, E.J., and F.S. Fay. 1998. Cytosolic free calcium and the cytoskeleton in the control of leukocyte chemotaxis. *Physiol Rev*. 78:949-67.

Pettit, E.J., and M.B. Hallett. 1998. Two distinct Ca2+ storage and release sites in human neutrophils. *J Leukoc Biol*. 63:225-32.

Propper, C., X. Huang, J. Roth, C. Sorg, and W. Nacken. 1999. Analysis of the MRP8-MRP14 protein-protein interaction by the two-hybrid system suggests a prominent role of the C-terminal domain of S100 proteins in dimer formation. *J Biol Chem*. 274:183-8.

Rahimi, F., K. Hsu, Y. Endoh, and C.L. Geczy. 2005. FGF-2, IL-1beta and TGF-beta regulate fibroblast expression of S100A8. *Febs J.* 272:2811-27.

Rammes, A., J. Roth, M. Goebeler, M. Klempt, M. Hartmann, and C. Sorg. 1997. Myeloid-related protein (MRP) 8 and MRP14, calcium-binding proteins of the S100 family, are secreted by activated monocytes via a novel, tubulin-dependent pathway. *J Biol Chem.* 272:9496-502.

Ravasi, T., K. Hsu, J. Goyette, K. Schroder, Z. Yang, F. Rahimi, L.P. Miranda, P.F. Alewood, D.A. Hume, and C. Geczy. 2004. Probing the S100 protein family through genomic and functional analysis. *Genomics.* 84:10-22.

Reeves, E.P., H. Lu, H.L. Jacobs, C.G. Messina, S. Bolsover, G. Gabella, E.O. Potma, A. Warley, J. Roes, and A.W. Segal. 2002. Killing activity of neutrophils is mediated through activation of proteases by K+ flux. *Nature.* 416:291-7.

Reynolds, L.E., F.J. Conti, M. Lucas, R. Grose, S. Robinson, M. Stone, G. Saunders, C. Dickson, R.O. Hynes, A. Lacy-Hulbert, and K. Hodivala-Dilke. 2005. Accelerated re-epithelialization in beta3-integrin-deficient- mice is associated with enhanced TGF-beta1 signaling. *Nat Med.* 11:167-74.

Rhee, S.G. 2001. Regulation of phosphoinositide-specific phospholipase C. *Annu Rev Biochem.* 70:281-312.

Rhee, S.G., and Y.S. Bae. 1997. Regulation of phosphoinositide-specific phospholipase C isozymes. *J Biol Chem.* 272:15045-8.

Ridinger, K., E.C. Ilg, F.K. Niggli, C.W. Heizmann, and B.W. Schafer. 1998. Clustered organization of S100 genes in human and mouse. *Biochim Biophys Acta.* 1448:254-63.

Rizzuto, R., M.R. Duchen, and T. Pozzan. 2004. Flirting in little space: the ER/mitochondria Ca2+ liaison. *Sci STKE.* 2004:re1.

Robinson, M.J., P. Tessier, R. Poulsom, and N. Hogg. 2002. The S100 family heterodimer, MRP-8/14, binds with high affinity to heparin and heparan sulfate glycosaminoglycans on endothelial cells. *J Biol Chem.* 277:3658-65.

Roderick, H.L., and M.D. Bootman. 2003. Bi-directional signalling from the InsP3 receptor: regulation by calcium and accessory factors. *Biochem Soc Trans.* 31:950-3.

Roes, J., B.K. Choi, D. Power, P. Xu, and A.W. Segal. 2003. Granulocyte function in grancalcin-deficient mice. *Mol Cell Biol.* 23:826-30.

Roos, D., R. van Bruggen, and C. Meischl. 2003. Oxidative killing of microbes by neutrophils. *Microbes Infect.* 5:1307-15.

Rossi, D., and A. Zlotnik. 2000. The biology of chemokines and their receptors. *Annu Rev Immunol.* 18:217-42.

Roth, J., F. Burwinkel, C. van den Bos, M. Goebeler, E. Vollmer, and C. Sorg. 1993. MRP8 and MRP14, S-100-like proteins associated with myeloid differentiation, are translocated to plasma membrane and intermediate filaments in a calcium-dependent manner. *Blood.* 82:1875-83.

Roth, J., T. Vogl, C. Sunderkotter, and C. Sorg. 2003. Chemotactic activity of S100A8 and S100A9. *J Immunol.* 171:5651.

Roulin, K., G. Hagens, R. Hotz, J.H. Saurat, J.H. Veerkamp, and G. Siegenthaler. 1999. The fatty acid-binding heterocomplex FA-p34 formed by S100A8 and S100A9 is the major fatty acid carrier in neutrophils and translocates from the cytosol to the membrane upon stimulation. *Exp Cell Res.* 247:410-21.

Rudolf, R., M. Mongillo, R. Rizzuto, and T. Pozzan. 2003. Looking forward to seeing calcium. *Nat Rev Mol Cell Biol.* 4:579-86.

Ryckman, C., C. Gilbert, R. de Medicis, A. Lussier, K. Vandal, and P.A. Tessier. 2004. Monosodium urate monohydrate crystals induce the release of the

proinflammatory protein S100A8/A9 from neutrophils. *J Leukoc Biol.* 76:433-40.

Ryckman, C., S.R. McColl, K. Vandal, R. de Medicis, A. Lussier, P.E. Poubelle, and P.A. Tessier. 2003a. Role of S100A8 and S100A9 in neutrophil recruitment in response to monosodium urate monohydrate crystals in the air-pouch model of acute gouty arthritis. *Arthritis Rheum.* 48:2310-20.

Ryckman, C., K. Vandal, P. Rouleau, M. Talbot, and P.A. Tessier. 2003b. Proinflammatory activities of S100: proteins S100A8, S100A9, and S100A8/A9 induce neutrophil chemotaxis and adhesion. *J Immunol.* 170:3233-42.

Saintigny, G., R. Schmidt, B. Shroot, L. Juhlin, U. Reichert, and S. Michel. 1992. Differential expression of calgranulin A and B in various epithelial cell lines and reconstructed epidermis. *J Invest Dermatol.* 99:639-44.

Saito, Y., K. Saito, Y. Hirano, K. Ikeya, H. Suzuki, K. Shishikura, S. Manno, Y. Takakuwa, K. Nakagawa, A. Iwasa, S. Fujikawa, M. Moriya, N. Mizoguchi, B.E. Golden, and M. Osawa. 2002. Hyperzincemia with systemic inflammation: a heritable disorder of calprotectin metabolism with rheumatic manifestations? *J Pediatr.* 140:267-9.

Sampson, B., M.K. Fagerhol, C. Sunderkotter, B.E. Golden, P. Richmond, N. Klein, I.Z. Kovar, J.H. Beattie, B. Wolska-Kusnierz, Y. Saito, and J. Roth. 2002. Hyperzincaemia and hypercalprotectinaemia: a new disorder of zinc metabolism. *Lancet.* 360:1742-5.

Santhanagopalan, V., B.L. Hahn, and P.G. Sohnle. 1995. Resistance of zinc-supplemented Candida albicans cells to the growth inhibitory effect of calprotectin. *J Infect Dis.* 171:1289-94.

Santoro, M.M., and G. Gaudino. 2005. Cellular and molecular facets of keratinocyte reepithelization during wound healing. *Exp Cell Res.* 304:274-86.

Schafer, B.W., R. Wicki, D. Engelkamp, M.G. Mattei, and C.W. Heizmann. 1995. Isolation of a YAC clone covering a cluster of nine S100 genes on human chromosome 1q21: rationale for a new nomenclature of the S100 calcium-binding protein family. *Genomics*. 25:638-43.

Schaffer, C.J., and L.B. Nanney. 1996. Cell biology of wound healing. *Int Rev Cytol*. 169:151-81.

Schmidt, M., R. Gillitzer, A. Toksoy, E.B. Brocker, U.R. Rapp, R. Paus, J. Roth, S. Ludwig, and M. Goebeler. 2001. Selective expression of calcium-binding proteins S100a8 and S100a9 at distinct sites of hair follicles. *J Invest Dermatol*. 117:748-50.

Schorr, W., D. Swandulla, and H.U. Zeilhofer. 1999. Mechanisms of IL-8-induced Ca2+ signaling in human neutrophil granulocytes. *Eur J Immunol*. 29:897-904.

Scott, K.A., R.J. Moore, C.H. Arnott, N. East, R.G. Thompson, B.J. Scallon, D.J. Shealy, and F.R. Balkwill. 2003. An anti-tumor necrosis factor-alpha antibody inhibits the development of experimental skin tumors. *Mol Cancer Ther*. 2:445-51.

Seemann, J., K. Weber, and V. Gerke. 1996. Structural requirements for annexin I-S100C complex-formation. *Biochem J*. 319 (Pt 1):123-9.

Segal, A.W. 2005. How neutrophils kill microbes. *Annu Rev Immunol*. 23:197-223.

Siegenthaler, G., K. Roulin, D. Chatellard-Gruaz, R. Hotz, J.H. Saurat, U. Hellman, and G. Hagens. 1997. A heterocomplex formed by the calcium-binding proteins MRP8 (S100A8) and MRP14 (S100A9) binds unsaturated fatty acids with high affinity. *J Biol Chem*. 272:9371-7.

Singer, A.J., and R.A. Clark. 1999. Cutaneous wound healing. *N Engl J Med.* 341:738-46.

Slaga, T.J., I.V. Budunova, I.B. Gimenez-Conti, and C.M. Aldaz. 1996. The mouse skin carcinogenesis model. *J Investig Dermatol Symp Proc.* 1:151-6.

Smith, A., M. Bracke, B. Leitinger, J.C. Porter, and N. Hogg. 2003. LFA-1-induced T cell migration on ICAM-1 involves regulation of MLCK-mediated attachment and ROCK-dependent detachment. *J Cell Sci.* 116:3123-33.

Sohnle, P.G., C. Collins-Lech, and J.H. Wiessner. 1991. The zinc-reversible antimicrobial activity of neutrophil lysates and abscess fluid supernatants. *J Infect Dis.* 164:137-42.

Sohnle, P.G., M.J. Hunter, B. Hahn, and W.J. Chazin. 2000. Zinc-reversible antimicrobial activity of recombinant calprotectin (migration inhibitory factor-related proteins 8 and 14). *J Infect Dis.* 182:1272-5.

Sopalla, C., N. Leukert, C. Sorg, and C. Kerkhoff. 2002. Evidence for the involvement of the unique C-tail of S100A9 in the binding of arachidonic acid to the heterocomplex S100A8/A9. *Biol Chem.* 383:1895-905.

Spassova, M.A., J. Soboloff, L.P. He, T. Hewavitharana, W. Xu, K. Venkatachalam, D.B. van Rossum, R.L. Patterson, and D.L. Gill. 2004. Calcium entry mediated by SOCs and TRP channels: variations and enigma. *Biochim Biophys Acta.* 1742:9-20.

Srikrishna, G., K. Panneerselvam, V. Westphal, V. Abraham, A. Varki, and H.H. Freeze. 2001. Two proteins modulating transendothelial migration of leukocytes recognize novel carboxylated glycans on endothelial cells. *J Immunol.* 166:4678-88.

Steiling, H., B. Munz, S. Werner, and M. Brauchle. 1999. Different types of ROS-scavenging enzymes are expressed during cutaneous wound repair. *Exp Cell Res.* 247:484-94.

Steinbakk, M., C.F. Naess-Andresen, E. Lingaas, I. Dale, P. Brandtzaeg, and M.K. Fagerhol. 1990. Antimicrobial actions of calcium binding leucocyte L1 protein, calprotectin. *Lancet.* 336:763-5.

Striggow, F., and B.E. Ehrlich. 1997. Regulation of intracellular calcium release channel function by arachidonic acid and leukotriene B4. *Biochem Biophys Res Commun.* 237:413-8.

Stuart, L.M., and R.A. Ezekowitz. 2005. Phagocytosis: elegant complexity. *Immunity.* 22:539-50.

Sugimoto, K., M. Nishida, M. Otsuka, K. Makino, K. Ohkubo, Y. Mori, and T. Morii. 2004. Novel real-time sensors to quantitatively assess in vivo inositol 1,4,5-trisphosphate production in intact cells. *Chem Biol.* 11:475-85.

Takashima, K., K. Tateda, T. Matsumoto, Y. Iizawa, M. Nakao, and K. Yamaguchi. 1997. Role of tumor necrosis factor alpha in pathogenesis of pneumococcal pneumonia in mice. *Infect Immun.* 65:257-60.

Taylor, S., S. Herrington, W. Prime, P.S. Rudland, and R. Barraclough. 2002. S100A4 (p9Ka) protein in colon carcinoma and liver metastases: association with carcinoma cells and T-lymphocytes. *Br J Cancer.* 86:409-16.

Teigelkamp, S., R.S. Bhardwaj, J. Roth, G. Meinardus-Hager, M. Karas, and C. Sorg. 1991. Calcium-dependent complex assembly of the myeloic differentiation proteins MRP-8 and MRP-14. *J Biol Chem.* 266:13462-7.

Thompson, R.D., K.E. Noble, K.Y. Larbi, A. Dewar, G.S. Duncan, T.W. Mak, and S. Nourshargh. 2001. Platelet-endothelial cell adhesion molecule-1 (PECAM-1)-deficient mice demonstrate a transient and cytokine-specific role

for PECAM-1 in leukocyte migration through the perivascular basement membrane. *Blood.* 97:1854-60.

Thorey, I.S., J. Roth, J. Regenbogen, J.P. Halle, M. Bittner, T. Vogl, S. Kaesler, P. Bugnon, B. Reitmaier, S. Durka, A. Graf, M. Wockner, N. Rieger, A. Konstantinow, E. Wolf, A. Goppelt, and S. Werner. 2001. The Ca2+-binding proteins S100A8 and S100A9 are encoded by novel injury-regulated genes. *J Biol Chem.* 276:35818-25.

Tian, W., S. Dewitt, I. Laffafian, and M.B. Hallett. 2004. Ca(2+), calpain and 3-phosphorylated phosphatidyl inositides; decision-making signals in neutrophils as potential targets for therapeutics. *J Pharm Pharmacol.* 56:565-71.

Treves, S., E. Scutari, M. Robert, S. Groh, M. Ottolia, G. Prestipino, M. Ronjat, and F. Zorzato. 1997. Interaction of S100A1 with the Ca2+ release channel (ryanodine receptor) of skeletal muscle. *Biochemistry.* 36:11496-503.

Underhill, D.M., and A. Ozinsky. 2002. Phagocytosis of microbes: complexity in action. *Annu Rev Immunol.* 20:825-52.

van den Bos, C., J. Roth, H.G. Koch, M. Hartmann, and C. Sorg. 1996. Phosphorylation of MRP14, an S100 protein expressed during monocytic differentiation, modulates Ca(2+)-dependent translocation from cytoplasm to membranes and cytoskeleton. *J Immunol.* 156:1247-54.

van Heyningen, V., C. Hayward, J. Fletcher, and C. McAuley. 1985. Tissue localization and chromosomal assignment of a serum protein that tracks the cystic fibrosis gene. *Nature.* 315:513-5.

Vandal, K., P. Rouleau, A. Boivin, C. Ryckman, M. Talbot, and P.A. Tessier. 2003. Blockade of S100A8 and S100A9 suppresses neutrophil migration in response to lipopolysaccharide. *J Immunol.* 171:2602-9.

Vicente-Manzanares, M., and F. Sanchez-Madrid. 2004. Role of the cytoskeleton during leukocyte responses. *Nat Rev Immunol.* 4:110-22.

Viemann, D., A. Strey, A. Janning, K. Jurk, K. Klimmek, T. Vogl, K. Hirono, F. Ichida, D. Foell, B. Kehrel, V. Gerke, C. Sorg, and J. Roth. 2005. Myeloid-related proteins 8 and 14 induce a specific inflammatory response in human microvascular endothelial cells. *Blood.* 105:2955-62.

Vogl, T., S. Ludwig, M. Goebeler, A. Strey, I.S. Thorey, R. Reichelt, D. Foell, V. Gerke, M.P. Manitz, W. Nacken, S. Werner, C. Sorg, and J. Roth. 2004. MRP8 and MRP14 control microtubule reorganization during transendothelial migration of phagocytes. *Blood.* 104:4260-8.

Vogl, T., J. Roth, C. Sorg, F. Hillenkamp, and K. Strupat. 1999. Calcium-induced noncovalently linked tetramers of MRP8 and MRP14 detected by ultraviolet matrix-assisted laser desorption/ionization mass spectrometry. *J Am Soc Mass Spectrom.* 10:1124-30.

Waisman, D.M. 1995. Annexin II tetramer: structure and function. *Mol Cell Biochem.* 149-150:301-22.

Wang, G., S. Zhang, D.G. Fernig, M. Martin-Fernandez, P.S. Rudland, and R. Barraclough. 2005. Mutually antagonistic actions of S100A4 and S100A1 on normal and metastatic phenotypes. *Oncogene.* 24:1445-54.

Ward, A.C., D.M. Loeb, A.A. Soede-Bobok, I.P. Touw, and A.D. Friedman. 2000. Regulation of granulopoiesis by transcription factors and cytokine signals. *Leukemia.* 14:973-90.

Weber, C. 2003. Novel mechanistic concepts for the control of leukocyte transmigration: specialization of integrins, chemokines, and junctional molecules. *J Mol Med.* 81:4-19.

Wicki, R., C. Franz, F.A. Scholl, C.W. Heizmann, and B.W. Schafer. 1997. Repression of the candidate tumor suppressor gene S100A2 in breast cancer is mediated by site-specific hypermethylation. *Cell Calcium.* 22:243-54.

Wilkinson, M.M., A. Busuttil, C. Hayward, D.J. Brock, J.R. Dorin, and V. Van Heyningen. 1988. Expression pattern of two related cystic fibrosis-associated calcium-binding proteins in normal and abnormal tissues. *J Cell Sci.* 91 (Pt 2):221-30.

Williams, R.L. 1999. Mammalian phosphoinositide-specific phospholipase C. *Biochim Biophys Acta.* 1441:255-67.

Witko-Sarsat, V., P. Rieu, B. Descamps-Latscha, P. Lesavre, and L. Halbwachs-Mecarelli. 2000. Neutrophils: molecules, functions and pathophysiological aspects. *Lab Invest.* 80:617-53.

Wu, D. 2005. Signaling mechanisms for regulation of chemotaxis. *Cell Res.* 15:52-6.

Wu, D., C.K. Huang, and H. Jiang. 2000. Roles of phospholipid signaling in chemoattractant-induced responses. *J Cell Sci.* 113 (Pt 17):2935-40.

Wu, D., G.J. LaRosa, and M.I. Simon. 1993. G protein-coupled signal transduction pathways for interleukin-8. *Science.* 261:101-3.

Xiong, Z., D. O'Hanlon, L.E. Becker, J. Roder, J.F. MacDonald, and A. Marks. 2000. Enhanced calcium transients in glial cells in neonatal cerebellar cultures derived from S100B null mice. *Exp Cell Res.* 257:281-9.

Xu, K., and C.L. Geczy. 2000. IFN-gamma and TNF regulate macrophage expression of the chemotactic S100 protein S100A8. *J Immunol.* 164:4916-23.

Yang, J., S. McBride, D.O. Mak, N. Vardi, K. Palczewski, F. Haeseleer, and J.K. Foskett. 2002. Identification of a family of calcium sensors as protein ligands

of inositol trisphosphate receptor Ca(2+) release channels. *Proc Natl Acad Sci U S A.* 99:7711-6.

Young, R.E., R.D. Thompson, and S. Nourshargh. 2002. Divergent mechanisms of action of the inflammatory cytokines interleukin 1-beta and tumour necrosis factor-alpha in mouse cremasteric venules. *Br J Pharmacol.* 137:1237-46.

Yui, S., M. Mikami, K. Tsurumaki, and M. Yamazaki. 1997. Growth-inhibitory and apoptosis-inducing activities of calprotectin derived from inflammatory exudate cells on normal fibroblasts: regulation by metal ions. *J Leukoc Biol.* 61:50-7.

Yui, S., M. Mikami, and M. Yamazaki. 1995a. Induction of apoptotic cell death in mouse lymphoma and human leukemia cell lines by a calcium-binding protein complex, calprotectin, derived from inflammatory peritoneal exudate cells. *J Leukoc Biol.* 58:650-8.

Yui, S., M. Mikami, and M. Yamazaki. 1995b. Purification and characterization of the cytotoxic factor in rat peritoneal exudate cells: its identification as the calcium binding protein complex, calprotectin. *J Leukoc Biol.* 58:307-16.

Zhang, S., B.S. Youn, J.L. Gao, P.M. Murphy, and B.S. Kwon. 1999. Differential effects of leukotactin-1 and macrophage inflammatory protein-1 alpha on neutrophils mediated by CCR1. *J Immunol.* 162:4938-42.

Zhang, T., T.L. Woods, and J.T. Elder. 2002. Differential responses of S100A2 to oxidative stress and increased intracellular calcium in normal, immortalized, and malignant human keratinocytes. *J Invest Dermatol.* 119:1196-201.

Zimmer, D.B., J. Chessher, and W. Song. 1996. Nucleotide homologies in genes encoding members of the S100 protein family. *Biochim Biophys Acta.* 1313:229-38.

Zoumpourlis, V., S. Solakidi, A. Papathoma, and D. Papaevangeliou. 2003. Alterations in signal transduction pathways implicated in tumour progression during multistage mouse skin carcinogenesis. *Carcinogenesis*. 24:1159-65.

10 Publications arising from this Thesis

Hobbs, J.A., R. May, K. Tanousis, E. McNeill, M. Mathies, C. Gebhardt, R. Henderson, M.J. Robinson, and N. Hogg. 2003. Myeloid cell function in MRP-14 (S100A9) null mice. Mol Cell Biol. 23:2564-76.